Universitat de Lleida

Non-edible triacylglycerols as feedstock to prepare phase change materials and pressure-sensitive adhesives

Pau Gallart Sirvent

http://hdl.handle.net/10803/405959

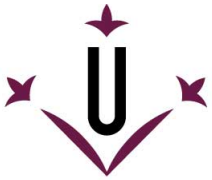

Universitat de Lleida

TESI DOCTORAL

Non-edible triacylglycerols as feedstock to prepare phase change materials and pressure-sensitive adhesives

Pau Gallart-Sirvent

Memòria presentada per optar al grau de Doctor per la Universitat de Lleida
Programa de Doctorat en Ciència i Tecnologia Agrària i Alimentària

Directors:
Ramon Canela-Garayoa
Gemma Villorbina Noguera

"Mother Earth is full of potential and mysteries; she can give life or take it away as simple as a snap. However, I also believe mother nature needs to be conserved so as to maintain its awesomeness. It is every man's duty to protect the environment and save our planet"

Kung Shing Yau

1992-2017

Agraïments

Wow! Doncs ja està! Després de 4 anyets ~~molestant~~ per Argònoms he après un munt de coses i fet grans amics! Així doncs, hi ha moltes persones que no surten a la portada d'aquesta tesi i han contribuït a la feina que s'explica més endavant. Per tant, vull regalar unes quantes paraules a tothom qui hi ha participat de forma directa o indirecta en aquesta empresa:

Vull donar gràcies al Ramon Canela, perquè m'has donat un enorme suport durant tots aquests anys i m'has guiat per aquest fantàstic camí. A la Gemma Villorbina, perquè m'has tractat com un amic des del primer dia i sempre has estat disposada a ajudar-me. També vull agraïr a l'empresa Subcarn Echevarría per aportar-me el greix animal i donar-me la possibilitat de tenir un contracte de doctorat.

A la Mercè Balcells i el Jordi Eras per les aportacions constructives que m'heu donat al llarg de tots els "lab meetings". A la Montse Llovera i la Sílvia Galitó dels serveis cientificotècnics per l'ajuda prestada i el bon tracte que sempre he rebut de vosaltres. A la Mireia Oromí perquè sempre has estat disposada a ajudar-me en l'RMN i el FT-IR i totes rialles que ens hem fet. No ens oblidem de la resta de la gent del Departament de Química que d'agrònom de ferro en agrònom de ferro sempre heu fet d'aquesta universitat una casa.

Als meus companys i ex-companys del laboratori de química orgànica Guerris, Remei, Carmen, Anna, Olalla, Silvia, Toni, Alexis, Marc,...dels quals sempre n'he après un munt. També vull donar ànims als nous companys del laboratòri de química orgànica Alberto, Diana, Nancy i Erika. Espero que gaudiu molt d'aquest camí que heu escollit! Una frase d'agraïment també pel Gonzalo i l'Alba els quals sou uns exel·lents treballadors i el vostre esforç ocupa més d'una pàgina en aquesta tesi. Finalment donar gràcies de compartir laboratòri amb uns grans personatges com són l'Albert i l'Edinson per tot el que he après de vosaltres, tot el que m'heu ajudat i tot el que n'hem gaudit.

A tota la gent del CREA que ha cooperat conjuntament amb el nostre grup i especialment durant el transcurs d'aquesta tesi. Aran, Camila i Marc us estic molt agraït per la vostra dedicació i l'ajuda prestada per preparar els manuscrits. Finalment, a la Lluïsa per haver-nos permès de fer tots els anàlisis de DSC i ciclatges, les correccions i totes les aportacions fetes a diferents nivells al llarg d'aquests anys.

To the people I met during my PhD internship in the US. Anlong and Kaichang, thank you so much to allow this internship by let me work in your lab and teach me as a son. To the OSU triathlon group to treat me as a friend and share some beautiful moments. To the friends I did, Günther, Zeno, Tomás and Lindsey: Few months were enough for a vast amount of adventures and nice moments I'll never ever forget.

Als meus companys del grup del Superbé per les desestressants rutes nocturnes, intersemanals, i a cop de pedal que fem a través del secà d'Artesa i voltants. A els meus col·legues del grup de triatló del Trèvol per tot el que gaudim aventura rere aventura, el bé que ens ho passem i l'enorme pinya que fem. A els Carlos, Franqui, Marc Daniel, Mariana, Mar, Maria i Mireia per les grans rialles que fem a cada moment que compartim. Als amics de la infància i la joventut, Kosta, Pagès, Eloi i Sole per totes les mil i una experiències que hem viscut i les que seguirem vivint! A la Gemma i el Zaka perquè sense la seva companyia mai hagués arribat a ser químic. Als grans amics de la facultat de química de Tarragona, Sergi, Monti, Guasch, Lore i Ribo perquè sempre és un luxe compartir amb vosaltres calçotades, paelles, sopars i qualsevol moment. De tots els químics, un petit i especial record pels doctors Sergi, Monti i Guasch, perquè tot i ser mesos més joves que jo, sempre n'he après molt de vosaltres.

A tots els meus tiets i cosins, pels fantàstics moments que han fet de nosaltres la nostra història i els demés que compartirem. Vull reservar també unes paraules pel Curial, aviat et recuperaràs i et tornarem a veure jugar al camp de l'Artesa! Per tot l'esforç que vareu ficar en jo mentre vaig creixer Aureli, Josep i Pepita, aquí teniu unes paraules per a la vostra eternitat: Moltes gràcies! A la meva padrina Carmina per totes les vegades que m'he quedat a dinar durant aquesta tesi i per tot el carinyo que sempre m'has donat al llarg de la vida. Finalment, he guardat les últimes paraules pels meus pares. El suport incondicional, dedicació, exemple i ensenyança que m'heu aportat m'han fet arribar fins aquí i qui sap fins on em portaran. Espero seguir-vos veient amb aquesta alegria, felicitat i...aviat...ballant com fins fa poc.

Pau

Summary

The research described in this document is focused on the utilization of vegetable and animal non-edible triacylglycerols to prepare value added products. Triacylglycerols appeared to be an excellent source to substitute petroleum since they come from distinct renewable sources and have various interesting chemical and physical properties. Nevertheless, although they are renewable, their utilization as starting materials to produce chemicals can cause some concerns. On the one hand, edible triacylglycerols compete directly with food and feed. To overpass these concerns, two distinct sources of non-edible triacylglycerols such as non-edible animal fat from slaughterhouses and vegetable oil from a Chinese three crop (*Vernicia fordii*) known as tung oil were used. On the other hand, some of the chemical procedures involved in the preparation of bio-based products have negative effects on the environment since high amount of wastes are generated and high temperatures and hazardous reagents are commonly employed. To overcome these issues, the present work takes advantage of the milder conditions and reusability of biocatalysts such as immobilized lipases and resting cells. Additionally, non-hazardous chemicals, low generating waste practices and cheap reagents were a priority to complete the transformation of non-edible animal fat and tung oil.

Non-edible animal fat was splitted into saturated fatty acids and unsaturated fatty acids by employing *R. oryzae* resting cells. Additionally, resting cells were reused by extracting the resulting fatty acids with supercritical CO_2 and glycerol was recovered and analyzed. To study and transform those saturated and unsaturated parts, the splitting was repeated in a multigram scale with cheap and common chemical reagents. Thus, the saturated fatty acids were thermally analyzed presenting good properties and reliability as Phase Change Materials (PCMs) and the unsaturated fatty acids were converted to *threo*-9, 10-dihydroxystearic acid (DHSA), a chemical block used in polymer chemistry. Besides, DHSA and some of their salts were also analyzed by DSC, although they did not present interesting properties as PCMs presumably due to their thermal degradation. Nevertheless, the esters of DHSA (DHSEs) were postulated to overcome this issue. Indeed, green and sustainable chemistry such as enzymatic hydrolysis, chemo-enzymatic epoxidation, hot water epoxide hydrolysis and enzymatic esterification were employed to prepare those DHSEs, which presented good properties and reliability as PCMs.

Finally, tung oil was used to prepare Pressure-Sensitive Adhesives (PSAs). The rare α-eleostearic acid mainly found in tung oil presents the particularity to afford Diels-Alders (D-A) reactions. Certainly, D-A reactions do not need a previous transformation of the triacylglycerols for polymerization allowing a direct

polymerization, which allowed the preparation of a non-waste generating polymer. The D-A polymerization of tung oil with some of the diacrylates used yielded PSAs with good properties such as peel strength, loop tack and aging resistance. Besides, the addition of dimaleimide lowered the curing time of the PSAs prepared.

Resumen

Este programa de investigación está enfocado en el aprovechamiento de triacilglicéridos vegetales y animales de origen no comestible para preparar productos con valor añadido. Los triacilglicéridos son una fuente excelente para substituir el petróleo ya que provienen de distintas fuentes renovables y tienen propiedades químicas y físicas interesantes. No obstante, aunque son renovables, su uso tiene que discutirse. Por un lado, debido al origen de los triacilglicéridos, ya que los comestibles compiten directamente con la alimentación. Por lo tanto, se han usado dos fuentes distintas como son la grasa animal no comestible de los mataderos municipales y un aceite vegetal no comestible proveniente de un árbol de cultivo chino (*Vernicia fordii*) llamado aceite de tung. Por el otro lado, parte de la química involucrada en la preparación de productos "bio-based" tiene efectos negativos para el medio ambiente ya que genera grandes cantidades de residuos y normalmente se usan altas temperaturas y reactivos peligrosos. Para superar este problema, este trabajo aprovecha las condiciones suaves y la reusabilidad de los biocatalizadores como las lipasas inmovilizadas y las "resting cells". Además, fueron una prioridad los reactivos químicos no peligrosos, practicas generadoras de pocos residuos y reactivos baratos para completar la transformación de la grasa animal no comestible y el aceite de tung.

La grasa animal no comestible se dividió en ácidos grasos saturados e insaturados usando "resting cells" de *R.Oryzae.* Además, las "resting cells" se reutilizaron usando CO_2 supercrítico y el glicerol se recuperó y analizó. Para estudiar y transformar estas partes saturadas e insaturadas la división se repitió a escala de multigramos con reactivos químicos comunes y baratos. Por lo tanto, los ácidos grasos saturados fueron analizados térmicamente presentando buenas propiedades cómo materiales de cambio de fase (PCMs) y los insaturados se convirtieron en un bloque químico usado para la síntesis de polímeros cómo es el ácido *threo*-9, 10-dihidroxiestearico (DHSA). Además, se analizaron térmicamente el DHSA y algunas de sus sales sin presentar atractivo como PCMs presumiblemente por degradación. No obstante, los esteres de DHSA (DHSEs) fueron postulados como alternativa para superar este problema. En efecto, se usó química verde y sostenible tal como la hidrólisis enzimática, la epoxidación químico-enzimática, la hidrólisis del epóxido con agua caliente y la esterificación enzimática para preparar estos DHSE los cuales presentaron buenas propiedades y confiabilidad como PCMs.

Para terminar, el aceite de tung se usó para preparar adhesivos sensibles a la presión (PSAs). El ácido α-eleoestearico, de origen poco común y mayoritariamente encontrado en el aceite de tung, presenta la particularidad de alcanzar reacciones

Diels-Alders (D-A). En efecto, las reacciones D-A no requieren de la transformación previa de los triacilgliceridos para ser polimerizados por lo que permiten polimerizaciones directas y, por lo tanto, preparar polímeros sin generar residuos. La polimerización mediante la reacción D-A del aceite de tung con algunos de los diacrilatos usados presentaron buenas propiedades para PSAs tales como ”peel strenght”, “loop tack”y resistencia al envejecimiento. Además, la adición de dimaleimidas bajó el tiempo de curado de los PSAs preparados.

Resum

Aquest programa de recerca està enfocat en l'aprofitament de triacilglicèrids vegetals i animals d'origen no comestible per preparar productes de valor afegit. Els triacilglicèrids són una font excel·lent per substituir el petroli ja que provenen de diferents fonts renovables i tenen propietats químiques i físiques interessants. No obstant, tot i que són renovables, el seu ús s'ha de discutir. D'una banda, a causa del origen dels triglicèrids, ja que els comestibles competeixen directament amb l'alimentació. Per tant, s'han fet servir dues fonts diferents com són el greix animal no comestible dels escorxadors municipals i un oli vegetal no comestible provinent d'un arbre de cultiu xinès (*Vernicia fordii*) anomenat oli de tung. D'altra banda, part de la química involucrada en la preparació de productes "bio-based" té efectes negatius per al medi ambient ja que genera grans quantitats de residus i normalment es fan servir altes temperatures i reactius perillosos. Per superar aquest problema, aquest treball aprofita les condicions suaus i la reusabilitat dels biocatalitzadors com les lipases immobilitzades i les "resting cells". A més, van ser una prioritat els reactius químics no perillosos, les practiques generadores de pocs residus i els reactius barats per tal de completar la transformació del greix animal no comestible i l'oli de tung.

El greix animal no comestible es va dividir en àcids grassos saturats i insaturats usant "resting cells" de *R.oryzae*. A més, les "resting cells" es van reutilitzar usant CO_2 supercrític i el glicerol es va recuperar i analitzar. Per estudiar i transformar aquestes parts saturades i insaturades la divisió es va repetir a escala de multigram usant reactius químics comuns i barats. Per tant, els àcids grassos saturats van ser analitzats tèrmicament presentant bones propietats com a materials de canvi de fase (PCMs) i els insaturats es van convertir en un bloc químic usat en la síntesi de polímers com és l'àcid *threo*-9, 10-dihidroxiesteàric (DHSA). A més, es van analitzar tèrmicament el DHSA i algunes de les seves sals sense presentar atractiu com PCMs, presumiblement per degradació. No obstant això, els èsters de DHSA (DHSEs) van ser postulats com alternativa per superar aquest problema. En efecte, es va usar química verda i sostenible tal com l'hidròlisi enzimàtica, l'epoxidació químico-enzimàtica, l'hidròlisi de l'epòxid amb aigua calenta i l'esterificació enzimàtica per tal de preparar aquests DHSEs els quals van presentar bones propietats i fiabilitat com PCMs.

Per acabar, l'oli de tung es va usar per obtenir adhesius sensibles a la pressió (PSAs). L'àcid α-eleoesteàric, d'origen poc comú i majoritàriament trobat en l'oli de tung, presenta la particularitat d'assolir reaccions Diels-Alders (D-A). A més, les reaccions D-A no requereixen de la transformació prèvia dels triacilglicèrids per ser polimeritzats per la qual cosa permeten polimeritzacions directes i, per tant, preparar polímers sense generar residus. La polimerització mitjançant la reacció D-A

de l’oli de tung amb alguns dels diacrilats usats va comportar la preparació de PSAs amb bones propietats com ara "peel strenght", "loop tack" i resistència a l'envelliment. A més, l'addició de dimaleimides va baixar el temps de curat dels PSAs preparats.

Abbreviations

ATR	Attenuated total reflectance
BPAGDA	Bisphenol A glycerolate diacrylate
^{13}C NMR	Carbon nuclear magnetic resonance
CAL-B	*Candida antarctica* Lipase-B
CDG	Conjugate diene group
CECT	"Colección Española de Cultivos Tipo"
DA reaction	Diels-Alder reaction
DG	Dienophile group
DHSA	*threo*-9, 10-Dihydroxystearic acid
DHSE	*threo*-9, 10-Dihydroxtstearate
DHW	Domestic hot water
DSC	Differential scanning calorimeter
ESO	Epoxidized soy bean oil
FFA	Free fatty acids
FT-IR	Fourier transform-infrared spectroscopy
GC-FID	Gas chromatography-flame ionization detector
^{1}H NMR	Proton nuclear magnetic resonance
IWH	Industrial waste heat
LHTES	Latent heat thermal energy storage
MSW	Municipal solid waste
MONG	Matter organic non glycerol
MPMI	4,4'-Methylene-bis(N-phenylmaleimide)
PA-SA	Palmitic acid-stearic acid
PCM	Phase change material
PET	Polyethylene terephthalate

PPGDA	Poly(propylene glycol) diacrylate
PSA	Pressure-sensitive adhesive
PVC	Polyvinyl chloride
SV	Saponification value
t-BuOH	*tert*-butyl alcohol
TES	Thermal energy storage
TOAA	An adduct from the reaction of tung oil and acrylic acid
U	One unit of activity

Table of contents

Chapter I

General introduction

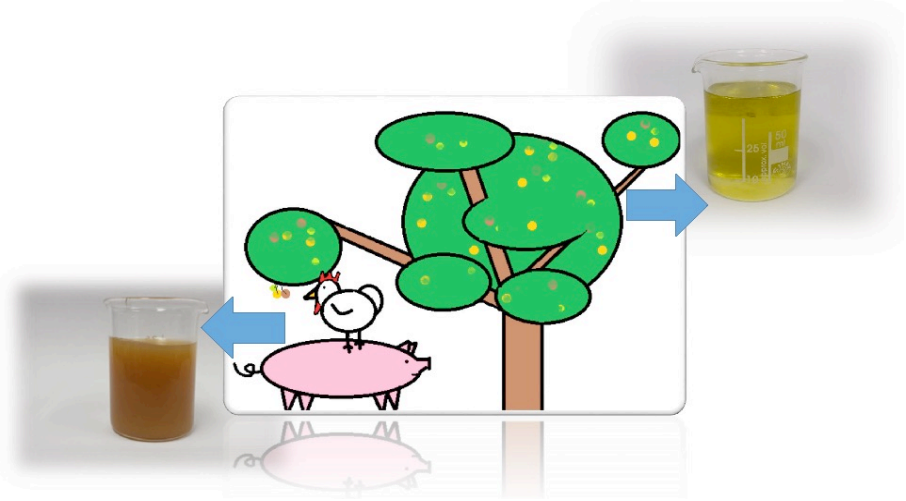

1.1. Circular economy

The current world system of economy dates from Industrial Revolution. This model uses a "take-make-use-dispose" system known as Linear Economy [1]. During the 20th century the market was stimulated by the invention of new products and services such as telephone, motor car, electric lighting and domestic appliances. Nevertheless, to keep stimulating the economy an idea called Planned Obsolescence was proposed [2]. The basis of Planned Obsolescence consider that consumer goods have to become rapidly obsolete and replaced. Designers and engineers have to develop goods following these criteria. On the one hand, the introduction of frequent esthetic changes may stimulate the desire to own something a little newer and a little better, sooner than necessary [3]. On the other hand, reducing the working life of products by replacing durable materials with others less durable. Planned Obsolescence certainly increased company profits but since 50 years ago it is recognized as "the systematic attempt of business to make us wasteful, debt-ridden, permanently discontented individuals" [4]. Besides, since 1960s global market prices made reuse became less economically attractive than buy new. For instance, products were not designed for disassembly. The Linear model has benefitted energy suppliers and raw materials producers such as the mining and oil industries. Nevertheless, environment has been damaged since huge amounts of waste were sent to landfill and/or combusted [5]. Disposal at end of life has never been a sustainable practice but as global population increased from approximately 1 billion in 1804 to 7.2 billion in 2014 and a further increase to 9.6 billion by 2050 is anticipated [6], the demand for energy and resources

will dramatically increase. As highlight, more minerals and fossil fuels were consumed during the 20th century than in all other centuries together [5].

A new alternative needs to be undertaken to solve the issues generated by Linear Economy. Circular Economy appears to be a sustainable alternative whereby it mirrors natural life cycles where dead organic material decomposes to become a nutrient for the next generation of living organisms. As natural systems, has to be highly efficient and not create waste. This concept was initially introduced during the 1970s enunciating that waste has to become a resource. Defined as a "Cradle-to-Cradle" system instead of the Linear Economy model described as "Cradle-to-Grave" [7] where the need to extend product life through repair and remanufacture was inherent [8]. On the basis of Linear Economy raw materials are extracted and processed, manufactured; used and disposed. In that way, products are used since end of life (see **Figure 1.1**). Conversely, Circular Economy keeps materials in circulation by remanufacturing and even though energy and resources will still be required for disassembly and recycling, the elimination of extraction and processing of bulk materials reduces the embodied energy, embodied water, associated emissions, environmental and other impacts [5].

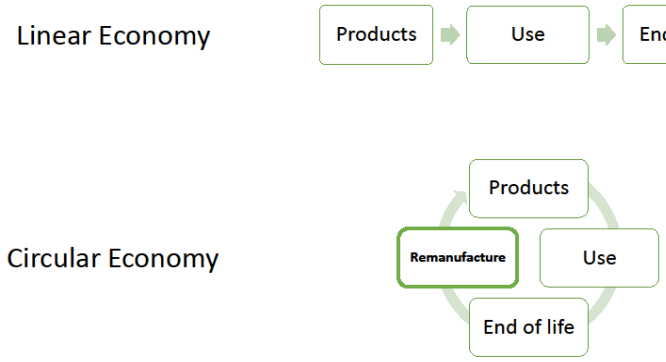

Figure 1.1. Simplified Linear and Circular Economy concepts.

1.2. Bioeconomy

Given the concept of Circular Economy, the use of renewable resources appears to be inherent to construct a model based in reusing and non-generating wastes. A bioeconomy can be understood as an economy using renewable biological resources as basic building blocks for materials, chemicals and energy [9–11]. With a good design and implementation, this sort of economy can meet many of the requirements for sustainability from environmental, social and economic perspectives. A bioeconomy can improve the reduction of greenhouse gas emissions, decrease dependence on fossil resources, wiser management of natural resources, and improved food security [10, 12]. Additionally, non-food markets such as bioenergy besides of existing food markets can give a major boost to rural areas [9]. The bioeconomy concept initially started from the life sciences and biotechnology spheres, sciences that use living beings to produce goods and services. On industrial scale it uses enzymes and micro-organisms to make

bio-based products matching up with the bioeconomy concept. In that way, by chemical and biotechnological approaches, as over 90% of the petroleum-based products could be replaced by bio-based alternatives [13].The technology needed to replace petroleum-based refineries is known as biorefienries and permits to apply the bioeconomy concept [14].

1.3. Biorefineries

Biomass is very likely to be the only viable alternative to fossil resources for production of fuels and chemicals, since it is the only C-rich material source available on the Earth, besides fossils. The replacement of petrochemicals by biomass for fuel and chemical production is an interesting option and is the driving force for the development of biorefinery complexes. The aim of this bio-industry is to be competitive in the market and lead to the progressive replacement of oil refinery products. In opposite to oil refineries, which are focused on very large plants, biorefinery industries will most probably encompass a whole range of different-sized installations and dispersed industrial complexes able to revitalize rural areas. Additionally, as circular economy concept, the residue from one bio-industry could become an input for other industries, giving rise to integrated bio-industrial systems [15].

The use of sustainable feedstock is not enough to ensure a prosperous future for the next generation; protection of the environment using greener methodologies is also required. These methods and techniques used have to minimize impact to the environment and the final products should be non-toxic, degradable into innocuous chemicals and with minimum production of waste. In order to establish a sustainable future production of these biofuels and biochemicals, the integration of green chemistry into biorefineries, along

with the use of low environmental impact technologies, is mandatory. Green chemistry can be considered as a set of principles (see **Figure 1.2**) for the manufacture and application of products that aim at eliminating the use or generation of environmentally harmful and hazardous chemicals. It offers a tool kit of techniques and underlying principles that any researcher should apply when developing the next generation of biorefineries. The overall goal of green chemistry combined with biomass achieves the production of genuinely green and sustainable chemical products [16].

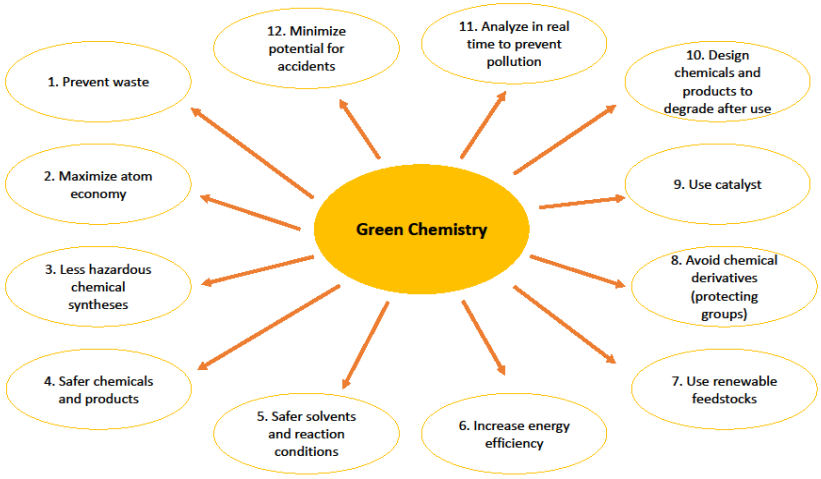

Figure 1.2. Schematic representation of the Green chemistry principles [17].

1.4. Biomass feedstocks

Biomass are non-fossilized and biodegradable organic materials originating from plants, animals, and microorganisms derived from biological sources. Biomass includes products, byproducts, residues and waste from agriculture, forestry and related industries, as well as the non-fossilized and biodegradable organic fractions of industrial and municipal solid wastes [18].

In other words, biomass is the solar energy stored as chemical energy via photosynthesis. Indeed, organisms evolved metabolic machineries for the photochemical reduction of carbon dioxide to organic matter. Thus, this solar energy is stored in chemical form in plant and animal materials [15, 18].

Feedstocks can be described as raw materials used in a biorefinery [15] whereby a large variety of sources have application. In that way, even matters such as organic fraction from Municipal Solid Waste (MSW), manure, wild fruits and crops, proteins and residues from fresh fruit and vegetable industries can be used to produce biogas [19]. Otherwise, carbohydrates (from starch, cellulose and hemicellulose) can be easily fermented to ethanol or used as a substrate for chemical reactions leading to a wide range of chemical products [20, 21]. Finally, oils and fats which are triacylglycerols consisting of glycerin and a variety of fatty acids present a substantial attractive scope for biorefinery purposes. Triacylglycerols can be used for biodiesel production by reacting with an alcohol, usually methanol. However, they are an excellent substrate for chemicals because their reactive sites can afford an enormous number of transformations [22]. **Figure 1.3** shows the most commonly used fatty acids as feedstocks.

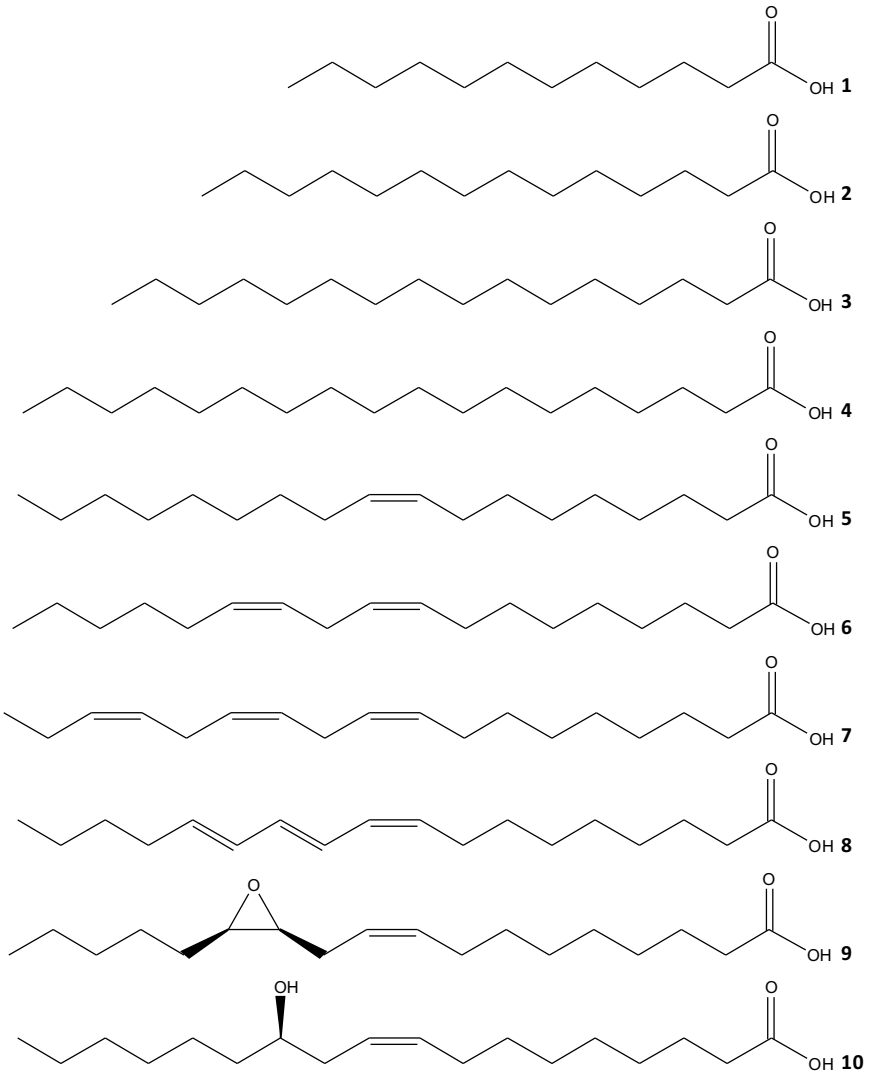

Figure 1.3. Major naturally occurring fatty acids: (**1**) Lauric acid. (**2**) Myristic acid. (**3**) Palmitic acid. (**4**) Stearic acid. (**5**) Oleic acid. (**6**) Linoleic acid. (**7**) Linolenic acid. (**8**) α-Eleostearic acid. (**9**) Vernolic acid. (**10**) Ricinoleic acid.

1.5. Sources of triacylglycerols

1.5.1. Edible oils

Edible oils have been used throughout human history. Certainly, for more than 6000 years, the olive oil cultivation has developed alongside Mediterranean civilizations for oil production [23]. Several edible oils from sources such as rapeseed [24], soybean [25], palm [26] and sunflower [27] have been extensive used as a feedstocks. Additionally, more than 95% of biodiesel production is produced from edible oils whereby soybean in USA while rapeseed and sunflower in Europe are the most used [28]. Unfortunately, the use of these edible sources has generated many problems, mainly due to their impact on global food markets and food security [29]. For instance, palm and soy are crops vital for human consumption. The use of these food crops on a large-scale production of non-food commodities could bring imbalance to the global food market [30], and as a consequence, the world could suddenly face a ‘‘food versus feedstock” crisis.

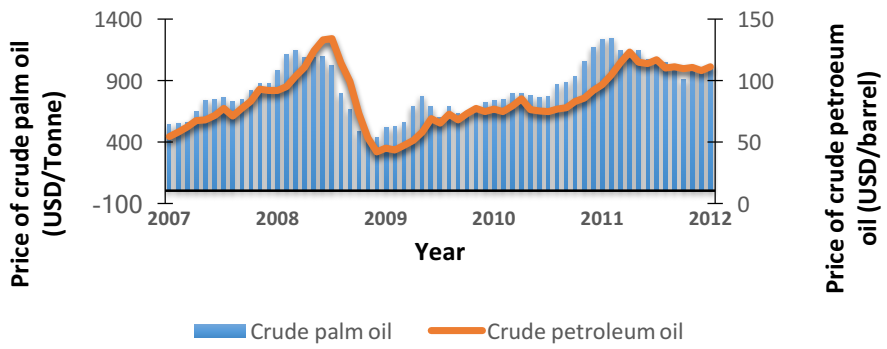

Figure 1.4. Price comparison of crude palm oil and crude petroleum oil from 2007 to 2012 [31].

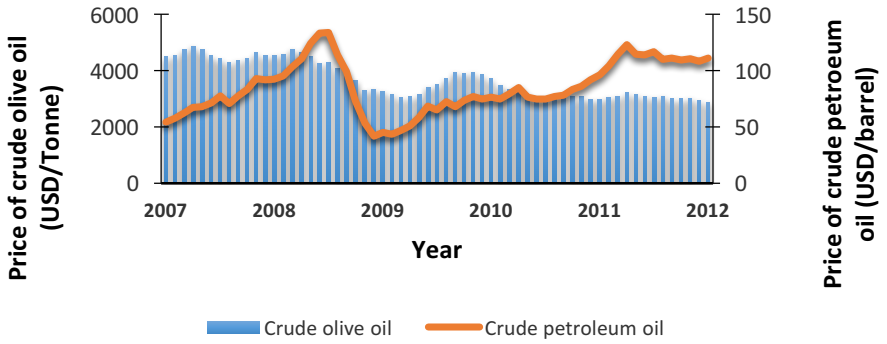

Figure 1.5. Price comparison of crude olive oil and crude petroleum oil from 2007 to 2012 [31].

This relation between petroleum oil and oils used as feedstocks for biodiesel production appears when comparing the market prices through years. **Figure 1.4** compares the price of petroleum oil and palm oil from 2007 to 2012. When petroleum oil price increases the palm oil price also increases to afford the demand. **Figure 1.5** shows the price of petroleum oil and olive oil in the same period. Conversely, an edible source such as olive oil whose price of production is unviable to produce biodiesel is not fixed by the price of petroleum oil. Additionally, using edible oils as feedstocks requires the use of much of the available arable land with a negative environmental impact. Hence, use of these feedstocks could cause deforestation in tropical countries such as Malaysia and Indonesia who account for about 80% of the world's supply of palm oil. Unfortunately, this deforestation is causing extensive damage to the environment and wildlife in those regions [28].

1.5.2. Non-edible oils

The “food versus feedstock” concern about using edible oils to substitute petroleum has increased the interest in non-edibles to produce chemicals and energy. Indeed, some feedstocks have the advantage of eliminate competition for food and feed due to be not suitable for human consumption [32]. Others, such as linseed oil [33] or some microalgae oil [34] are used for nutritional supplementation. Nevertheless, the present work will consider these oils as non-edibles because they are only used as supplements in the diet. Biomass provides a wide range of non-edible feedstocks from vegetable, animal or microbiological sources. On the one hand, vegetable crops as linseed [35], jatropha [36], jojoba [37], tobacco [38], seamango [39], tung [40], euphorbia [41] or castor [42] present attractive properties as feedstocks. On the other hand, waste animal fats [43], waste cooking oils [44] or microalgae [28] enhance the feedstock range.

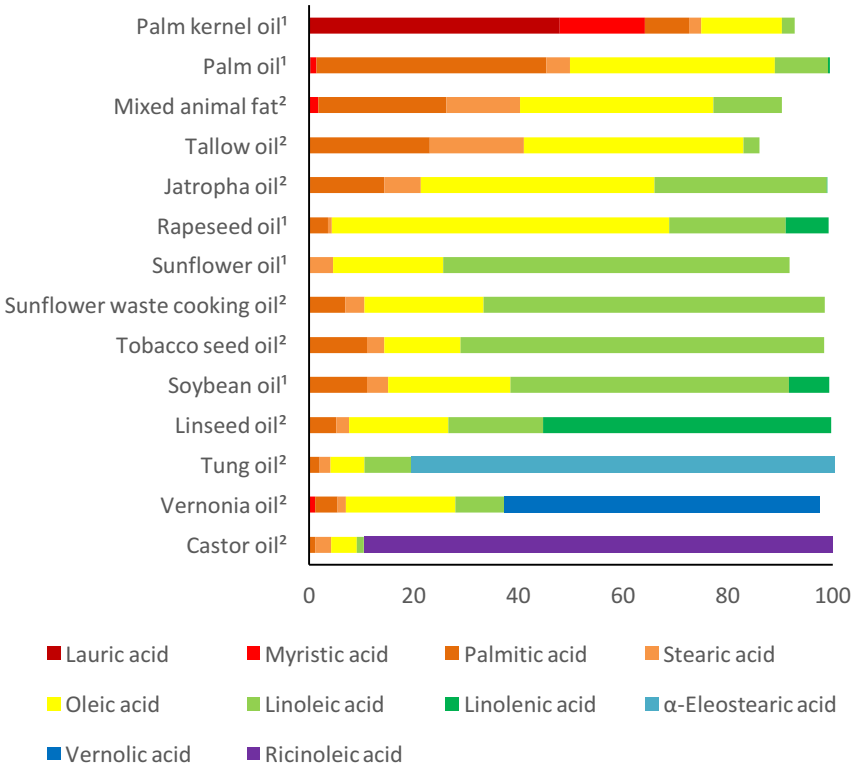

Figure 1.6. Account of the major naturally occurring fatty acids in: Palm kernel oil[1] [45], palm oil[1] [45], mixed animal fat[2] [46], tallow oil[2] [45], jatropha oil[2] [45], rapeseed oil[1] [47], sunflower oil[1] [45], sunflower waste cooking oil[2] [48], tobacco seed oil[2] [45], soybean oil[1] [45], linseed oil[2] [45], tung oil[2] [49], vernonia oil[2] [50], castor oil[2] [45].

[1]Edible oil. [2]Non-edible oil.

Figure 1.6 shows the fatty acids content in several sources of edible and non-edible feedstock. In the figure, sources are organized by the distinct fatty acids present in each. Thus, mostly saturated sources can be spotted on the top while most unsaturated and rare are present on the bottom. As an

example, although whose composition is similar, soybean oil is widely used in human consumption while tobacco seed is non-edible. In that way, depending on the chemistry needed and the final use of the prepared products, non-edible oils are suitable to replace edible oils. Hence, sunflower waste cooking oil would be a good choice as raw material instead of sunflower oil since it is cheaper and non-edible [51]. Additionally, the amount of waste cooking oil generated in each country is huge while unsuccessful management causes possible contamination of water and land resources [52]. On the case of rapeseed oil, is widely used in Europe to prepare biodiesel, nevertheless, India and Africa mainly use a non-edible source such as jatropha oil [28]. Palm oil is a source of mainly saturated and monounsaturated acids which could be replaced by non-edible animal fat. It is known that many animal meat processing facilities and animal mortalities lead to large amounts of cheap waste animal fats [53]. This non-edible source can be found worldwide and could be an alternative to palliate the increasing production of palm oil [54]. Finally, non-edible sources such as tung oil, vernonia oil and castor oil present high amounts of α-eleostearic acid, vernolic acid and ricinoleic acid, respectively. These sources contain moieties such as conjugated double bonds, epoxide or alcohol groups very attractive for polymer chemistry [55].

1.6. Applications of triacylglycerols

The wide range of sources of triacylglycerols available from feedstocks is translated into an enormous number of applications. In that way, triacylglycerols are a green alternative to petroleum based commodities such as lubricants [56], diesel [57], polymers [55], paraffins [58], etc. The range of

available sources and the procedure to prepare each product depends on the application needed. Whereas that biodiesel can be prepared from a vast number of sources, Phase Change Materials (PCMs) need pure saturated fatty acids in opposite to polymers who need some functionalized sources. The preparation of biodiesel, PCMs and polymers from triacylglycerols as feedstocks will further discussed.

1.6.1. Biodiesel

Biodiesel is a mixture of mono-alkyl esters produced from renewable biological sources to substitute conventional diesel as a fuel. Pure biodiesel can be used as a combustible in cars or blended with diesel. Hence, the designation of pure biodiesel is B100 while i.e. designation B20 means that contains a 20% of B100 and 80% of conventional diesel [59]. Biodiesel preparation needs a vast part of the triacylglycerols used as feedstock. Certainly, the preparation of biodiesel is continuously under extensive study and review and can be achieved by a wide range of feedstocks. Unfortunately, biodiesel is mainly prepared from edible oils such as rapeseed, soybean, sunflower and palm [48]. Nevertheless, in order to palliate the food versus fuel issue, it can be prepared from non-edible vegetable sources such as karanja, polanga, mahua, rubber seed, cottonseed, jojoba, tobacco, neem, linseed or jatropha [60]. Besides, it can be prepared from waste cooking vegetable oil [44], animal fats waste [61] or microalgae [28].

Biodiesel preparation consists mainly in a transesterification whereby trigacylglycerols are converted into mono-alkyl esters. **Figure 1.7** shows a common transesterification with the presence of free fatty acids (FFA)

catalyzed by acids (A) and bases (B). The homogeneous alkali-catalyzed transesterification has been the commonest method used at laboratory, pilot and industrial scale levels [62]. This process is catalyzed by alkaline metal hydroxides (such as NaOH) and alkoxides [63] as well as sodium or potassium carbonates [57]. These catalysts are cheap and show a very high performance when feedstocks contain low FFA concentration. However, when the raw materials have a high percentage of FFA or water, the alkali catalyst will react with the FFA to form soaps resulting in the consumption of the catalyst [32]. In the case of feedstocks containing high amounts of FFA the acid catalysis is more suitable [64]. The acid catalysts used include sulphuric, hydrochloric, sulfonic and phosphoric acids. However, this method is sensitive to the presence of water. In fact, water and acid release FFA from triacylglycerols. Additionally, this method is slower and needs higher amounts of alcohol [45, 65].

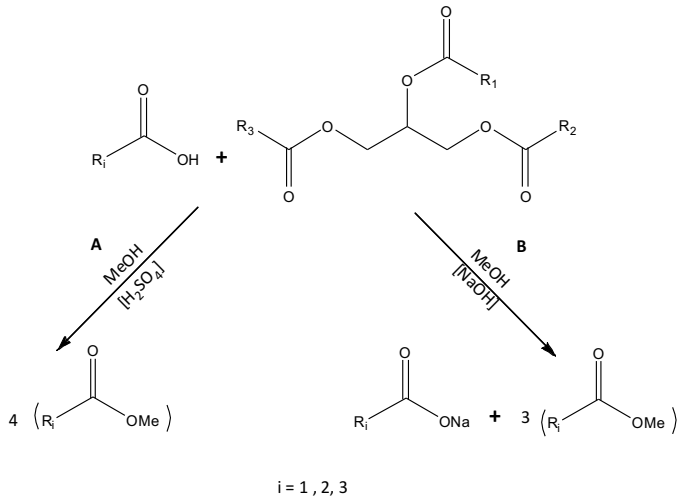

Figure 1.7. Esterification of triacylglycerols containing FFA via acid (A) and base (B) catalysis.

Usually, in industrial application, the base catalysts are preferred over acid catalysts due to their capability of completion of reaction at higher speed, lower reaction temperature and higher conversion efficiency [66]. However, reactions catalyzed by chemical catalysts have several collective drawbacks, such as being energy-intensive, tedious to recover glycerol, difficulty in the removal of acid or base catalyst from the product, further treatment of alkaline wastewater, and interference of FFA and water in the reaction. Alternatives such as supercritical alcohol method can overcome these problems; nevertheless, high pressure and temperature are used to carry out the transesterification reaction [67].

On the other hand, enzyme-catalyzed processes have shown interesting results [68]. Biocatalysts such as lipases have high activity and selectivity, and their reactions take place under mild conditions, producing less wastewater and consuming less energy. Although large-scale application of enzymatic processes is less frequent due to the high cost of enzymes. Nevertheless, the lipase production price is decreasing whereas enzymes are most used in industry, and immobilized lipases as well as resting cells can be reused several times [69].

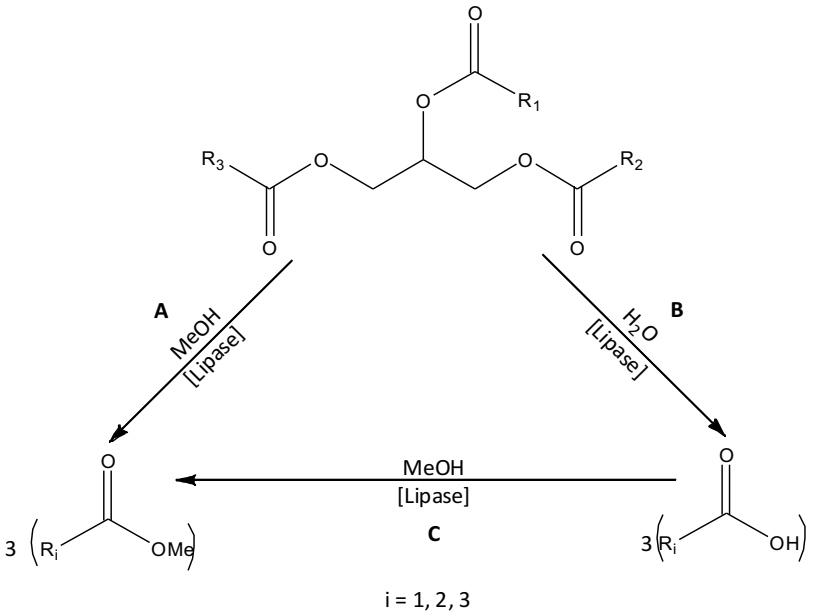

Figure 1.8. Schematic representation of the: Transesterification of triacylglycerols catalyzed by a lipase (A). Hydrolysis of triacylglycerols catalyzed by a lipase (B). Esterification of fatty acids catalyzed by a lipase (C).

When compared with the use of conventional chemical catalysis and supercritical methanol, enzymatic transesterification for biodiesel production is one of the most promising strategies. **Figure 1.8** shows the capability of lipases to transform triacylglycerides into methyl esters (A) or FFA (B) and the latters to methyl esters (C). In addition, lipases have the ability to transfer both triacylglycerols and FFA into biodiesel, which means they are able to catalyze oils from varied resources, including waste oils with a high content of FFA [68].

1.6.2 PCMs from fatty acids

The stability of unsaturated and functionalized triacylglycerols against temperature or storing is committed. In that way, poly-unsaturated oils present lower stability than monounsaturated. Nevertheless, monounsaturated oils are also affected [70]. Regarding to stability, the poor reactive alkyl chain of saturated fatty acids provides excellent thermal stability properties [71]. This fact acquires special importance in thermal energy storage (TES) applications. Thermal energy can be stored in the form of sensible heat storage, latent heat storage and chemical reaction heat storage [72]. Among these forms, latent heat thermal energy storage (LHTES) is afforded by using PCMs which can store or release heat energy during the phase change process when the surrounding temperature increases or decreases [73]. At present, a large number of inorganic, organic and their mixtures PCMs have been studied. Among all investigated PCMs, fatty acids have many superior properties, including proper melting temperature range, high heat capacity, congruent melting, little or no supercooling during phase transition, lower vapor pressure, non-toxic, non-corrosive to metal containers, good chemical and thermal stability, low cost, non-flammability and small volume change [74]. In general, fatty acids and fatty acid derivatives used for PCMs purposes can include pure fatty acids, eutectic mixtures of fatty acids and fatty acid esters.

1.6.2.1 Pure fatty acids

The phase change temperature and latent heat are two basic parameters of PCMs. The former determines the temperature to store or release energy while the later the energy that can store or release per mass. In that way,

many researchers have tested many of these parameters with fatty acids. Since distinct carbon chains (from 10 to 18 carbon atoms) of FFA have been studied various phase change temperatures are available due to the specific melting and solidification points of each fatty acid. Most of the pure fatty acids studied are saturated, indeed, almost no research has been done about the unsaturated acids as PCMs [74].

Table 1.1 shows the thermal properties of various fatty acids. Literature data are slightly different from each other due to the individual experimental conditions, purity, etc [75]. Regarding to saturated fatty acids, as the carbon number increase the melting temperatures as well as latent heat also increase. Nevertheless, oleic acid (18 carbon atoms) presents the lower melting temperature and the lower latent heat. The purity of the fatty acid is also crucial to evaluate the latent heats whereby the fatty acids with higher purities achieve higher latent heats. This fact is highlighted in **Table 1.1** when comparing industrial grade stearic acid (≥90%) and reagent grade stearic acid (>98%) the latent heat and the melting temperature differs.

Table 1.1. Thermal properties of fatty acids studied as PCMs.

Fatty acid	Melting temperature (˚C)	Melting latent heat ($kJ \bullet kg^{-1}$)	Freezing temperature (˚C)	Freezing latent heat ($kJ \bullet kg^{-1}$)	Purity (%)	Reference
Caprylic acid	16.1	144.2	-	-	>99.9	[76]
Capric acid	32.14	156.40	32.53	154.24	98	[77]
Lauric acid	44.02	182.3	42.09	182.4	-	[78]
	42.64	176.6	-	-	97	[79]
Myristic acid	53.73	187.3	52.09	184.9	-	[78]
	52.99	181.0	-	-	95	[79]
	51.80	178.14	51.74	181.63	>98	[80]
Palmitic acid	62.11	212.1	60.38	214.6	-	[78]
	61.31	197.9	-	-	96	[79]
	60.42	233.24	59.88	237.11	98	[80]
Stearic acid	68.96	222.8	67.06	226.7	-	[78]
	54.70	159.3	-	-	≥90	[79]
	66.82	258.98	66.36	263.32	>98	[80]
Oleic acid	13.6	138.07	-	-	>99.9	[81]

Although these fatty acids proceed from feedstocks the preparation needs to be discussed. The common procedure to prepare stearic acid of industrial grade proceeds by hydrogenation of a highly unsaturated edible vegetable source such as soybean oil. The unsaturated triacylglycerols are converted in stearine. To release stearic acid, the stearine is treated with sodium

hydroxide and sulfuric acid [82]. The purification of stearic acid to acquire a reagent grade mixture will need some crystallization procedures. Fatty acids such as lauric, myristic or palmitic could proceed from palm industry. Additionally, a common industrial grade preparation of palmitic acid starts from the hydrogenation of vegetable oils such as cottonseed oil followed by the reaction with excess of caustic alkali at high temperatures from 300 to 400˚C and the acidification of the mixture [83]. This 90% palmitic acid will additionally need some crystallization steps to acquire a reagent grade mixture.

1.6.2.2 Eutectic mixtures of fatty acids

Another approach to prepare PCMs from fatty acids is the combination of two or more fatty acids. This mixture has a eutectic temperature which is the lowest melting temperature of a mixture of various components, and such mixture features the same stability of a single component. Certainly, the eutectic temperature is lower than the melting temperature of each pure compound.

Each fatty acid can be combined with various fatty acids. These combinations increase the number of phase change temperatures and thus the application range. As example, capric acid can be mixed with lauric, palmitic or stearic acids with melting temperatures of 19.62, 23.12 and 25.39˚C, respectively. This decrease on the phase change temperature respect pure capric acid matches with low temperature TES applications such as building heating/cooling and indoor temperature controlling [84]. On another hand, stearic and palmitic acids have phase change temperatures too high for applications such as air conditioning condensation heat recovery system.

Nevertheless, the eutectic mixture of palmitic and stearic acids lowers the melting temperature to 53.95˚C [73] allowing the possibility to be used for this application.

Generally, a eutectic mixture of fatty acids is prepared by slowly cooling down uniformly mixed two kinds of fatty acids melted with different proportions. The phase change temperature and latent heat of the eutectic mixture are obtained via the differential scanning calorimeter (DSC) test [74]. Indeed, pure reagent grade fatty acids are mixed together to prepare these eutectic mixtures. Unfortunately, these mixtures will belong from commercial fatty acids with the drawback of being prepared by hydrogenation of edible feedstocks, high temperatures, etc.

1.6.2.3 Fatty acid esters

Fatty acids can present a certain corrosivity, bad odor and sublimation during heating process. By that way, some researchers have replaced them with fatty acid esters [74]. The combination of fatty acids and alcohols expands the scope of phase-change temperatures. Certainly, each fatty acids can be mixed with distinct alcohols. On the one hand, the esterification with short-chain alcohols will lower the phase change temperature respect the pure fatty acid [85]. On the other hand, higher phase change temperatures are achieved by esterification with longer-chain alcohols [86, 87]. Nevertheless, the preparation of PCMs esters is not subjected by only reacting linear fatty acids and mono-hydric alcohols. For instance, binary mixtures of esters [88], esterification of diacids [89] as well as esterification with diols [90], glycerol [91, 92], erythritol [93], xylitol [94] and galactitol [95] rendered PCMs.

From all the esters prepared stearic acid has been the most used. Feldman et al. [96] prepared short-chain monohydric alcohol stearates via the esterification of four kinds of industrial grade stearic acids with distinct purities with methyl, propyl and butyl alcohols, respectively. The melting latent heats of methyl stearates were in the range of 180–202 $kJ \bullet kg^{-1}$ while propyl stearates were in the range of 152–182 $kJ \bullet kg^{-1}$ and that of butyl stearates were in the range of 138-145 $kJ \bullet kg^{-1}$. The results also showed that the most pure stearates presented higher melting and freezing temperatures and latent heats. Suppes et al. [85] also evaluated combinations of mixtures of methyl and ethyl esters of palmitic, stearic and oleic acids. Pure methyl stearate showed a melting temperature of 38˚C and a melting latent heat of 208 $kJ \bullet kg^{-1}$ while pure ethyl stearate shown a melting temperature of 33˚C and a melting latent heat of 188 $kJ \bullet kg^{-1}$. In the study, methyl esters shown higher melting temperatures and latent heats compared with ethyl esters while oleic acid derivatives presented broad latent heat transitions and lower latent heats. In both studies the odd numbered esters had shown higher melting temperatures as well as latent heats. Besides, to prepare mixtures with good performance as PCMs the need of a purity higher than 90% was inherent.

Since Suppes et al. [85] postulated that at least a 90% purity of stearic acid was needed. They also realized that this ratio is not found naturally in any of the large-volume fat and oil feedstocks. Indeed, to meet the demands of PCMs applications, fats and oils had to be modified or purified by hydrogenation and distillation. Following these approaches, novel bio-based phase change materials have appeared. Such studies were based on commercially available organic compounds from triacylglycerol

feedstocks [71, 97–100]. These products are partially hydrogenated soy-wax [97, 98] or saturated fatty esters resulting from the hydrogenation of unsaturated fatty acids obtained from several sources [71, 99, 100]. Unfortunately, the unsaturated fatty acids are hydrogenated to the corresponding saturated fatty acids, losing all the opportunities to be converted in other potential applications.

1.6.3 Polymers from triacylglycerols

The use of triacylglycerols to prepare polymers is having a special attention since they are renewable and can substitute petroleum-based polymers. Certainly, the use of plant oils as a source for polymer industry is a theme continuously studied and reviewed [55, 101–103]. Edible sources such as soybean, palm, rapeseed and sunflower are the most studied to prepare bio-based polymers since they are cheap and easily available [55, 101–104]. However, non-edible vegetable oils including linseed oil [104], tung oil [105], vernonia oil [106] and castor oil [107], are widely used in lubricants, paints, coatings, cosmetics, and pharmaceuticals.

Whereas the saturated fatty acids are not reactive, the distinct active sites present in triacylglycerides can be used to create polymers. Moieties such as double bonds, allylic carbons, ester groups as well as epoxides or alcohols provide the reactivity necessary to prepare a vast number of macromolecules. One approach to evaluate the availability to functionalize a triacylglycerol is the unsaturation degree [104]. Oils such as soybean or linseed, present high amounts of linoleic acid and linolenic acid, respectively. Indeed, the most unsaturated the oil the most susceptible to functionalization. This means that linseed oil will be easier to modify than soybean oil. Certainly, highly unsaturated oils such as linseed or tung oil are

considered drying oils, since they can polymerize even on the merely presence of oxygen [104, 108, 109]. Thus, unsaturated sources such as many vegetable oils are more usable in polymer chemistry than more saturated sources such as palm oil or animal fats. Nevertheless, the preparation of polymers from triacylglycerols can undergo various pathways (see **Figure 1.9**). The first approach is the direct polymerization through the double bonds or other reactive functional group present in the fatty acid chain. A second way consists on the chemical modification of the double bonds, introducing functional groups easier to polymerize, and the third is the chemical transformation of plant oils to produce platform chemicals, which can be used to produce monomers for the polymer synthesis [110].

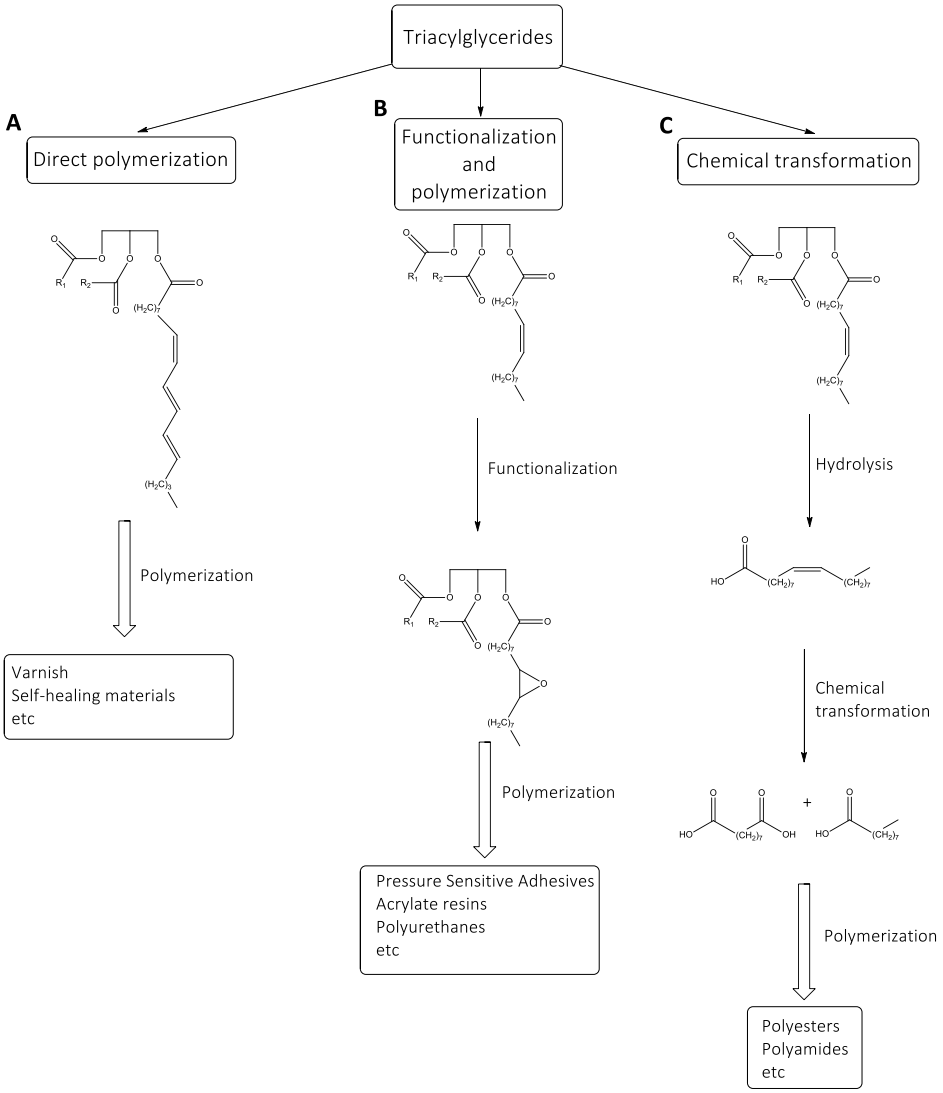

Figure 1.9. Exemplified approaches to prepare polymers from triacylglycerols: Direct polymerization (A). Functionalization and polymerization (B). Chemical transformation (C).

1.6.3.1 Direct polymerization

The number of active functional groups present in fatty acids is scarce when compared to the transformations that these groups can undergo to increase their reactivity towards polymerization. By that reason, the direct polymerization of vegetable oils is generally considered difficult. However, it matches some green chemical principles, since the direct conversion of the oil into a polymer prevents the generation of waste and maximizes the atom economy.

An example of direct polymerization is traditional drying oils as linseed oil or tung oil used for painting formulations or resin applications [55] as well as novel applications such as the self-healing repairing properties of tung oil [109]. The studies in linoleic acid revealed that a radical alkyl reacts with oxygen to form a hydroperoxide. This moiety can lead to alkyoxyl or peroxyl radicals, which besides of the alkyl radical can react with an analogous radicals to produce cross-links and consequently polymers [111].

Another approach is the metathesis of vegetable oils such as olive, soybean or linseed. The olefin metathesis of vegetable oil derivatives, such as fatty acid esters, has been investigated since 1972 [112]. This type of chemistry is able to convert unsaturated feedstocks to useful chemicals and contribute to a sustainable chemical industry. Some catalyst as reusable heterogeneous rhenium oxide or homogeneous ruthenium can be used in these reactions. Metathesis of fatty oils containing triacylglycerides of unsaturated long-chain fatty acids proceeds by the reaction between an olefin and a transition metal complex in a 2+2 fashion to generate an unstable metallacyclobutane intermediate. This intermediate can either revert to the starting material or open productively to afford a new metal carbene and produce a new olefin.

The reaction (see **Figure 1.10**) can proceed by intramolecularly as well as intermolecularly, the latter reaction strongly predominates [113].

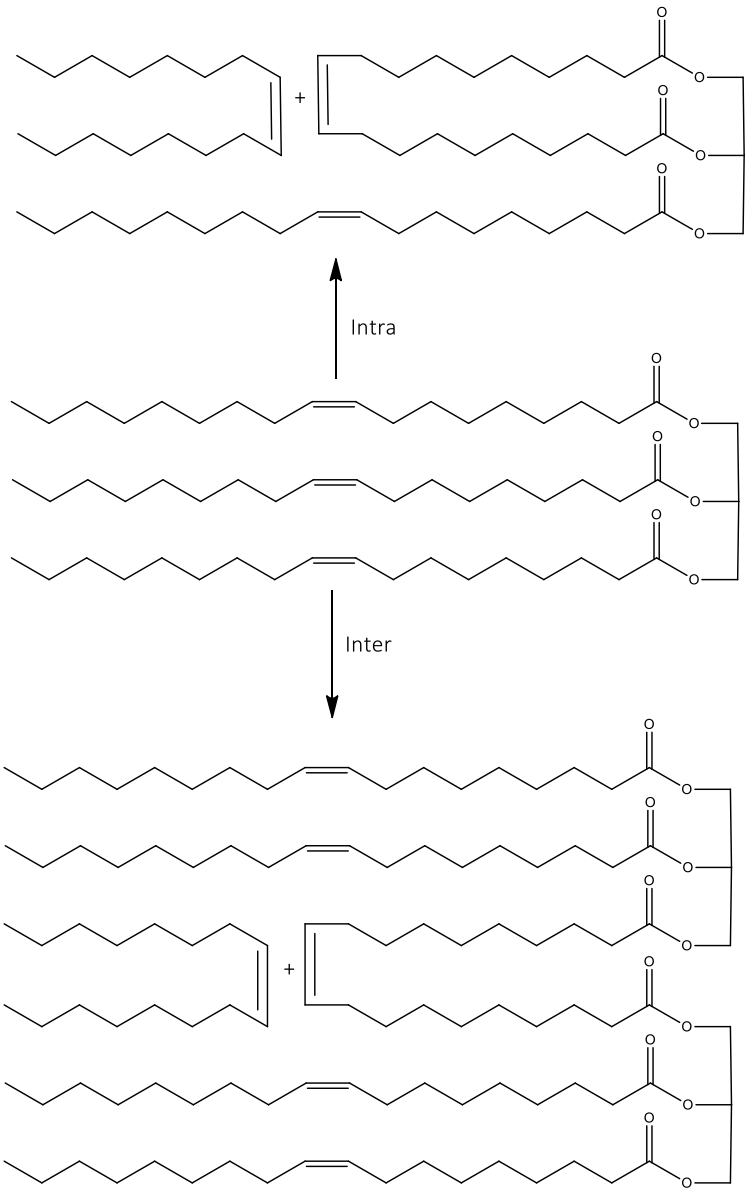

Figure 1.10. Intramolecular and intermolecular triolein metathesis [113].

The last approach to prepare polymers by direct polymerization takes advantage of the conjugated double bonds of tung oil. This non-edible source of triacylglycerols contains about 80% of α-eleostearic acid. The conjugated double bonds can also undergo Diels−Alder (DA) reaction easily with a dienophile [114]. DA reaction, one of the most useful reactions in modern organic chemistry, is a 4+2 cycloaddition between a conjugated diene and a dienophile to form a cyclohexene (see **Figure 1.11**). In macromolecular chemistry, it has been successfully applied to the construction of different kinds of poly adducts. The DA reaction is considered as effective, versatile, and selective, which also fulfills most of the requirement for the "click" polymer chemistry [115]. In that way, tung oil has been recently cross-linked to form polymers by reaction with dimaleimides [116, 117]. Although the combination of a non-edible source such as tung oil with DA reactions can lead directly to polymers, the exploitation of that chemistry is recent and scarce.

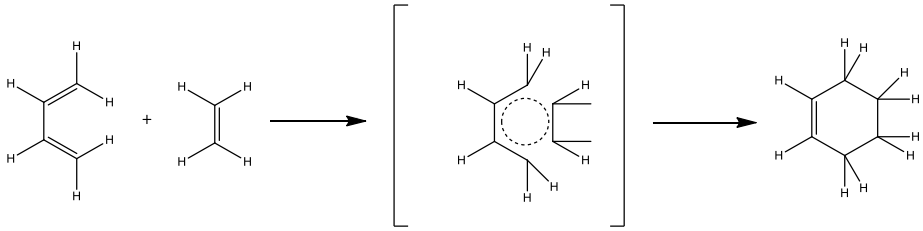

Figure 1.11. Diels-Alder reaction of a diene with a dienophile to form a cyclohexene [118].

1.6.3.2 Chemical modification

The reactivity of the double bonds from triacylglycerols raises exponentially the scope of bio-based polymer chemistry at expense of adding reaction steps to prepare polymers. Probably, the most frequently studied

polymerization of plant oils in recent years involves epoxidized plant oils and fatty acids. Certainly, epoxidized sources such as linseed or soybean oil are commercially available for bulk as well as research purposes [55]. Industrially, vegetable oil epoxides are currently used mainly as PVC stabilizers. Additionally, they can be converted to aziridines [101], episulfides [101], rubbers [55], coatings [55], polyurethanes [55] or acrylate resins [55]. Another potential use of epoxidized plant oils is the preparation of pressure-sensitive adhesives (PSAs). PSAs are tacky adhesives that can quickly bond with adherents under light pressure and their cohesion strength permits to be clearly removed from the adherents [119]. In that way, epoxide moiety has been the key steep to prepare bio-based PSAs from triacylglycerols such as epoxidized soybean oil [119–121] as well as FFA such as epoxidized oleic acid (see **Figure 1.12**).

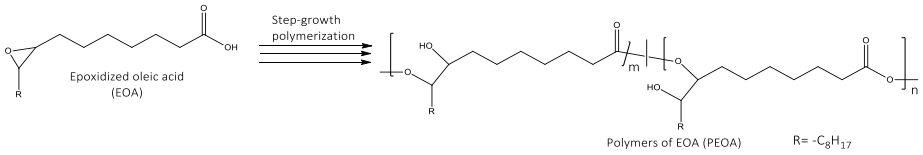

Figure 1.12. Polymerization of *cis*-9, 10-epoxystearic acid to prepare PSAs [122].

The epoxidation of unsaturated fatty acids or triacylglycerides on an industrial scale takes place by a Prilezhaev reaction [123]. **Figure 1.13** shows the Prilezhaev epoxidation of an olefin by a peroxoacid. This reaction uses hydrogen peroxide as an oxidant and formic acid as an oxygen carrier to epoxidize the double bonds [124, 125]. Nevertheless, the use of these acids is prone to loss of yield and side reactions like the acid-catalyzed ring-opening of the oxirane group by FFA, formic acid or water [126].

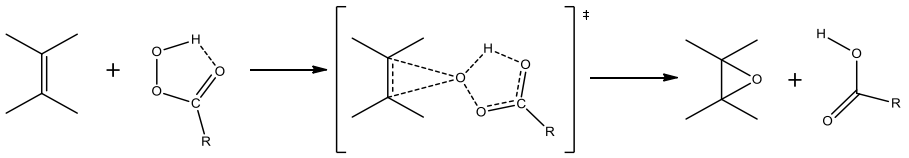

Figure 1.13. Prileshajev epoxidation of an olefin [125].

Chemo-enzymatic epoxidation (see **Figure 1.14**) is of considerable interest because the conditions of this method minimizes undesirable epoxide ring opening [101]. Initially, the unsaturated fatty acid or ester is converted into a percarboxylic acid by a lipase-catalyzed reaction with H_2O_2 and then, the second reaction step occurs without involvement of the enzyme, following the rules of the Prileshajev epoxidation [126]. Additionally, it can be used in triacylglycerides by adding a 5% mol of FFA (see **Figure 1.15**).

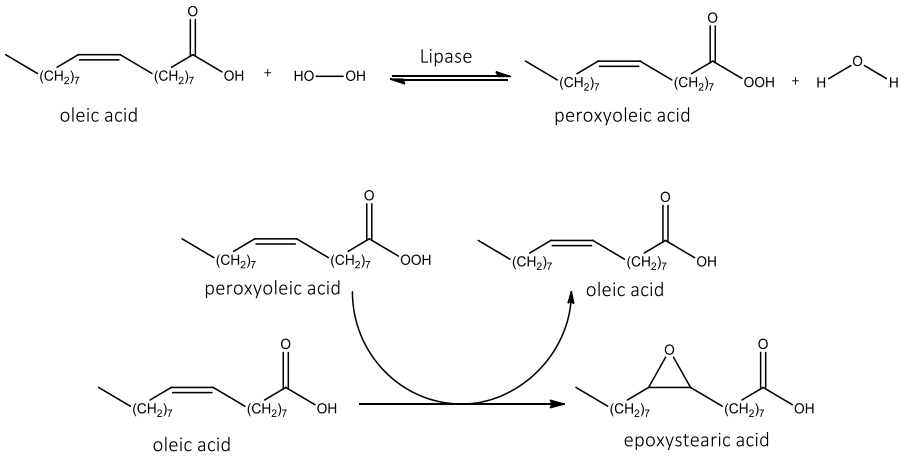

Figure 1.14. Schematic representation of the chemoenzymatic epoxidation of oleic acid [127].

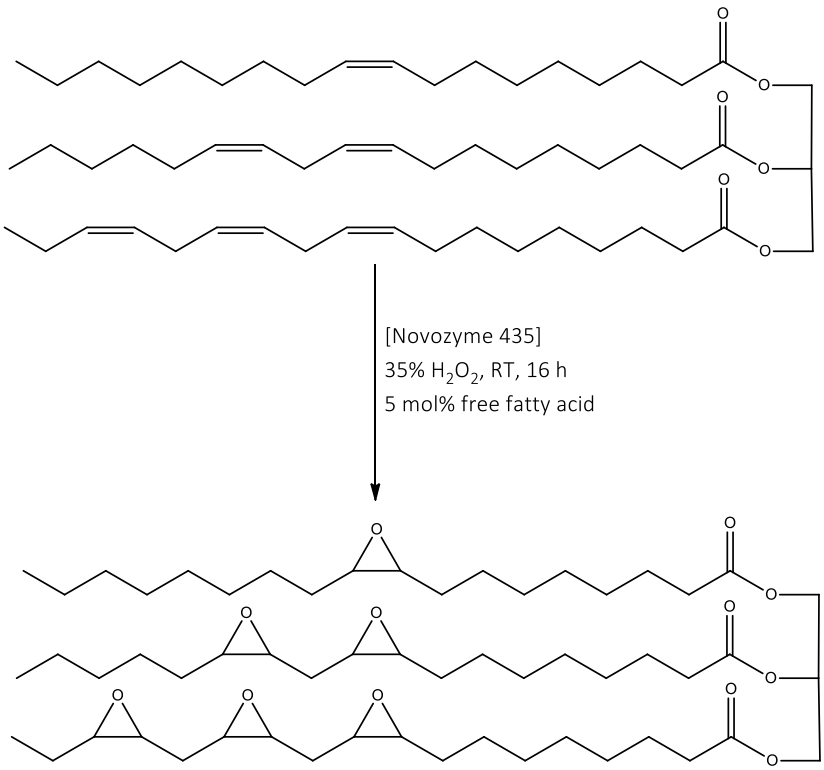

Figure 1.15. Chemoenzymatic epoxidation of triacylglycerols [128].

1.6.3.3 Chemical transformation

The chemical transformation of triacylglycerols to building blocks for polymer chemistry presents some attractive aspects. Building blocks such as sebacic acid, azelaic acid or undecylenic acid have some industrial applications and are mainly studied and reviewed. Nevertheless, the industrial chemistry involved in the preparation of these building blocks is not always prone to match the green chemistry principles [55, 107, 110, 129]. The two major fatty acids used for preparation of building blocks are ricinoleic acid and oleic acid.

Castor oil, presents a toxic protein called ricine with laxative and vomitive properties making it non-edible [107]. Is the main source of ricinoleic acid which is used in applications such as polyurethane polymers, plasticizers, lubricants, cosmetics, soaps, inks, paints, and others [130]. Thus, ricinoleic acid is mainly transformed into undecylenic acid or sebacic acid following distinct routes. The pyrolysis of castor oil needs high temperatures of about 550˚C and reduced pressure to achieve heptaldehyde and undecylenic acid [131]. On the one hand, heptaldehyde can be hydrogenated to be a building block for plasticizers [130]. On the other hand, undecylenic acid has been studied and reviewed showing antifungal activity, antiviral activity, as insecticide and being the building block for chemicals and polymers [107, 110]. The preparation of sebacic acid is afforded by subjecting castor oil at high temperatures (about 280˚C) with alkali. This treatment results in saponification of the castor oil to ricinoleic acid that is then cleaved to give capryl alcohol and sebacic acid [129]. Capryl and sebacyl esters are used as plasticizers [130], while sebacic acid reacts with hexamethylene diisocyanate to produce nylon 6, 10 [107, 130].

Oleic acid is the main fatty acid from sources such as olive oil [45], high oleic peanut oil [132], and high oleic sunflower oil [133]. Additionally, in spite of oleic acid accounts for less than the half of the fatty acids present in palm oil [45], several oleic acid derivatives can be prepared from palm oil [134]. In oleochemistry, the industrially most important application of ozonolysis is the oxidation of the double bond of oleic acid to yield azelaic and pelargonic acids [55, 123]. Azelaic acid has important applications in textiles (polyesters and polyamides) and pharmaceuticals (antiacne) [135]. However, an improvement of this process towards a more ecologically benign one is highly desired due to the toxicity of ozone, serious safety risks and the high energy

demand of the ozonolysis [136]. A valid alternative but not industrial is hydrogen peroxide (see **Figure 1.16**), because it is capable to oxidize with excellent atom economy and is safer than gaseous reactants [137]. First, oleic acid is converted to *threo*-9, 10-dihydroxystearic acid (DHSA) or *erythro*-9, 10-dihydroxystearic acid. Then, in a second step the diol is cleaved to azelaic acid by using H_2O_2 or O_2 [135, 136].

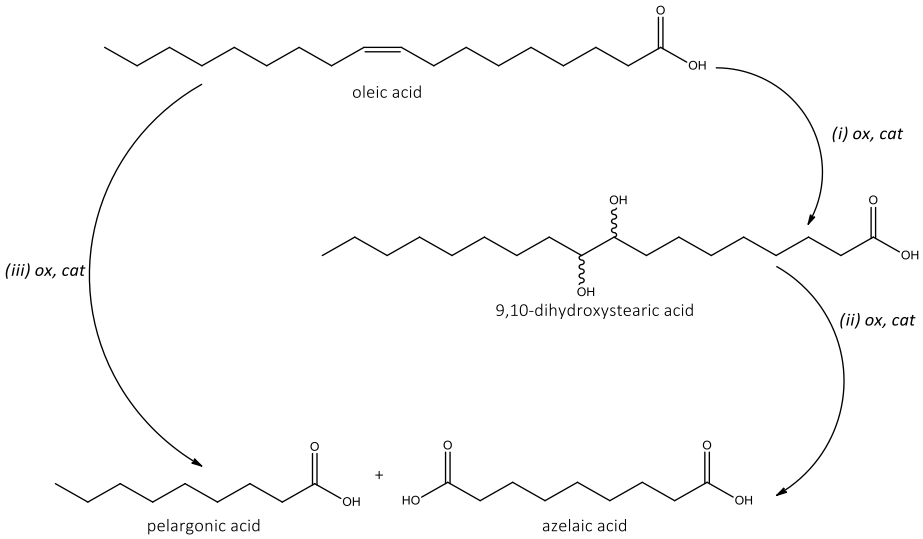

Figure 1.16. Distinct approaches to prepare azelaic and pelargonic acids from oleic acid [135].

1.7. References

[1] Smith A. The Wealth of Nations. New York, NY: Modern Library; 2000.

[2] London B. Ending the depression through planned obsolescence. New York, NY: New York; 1932.

[3] Adamson G. Industrial strength design : How Brooks Stevens shaped your world. Milwaukee, Wis: Milwaukee Art Museum; 2003.

[4] Packard V. The waste makers London, UK: Lowe & Brydone; 1960.

[5] Andrews D. The circular economy, design thinking and education for sustainability. Local Econ 2015;30:305–15.

[6] United Nations. World population prospects: The 2012 revision. Highlights and advance tables. Popul Dev Rev 2013;36:775–801.

[7] Stahel WR, Giarini O. The limits to certainty. Dordrecht: Kluwer academic publishers; 1989.

[8] Stahel WR. Jobs for tomorrow. New York, NY: Vantage; 1981.

[9] European Comision. Building a bio-based economy for europe in 2020. 2011.

[10] European Comision. Innovating for Sustainable Growth: A Bioeconomy for Europe. 2012

[11] OECD. The Bioeconomy to 2030. Main findings and conclusions. 2009.

[12] Langevald H, Sanders J, Meeusen M. The biobased economy: Biofuels, materials and chemicals in the post-oil era. New York, NY: Earthscan; 2010.

[13] McCormick K, Kautto N. The Bioeconomy in Europe: An Overview. Sustain 2013;5:2589–608.

[14] Kamm B, Kamm M. Principles of biorefineries. Appl Microbiol Biotechnol 2004;64:137–45.

[15] Cherubini F. The biorefinery concept: Using biomass instead of oil for producing energy and chemicals. Energy Convers Manag 2010;51:1412–21.

[16] Axelsson L, Franzén M, Ostwald M, Berndes G, Lakshmi G, Ravindranath NH. Perspective: Jatropha cultivation in southern India: Assessing farmers' experiences. Biofuels, Bioprod Biorefining 2012;6:246–56.

[17] Anastas P, Eghbali N. Green Chemistry: Principles and Practice. Chem Soc Rev 2009;39:301.

[18] Demirbas A. Biomass feedstocks. Biofuels 2009:45–85.

[19] Cherubini F, Bargigli S, Ulgiati S. Life cycle assessment of urban waste management: Energy performances and environmental impacts. The case of Rome, Italy. Waste Manag 2008;28:2552–64.

[20] Rajagopal D, Zilberman D. Environmental, economic and policy aspects of biofuels. Foundations and trends in microeconomics. 2007,4:353-468.

[21] Hoogwijk M, Faaij A, van den Broek R, Berndes G, Gielen D, Turkenburg W. Exploration of the ranges of the global potential of biomass for energy. Biomass Bioenerg 2003;25:119–33.

[22] Biermann U, Bornscheuer U, Meier MAR, Metzger JO, Schäfer HJ. Oils and fats as renewable raw materials in chemistry. Angew Chem Int Ed 2011;50:3854–71.

[23] Vossen P. Olive oil: History, production, and characteristics of the world's classic oils. Hort Science 2007;42:1093–100.

[24] Lang X, Dalai AK, Bakhshi NN, Reaney MJ, Hertz PB. Preparation and characterization of bio-diesels from various bio-oils. Bioresour Technol 2001;80:53–62.

[25] Alcantara R, Amores J, Canoira L, Fidalgo E, Franco MJ, Navarro A. Catalytic production of biodiesel from soy-bean oil, used frying oil and tallow. Biomass Bioenerg 2000;18:515–27.

[26] Kalam M., Masjuki H. Biodiesel from palm oil—an analysis of its properties and potential. Biomass Bioenerg 2002;23:471–9.

[27] Antolín G, Tinaut F V., Briceo Y, Castao V, Pérez C, Ramírez AI. Optimisation of biodiesel production by sunflower oil transesterification. Bioresour Technol 2002;83:111–4.

[28] Ahmad AL, Yasin NHM, Derek CJC, Lim JK. Microalgae as a sustainable energy source for biodiesel production: A review. Renew Sustain Energy Rev 2011;15:584–93.

[29] Brennan L, Owende P. Biofuels from microalgae-A review of technologies for production, processing, and extractions of biofuels and co-products. Renew Sustain Energy Rev 2010;14:557–77.

[30] Gui MM, Lee KT, Bhatia S. Feasibility of edible oil vs. non-edible oil vs. waste edible oil as biodiesel feedstock. Energy 2008;33:1646–53.

[31] Index mundi commodities, http://www.indexmundi.com/commodities/ n.d; 2017 [acessed 13/3/2017].

[32] Leung DYC, Wu X, Leung MKH. A review on biodiesel production using catalyzed transesterification. Appl Energy 2010;87:1083–95.

[33] Cunnane S, Ganguli S, Menard C, Liede A, Hamadeh JM, Chen ZY, Woleverd TMS, Jenkins DJA. High a-linolenic acid flaxseed (Linurn usiiaiissimurn) : some nutritional properties in humans. Br J Nutr 1993, 69:443-53.

[34] Mata TM, Martins AA, Caetano NS. Microalgae for biodiesel production and other applications: A review. Renew Sustain Energy Rev 2010;14:217–32.

[35] Cakmakli B, Hazer B, Tekin IO, Kizgut S, Koksal M, Menceloglu Y. Synthesis and characterization of polymeric linseed oil grafted methyl methacrylate or styrene. Macromol Biosci 2004;4:649–55.

[36] Freire LMS, Bicudo TC, Rosenhaim R, Sinfrônio FSM, Botelho JR, Carvalho Filho JR, et al. Thermal investigation of oil and biodiesel from jatropha curcas L. J Therm Anal Calorim 2009;96:1029–33.

[37] Canoira L, Alcántara R, Jesús García-Martínez M, Carrasco J. Biodiesel from Jojoba oil-wax: Transesterification with methanol and properties as a fuel. Biomass Bioenerg 2006;30:76–81.

[38] Usta N. Use of tobacco seed oil methyl ester in a turbocharged indirect injection diesel engine. Biomass Bioenerg 2005;28:77–86.

[39] Ang GT, Ooi SN, Tan KT, Lee KT, Mohamed AR. Optimization and kinetic studies of sea mango (Cerbera odollam) oil for biodiesel production via supercritical reaction. Energy Convers Manag 2015;99:242–51.

[40] Park JY, Kim DK, Wang ZM, Lu P, Park SC, Lee JS. Production and characterization of biodiesel from tung oil. Appl Biochem Biotechnol 2008;148:109–17.

[41] Liu Z, Shah SN, Evangelista RL, Isbell TA. Polymerization of euphorbia oil with Lewis acid in carbon dioxide media. Ind Crops Prod 2013;41:10–6.

[42] Reis JML dos, Motta EP. Mechanical properties of castor oil polymer mortars. Mater Res 2014;17:1162–6.

[43] Banković-Ilić IB, Stojković IJ, Stamenković OS, Veljkovic VB, Hung YT. Waste animal fats as feedstocks for biodiesel production. Renew Sustain Energy Rev 2014;32:238–54.

[44] Phan AN, Phan TM. Biodiesel production from waste cooking oils. Fuel 2008;87:3490–6.

[45] Aransiola EF, Ojumu T V., Oyekola OO, Madzimbamuto TF, Ikhu-Omoregbe DIO. A review of current technology for biodiesel production: State of the art. Biomass Bioenerg 2014;61:276–97.

[46] Gallart-Sirvent P, Yara E, Villorbina G, Balcells M, Sala N, Canela-Garayoa R. Recycling Rhizopus oryzae resting cells as biocatalyst to prepare near eutectic palmitic-stearic acid mixtures from non-edible fat. J Mol Catal B Enzym 2016;134:172–7.

[47] Goering, C.E., Schwab, A.W., Dangherty, M.J., Pryde, E.H., Heakin AJ. Fuel properties of eleven vegetable oils. Trans Am Soc Agric Eng 1982;25:1472–7.

[48] Balat M. Potential alternatives to edible oils for biodiesel production - A review of current work. Energy Convers Manag 2011;52:1479–92.

[49] Schönemann A, Frenzel W, Unger A, Kenndler E. An investigation of the fatty acid composition of new and aged tung oil. Stud Conserv 2006;51:99–110.

[50] Baye T, Becker HC. Exploration of Vernonia galamensis in Ethiopia, and variation in fatty acid composition of seed oil. Genet Resour Crop Evol 2005;52:805–11.

[51] Hameed BH, Goh CS, Chin LH. Process optimization for methyl ester production from waste cooking oil using activated carbon supported potassium fluoride. Fuel Process Technol 2009;90:1532–7.

[52] Chhetri AB, Watts KC, Islam MR. Waste cooking oil as an alternate feedstock for biodiesel production. Energies 2008;1:3–18.

[53] Janaun J, Ellis N. Perspectives on biodiesel as a sustainable fuel. Renew Sustain Energy Rev 2010;14:1312–20.

[54] Corley RH V. How much palm oil do we need? Environ Sci Policy 2009;12:134–9.

[55] Meier MAR, Metzger JO, Schubert US. Plant oil renewable resources as green alternatives in polymer science. Chem Soc Rev 2007;36:1788–802.

[56] Filley J. New lubricants from vegetable oil: Cyclic acetals of methyl 9, 10-dihydroxystearate. Bioresour Technol 2005;96:551–5.

[57] Ma F, Hanna MA. Biodiesel production: A review. Bioresour Technol 1999;70:1–15.

[58] Zalba B, Marín JM, Cabeza LF, Mehling H. Review on thermal energy storage with phase change: Materials, heat transfer analysis and applications. vol. 23. 2003.

[59] Demirbas A. Importance of biodiesel as transportation fuel. Energy Policy 2007;35:4661–70.

[60] Ashraful AM, Masjuki HH, Kalam MA, Rizwanul Fattah IM, Imtenan S, Shahir SA. Production and comparison of fuel properties, engine performance, and emission characteristics of biodiesel from various non-edible vegetable oils: A review. Energy Convers Manag 2014;80:202–28.

[61] Adewale P, Dumont MJ, Ngadi M. Recent trends of biodiesel production from animal fat wastes and associated production techniques. Renew Sustain Energy Rev 2015;45:574–88.

[62] Frascari D, Zuccaro M, Pinelli D, Paglianti A. A pilot-scale study of alkali-catalyzed sunflower oil transesterification with static mixing and with mechanical agitation. Energy and Fuels 2008;22:1493–501.

[63] Karaosmanog F. Optimization of base-catalyzed transesterification 2004;5:1888–95.

[64] Maaira J, Santana A, Recasens F, Angeles Larrayoz M. Biodiesel production using supercritical methanol/carbon dioxide mixtures in a continuous reactor. Fuel 2011;90:2280–8.

[65] Sinha S, Agarwal AK, Garg S. Biodiesel development from rice bran oil: Transesterification process optimization and fuel characterization. Energy Convers Manag 2008;49:1248–57.

[66] Shahid EM, Jamal Y. Production of biodiesel: A technical review. Renew Sustain Energy Rev 2011;15:4732–45.

[67] Abbaszaadeh A, Ghobadian B, Omidkhah MR, Najafi G. Current biodiesel production technologies: A comparative review. Energy Convers Manag 2012;63:138–48.

[68] Yan Y, Li X, Wang G, Gui X, Li G, Su F. Biotechnological preparation of biodiesel and its high-valued derivatives: A review. Appl Energy 2014;113:1614–31.

[69] Liu Y, Liu T, Wang X, Xu L, Yan Y. Biodiesel synthesis catalyzed by Burkholderia cenocepacia lipase supported on macroporous resin NKA in solvent-free and isooctane systems. Energy and Fuels 2011;25:1206–12.

[70] Halvorsen BL, Blomhoff R. Determination of lipid oxidation products in vegetable oils and marine omega-3 supplements. Food Nutr Res 2011;55.

[71] Yu S, Jeong SG, Chung O, Kim S. Bio-based PCM/carbon nanomaterials composites with enhanced thermal conductivity. Sol Energy Mater Sol Cells 2014;120:549–54.

[72] Chen C, Wang L, Huang Y. Morphology and thermal properties of electrospun fatty acids/polyethylene terephthalate composite fibers as novel form-stable phase change materials. Sol Energy Mater Sol Cells 2008;92:1382–7.

[73] Zhang N, Yuan Y, Du Y, Cao X, Yuan Y. Preparation and properties of palmitic-stearic acid eutectic mixture/expanded graphite composite as phase change material for energy storage. Energy 2014;78:950–6.

[74] Yuan Y, Zhang N, Tao W, Cao X, He Y. Fatty acids as phase change materials: A review. Renew Sustain Energy Rev 2014;29:482–98.

[75] Rozanna D, Chuah TG, Salmiah A, Choong TSY, Sa'ari M. Fatty Acids as Phase Change Materials (PCMs) for Thermal Energy Storage: A Review. Int J Green Energy 2004;1:495–513.

[76] Inoue T, Hisatsugu Y, Suzuki M, Wang Z, Zheng L. Solid-liquid phase behavior of binary fatty acid mixtures: 3. Mixtures of oleic acid with capric acid (decanoic acid) and caprylic acid (octanoic acid). Chem Phys Lipids 2004;132:225–34.

[77] Karaipekli A, Sari A. Capric acid and palmitic acid eutectic mixture applied in building wallboard for latent heat thermal energy storage. J Sci Ind Res (India) 2007;66:470–6.

[78] Cai Y, Ke H, Lin L, Fei X, Wei Q, Song L. Preparation, morphology and thermal properties of electrospun fatty acid eutectics/polyethylene terephthalate form-stable phase change ultrafine composite fibers for thermal energy storage. Energy Convers Manag 2012;64:245–55.

[79] Sari A. Thermal reliability test of some fatty acids as PCMs used for solar thermal latent heat storage applications. Energy Convers Manag 2003;44:2277–87.

[80] Sari A, Alkan C, Kolemen U, Uzun O. Eudragit S (methyl methacrylate methacrylic acid copolymer)/fatty acid blends as form-stable phase change material for latent heat thermal energy storage. J Appl Polym Sci 2006;101:1402–6.

[81] Inoue T, Hisatsugu Y, Ishikawa R, Suzuki M. Solid-liquid phase behavior of binary fatty acid mixtures: 2. Mixtures of oleic acid with lauric acid, myristic acid, and palmitic acid. Chem Phys Lipids 2004;127:161–73.

[82] Preparation of crystallizable stearic acid. US Pat., 2985674, 1961.

[83] Production of palmitic acid. US Pat., 2682549, 1951.

[84] Karaipekli A, Sari A. Preparation, thermal properties and thermal reliability of eutectic mixtures of fatty acids/expanded vermiculite as novel form-stable composites for energy storage. J Ind Eng Chem 2010;16:767–73.

[85] Suppes GJ, Goff MJ, Lopes S. Latent heat characteristics of fatty acid derivatives pursuant phase change material applications. Chem Eng Sci 2003;58:1751–63.

[86] Alper Aydn A. High-chain fatty acid esters of 1-octadecanol as novel organic phase change materials and mathematical correlations for estimating the thermal properties of higher fatty acid esters' homologous series. Sol Energy Mater Sol Cells 2013;113:44–51.

[87] Aydın AA, Aydın A. High-chain fatty acid esters of 1-hexadecanol for low temperature thermal energy storage with phase change materials. Sol Energy Mater Sol Cells 2012;96:93–100.

[88] Liston LC, Farnam Y, Krafcik M, Weiss J, Erk K, Tao BY. Binary mixtures of fatty acid methyl esters as phase change materials for low temperature applications. Appl Therm Eng 2016;96:501–7.

[89] Aydn AA. Diesters of high-chain dicarboxylic acids with 1-tetradecanol as novel organic phase change materials for thermal energy storage. Sol Energy Mater Sol Cells 2012;104:102–8.

[90] Li WD, Ding EY. Preparation and characterization of a series of diol di-stearates as phase change heat storage materials. Mater Lett 2007;61:4325–8.

[91] Sarı A, Biçer A, Karaipekli A. Synthesis, characterization, thermal properties of a series of stearic acid esters as novel solid–liquid phase change materials. Mater Lett 2009;63:1213–6.

[92] Sar A, Bier A, Karaipekli A, Alkan C, Karadag A. Synthesis, thermal energy storage properties and thermal reliability of some fatty acid esters with glycerol as novel solidliquid phase change materials. Sol Energy Mater Sol Cells 2010;94:1711–5.

[93] Sari A, Eroglu R, Biçer A, Karaipekli A. synthesis and thermal energy storage properties of erythritol tetrastearate and erythritol tetrapalmitate. Chem Eng Technol 2011;34:87–92.

[94] Biçer A, Sar A. Synthesis and thermal energy storage properties of xylitol pentastearate and xylitol pentapalmitate as novel solid-liquid PCMs. Sol Energy Mater Sol Cells 2012;102:125–30.

[95] Sari A, Biçer A, Lafçi Ö, Ceylan M. Galactitol hexa stearate and galactitol hexa palmitate as novel solid-liquid phase change materials for thermal energy storage. Sol Energy 2011;85:2061–71.

[96] Feldman D, Banu D, Hawes D. Low chain esters of stearic acid as phase change materials for thermal energy storage in buildings. Sol Energy Mater Sol Cells 1995;36:311–22.

[97] Hu W, Yu X. Thermal and mechanical properties of bio-based PCMs encapsulated with nanofibrous structure. Renew Energy 2014;62:454–8.

[98] Hu W, Yu X. Encapsulation of bio-based PCM with coaxial electrospun ultrafine fibers. RSC Adv 2012;2:5580–4.

[99] Jeong SG, Chung O, Yu S, Kim S, Kim S. Improvement of the thermal properties of bio-based PCM using exfoliated graphite nanoplatelets. Sol Energy Mater Sol Cells 2013;117:87–92.

[100] Jeong SG, Lee JH, Seo J, Kim S. Thermal performance evaluation of bio-based shape stabilized PCM with boron nitride for energy saving. Int J Heat Mass Transf 2014;71:245–50.

[101] Biermann U, Friedt W, Lang S, Lühs W, Machmüller G, Metzger JO, et al. New syntheses with oils and fats as renewable raw materials for the chemical industry. Angew Chem Int Ed 2000;39:2206–2224.

[102] Montero De Espinosa L, Meier MAR. Plant oils: The perfect renewable resource for polymer science?! Eur Polym J 2011;47:837–52.

[103] Seniha F, Yagci Y, Tuncer A. Polymers from triacylglyceride oils. Prog Polym Sci 2006;31:633–70.

[104] Adekunle KF. A review of vegetable oil-based polymers : Synthesis and applications. Open J Polym Chem 2015;5:34–40.

[105] Li A, Li K. Pressure-sensitive adhesives based on tung oil. RSC Adv 2015;5:85264–71.

[106] Kimwomi RRK, Kossmehl G, Zeinalov EB, Gitu PM, Bhatt BP. Polymeric antioxidants from vernonia oil. Macromol Chem Phys 2001;202:2790–6.

[107] Steen M Van Der, Stevens C V. Undecylenic Acid : A Valuable and physiologically active renewable building block from castor Oil 2009:692–713.

[108] Li F, Larock RC. Thermosetting polymers from cationic copolymerization of tung oil: synthesis and characterization. J Appl Polym Sci 2000;78:1044–56.

[109] Samadzadeh M, Boura SH, Peikari M, Ashrafi A, Kasiriha M. Tung oil: An autonomous repairing agent for self-healing epoxy coatings. Prog Org Coatings 2011;70:383–7.

[110] Ronda JC, Lligadas G, Galià M, Cádiz V. Vegetable oils as platform chemicals for polymer synthesis. Eur J Lipid Sci Technol 2011;113:46–58.

[111] Frankel EN. Lipid oxidation. Pro Lipid Res 1980;19:1–22.

[112] Xia Y, Larock RC. Vegetable oil-based polymeric materials: synthesis, properties, and applications. Green Chem 2010;12:1893.

[113] Mol JC. Application of olefin metathesis in oleochemistry: an example of green chemistry. Green Chem 2002;4:5–13.

[114] Huang K, Zhang P, Zhang J, Li S, Li M, Xia J. Preparation of biobased epoxies using tung oil fatty acid-derived C21 diacid and C22 triacid and study of epoxy properties. Green Chem 2013;15:2466–75.

[115] Tasdelen MA. Diels–Alder "click" reactions: recent applications in polymer and material science. Polym Chem 2011;2:2133.

[116] Lacerda TM, Carvalho AJF, Gandini A. Two alternative approaches to the Diels–Alder polymerization of tung oil. RSC Adv 2014;4:26829.

[117] Huang K, Liu Z, Zhang J, Li S, Li M, Xia J, et al. Epoxy monomers derived from tung oil fatty acids and its regulable thermosets cured in two synergistic ways. Biomacromolecules 2014;15:837–43.

[118] McMurry JE. Química Orgánica. Mexico D.F, Mexico: CENGAGE Learning; 2008.

[119] Li A, Li K. Pressure-sensitive adhesives based on soybean fatty acids. RSC Adv 2014.

[120] Li A, Li K. Pressure-sensitive adhesives based on epoxidized soybean oil and dicarboxylic acids. ACS Sustain Chem Eng 2014.

[121] Ahn BK, Kraft S, Wang D, X Susan Sun. Thermally stable, transparent, pressure-sensitive adhesives from epoxidized and dihydroxil soybean oil. Biomacromolecules 2011;12:1839–43.

[122] Wu Y, Li A, Li K. Pressure sensitive adhesives based on oleic acid. J Am Oil Chem Soc 2015;92:111–20.

[123] Baumann H, Bühler M, Fochem H, Hirsinger F, Zoebelein H, Falbe J. Natural fats and oils???Renewable raw materials for the chemical industry. Angew Chem Int Ed 1988;27:41–62.

[124] Dryuk VG. The mechanism of epoxidation of olefins by peracids. Tetrahedron 1976;32:2855–66.

[125] Bach RD, Canepa C, Winter JE, Blanchette PE. Mechanism of acid-catalyzed epoxidation of alkenes with peroxy acids. J Org Chem 1997;62:5191–7.

[126] Hilker I, Bothe D, Prüss J, Warnecke HJ. Chemo-enzymatic epoxidation of unsaturated plant oils. Chem Eng Sci 2001;56:427–32.

[127] Törnvall U, Orellana-Coca C, Hatti-Kaul R, Adlercreutz D. Stability of immobilized Candida antarctica lipase B during chemo-enzymatic epoxidation of fatty acids. Enzyme Microb Technol 2007;40:447–51.

[128] Klaas M, Warwel S. Chemoenzymatic epoxidation of unsaturated fatty acid esters and plant oils. J Am Oil Chem Soc 1996;73:9–13.

[129] Vasishtha AK, Trivedi RK, Das G. Sebacic acid and 2-octanol from castor oil. J Am Oil Chem Soc 1990;67:333–7.

[130] Ogunniyi DS. Castor oil: A vital industrial raw material. Bioresour Technol 2006;97:1086–91.

[131] Das G, Trivedi RK, Vasishtha AK. Heptaldehyde and undecylenic acid from castor oil. J Am Oil Chem Soc 1989;66:938–41.

[132] O'Keefe SF, Wiley VA, Knauft DA. Comparison of oxidative stability of high- and normal-oleic peanut oils. J Am Oil Chem Soc 1993;70:489–92.

[133] Smith SA, King RE, Min DB. Oxidative and thermal stabilities of genetically modified high oleic sunflower oil. Food Chem 2007;102:1208–13.

[134] KosheelaDevi PP, Tuan Noor Maznee TI, Hoong SS, Nurul 'Ain H, Mohd. Norhisham S, Norhayati MN. Performance of palm oil-based dihydroxystearic acid as ionizable molecule in waterborne polyurethane dispersions. J Appl Polym Sci 2016;133:1–10.

[135] Benessere V, Cucciolito ME, De Santis A, Di Serio M, Esposito R, Ruffo F. Sustainable process for production of azelaic acid through oxidative cleavage of oleic acid. J Am Oil Chem Soc 2015;92:1701–7.

[136] Kulik A, Martin A, Pohl M-M, Fischer C, Köckritz A. Insights into gold-catalyzed synthesis of azelaic acid. Green Chem 2014;16:1799.

[137] Sato K. Green oxidation with aqueous hydrogen peroxide. Trends Sci 2009;14:60–3.

AIMS AND OBJECTIVES

The main aim of my dissertation was to use triacylglycerols from vegetable and animal non-edible sources to prepare value-added products.

The specific objectives were to:

1. Hydrolyze non-edible animal fat with biocatalysts to separate in saturated and unsaturated fatty acids.
2. Evaluate the thermal properties of the saturated fatty acids, *threo*-9, 10-dihydroxystearic acid (DHSA) and DHSA-salts prepared by applying chemical approaches to non-edible animal fat.
3. Evaluate the thermal properties of the *threo*-9, 10-dihydroxystearates (DHSEs) prepared via green and bio-catalytic approaches from non-edible animal fat to improve the DHSA thermal and chemical stability.
4. Evaluate the properties as PSAs of the polymers prepared by direct polymerization of tung oil.

Chapter II

Recycling Rhizopus oryzae resting cells as biocatalyst to prepare near eutectic palmitic-stearic acid mixtures from non-edible fat

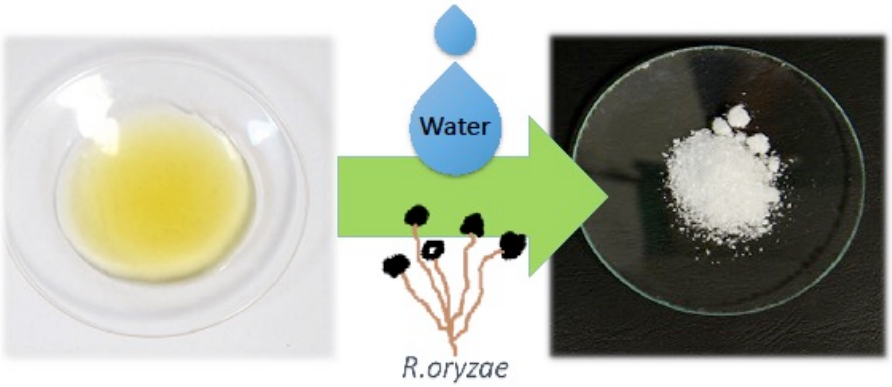

Results described in this chapter have been published in: Journal of Molecular Catalysis B: Enzymatic. 2016; 134; 172-7.

2.1. Abstract

Non-edible fat waste was studied as a starting material to prepare eutectic mixtures of biomaterials. Initially, the fat was hydrolyzed using water and *R. oryzae* resting cells. The hydrolysis was performed in organic solvent-free media and the degree of hydrolysis at 1 h was 42% while hydrolytic values of 86 and 98% were achieved at 12 and 48 h, respectively. To recover the resting cells, they were extracted in consecutive cycles with solvents or supercritical CO_2. Compared with solvents, supercritical CO_2 allowed the highest reuse. Hence, *R. oryzae* was used for 336 h (7 reaction cycles), yielding 56.5 g of FFA/g biocatalyst. Crude glycerol was recovered, showing a purity of 66.0% and an ash and water content of 2.3 and 1.8%, respectively. The hydrolyzed fat was crystallized with several solvents to yield palmitic and stearic acid mixtures with melting point characteristics of eutectic mixtures. From 76 to 90% of the palmitic and stearic acids present in the initial hydrolyzed animal fat were recovered, depending on the solvent. The palmitic:stearic acid ratios determined by GC-FID were similar to those reported for eutectic mixtures whit PCMs (phase change materials) properties, as were the melting points, which ranged from 51.5 to 54.8˚C.

Keywords: Supercritical CO_2, biocatalysis, glycerol recovery, bio-based materials, bioeconomy.

Abbreviations of this chapter: CAL-B, *Candida antarctica* Lipase-B; CECT, "Colección Española de Cultivos Tipo"; FFA, free fatty acids; GC-FID, gas chromatography-flame ionization detector; MONG, matter organic non glycerol; PCM, phase change material; SV, saponification value; TES, thermal energy storage; U, one unit of activity.

2.2. Introduction

Only Europe is producing near 10 mil MT/year of animal fat byproducts from slaughterhouses [1]. Certainly, current industrial practices have led to the production of various crude fatty materials that are difficult to treat and valorize [2]. These animal fats are composed mainly of triacylglycerols derived from glycerol and fatty acids.

The high thermal and chemical stability and high heat capacity of fatty acids have been widely studied for TES (thermal energy storage) purposes [3]. TES matches the thermal energy supply and demand in time or space, thereby improving energy utilization efficiency and contributing to environmental protection. Thermal energy can be stored in the form of latent heat in PCMs such as fatty acids. In this regard, heat energy is stored or released during the phase-change process. Furthermore, fatty acids and fatty acid derivatives are an excellent source of renewable materials and provide alternatives to paraffin and salt products, which are currently predominant in this technology [4, 5].

Novel bio-based organic PCMs derived from fatty acid feedstock have been described by Yu, Jeong and Kosny [6–8]. These products comprise saturated fatty esters that result from the hydrogenation of fats and oils containing a high percentage of unsaturated fatty acid. The hydrogenation process leads to saturated fatty acids with at least 90% purity a level that is essential if they are to be used as feedstock in PCMs [9]. Nevertheless, in this approach, the unsaturated fatty acids are converted to the corresponding saturated fatty acids, thus ruling out the opportunity to use them for other potential applications. Eutectic mixtures of fatty acids have also been prepared from pure fatty acids and haven shown satisfactory performance as PCMs

[3, 4, 10, 11]. In this strategy, although the purity requirements decrease, no study has addressed the preparation of PCMs based on eutectic mixtures from triacylglycerols as feedstock.

The splitting of lipids into fatty acids and glycerol in the industrial sector is usually conducted at high temperatures and pressure. Although the conversion achieves yields of between 96 and 99%, the polymerization of fats and formation of byproducts occurs under these extreme conditions, resulting in dark fatty acids and colored aqueous glycerol solutions. Consequently, final distillation processes are required to remove the color and the byproducts [12]. In contrast, fats and oils can also be hydrolyzed using lipases and less harsh conditions. Temperatures below 70˚C and atmospheric pressure prevent polymerization and byproduct formation. Hence, these enzymatic processes are considered environmentally advantageous over the physical-chemical process previously described [2, 12, 13].

As early as the 1990s, Fu et al. described the use of a lipase from *Candida cylindracea* in the hydrolysis of beef tallow and linseed oil—an approach that yielded 4000 t of fatty acids per year [14]. Several studies have addressed the hydrolysis of various kinds of animal fats catalyzed by commercial lipases [13–19]. Furthermore, enzyme stability in the hydrolysis of such fats has been studied [17–19]. Recent years have brought about considerable interest in the direct use of intracellular lipases as whole-cell biocatalysts. Their application in organic synthesis offers many advantages, one being the preparation of the biocatalyst in a straightforward and inexpensive manner [20]. Adamczak's et al. recent study reported that animal fat hydrolysis catalyzed by resting cells for 72 h led to a 68% yield [2]. To the best of our knowledge, the reuse of resting cells in the hydrolysis of animal fats

has not been reported to date. Neither has glycerol recovery in enzymatic animal fat hydrolysis been reported.

The present study takes advantage of the fatty acid composition of non-edible animal fats to prepare palmitic and stearic acid mixtures with melting points specific of eutectic mixtures. We also describe the hydrolysis of the fats using *Rhizopus oryzae* resting cells and their reuse—a practice that reduces processing costs. The effect of reaction time was compared with that required by a commercial lipase. The hydrolysis was performed in an organic solvent-free medium, and the final extraction was accomplished using either supercritical CO_2 or various common solvents. Glycerol was recovered from the aqueous phase and analyzed. Finally, unsaturated and saturated fatty acids were separated by crystallization.

2.3. Materials and methods

2.3.1. Materials

CO_2 was obtained from Messer Iberica de Gases S.A (Tarragona, Spain). Immobilized lipase-B from *C.antarctica* (Immobilized CAL-B) was a gift sample from Novozymes A/S (Bagsvaerd, Denmark). All the reagents were used as received. Animal fat was a kind gift from Subproductos Cárnicos Echevarria y Asociados S.L (Cervera, Spain).

2.3.2. Characterization of waste fat

The waste fat was composed of non-edible fatty pig and chicken parts. It consisted mainly of triacylglycerides and had a saponification value (SV) of 196. The percentage of unsaturated fatty acids was 55.14%, in which monounsaturated and polyunsaturated fatty acids accounted for 40.50 and

14.64%, respectively, as determined by a chromatographic method [21]. Of all the unsaturated fatty acids in the animal fat, oleic acid was the most abundant, accounting for about 36.97% of the total fatty acids present. Saturated fatty acids accounted for 43.99% of the total fatty acids and palmitic and stearic acids for 24.57 and 14.05% of this total, respectively.

2.3.3. Preparation of resting cells

Rhizopus oryzae cells were grown in a synthetic liquid medium containing 2 g of asparagine, 1 g of K_2HPO_4, 0.5 g of $MgSO_4$, 5 mg of thiamine hydrochloride, 1.45 mg of $Fe(NO_3)_3 \bullet 9H_2O$, 0.88 mg of $ZnSO_4 \bullet 7H_2O$, and 0.235 mg of $MnSO_4 \bullet H_2O$ per liter of distilled water. The initial pH of the medium was adjusted to pH 6.0. Next, 250-mL aliquots of the medium were sterilized at 121°C for 15 min, and 1% (v/v) of refined sunflower oil was added aseptically. The medium was inoculated with 2.5 mL of a *R. oryzae* spore suspension (1-4 × 106 spores/mL) and then incubated at 28°C for 5 days using an orbital shaker at 200 rpm. Mycelium was harvested from the culture medium using a Buchner funnel and washed with distilled water followed by acetone. It was then dried under vacuum for 18 h and ground to a powder. The *R. oryzae* (CECT20476) strain is housed in the Spanish Type Culture Collection (CECT).

2.3.4. Lipase assay

The lipolytic activity of the *R. oryzae* resting cells was determined using a modification of the method developed by Méndez et al. [22]. The reaction consisted of methyl stearate hydrolysis by 10 mg of mycelia at 40˚C in 0.5 mL of *t*-BuOH for 1 h. One unit of activity (U) was defined as the amount (in mg) of resting cells releasing 1 µmol of stearic acid in 1 min under assay conditions. One gram of *R. oryzae* resting cells reached 78.65 U under the

mentioned conditions.

2.3.5. Biocatalytic hydrolysis of waste fat- Reaction progress study

An amount of 20 g of water was added to a 50-mL falcon tube containing 20 g of animal fat and 2 g of biocatalyst. The falcon tube was fixed horizontally in a Labnet 211DS orbital oven and then shaken at 220 rpm at 40˚C in reaction times ranging from 1 to 72 h. Finally, the reaction mixture was centrifuged at 6000 rpm for 10 min, and the non-aqueous and aqueous phases were separated. The resulting non-aqueous viscous liquid was recovered, and two aliquots were titrated to determine the acid value in duplicate. The degree of hydrolysis was calculated using the following equation:

Degree of hydrolysis (%) = acid value / saponification value • 100

2.3.6. Biocatalytic hydrolysis of waste fat- Reuse study

Once the reaction had been performed as indicated above, the resting cells were recovered by passing them through a Pyrex crucible n˚3 and then washed with water and dried under vacuum for 24 h. Finally, the cells were extracted with a common solvent or using a lab-scale supercritical fluid extractor (Speed SFE-Applied separations). Regarding the common solvent extraction, resting cells were extracted three times with 20 mL of solvent, and the fractions were pooled and taken to complete dryness under vacuum. During the supercritical CO_2 extraction, the extraction vessel was packed with the resting cells recovered. The extraction temperature, pressure, CO_2 outflow rate, and residence time were set at 45 °C, 35 MPa, 4 L•min^{-1}, and 45 min, respectively. The remaining fatty matter obtained from the common

or the supercritical CO_2 extraction was mixed with the non-aqueous layer previously obtained. These hydrolyzed fatty acids were titrated in duplicate to determine the acid value to be used to determine the degree of hydrolysis. The washed resting cells were recovered for a reuse study.

2.3.7. Glycerol recovery

The aqueous phases of six 50-mL falcon tubes (133.00 g) resulting from the hydrolysis of waste fat by *R. oryzae* resting cells were pooled in a 250-mL flat-bottomed flask, and the solution was concentrated under vacuum. The concentrate was placed in a Speedvac concentrator (mod. SPD131 DDA-230) at 50˚C for 8 h until constant weight. Crude glycerol (12.94 g) was obtained and analyzed in duplicate following the procedures described below:

Glycerol content. European standard EN 14106

Ash content. Standard method ISO 6245

Water content. Determined using a DL 39 coulometer (Mettler Toledo, Switzerland) and validated with a standard containing 0.5% water (Hydranal Titrant 5, Fluka)

MONG (matter organic non glycerol). Standard method ISO 2464

Acidity. European Standard EN 14104

2.3.8. Crystallization study of hydrolyzed animal fat

Crystallization studies were performed by dissolving 5 g of the hydrolyzed animal fat in various common solvents under reflux. Crystallizations were performed for 24 h at temperatures from 25 to -20˚C and solute/solvent ratios from 1/1 to 1/6 (w/v). The resulting solid material was recovered by filtration under vacuum in a Pyrex crucible n˚3 and then washed three times with the corresponding cold solvent. The fatty solids were analyzed by

GC-FID [21], and their uncorrected melting points were determined in a Gallenkamp melting-point apparatus.

2.4. Results and Discussions

2.4.1 Reaction progress study

Figure 2.1 shows the progress of the reaction using Immobilized CAL-B and *R. oryzae* resting cells as biocatalyst for the hydrolysis of non-edible animal fats. 42% Of hydrolysis was attained at 1 h, 86% at 12 h, and 98% at 48 h. In contrast, the immobilized CAL-B presented a more lineal slope, with a lower degree of hydrolysis than that achieved by the resting cells. At 72 h, CAL-B had hydrolyzed 36% of the animal fat, while *R. oryzae* resting cells had achieved 99% of hydrolysis. Moreover, the degree of hydrolysis attained with the latter was comparatively higher than that achieved with *Aspergillius niger* whole cells (52.6%) at 24 h [23] and that reported for beef tallow using the immobilized whole cells of *Rhizomucor miehei* (68%) [2] or *Yarrowia lipolytica* (61%) [2] at 72 h. However, a comparative degree of hydrolysis (95%) [19] was achieved using immobilized commercial *Candida rugosa* lipase to hydrolyze edible pork lard for 24 h.

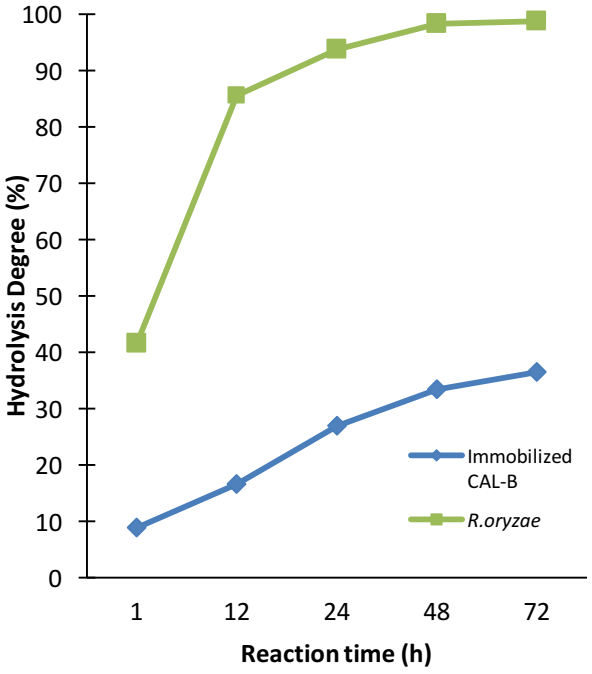

Figure 2.1. Effect of time on the hydrolysis of non-edible animal fat by *R. oryzae* resting cells and immobilized CAL-B. Experimental details are described in the experimental subsection (2.3.5 Biocatalytic hydrolysis of waste fat- Reaction progress study).

In addition, the animal fat and water were mixed at a ratio of 1:1 (w/w) [13, 19]. Hence, this relative water amount makes the process sustainable and realistic for scale-up purposes. In order to keep the animal fat in a melted state [2] and respecting the stability conditions for *R. oryzae* [24], the temperature was set at 40˚C. In order to improve the phase interaction, the Falcon tubes were fixed in a horizontal position in a Labnet 211DS orbital oven (220 rpm). In addition, the use of these tubes

allows the reaction and centrifugation processes to take place in the same vessel, thereby facilitating recovery of the non-aqueous layer in the non-organic solvent conditions used to perform the hydrolysis.

2.4.2 Reusability of *R. oryzae* resting cells after extraction with supercritical CO_2 or common solvents

The reusability studies of *R. oryzae* resting cells were conducted at 40˚C for 48 h. **Figure 2.2** shows the results from three consecutive hydrolysis cycles performed using resting cells treated with common solvents or a lab-scale supercritical fluid extractor (Speed SFE-Applied separations) to extract the fatty matter. Compared with common solvents, supercritical CO_2 achieved the highest degrees of hydrolysis after the three cycles (above 90%). In contrast, a considerable decrease in hydrolysis was observed in the second cycle of cells extracted with the common solvents. This decrease was parallel to the loss of resting cell mass after the first washing cycle using said solvents (up to 50% weight loss related to the starting resting cell weight). Enzyme leakage of the resting cells to the aqueous phase presumably occurs during the first solvent extraction, which may promote the partial leakage. Although the resting cell mass in the third cycle remained constant with respect to that registered in the second, the degree of hydrolysis with diethyl ether and ethyl acetate decreased from the second to the third cycle, while it remained constant using heptane, benzene, or hexane. These results suggest a progressive inhibition of the enzyme by oxygenated solvents but not by hydrocarbonated ones.

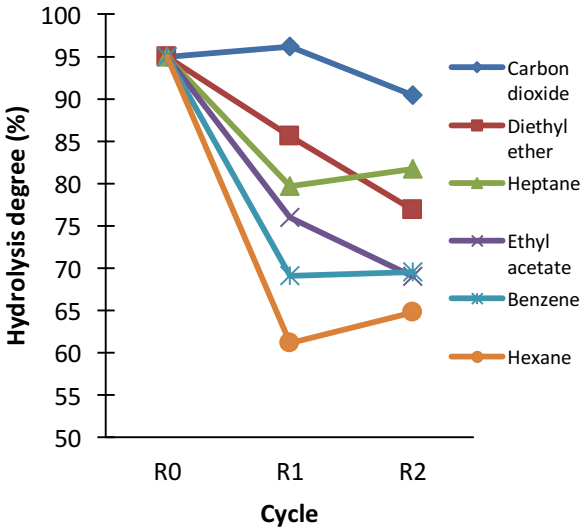

Figure 2.2. Three consecutive hydrolysis cycles of non-edible animal fat by *R. oryzae* resting cells extracted with common solvents or supercritical CO_2. Experimental details are described in the experimental subsection (2.3.6 Biocatalytic hydrolysis of waste fat- Reuse study).

2.4.3 Productivity of the *R. oryzae* resting cells using supercritical CO_2

In the enzymatic treatment, the cost of the enzyme is a crucial for the economic feasibility of the process. Logically, reusing the enzyme can reduce the cost of the process. Encouraged by the results achieved with the preliminary studies described above, we extended the reusability studies of resting cells extracted using supercritical CO_2. Commonly, studies of the lipase hydrolysis of animal fat determined the progress of the reaction in terms of the degree of hydrolysis [13–19]. To the best of our knowledge, this is the first report to provide data on the final yield of the process and thus allowing the determination of the true productivity of a given biocatalyst. In

this case, the biocatalyst was used in 7 cycles for 48 h each. The hydrolytic reaction was followed by resting cell extraction with supercritical CO_2 after each cycle. The same biocatalyst allowed the hydrolysis of animal fat for 336 h (**Figure 2.3**). Yields ranged from 94 to 69% depending on the cycle. The recovery of the non-aqueous layer supernatant in combination with the supercritical CO_2 extraction of resting cells achieved mass recoveries from 95.93 to 99.59%. Certainly, a total amount of 140 g of animal fat reacted with 140 g of water and catalyzed by 2 g of resting cells yielded 113 g of FFA.

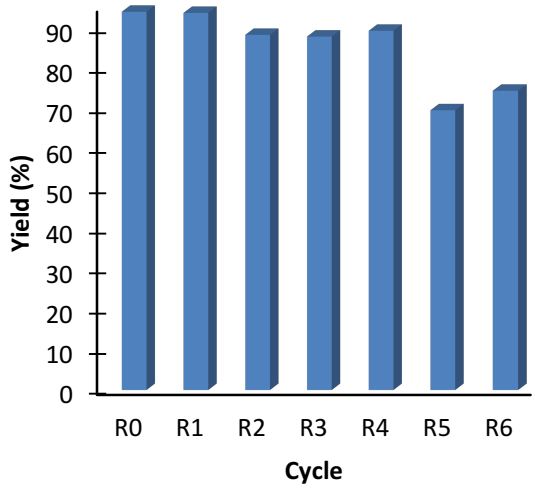

Figure 2.3. Non-edible animal fat hydrolysis yields from 7 cycles with *R. oryzae* resting cells extracted by supercritical CO_2. Experimental details are described in the experimental subsection (2.3.6 Biocatalytic hydrolysis of waste fat- Reuse study).

Considering these results, we proceed to perform a mass and energy balances comparing the single process without biocatalyst recovering and the 7 cycle process. **Table 2.1** shows that mass and energy consumptions are

always favorable in the second approach considering the amount of FFA obtained.

Table 2.1. Mass and energy balances comparing the single process without biocatalyst recovering and the 7-cycle process.

	Without using CO_2		**Using CO_2 for biocatalyst recovering**	
	Mass balance	Energy balance	Mass balance	Energy balance
g biocatalyst	2		2	
g FFA	14		113	
g•g^{-1} biocatalyst	560[a]		2382[e]	
g•g^{-1} FFA	79[b]		43[f]	
kJ•g^{-1} biocatalyst		77869[c]		88287[g]
kJ•g^{-1} FFA		12630[d]		3169[h]

[a]The mass of the following compounds and solvents were considered: growth media, washing water, washing acetone.[b]The mass of the following compounds and solvents were considered: growth media, washing water, washing acetone and water used as reagent.[c]The energy consumption for the following equipment were considered: autoclave, LAF-bench, incubator and freeze dryer. [d]The energy consumption for the following equipment were considered: autoclave, LAF-bench, incubator and freeze dryer. In addition, the energy consumption used during the hydrolysis process was also considered. [e]The mass of the following compounds and solvents were considered: growth media, washing water, washing acetone.[f]The mass of the following compounds and solvents were considered: growth media, washing water, washing acetone and CO_2 and water (reagent) used for the 7 cycles. [g]The energy consumption for the following equipment were considered: autoclave, LAF-bench, incubator, freeze dryer. [h]The energy consumption for the following equipment were considered: autoclave, LAF-bench, incubator, freeze dryer. In addition, the use for the 7 cycles of the incubator, vacuum pump and SFE extractor were also considered.

2.4.4 Crude glycerol analysis

Glycerol accounted for 10% of the total hydrolyzed fat. Consequently, its recovery and purity is relevant for the evaluation of the environmental impact of the process. **Table 2.2** shows the main characteristics of the crude glycerol co-produced with the corresponding fatty acids. The crude glycerol had a purity of 66.0% and an ash and water content of 2.3 and 1.8%, respectively. The matter organic non-glycerol (MONG) in the crude glycerol accounted for 29.9%. Similar purities of glycerol and ash content were obtained from crude glycerol resulting from the transesterification of vegetable feedstocks with sodium methylate [25] or sodium hydroxide [26] as catalysts. Higher amounts of water (8.9%) [26] appeared when sodium hydroxide was the catalyst. In contrast, no water is observed in sodium methylate catalysis but a high content of methanol (up to 32.68%) remains in the crude glycerol phase [25]. To date, no study has addressed the analysis of crude glycerol from feedstocks resulting from biocatalytical hydrolysis. Indeed, although the biocatalytical transesterification of feedstocks to produce biodiesel has been widely described and reviewed [27, 28], information on crude glycerol isolation and analysis is scarce [29].

Table 2.2. Chemical composition of crude glycerol from the non-edible animal fat. The hydrolysis was catalyzed by *R. oryzae* resting cells.

Product	%
Glycerol	66.0
Ash	2.3
Water content	1.8
MONG	29.9
Acidity	25[a]

[a] mg KOH•g^{-1}

2.4.5. Crystallization of the hydrolyzed animal fat to yield eutectic-like palmitic-stearic acid mixtures

The animal fat used showed a 3:2 palmitic:stearic acid ratio (w/w). This ratio is very close to the palmitic:stearic acid ratios which had been described that shown eutectic properties, which allows good performance as PCMs [4, 30]. Hence, we realized that an optimal crystallization could provide a eutectic palmitic-stearic mixture free of unsaturated fatty acids. **Table 2.3** shows the results of crystallizing the hydrolyzed animal waste fat with several solvents. To achieve a eutectic-like saturated fatty acid mixture, crystallizations were performed at temperatures ranging from 25 to -20˚C and solute/solvent ratios from 1/1 to 1/6 (w/v). The solute/solvent ratio fixed for each crystallization temperature implies higher saturated fatty acid recovery with no presence of unsaturated fatty acids.

Nevertheless, higher recovery yields were attained when crystallizations were performed at -20˚C and a solute/solvent ratio of 1:6 (w/v) was used. In these conditions, between 76 to 90% of the palmitic and stearic acids present in the starting hydrolyzed animal fat were recovered. The palmitic:stearic acid ratios determined by GC-FID [21] were similar to those reported for eutectic mixtures. In fact, the sharp melting points of the mixtures (**Table 2.3**), which were lower than the melting points of the pure palmitic or stearic acids, were very similar to those of mixtures with palmitic:stearic acid ratios of 62:38 [4] and 64.2:35.8 [30], which show melting points of 53.89 [4] and 52.3˚C [30], respectively. Indeed, these mixtures have already showed satisfactory performance as PCMs [4, 30].

Table 2.3. Effect of solvent and temperature on the crystallization of the hydrolyzed non-edible animal fat.

Solvent	Solute/ solvent ratio (g/mL)	Crystallization temperature (˚C)	Palmitic and Stearic acids recovered (%)	Palmitic/Stearic mass ratio [21]	Melting point (˚C)
Ethyl Acetate	1/1	25	23	52.4/47.6	54.0
	1/2	4	50	58.2/41.8	52.5
	1/6	**-20**	**88**	**63.2/36.8**	**51.5**
Acetone	1/1	25	16	52.5/47.5	54.8
	1/2	4	70	61.3/38.7	53.5
	1/6	**-20**	**76**	**62.5/37.5**	**52.8**
Ethanol	1/1	25	6	47.8/52.2	54.5
	1/2	4	42	56.0/44.0	54.0
	1/6	**-20**	**79**	**61.2/38.8**	**53.4**
Hexane	1/1	25	17	53.1/46.9	54.0
	1/2	4	53	59.7/40.3	53.5
	1/6	**-20**	**89**	**62.4/37.6**	**52.5**
Methanol	1/1	25	0	-	-
	1/2	4	46	53.6/46.4	54.8
	1/6	**-20**	**90**	**58.7/41.3**	**53.0**

2.5. Conclusions

Non-edible animal fat waste was subjected to biocatalytic hydrolysis in order to prepare eutectic-like mixtures of saturated fatty acids. The hydrolysis was studied using either *R. oryzae* resting cells or Immobilized CAL-B. The former showed higher degrees of hydrolysis than the latter. To the best of our knowledge, the degree of animal fat hydrolysis achieved with *R. oryzae* resting cells was the highest among the values reported using resting cells of other fungi. In fact, our results are similar to those reported for commercial lipases. Moreover, this is the first study to report on a clean process to reuse the resting cells from several hydrolytic cycles and the recovery and characterization of the crude glycerol obtained. We propose that an inexpensive biomaterial for thermal energy storage can be achieved by exploiting both the initial animal fat composition and the degree of hydrolysis. This material will results from the crystallization of the crude product of the reaction, which yields palmitic and stearic acid mixtures with a composition and melting point characteristic of eutectic mixtures. The transformation of the remaining unsaturated fatty acids into new added-value compounds is now underway.

2.6. References

[1] Fava F, Totaro G, Diels L, Reis M, Duarte J, Beserra Carioca O. Biowaste biorefinery in Europe: opportunities and research & development needs. New Biotechnol 2015;32: 100-8.

[2] Adamczak M, Bednarski W. Enhanced activity of intracellular lipases from Rhizomucor miehei and Yarrowia lipolytica by immobilization on biomass support particles. Process Biochem 2004;34:1347–61.

[3] Yuan Y, Zhang N, Tao W, Cao X, He Y. Fatty acids as phase change materials: A review. Renew Sustain Energy Rev 2014;29: 482-98.

[4] Zhang N, Yuan Y, Du Y, Cao X, Yuan Y. Preparation and properties of palmitic-stearic acid eutectic mixture/expanded graphite composite as phase change material for energy storage. Energy 2014;78:950–6.

[5] Farid MM, Khudhair AM, Razack SAK, Al-Hallaj S. A review on phase change energy storage: Materials and applications. Energy Convers Manag 2004;45:1597–615.

[6] Yu S, Jeong SG, Chung O, Kim S. Bio-based PCM/carbon nanomaterials composites with enhanced thermal conductivity. Sol Energy Mater Sol Cells 2014;120:549–54.

[7] Jeong SG, Chung O, Yu S, Kim S, Kim S. Improvement of the thermal properties of Bio-based PCM using exfoliated graphite nanoplatelets. Sol Energy Mater. Sol Cells 2013;117:87–92.

[8] Kosny J, Kossecka E, Brzezinski A, Tleoubaev A, Yarbrough D. Dynamic thermal performance analysis of fiber insulations containing bio-based phase change materials (PCMs). Energy Build 2012;52:122–31.

[9] Suppes GJ, Goff MJ, Lopes S. Latent heat characteristics of fatty acid derivatives pursuant phase change material applications. Chem Eng Sci 2003;58:1751–63.

[10] Zhang N, Yuan Y, Yuan Y, Li T, Cao X. Lauric-palmitic-stearic acid/expanded perlite composite as form-stable phase change material: Preparation and thermal properties. Energy Build 2014;82:505–11.

[11] Yanping Y, Wenquan T, Xiaoling C, Li B. Theoretic prediction of melting temperature and latent heat for a fatty acid eutectic mixture. J Chem Eng Data 2011;56:2889–91.

[12] Abdelmoez W, Mustafa A. Oleochemical industry future through biotechnology. J Oleo Sci 2014;63:545–54.

[13] Teng D, Le R, Yuan F, Yang J, He L, Gao Y. Optimization of enzymatic hydrolysis of chicken fat in emulsion by response surface methodology. J Am Oil Chem Soc 2009;86:485–94.

[14] Fu J, Zhu X, Gao X, Duan K. Oil and fat hydrolysis with lipase from Aspergillus sp.. J Am Oil Chem Soc 1995;527–31.

[15] Linfield WM, Barauskas RA, Sivieri L, Serota S, Stevenson Sr. RW. Enzymatic fat hydrolysis and synthesis. J Am Oil Chem Soc 1984; 61:191–95.

[16] Moskowitz GJ, Cassaigne R, West IR, Shen T, Feldman LI. Hydrolysis of animal fat and vegetable oil with Mucor miehei esterase. Properties of the enzyme. J Agric Food Chem 1977;25:1146–50.

[17] Sharma A, Chaurasia SP, Dalai AK. Non-selective hydrolysis of tuna fish oil for producing free fatty acids containing docosahexaenoic acid. Can J Chem Eng 2014;92: 344–54.

[18] Kosugi T, Suzuki Y, Funada H. Hydrolysis of beef tallow by lipase from Pseudomonas sp.. Biotechnol Bioeng 1988;31: 349–56.

[19] Virto MD, Agud I, Montero S, Blanco A, Solozabal R, Lascaray JM, et al. Hydrolysis of animal fats by immobilized Candida rugosa lipase. Enzym Microb Technol 1994;16:61–65.

[20] Grogan G. Practical Biotransformations: a beginner's guide, Wiley & Sons, Chichester, 2009.

[21] Eras J, Montañes J, Ferran J, Canela R. Chlorotrimethylsilane as a reagent for gas chromatographic analysis of fats and oils. J Chromatogr A 2001;918:227–32.

[22] Méndez J, Canela R, Torres M. Kinetic study of palmitic acid esterification catalyzed by Rhizopus oryzae resting cells. Acta Biológica Colombiana 2009;14:1–12.

[23] Edwinoliver NG, Thirunavukarasu K, Naidu RB, Gowthaman MK, Kambe TN, Kamini NR. Scale up of a novel tri-substrate fermentation for enhanced production of Aspergillus niger lipase for tallow hydrolysis. Bioresour Technol 2010;101:6791–6.

[24] Meussen BJ, De Graaff LH, Sanders JPM, Weusthuis RA. Metabolic engineering of Rhizopus oryzae for the production of platform chemicals. Appl Microbiol Biotechnol 2012;9:875-86.

[25] Thompson JC, He BB. Characterization of crude glycerol from biodiesel production from multiple feedstocks. Appl Eng Agric 2006;22:261–5.

[26] Ooi AH, Yong TL, Dzulkefly KC, Wanyunus K, Hazimah WMZ. Crude glycerine recovery from glycerol residue waste from a palm kernel oil methyl ester plant. J Oil Palm Res 2001;13:16–22.

[27] Bajaj A, Lohan P, Jha PN, Mehrotra R. Enzymatic biodiesel production through lipase catalyzed transesterification : An overview. J Mol Catal B: Enzym 2010;62:9–14.

[28] Tan T, Lu J, Nie K, Deng L, Wang F. Biodiesel production with immobilized lipase : A review. Biotechnol Adv 2010;28:628–34.

[29] Shimada Y, Watanabe Y, Sugihara A, Tominaga Y. Enzymatic alcoholysis for biodiesel fuel production and application of the reaction to oil processing. J Mol Catal B: Enzym 2002;17: 133–42.

[30] Baran G, Sari A. Phase change and heat transfer characteristics of a eutectic mixture of palmitic and stearic acids as PCM in a latent heat storage system. Energy Convers Manag 2003;44:3227–46.

Chapter III

Fatty acids and derivatives from non-edible animal fat as phase change materials

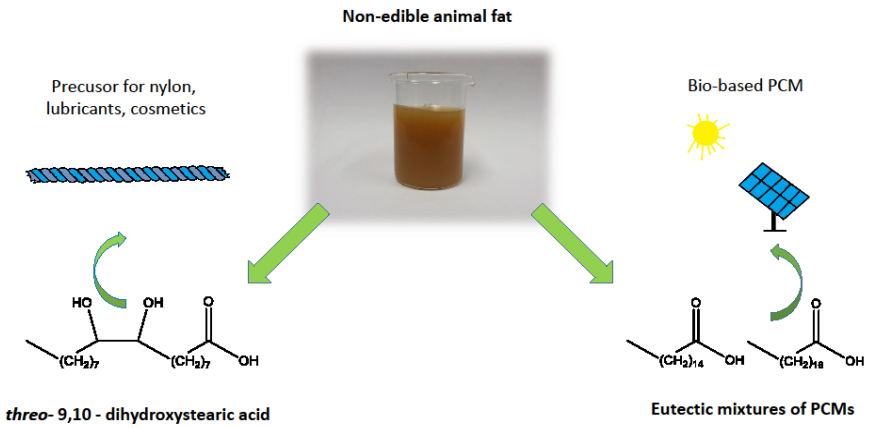

Results described in this chapter have been published in: RSC Advances. 2017; 7; 24133-24139.

3.1. Abstract

A set of compounds from non-edible fat waste was prepared and their thermal behavior was studied. The fat was hydrolyzed and crystallized in a simple and robust process to yield palmitic acid-stearic acid (PA-SA) mixtures. The PA-SA mass ratios determined by GC-FID (gas chromatography-flame ionization detector) were similar to those reported for eutectic mixtures of PCMs (phase change materials). DSC (differential scanning calorimeter) results indicated that the melting and solidification temperatures were around 55 and 52˚C and the latent heat of the crystallized fractions measured was around 180 $kJ \bullet kg^{-1}$. The thermal cycling reliability of the eutectic mixtures was also tested during 1000 melting/freezing cycles. The lost in melting and solidification enthalpies was below 14% in all mixtures showing a promising behavior for PCM applications. Additionally, the unsaturated fatty acids were recovered and transformed to *threo*-9,10-dihydroxystearic acid (DHSA) and some of their inorganic salts, which were analyzed by FT-IR (fourier transform-infrared spectroscopy) and tested by first time using the DSC technique.

Keywords: Bioeconomy; differential scanning calorimeter; *threo*-9, 10-dihydroxystearic acid; *threo*-9,10-dihydroxystearate salts; eutectic fatty acids; PCM.

Abbreviations of this chapter: ATR, attenuated total reflectance; DHSA, *threo*-9,10-dihydroxystearic acid; DHW, domestic hot water; DSC, differential scanning calorimeter; FT-IR, fourier transform-infrared spectroscopy; FFA, free fatty acids, GC-FID, gas chromatography-flame ionization detector; IWH, industrial waste heat; PA-SA, palmitic acid-stearic acid; PCM, phase change material; TES, thermal energy storage.

3.2. Introduction

Animal fats are triacylglycerols containing saturated and unsaturated fatty acids. Nowadays, enormous amounts of animal fat are produced annually as a co-product by agro-industrial practices generating crude fatty materials difficult to treat and valorize [1, 2]. Since fatty acids present high thermal and chemical stability and high heat capacity, TES (thermal energy storage) applications are considered a potential solution to revalorize these materials. Thermal energy is stored and released during the phase change process by fatty acids, acting as PCMs, when the surrounding temperature increases or decreases [3]. Indeed, fatty acids and fatty acid derivatives are considered an alternative to other PCMs, such as paraffin and salt products, with the improvement of being sustainable bio-based materials [3, 4].

Recently, various studies of bio-based organic PCMs from feedstocks have appeared. Such studies were based on commercially available organic compounds [5–9]. These products are partially hydrogenated soy-wax [6, 7] or saturated fatty esters resulting from the hydrogenation of unsaturated fatty acid obtained from several sources [5, 8, 9]. The hydrogenation process is essential in these bio-based PCMs whereby they can remain stable during phase change cycles with no risk of oxidation [8, 10]. Unfortunately, the

unsaturated fatty acids are converted to the corresponding saturated fatty acids, losing the opportunity of use them in other potential applications. On the other hand, eutectic mixtures of fatty acids have also been prepared from pure commercial fatty acids and have shown satisfactory performance as phase change materials [3, 11–13]. However, no study has addressed the preparation of PCMs based on eutectic mixtures directly recovered from acylglycerols as feedstock. Indeed, near eutectic mixtures of PA-SA and unsaturated fatty acids can be separated hydrolyzing animal fat waste with biocatalysts (see **Chapter II**) [14].

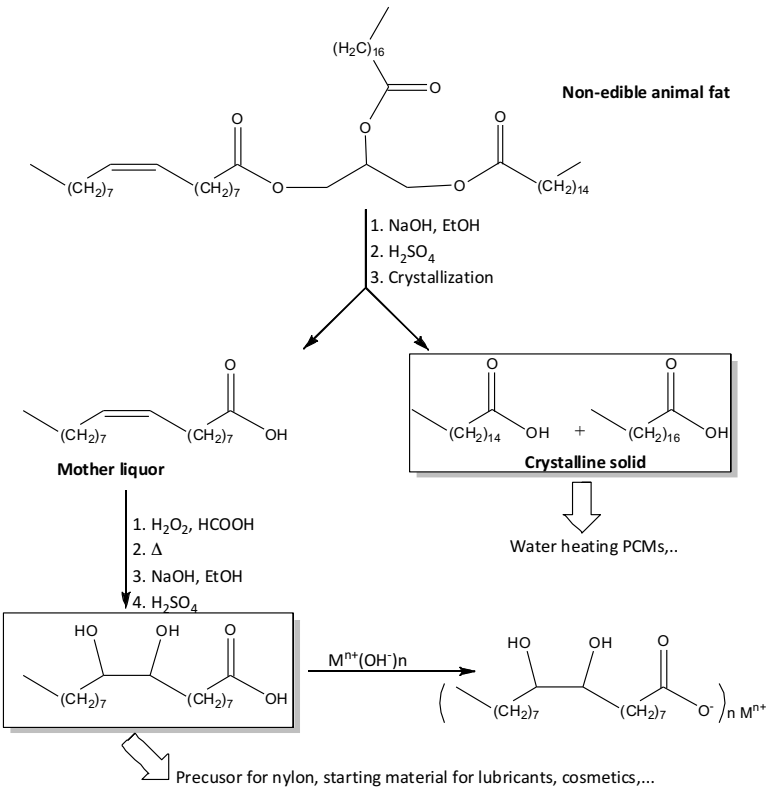

Figure 3.1. Synthesis afforded in this study. The triacylglyceride represents the three fatty acids usable to prepare the products studied.

The remaining unsaturated fatty acids could be an excellent starting material to prepare high-value molecules [15]. In that way, oleic acid has been epoxidated, hydroxylated, and cleaved oxidatively to azealic acid [16–18]. One of the intermediates of this process, DHSA, also plays an important role as a building bloc. Recently, it has been used as an ionizable molecule in waterborne polyurethane dispersions [19] and as a starting material for the preparation of lubricants [20], estolides [21], soaps [21], deodorant sticks [21] and shampoos [21].

The aim of the present study is to determine the actual thermal energy storage capacity as PCM of eutectic mixtures of PA-SA prepared from non-edible animal fat through a simple process involving hydrolysis and crystallization steps. Moreover, the remaining unsaturated fatty acids were transformed to pure DHSA. DHSA and some of it inorganic salts (**Figure 3.1**) have also been analyzed by FT-IR and tested using a DSC technique to study their potential as PCM.

3.3. Experimental

3.3.1. Materials

Animal fat was a kind gift from Subproductos Cárnicos Echevarria y Asociados S.L (Cervera, Spain). This fat was composed of non-edible fatty pig and chicken parts. It consisted mainly of triacylglycerides and had a saponification value (SV) of 196. The percentage of unsaturated fatty acids was 55.14%, in which monounsaturated and polyunsaturated fatty acids accounted for 40.50 and 14.64%, respectively, as determined by a chromatographic method [22]. Of all the unsaturated fatty acids in the animal fat, oleic acid was the most abundant, accounting for about 36.97% of the total fatty acids

present. Saturated fatty acids accounted for 43.99% of the total fatty acids and palmitic and stearic acids for 24.57 and 14.05% of this total, respectively.

Animal fat hydrolysis and DHSA synthesis were conducted in a mechanically stirred cylindrical jacketed glass reactor (5 L). Stirring was performed using a stirring glass rod with three Teflon baffles. The reactor temperature was regulated using regular motor antifreeze heated using a B. Braun Thermomix 1441 Recirculating Bath Pump.

3.3.2. Synthesis pretreatments

3.3.2.1 Non-edible animal fat hydrolysis

Ethanol (1000 mL) was added to the mechanically stirred cylindrical jacketed glass reactor (5 L) containing 1000 g of animal fat at 80˚C. The mixture was stirred at 300 rpm. Afterwards, 2000 mL of 14.2% NaOH solution at 60˚C were added drop wise and the reaction mixture was refluxed for 30 min under stirring. The reaction mixture was driven at pH=2 by adding drop wise 250 mL of a 98% H_2SO_4. This addition should be performed carefully and drop wise during at least 30 min to avoid as much as possible the overheating and the organic matter oxidation. Finally, the aqueous layer was discarded and the organic phase was washed twice with 2000 mL of a 20% NaCl aqueous solution at 60˚C. The upper phase was recovered yielding 944 g of crude FFA (99% yield).

- Crystallization of hydrolyzed animal fat to prepare PA-SA eutectic mixtures and a highly unsaturated fatty acid mixture:

Crystallization studies were performed by dissolving under reflux 5 g of the hydrolyzed animal fat using various common solvents according the

procedure already described in **Chapter II** [14]. The crystallization process was performed at -20˚C using a solute/solvent ratio of 1:6 (w:v). Recovered solids were analyzed for their PCMs properties. These solid fatty acids were also analyzed by GC-FID [22] and FT-IR. To prepare DHSA the crystallization process was scaled up to 200 g of FFA using methanol at -20˚C. The mother liquor was concentrated under vacuum to achieve a highly unsaturated fatty acid mixture.

3.3.2.2 Synthesis of DHSA from the high unsaturated fatty acid mixture

The synthesis of DHSA has been widely described appearing as early as end 19th and early 20th [21]. Swern described on 1959 the synthesis of DHSA from commercial oleic acid [23]. In this procedure, a high amount of hazardous formic acid and hydrogen peroxide are mixed with oleic acid producing a high exothermic reaction. Once the formic acid is removed by distillation, sodium hydroxide is added to hydrolyze the ester moiety and hydrochloric acid is finally added to liberate the FFA. Recently, the epoxidation and hydrolysis of triacylglycerols [24, 25] has been described and patented [26]. These publications studied and optimized the amount of reactants and the conditions to achieve the products using less amounts of reactants and also involving milder conditions. Even though the preparation of crude DHSA from animal sources is claimed, the patented procedure is described and preferred for palm oil-based oleic acid [26]. These last decades palm oil production has been revised and reviewed due to their contribution in deforestation and their affect in biodiversity [27–29]. Malaysia and Indonesia produce more than the 80% of all palm oil [28]. Unfortunately, 55-59% of oil palm expansion in Malaysia, and at least 56% of that in Indonesia occurred at the expense of forests during the period 1990–

2005 [29]. Besides, demand of palm oil is predicted to continue increasing [30] with potentially suitable areas for oil palm cultivation in Southeast Asia, Latin America and Central Africa [28, 29]. In opposite, this study uses non-edible animal fats as a source to prepare DHSA. As a summary, the mixture of highly unsaturated FFA recovered from the mother crystallization liquor was mixed with moderate amounts of formic acid and then hydrogen peroxide was added drop wise [24–26]. Once the double bonds were epoxidized, the temperature was increased to lead all the epoxide groups react with the FFA and formic acid yielding the corresponding esters. Subsequently, sodium hydroxide was added to hydrolyze the ester groups and sulfuric acid was finally added to liberate the FFA [23]. Finally, the crude mixture of reaction was crystallized to recover pure DHSA.

Thereby, 8.32 mL (208.1 mmol) of formic acid were added to a mechanically stirred cylindrical jacketed glass reactor (5 L) containing 100 g of the highly unsaturated fatty acids previously obtained from the mother liquor. The mixture was stirred at 300 rpm. Afterwards, 130 mL of 30% H_2O_2 (1.141 mol) solution were added drop wise at 4˚C. Once the addition was finished, the temperature was driven up to 60˚C and the reaction mixture was stirred for 18 h at 60˚C. The resulting epoxide groups were hydrolyzed for 3 h at 100˚C. Ethanol (100 mL) was added to the reactor, and esters were hydrolyzed by a drop wise addition of 100 mL of 20% NaOH solution at 60˚C. The reaction mixture was stirred under reflux for 30 min and afterwards driven at pH=2 by adding drop wise 25 mL of 98% H_2SO_4. The aqueous layer was discarded and the organic phase was washed twice with 300 mL of a 20% NaCl aqueous solution at 60˚C. The crude DHSA was recovered yielding 106 g (95% yield). The crude was dissolved in hot ethyl acetate (1 g of solute:1 mL of solvent) and let to crystallize for 24 h at 4˚C.

The resulting white powder was recovered by filtration under vacuum in a Pyrex crucible n° 3 and then washed three times with cold ethyl acetate (74% isolated yield). M.P: 94.5°C (DSC first cycle). The final white powder was analyzed by FT-IR and ^{1}H NMR (see **Annexes I** and **II**):

DHSA: ^{1}H RMN (400 MHz, $CDCl_3$) δ ppm: 0.88 (t, J=6.9 Hz, CH_3), 1.19 - 1.55 (m, CH_2), 1.63 (m, βCH_2), 2.34 (t, J=7.4 Hz, αCH_2), 3.40 (m, HCOH).

3.3.2.3 Synthesis of DHSA salts

To a solution containing 1 g (3.16 mmol) of DHSA in 10 mL of methanol, 3.32 mmol of NaOH or LiOH•H_2O in 10 mL of water were added under high stirring speed. Afterwards, the reaction temperature was increased until the solution became transparent and then let it cold until precipitated appeared. The calcium and magnesium salts were prepared from the sodium salt solution by adding drop wise 3.48 mmol of $CaCl_2$ or $MgCl_2$ in 10 mL of water. The precipitates were recovered by filtration under vacuum in a Pyrex crucible n°3. All the products were analyzed by FT-IR and NMR (see **Annexes I** and **II**):

Litium salt of DHSA: ^{1}H RMN (400 MHz, $DOCD_3$) δ ppm: 0.90 (t, J=6.9 Hz, C**H$_3$**), 1.22 - 1.54 (m, C**H$_2$**), 1.60 (m, β**CH$_2$**), 2.17 (t, J=7.5 Hz, αC**H$_2$**), 3.32 (m, **H**COH). ^{13}C RMN (400 MHz, $DOCD_3$) δ ppm: 13.08 (**C**H_3), 22.36 (**C**H_2CH_3), 25.69, 25.72 (**C**H_2CH_2CHOH), 26.60-29.57 (**C**H_2), 31.70 (CH_3CH_2**C**H_2), 32.68, 32.69 (**C**H_2CHOH), 37.39 (α**C**H_2), 73.80 (**C**HOH), 181.72 (**C**OO^-).

Sodium salt of DHSA: ^{1}H RMN (400 MHz, $DOCD_3$) δ ppm: 0.94 (m, C**H$_3$**), 1.28-1.60 (m, C**H$_2$**), 1.64 (m, β**CH$_2$**), 2.19 (t, J=7.5 Hz, αC**H$_2$**), 3.41 (m, **H**COH). ^{13}C RMN (400 MHz, $DOCD_3$) δ ppm: 13.09 (**C**H_3), 22.37 (**C**H_2CH_3), 25.69, 25.72 (**C**H_2CH_2CHOH), 26.63-29.61 (**C**H_2), 31.70 (CH_3CH_2**C**H_2), 32.68, 32.69 (**C**H_2CHOH), 37.93 (α**C**H_2), 73.85 (**C**HOH), 181.73 (**C**OO^-).

Magnesium salt of DHSA: ^{1}H RMN (400 MHz, $DOCD_3$) δ ppm: 0.92 (m, C**H$_3$**), 1.25-1.56 (m, C**H$_2$**), 1.64 (m, β**CH$_2$**), 2.19 (t, J=7.5 Hz, αC**H$_2$**), 3.38 (m, **H**COH). ^{13}C RMN (400 MHz, $DOCD_3$) δ ppm: 13.08 (**C**H_3), 22.36 (**C**H_2CH_3), 25.69, (**C**H_2CH_2CHOH), 26.05-29.60 (**C**H_2), 31.70 (CH_3CH_2**C**H_2), 32.58 (**C**H_2CHOH), 37.38 (α**C**H_2), 73.92 (**C**HOH), 182.27 (**C**OO^-).

Calcium salt of DHSA: ^{1}H RMN (400 MHz, $DOCD_3$) δ ppm: 0.90 (m, C**H$_3$**), 1.25-1.56 (m, C**H$_2$**), 1.64 (m, β**CH$_2$**), 2.17 (t, J=7.5 Hz, αC**H$_2$**), 3.37 (m, **H**COH). ^{13}C RMN (400 MHz, $DOCD_3$) δ ppm: 13.08 (**C**H_3), 22.35 (**C**H_2CH_3), 25.70, (**C**H_2CH_2CHOH), 26.04-29.59 (**C**H_2), 31.72 (CH_3CH_2**C**H_2), 32.55 (**C**H_2CHOH), 37.38 (α**C**H_2), 73.92 (**C**HOH), 182.30 (**C**OO^-).

3.3.3. Characterization

FT-IR spectroscopy was performed in order to identify the characteristic structure of PA-SA eutectic mixture, DHSA and DHSA salts. FT-IR spectra were recorded with a Jasco 6300 FT-IR spectrometer coupled with an ATR accessory.

The DHSA structure and purity was determined by ^{1}H NMR spectroscopy. This technique allowed the evaluation of the purity of this product by comparing the signals related to **H**-COH (hydrogen bonded to a secondary alcohol) and R_1C**H$_2$**COOH (hydrogen bonded to the α-carbon of the carboxylic acid) [31]. Moreover, this technique was also used to evaluate the DHSA content after this product was analyzed by DSC technique. ^{1}H NMR spectra were recorded

with a MERCURY plus NMR Spectrometer Systems VARIAN Imant AS operating at 400 MHz.

GC-FID is commonly used on the analysis of mixtures of FFA to determine the percentage of each fatty free acid. GC-FID was used to characterize the fatty acid contents in the non-edible animal fat, the PA-SA eutectic mixtures and the highly unsaturated fatty acid mixture. These fatty maters were analyzed in triplicate using a ThermoQuest series 2000 chromatograph equipped with a FID detector, an EEP system (Fisons, Barcelona, Spain), a split/ split-less injection system and an autosampler. The analytical column (Supelco, Madrid, Spain) was a 30 m x 0.25 mm fused-silica capillary coated with 0.25 mm film thickness of poly(80% biscyanopropyl–20% cyanopropylphenyl siloxane) (SP-2330), and was temperature programmed from 150 to 220˚C at 5˚C•min^{-1} then held at 220˚C for 6 min.

Thermophysical characterization was performed with differential scanning calorimetry (DSC 822e from Mettler Toledo) in order to analyze the phase change temperature and phase change enthalpies (melting and solidification). Measurements were conducted using a three cycle program repetitions. The first cycle was disregarded and, thus, the mean value of the two following cycles was calculated and the results were presented in a confidence interval of 95%. The second and the third cycle were performed at 0.5˚C•min^{-1} under flowing 80 mL•min^{-1} nitrogen gas. The DSC analyses were performed between 30 and 250˚C depending on the melting point of the product studied. The mass of sample used was around 5 mg and the samples were located into 40 µL aluminum crucibles. The equipment accuracy was ± 0.1˚C for temperature and ±3 kJ•kg^{-1} for enthalpy determinations.

The thermal cycling reliability is crucial for the application of PCMs, in fact only a thermal stable phase change temperature and latent heat of PCMs after a large number of thermal cycles makes possible the PCMs purpose. To study the thermal cycling reliability, an accelerated thermal cycle experiment was performed to analyze the changes of the phase change temperature and latent heat of the PA-SA eutectic mixtures after 1000 thermal cycles. In order to study the thermal cycling stability and reliability, new material samples were cycled in a thermal cycler Bioer Gene Q T-18. A tube volume of 0.5 mL was used for each compound. A dynamic method was established using a temperature range between 30 and 70˚C and at 4˚C•s^{-1} for cooling and 5˚C•s^{-1} for heating. A total of 1000 cycles were performed under the described conditions. Finally, the compounds were recovered and a new DSC test was performed. Notice that this study presents results when performing 1000 cycles, which would be around 3 years of operation if the PCM implemented in a system cycled once per day [32].

3.4. Results and Discussions

3.4.1. FT-IR characterization of the PA-SA eutectic mixture, DHSA and their salts

Table 3.1 shows the assigned wave number (cm^{-1}) of the compounds synthesized. PA-SA eutectic mixture FT-IR spectra shows a band signal at 2955 cm^{-1} associated to the asymmetrical stretching vibration of -CH_3 while the bands at 2917 cm^{-1} and 2845 cm^{-1} responds to the symmetrical and asymmetrical stretching modes of –CH_2 group, respectively. A characteristic band at 1697 cm^{-1} represents the asymmetrical stretching vibration (ω_2) of C=O. The band at 1460 cm^{-1} is the -CH_2 deformation while 1409 cm^{-1} has its

origin in the C=O symmetrical stretching vibration (ω_1). The band at 1295 cm^{-1} represents -CH_2 twist and wag and the band at 935 cm^{-1} responds to C=O deformation (ω_3). The -CH_2 rocking vibration and bending is associated to a band at 721 cm^{-1}.

The bands at 3332 cm^{-1} and 3244 cm^{-1} correspond to DHSA (O-H stretching vibration). A characteristic band signal at 2952 cm^{-1} responds to the asymmetrical stretching vibration of -CH_3 while the bands at 2910 cm^{-1} and 2848 cm^{-1} are associated with the symmetrical and asymmetrical stretching modes of –CH_2 group, respectively. The band at 1704 cm^{-1} is the characteristic absorption band for asymmetrical stretching vibration (ω_2) of C=O. The band at 1468 cm^{-1} corresponds to the -CH_2 deformation while 1411 cm^{-1} respond to the C=O symmetrical stretching vibration (ω_1). The bands at 1331 cm^{-1} and 1295 cm^{-1} have its origins on the –OH bending and -CH_2 twist and wag, respectively. The –OH stretching is associated with a band at 1078 cm^{-1}. At 923 cm^{-1} and 721 cm^{-1} are observed the C=O deformation (ω_3) and -CH_2 rocking vibration and bending, respectively.

Table 3.1. Absorption Maxima (cm^{-1}) in the FT-IR spectra of PA-SA eutectic mixture, DHSA and their salts. (see **Annex II**).

Wave number (cm^{-1})						Assignment
PA-SA eutectic	**DHSA**	**Litium salt of DHSA**	**Sodium salt of DHSA**	**Calcium salt of DHSA**	**Magnesium salt of DHSA**	
-	3332 3244	3284	3290	3266	3300	**Broad absorption of O-H stretching vibration**
2955	2952	-	2950	2952	-	**CH_3, C-H asymmetrical stretching**
2917	2910	2916	2917	2917	2920	**CH_2, C-H asymmetrical stretching**
2845	2848	2847	2848	2848	2852	**CH_2, C-H symmetrical stretching**
1697	1704	1562	1558	1571 1535	1600	**C=O asymmetrical stretching vibration (ω_2)**
1460	1468	1463	1463	1464	1468	**CH_2 deformation**
1409	1411	1399	1435- 1415	1428	1399	**C=O symmetrical stretching vibration (ω_1)**
-	1331	1335	1328	1325	1335	**O-H bending**
1295	1295	-	-	-	-	**-CH_2 twist and wag**
-	1078	1078	1078	1078	1078	**O-H stretching**
935	923	-	-	-	-	**C=O deformation (ω_3)**
721	721	718	718	718	721	**-CH_2 rocking and bending**

The broad absorption band of O-H stretching vibration band is present in all the salts within 3300 cm^{-1} and 3266 cm^{-1} depending on the salt. The band corresponding to the asymmetrical stretching vibration of -CH_3 is only observed in calcium (2952 cm^{-1}) and sodium (2950 cm^{-1}) spectra salts. Otherwise, the bands at ~2920 cm^{-1} and ~2850 cm^{-1} associated to the symmetrical and asymmetrical stretching modes of –CH_2 group are present

in all spectra. The band at 1704 cm^{-1} characteristic for asymmetrical stretching vibration (ω_2) of C=O previously observed in DHSA spectra can now be found at the region around 1600-1535 cm^{-1} upon formation of the carboxylate anion. Moreover, calcium salt spectra presents two bands for the asymmetrical stretching vibration (ω_2) of C=O (1571 and 1535 cm^{-1}). The band at around 1460 cm^{-1} characteristic for the -CH_2 deformation and the band at around 1400-1430 cm^{-1} for the C=O symmetrical stretching vibration (ω_1) are present in all the spectra. The –OH bending and –OH stretching are also present, which have its origins in bands at ~1330 cm^{-1} and 1078 cm^{-1}, respectively. Finally, the band corresponding to the C=O deformation (ω_3) observed in the previous FFA analyzed disappears in all the salts but the -CH_2 rocking vibration and bending is maintained at ~720 cm^{-1}.

3.4.2. Composition, thermal properties and reliability of the PA-SA eutectic mixture prepared by crystallization

The preparation of a eutectic mixture from PA-SA allows of the preparation of PCMs useful in applications such as to improve the thermal comfort in buildings through heating applications, improve domestic hot water (DHW) tanks efficiency [33, 34], air conditioning condensation heat recovery systems [3], and low temperature industrial waste heat (IWH) recovery [35]. Depending on the application, palmitic acid and stearic acid present too high phase change temperatures (*Tm*). Eutectic mixtures allow the decrease of the *Tm*. In this case, the animal fat used showed a 3:2 palmitic/stearic acid ratio (w:w). This ratio is very close to the palmitic/stearic acid ratio showing eutectic properties, which can lead to the PCM indicated above [3, 36]. Hence, authors realized that by an optimal crystallization, the unsaturated

fatty acids and the saturated fatty acids could be separated with the advantage of preparing in the crystallization process a eutectic PA-SA mixture [14]. **Table 3.2** shows the thermal properties of the PA-SA eutectic mixtures. The solute/solvent ratio and crystallization temperature implied higher saturated fatty acid recovery with no presence of unsaturated fatty acids. In these conditions, between 76 to 90% of the palmitic and stearic acids present in the starting hydrolyzed animal fat were recovered in form of eutectic mixtures.

The palmitic/stearic acid ratios determined by GC-FID [22] ranged from 63.2:36.8 for the ethyl acetate crystallization to 58.7:41.3 in the case of the methanol crystallization. Similar compositions such as 62:38 [3] and 64.2:35.8 [36] were described in the preparation of eutectic mixtures starting from commercially pure palmitic and stearic acids. The DSC curve of the bio-based mixtures prepared from non-edible fats showed one sharp endothermic peak during the melting process and one sharp exothermic peak on the solidification process, which indicates that only one real eutectic mixture has been obtained after crystallization. The melting and solidification temperatures around 55 and 52˚C, respectively, measured by DSC analysis were lower than the melting points of the pure palmitic or stearic acids [3]. These results were close to those reported on the preparation of PA-SA eutectic mixtures of commercial palmitic and stearic acids, with melting points of 53.89 [3] and 52.3˚C [36] and a solidification temperature of 54.37˚C [3]. The latent heats of melting of the eutectic mixtures prepared ranged from 183 to 176 $kJ \bullet kg^{-1}$ and the solidification latent heats from 181 to 172 $kJ \bullet kg^{-1}$ depending on the mixture achieved. Similar results of latent solidification heat, 177.67 $kJ \bullet kg^{-1}$ [3] and

181.7 kJ•kg^{-1} [36], were described in the PA-SA eutectic mixtures prepared from commercial palmitic and stearic acids.

Table 3.2. Thermal properties of the PA-SA mixtures prepared from the hydrolyzed animal fat by crystallization with various solvents. (see **Annex III**)

Crystallization solvent	**Cycling aspects**	**H $_{Melting}$ (kJ•kg^{-1})**	**H $_{Solidification}$ (kJ•kg^{-1})**	**T $_{Melting}$ (˚C)**	**T $_{Solidification}$ (˚C)**
Ethyl acetate	Not-cycled	182±8	181±14	54.9	52.0
	Cycled (1000)	161±3	160±1	54.9	52.2
	Property loss (%)	11	11	-0.1	-0.3
Acetone	Not-cycled	183±5	181±5	54.1	52.5
	Cycled (1000)	161±3	158±2	54.8	52.3
	Property loss (%)	12	13	-1.2	0.5
Ethanol	Not-cycled	183±8	180±8	55.2	52.3
	Cycled (1000)	158±2	155±2	55.0	52.2
	Property loss (%)	14	14	0.4	0.1
Hexane	Not-cycled	176±6	172±10	53.4	52.1
	Cycled (1000)	157±1	153±1	54.3	51.5
	Property loss (%)	11	11	-1.8	1.1
Methanol	Not-cycled	179±11	178±10	55.0	52.1
	Cycled (1000)	164±2	158±2	55.0	52.6
	Property loss (%)	9	11	0.0	-1.1

In general terms, after thermal cycling, solidification and melting enthalpies present similar reduction in their values with a maximum decrease of 14% (**Table 3.2**). These loses are below 15% after thermal cycling, which indicated that the material shows good thermal cycling stability [37]. Moreover, phase-change temperature (i.e. melting and solidification) does not present outstanding changes, ranging from -1.8 to 1.1 %. According to the distinct mixtures prepared, the product crystallized in methanol presented the best thermal cycling stability since melting enthalpy only decreased by 9% and solidification enthalpy by 11% while the ones crystallized in ethanol present the worst (14% reduction). Moreover, the mixtures crystallized in methanol showed the highest latent heat after 1000 heating/cooling cycles of the whole materials under study: 164 $kJ \bullet kg^{-1}$ (melting enthalpy), 158 $kJ \bullet kg^{-1}$ (solidification enthalpy). Thus, these mixtures prepared in an easy and robust process can be considered as potential PCM candidates due to their thermal performance and thermal cycling stability and reliability.

3.4.3. Determination of the thermal properties of DHSA and their salts

Table 3.3 shows the thermal properties of DHSA and their salts prepared from the animal fat waste. The variation of enthalpy and melting point observed along the two recorded cycles announced the poor cycling stability of DHSA. Presumably, the diol and carboxylic acid moieties present in DHSA reacted forming an estolide with a decreasing response on the enthalpies as well as a modification on the phase change temperature. To confirm this hypothesis, the content in the DSC crucible was recovered and analyzed by

^{1}H NMR spectroscopy (see **Annex I**). Two new signals appeared at 3.58 ppm and 4.83 ppm, which can be assigned to **H**-COH (hydrogen bonded to a secondary alcohol) and R1COOC**H**R_2 (hydrogen bonded to a secondary alcoxyester), respectively. These signals are characteristics of a DHSA-estolide [38]. Nevertheless, the first DSC analysis cycle recorded a melting temperature of 94.5˚C [39] and also the narrow enthalpy peaks observed indicated that the developed process allowed the preparation of pure DHSA. Therefore, the melting enthalpy on the first recorded cycle (168 kJ•kg^{-1}) and a phase change temperature higher than non-derivatized fatty acids are remarkable. These values are promising for PCM interests but the low cycling stability makes obvious the need of avoiding the formation of the detected DHSA-estolides.

The DHSA salts were synthesized presupposing the maintenance of the good enthalpy values of DHSA and trying to improve the poor cycling stability. Nevertheless, **Table 3.3** shows that none of the salts synthesized presented a suitable behavior to be used as PCMs. Only calcium diol salt shows melting and solidification, but with a low phase change enthalpy value, whereas magnesium salt does not show melting process. Unfortunately, lithium salt did not shown solidification capability, although showed a very promising melting enthalpy value (236 kJ•kg^{-1}).

Table 3.3 Thermal properties of DHSA and their salts. (see **Annex III**).

Product	**$H_{Melting}$** **(kJ•kg^{-1})**	**$H_{Solidification}$** **(kJ•kg^{-1})**	**$T_{Melting}$** **(˚C)**	**$T_{Solidification}$** **(˚C)**
DHSA	161±11	151±7	93.8	82.8
Lithium salt of DHSA	236	-	231.6	-
Sodium salt of DHSA	82	-	204.7	-
Calcium salt of DHSA	76±2	68±4	160±1	127±1

3.5. Conclusions

This paper shows new applications to non-edible animal fat waste by preparing eutectic mixtures of PA-SA and pure DHSA. These compounds were achieved from animal fat by a conventional hydrolysis (99% yield) process. Various solvents can be used to perform the crystallization process. This led to recoveries up to 90% of the PA-SA content in the animal fat. These eutectic mixtures of PA-SA showed good performance as PCMs. The melting and solidification temperatures of the various PA-SA PCM prepared were around 55 and 52˚C, respectively. Moreover, the latent heats of the crystallized fractions ranged from 172 to 181 kJ•kg^{-1}. Thermal cycling test results indicated a good thermal cycling reliability of PA-SA because the

melting and solidification temperatures of PA-SA PCM oscillated only up to 1.8 and 1.1%, respectively. Concerning the melting and solidification latent heats of the eutectic PCM, they decreased up to 14% after 1000 thermal cycles in the most pronounced case. Moreover, DHSA was synthesized from non-edible animal fat. This dihydroxy fatty acid was prepared from the unsaturated fatty acids present in the mother crystallization liquor, which evidences the opportunity of provide distinct applications to animal fat. The DSC analysis performed for first time on DHSA and their salts revealed no potential use as PCM. Nevertheless, a good melting enthalpy and a phase-change temperature higher than common fatty acids could be promising for PCM interests. The modification of DHSA to new phase change materials with improved cycling stability is now undergone.

3.6. References

[1] Ramani K, John Kennedy L, Ramakrishnan M, Sekaran G. Purification, characterization and application of acidic lipase from Pseudomonas gessardii using beef tallow as a substrate for fats and oil hydrolysis. Process Biochem 2010;45:1683–91.

[2] Adamczak M, Bednarski W. Enhanced activity of intracellular lipases from Rhizomucor miehei and Yarrowia lipolytica by immobilization on biomass support particles. Process Biochem 2004;39:1347–61.

[3] Zhang N, Yuan Y, Du Y, Cao X, Yuan Y. Preparation and properties of palmitic-stearic acid eutectic mixture/expanded graphite composite as phase change material for energy storage. Energy 2014;78:950–6.

[4] Farid MM, Khudhair AM, Razack SAK, Al-Hallaj S. A review on phase change energy storage: Materials and applications. Energy Convers Manag 2004;45:1597–615.

[5] Yu S, Jeong SG, Chung O, Kim S. Bio-based PCM/carbon nanomaterials composites with enhanced thermal conductivity. Sol Energy Mater Sol Cells 2014;120:549–54.

[6] Hu W, Yu X. Thermal and mechanical properties of bio-based PCMs encapsulated with nanofibrous structure. Renew Energy 2014;62:454–8.

[7] Hu W, Yu X. Encapsulation of bio-based PCM with coaxial electrospun ultrafine fibers. RSC Adv 2012;2:5580–4.

[8] Jeong SG, Chung O, Yu S, Kim S, Kim S. Improvement of the thermal properties of Bio-based PCM using exfoliated graphite nanoplatelets. Sol Energy Mater Sol Cells 2013;117:87–92.

[9] Jeong SG, Lee JH, Seo J, Kim S. Thermal performance evaluation of bio-based shape stabilized PCM with boron nitride for energy saving. Int J Heat Mass Transf 2014;71:245–50.

[10] Kosny J, Kossecka E, Brzezinski A, Tleoubaev A, Yarbrough D. Dynamic thermal performance analysis of fiber insulations containing bio-based phase change materials (PCMs). Energy Build 2012;52:122–31.

[11] Yuan Y, Zhang N, Tao W, Cao X, He Y. Fatty acids as phase change materials: A review. Renew Sustain Energy Rev 2014;29:482–98.

[12] Zhang N, Yuan Y, Yuan Y, Li T, Cao X. Lauric-palmitic-stearic acid/expanded perlite composite as form-stable phase change material: Preparation and thermal properties. Energy Build 2014;82:505–11.

[13] Yanping Y, Wenquan T, Xiaoling C, Li B. Theoretic prediction of melting temperature and latent heat for a fatty acid eutectic mixture. J Chem Eng Data 2011;56:2889–91.

[14] Gallart-Sirvent P, Yara E, Villorbina G, Balcells M, Sala N, Canela-Garayoa R. Recycling Rhizopus oryzae resting cells as biocatalyst to prepare near eutectic palmitic-stearic acid mixtures from non-edible fat. J Mol Catal B Enzym 2016;134:172–7.

[15] Godard A, Thiebaud-Roux S, De Caro P, Vedrenne E, Mouloungui Z. New one-pot syntheses of ketals and acetals from oleic acid. Ind Crops Prod 2014;52:111–7.

[16] Kulik A, Martin A, Pohl M-M, Fischer C, Köckritz A. Insights into gold-catalyzed synthesis of azelaic acid. Green Chem 2014;16:1799.

[17] Kulik A, Janz A, Pohl MM, Martin A, Köckritz A. Gold-catalyzed synthesis of dicarboxylic and monocarboxylic acids. Eur J Lipid Sci Technol 2012;114:1327–32.

[18] Benessere V, Cucciolito ME, De Santis A, Di Serio M, Esposito R, Ruffo F. Sustainable process for production of azelaic acid through oxidative cleavage of oleic acid. J Am Oil Chem Soc 2015;92:1701–7.

[19] KosheelaDevi PP, Tuan Noor Maznee TI, Hoong SS, Nurul 'Ain H, Mohd. Norhisham S, Norhayati MN. Performance of palm oil-based dihydroxystearic acid as ionizable molecule in waterborne polyurethane dispersions. J Appl Polym Sci 2016;133:1–10.

[20] Filley J. New lubricants from vegetable oil: Cyclic acetals of methyl 9, 10-dihydroxystearate. Bioresour Technol 2005;96:551–5.

[21] Koay GFL, Chuah T, Zainal-abidin S, Ahmad S, Choong TSY. Development, characterization and commercial application of palm based dihydroxystearic acid and Its derivatives : an overview 2011;265:237–65.

[22] Eras J, Montañes F, Ferran J, Canela R. Chlorotrimethylsilane as a reagent for gas chromatographic analysis of fats and oils. J Chromatogr A 2001;918:227–32.

[23] Swern, D, Scanlan JT, Dickel GB. 9, 10-Dihydroxystearic Acid. Org Synth 1959;39:15.

[24] Gamage PK, O'Brien M, Karunanayake L. Epoxidation of some vegetable oils and their hydrolysed products with peroxyformic acid - optimised to industrial scale. J Natl Sci Found Sri Lanka 2009;37:229–40.

[25] Okieimen FE, Pavithran C, Bakare IO. Epoxidation and hydroxlation of rubber seed oil: One-pot multi-step reactions. Eur J Lipid Sci Technol 2005;107:330–6.

[26] Palm oil-based hydroxy fatty acids. EP., EP001588999A2, 2005.

[27] Gaveau DL, Wich S, Epting J, Juhn D, Kanninen M, Leader-Williams N. The future of forests and orangutans (Pongo abelii) in Sumatra: predicting impacts of oil palm plantations, road construction, and mechanisms for reducing carbon emissions from deforestation. Environ Res Lett 2009;4:19.

[28] Fitzherbert EB, Struebig MJ, Morel A, Danielsen F, Brühl CA, Donald PF. How will oil palm expansion affect biodiversity? Trends Ecol Evol 2008;23:538–45.

[29] Koh LP, Wilcove DS. Is oil palm agriculture really destroying tropical biodiversity? Conserv Lett 2008;1:60–4.

[30] Carter C, Finley W, Fry J, Jackson D, Willis L. Palm oil markets and future supply. Eur J Lipid Sci Technol 2007;109:307–14.

[31] Wu Y, Li A, Li K. Pressure sensitive adhesives based on oleic acid. J Am Oil Chem Soc 2014;92:111–20.

[32] Sari A. Thermal reliability test of some fatty acids as PCMs used for solar thermal latent heat storage applications. Energy Convers Manag 2003;44:2277–87.

[33] Cabeza LF, Castell A, Barreneche C, De Gracia A, Fernández AI. Materials used as PCM in thermal energy storage in buildings: A review. Renew Sustain Energy Rev 2011;15:1675–95.

[34] Kousksou T, Bruel P, Cherreau G, Leoussoff V, El Rhafiki T. PCM storage for solar DHW: From an unfulfilled promise to a real benefit. Sol Energy 2011;85:2033–40.

[35] Brückner S, Liu S, Miró L, Radspieler M, Cabeza LF, Lävemann E. Industrial waste heat recovery technologies: An economic analysis of heat transformation technologies. Appl Energy 2015;151:157–67.

[36] Baran G, Sari A. Phase change and heat transfer characteristics of a eutectic mixture of palmitic and stearic acids as PCM in a latent heat storage system. Energy Convers Manag 2003;44:3227–46.

[37] Solé A, Neumann H, Niedermaier S, Cabeza LF, Palomo E. Thermal stability test of sugar alcohols as phase change materials for medium temperature energy storage application. Energy Procedia 2014;48:436–9.

[38] Awang R, Azizan A, Ahmad S, Yunus W. Characterization of estolides from dihydroxystearic acid. J Oil Palm Res 2007;19:350–5.

[39] Swern D, Jordan EF. Aliphatic esters of the 9, 10-dihydroxystearic acids. J Am Chem Soc 1945;67:902–3.

Chapter IV

A sustainable approach to prepare new phase change materials from non-edible animal fat

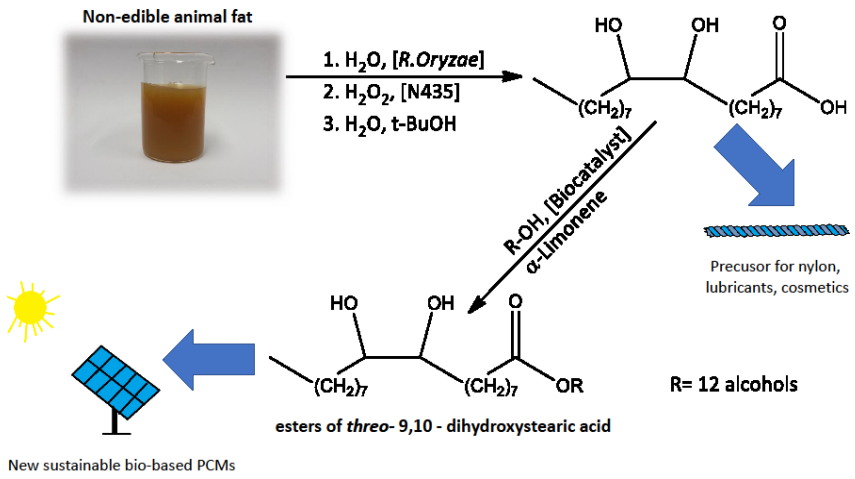

Part of the results described in this chapter have been submitted to: Green Chemistry.

4.1. Abstract

The thermal properties of various alkyl *threo*-9, 10-dihydoxy stearates (DHSEs) prepared from non-edible fat were studied. These esters were synthesized by combining *R. orzyzae* resting cells, immobilized CAL-B, and hot water. Specifically, non-edible animal fat was hydrolyzed in a 93% yield with *R. orzyzae* resting cells. Crude unsaturated fatty acids were recovered after performing a crystallization step to obtain the saturated fatty acids. The unsaturated fatty acids were epoxidized with 30% H_2O_2 using immobilized CAL-B. The epoxy ring was cleaved with hot water in the presence of *tert*-butanol (*t*-BuOH). The two reactions were also studied using commercial oleic acid as substrate. Pure *threo*-9, 10-dihydroxystearic acid (DHSA) from animal fat was recovered by crystallization (51% yield). Subsequently, DHSA was enzymatically esterified in α-limonene to produce twelve DHSEs (58-90% yield). DSC (differential scanning calorimetry) analysis of these esters revealed potential latent heats ranging from 136.83 to 234.22 kJ•kg^{-1}. The melting temperatures of these compounds ranged from 52.45 to 76.88°C, as also determined by DSC. Finally, the compounds with enthalpies above 200 kJ•kg^{-1} were subjected to 100 and 1000 thermal cycles and were observed to present good thermal reliability. The novel sustainable approach described herein is valuable for the preparation of DHSEs from non-edible animal fat. In addition, these esters showed thermal reliability from 50 to 77°C and thus show promise for thermal energy storage applications.

Keywords: bioeconomy, bio-based PCM, *threo*-9, 10-dihydroxystearic acid synthesis, α-limonene, fatty acids, differential scanning calorimeter.

Abbreviations of this chapter: CAL-B, *Candida antarctica* Lipase-B; DHSA, *threo*-9, 10-dihydroxystearic acid; DHSE, *threo*-9, 10-dihydroxy stearate; DHW, domestic hot water; DSC, differential scanning calorimetry; GC-FID, gas chromatography-flame ionization detector; IWH, industrial waste heat; PCM, phase-change material; *t*-BuOH, *tert*-butanol.

4.2. Introduction

It has been estimated that the world population will reach 9.2 billion by 2050 [1]. Such growth will bring with it a significant increase in livestock production and animal by-products. In this regard, by-products account for almost 60% of the body weight of a farm animal, while 20% corresponds to non-edible ones. Furthermore, dead and fallen animals increase the amount of non-edible by-products. In this scenario, the reuse of non-edible by-products gains increasing relevance given the public health concerns associated with the non-utilization of such products [2]. Fatty non-edible animal parts comprise mainly triacylglycerides, which contain saturated and unsaturated fatty acids and glycerol. These fats are an interesting source to prepare biodiesel [3] and recently they have been used to prepare phase change materials (PCMs) as shown in **Chapter III** [4].

PCMs have the capacity to store heat energy during the phase-change that occurs during melting and solidification processes. In this regard, fatty acids present good purposes due to a high thermal and chemical stability and a high heat capacity [5, 6]. In addition, fatty acids and their derivatives are an excellent source of renewable materials, providing alternatives to currently predominant PCMs such as paraffins and salts [7, 8]. Commercially available fatty acid derivatives have recently been proposed as bio-based organic

PCMs. These acids result from the partial hydrogenation of soy-wax [9, 10] or from the hydrogenation of unsaturated triacylgicerides [11-14]. These approaches allow the substitution of paraffin; however, the use of edible oil raises concerns about the likely surplus of food that might cause starvation, especially in the developing countries [15]. Furthermore, although hydrogenation promotes stability during phase-change cycles with no risk of oxidation [12, 13], the conversion of unsaturated fatty acids to saturated fatty acids circumvents the opportunity of using them for other potential applications.

The unsaturated moieties in fatty acids play an important role in the synthesis of monomers and polymers from fats and oils. The epoxy fatty acid derivatives produced from unsaturated oils allow the formation of pressure-sensitive adhesives (PSAs) [16, 17], rubbers [18], coatings [18], polyurethanes [18], and acrylate resins [18]. In addition, oleic acid can be converted to DHSA and cleaved in an oxidative manner to azelaic acid in a green and efficient gold-catalyzed system [19, 20]. DHSA has recently been used as starting material for the preparation of lubricants [21], estolides [22], soaps [22], deodorant sticks [22], and shampoos [22]. Nevertheless, common lab-scale synthesis of DHSA from commercial oleic acid usually involves the use of chemicals, including formic acid, NaOH and HCl [23] or $MgSO_4$, Na_2SO_3 and hexane [19]. In terms of the bio-based production of DHSA, a recently patented procedure using formic acid and hydrogen peroxide allows the preparation of crude DHSA from palm oil-based oleic acid [24]. Nevertheless, palm oil production has been revised and reviewed due its contribution to deforestation and the resulting effects on biodiversity [25-27].

In **Chapter III**, a procedure was described using conventional chemistry to achieve eutectic mixtures of palmitic-stearic acid with thermal energy

storage capabilities (as PCM) from non-edible animal fats. The remaining unsaturated fatty acids were converted into DHSA using formic acid and hydrogen peroxide. In that study, the performance of DHSA as a PCM was also tested by DSC. Although DHSA presented satisfactory enthalpies, a high decrease in enthalpy was observed when cycling, thereby highlighting low chemical stability, presumably caused by the formation of estolides between the diol and fatty acid moieties. To avoid this esterification during cycling, some salts were prepared and also analyzed by DSC; however, DHSA showed poor performance as a PCM [4]. Since the use of esters of fatty acids as PCMs [28-32] has been widely described, the preparation of alkyl *threo*-9, 10-dihydoxy stearates (DHSEs) could allow the preparation of products with acceptable enthalpies and improved thermal cycling stability. Certainly, the presence of the ester group should prevent estolide formation. In addition, alkyl hydroxyl stearates have shown interesting applications as lubricants [21], plasticizers [33, 34], mold-release agents [33, 34], waxes [33, 34], surfactants [33, 34], and chemical intermediates [33, 34].

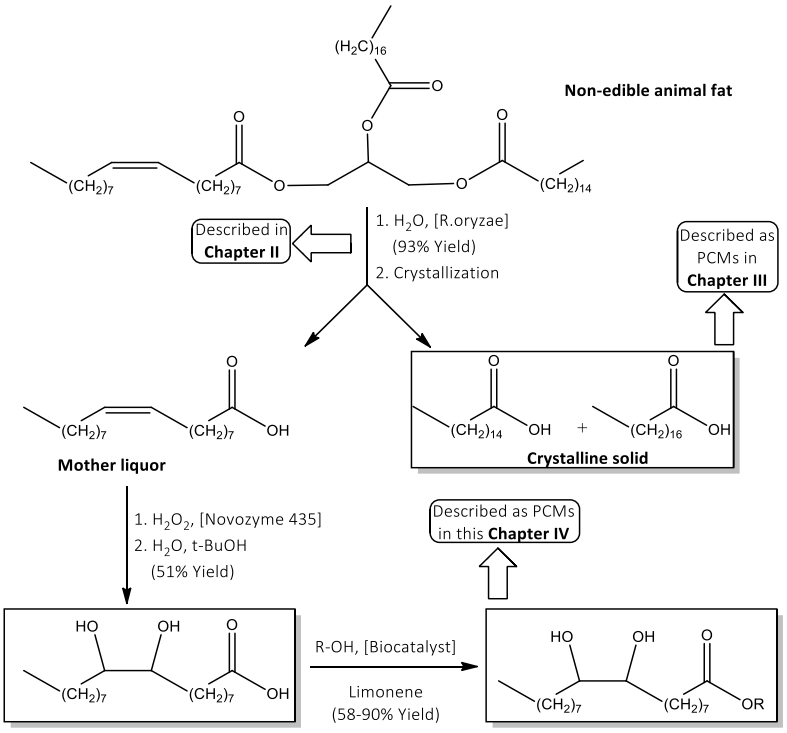

Figure 4.1. Green syntheses afforded in this study. The triacylglycerol represents three different fatty acids present on the starting material.

The present work is the first to apply sustainable chemistry and biocatalysts to prepare PCMs (**Figure 4.1**). Furthermore, the pathways used in this study (without hydrogenation of the triacylglycerols) allow the sustainable preparation of various products from non-edible animal fat. Hence, the non-edible animal fat was hydrolyzed using a recent bio-catalytic procedure [35], and the crude free acids were split into saturated and unsaturated fatty acids. The unsaturated fatty acids were epoxidized using immobilized CAL-B in a solvent-free media, the epoxy ring was cleaved with hot water, and the resulting DHSA was crystallized using *t*-BuOH and H_2O. Twelve DHSEs were prepared from DHSA and the corresponding alcohol using immobilized CAL-B

as catalyst and α-limonene as solvent. DSC was used to test the performance of these esters as PCMs.

4.3. Materials and methods

4.3.1. Materials

Methanol (≥99.9%), 1-butanol (≥99.5%), 1-dodecanol (98%), 1-hexanol (98%) and oleic acid (90%) were purchased from Sigma-Aldrich Corp. (St. Louis, USA). Ethanol (≥99.9%) was purchased from Scharlau (Barcelona, Spain). 1-Propanol (≥99.8%), 1-pentanol (99%), 1-decanol (97%), 1-tetradecanol (97%) and 1-hexadecanol (99%) were purchased from Fluka (Buchs, Switzerland). 1-Octadecanol (97%) was purchased from Alfa Aesar (Karlsruhe, Germany). 1-Octanol (99%) was purchased from Acros (New Jersey, USA). Hydrogen peroxide (30%) (w/v) solution was purchased from Fischer Scientific UK (Leicester, UK). CO_2 was obtained from Messer Iberica de Gases S.A (Tarragona, Spain). *R. oryzae* resting cells were prepared as described [35]. Immobilized lipase-B from *C. antarctica* (Immobilized CAL-B) was a gift sample from Novozymes A/S (Bagsvaerd, Denmark). Animal fat was a kind gift from Subproductos Cárnicos Echevarria y Asociados S.L (Cervera, Spain). α-Limonene was a kind gift from Creaciones Aromaticas Industriales (Sant Quirze del Vallès, Spain).

4.3.2. Analyses

NMR spectra were recorded with a MERCURY plus NMR Spectrometer Systems VARIAN Imant AS operating at 400 MHz. DSC analyses were performed with a DSC 822e from Mettler Toledo. Thermophysical

characterization was performed with differential scanning calorimetry (DSC 822e from Mettler Toledo) in order to analyze the phase change temperature and phase change enthalpies (fusion and solidification). Measurements were conducted using a three cycle program repetitions. The first cycle was disregarded and, thus, the mean value of the two following cycles was calculated. The second and the third cycle were performed at 0.5˚C•min^{-1} under flowing 80 mL•min^{-1} nitrogen gas. The DSC analyses were performed between 30 and 95˚C depending on the melting point of the product studied. The amount of sample used was around 5 mg and the samples were located into 40 µL aluminum crucibles. The equipment accuracy was ± 0.1˚C for temperature and ±3 kJ• kg^{-1} for enthalpy determinations. To study thermal cycling reliability, a Bioer Gene Q T-18 thermal cycler was used to analyze the changes of the phase-change temperature and latent heat of the esters after 100 and 1000 thermal cycles. A 0.5-mL vial was used for each compound. A dynamic method was established using a temperature range between 30 °C and 95 °C and at 4°C•s^{-1} for cooling and 5°C•s^{-1} for heating. A total of 1000 cycles were performed under the described conditions. Finally, the compounds were tested again by DSC to identify changes in their thermos-physical properties.

4.3.3. Characterization of waste fat

The fat was composed of non-edible fatty parts of pig and chicken origin. It consisted mainly of triacylglycerides. The fat had a saponification value (SV) of 196. The percentage of unsaturated fatty acids was 55.14%, in which monounsaturated and polyunsaturated fatty acids accounted for 40.50 and 14.64%, respectively, as determined by gas chromatography [36]. Of all the unsaturated fatty acids in the animal fat, oleic acid was the most abundant,

accounting for about 36.97% of the total fatty acids present. Saturated fatty acids accounted for 43.99% of the total fatty acids and palmitic and stearic acids for 24.57 and 14.05% of this total, respectively.

4.3.4. Chemo-enzymatic epoxidation of oleic acid – Reuse study

A volume of 5.42 mL (47.81 mmol) of a 30% H_2O_2 solution (4˚C) was added to a 50-mL Falcon vial containing 10 g (31.86 mmol of double bonds) of 90% oleic acid and 1 g of immobilized CAL-B. The Falcon vial was fixed horizontally in a Labnet 211DS orbital oven and then shaken at 220 rpm at 55˚C for 150 min. The vial was centrifuged at 6000 rpm for 5 min, and the non-aqueous and aqueous phases were separated. Immobilized CAL-B was recovered by filtering the crude mixture through a Pyrex crucible n˚3, washing with water and drying the biocatalyst under vacuum for 24 h. Finally, the biocatalyst was extracted with a lab-scale supercritical fluid extractor (Speed SFE-Applied separations). The extraction vessel was packed with the immobilized CAL-B recovered. The extraction temperature, pressure, CO_2 outflow rate, and residence time were set at 60°C, 35 MPa, 4 L•min^{-1}, and 45 min, respectively. The epoxide recovered from the supercritical CO_2 extraction was joined to the non-aqueous layer previously obtained. The washed immobilized CAL-B was recovered for a reuse study. The crude of reaction was analyzed by ^{1}H NMR spectroscopy (see **Annex I**) after each reuse.

cis- 9, 10-Epoxyestearic acid: ^{1}H RMN (400 MHz, $CDCl_3$) δ ppm: 0.88 (t, J=6.9 Hz, C**H₃**), 1.19-1.55 (m, C**H₂**), 1.63 (m, β**CH₂**), 2.34 (t, J=7.4 Hz, αC**H₂**), 2.90 (m, **H**COC**H**).

4.3.5. Chemo-enzymatic epoxidation of oleic acid – Remaining activity of the enzyme

A volume of 542 µL (4.78 mmol) of a 30% H_2O_2 solution (4˚C) was added to a 15-mL Falcon vial containing 1 g (3.19 mmol) of 90% oleic acid and 0.1 g of immobilized CAL-B. The vial was fixed horizontally in a Labnet 211DS orbital oven and then shaken at 220 rpm at 55˚C for 150 min. Subsequently, the vial was centrifuged at 6000 rpm for 5 min, and the non-aqueous and aqueous phases were separated. Then, the final mixture was extracted twice with 5 mL of common solvents or α-limonene. Immobilized CAL-B was recovered by filtering the mixture through a Pyrex crucible n˚3 and washing with the main solvent. The washed biocatalyst was used for a new solvent-free reaction and the remaining activity of immobilized CAL-B evaluated. An aliquot of this new reaction was analyzed by ^{1}H NMR spectroscopy.

4.3.6. Preparation of DHSA from oleic acid

A volume of 5.42 mL (47.81 mmol) of a 30% H_2O_2 solution (4˚C) was added to a 50-mL Falcon vial containing 10 g (31.86 mmol of double bonds) of 90% oleic acid and 1 g of immobilized CAL-B. The vial was fixed horizontally in a Labnet 211DS orbital oven and shaken at 220 rpm at 55˚C for 150 min. The epoxide was recovered by extracting the final mixture twice with 25 mL of *t*-BuOH. This organic solution was placed in a 150 mL reaction tube containing 50 mL of water. The tube was closed and stirred magnetically in an oil bath at 130˚C for 12 h. The tube was cooled to room temperature and the content was placed in a funnel. The aqueous phase was discarded and the organic phase was chilled at 4˚C for 24 h. The final crystals were

recovered using a Pyrex crucible n˚3 and washed three times with cold ethyl acetate. (5.50 g, 55% isolated yield).

The final white powder (m.p. 94.2˚C) [37] was analyzed by ^{1}H NMR (see **Annex I**):

DHSA: ^{1}H RMN (400 MHz, $CDCl_3$) δ ppm: 0.88 (t, J=6.9 Hz, C**H$_3$**), 1.19-1.55 (m, C**H$_2$**), 1.63 (m, β**CH$_2$**), 2.34 (t, J=7.4 Hz, αC**H$_2$**), 3.40 (m, **H**COH).

4.3.7. Bio-catalytic hydrolysis of non-edible waste fat

The bio-catalytic hydrolysis of the fat and the separation of the resulting FFA by crystallization was performed following the procedure already described [35]. Thus, we added 20 g of water to each 50-mL Falcon vial (six in total) containing each 20 g of animal fat and 2 g of *Rhizopus oryzae*. The vials were fixed horizontally in a Labnet 211DS orbital oven and shaken at 220 rpm at 40˚C for 48 h. Finally, the vials were centrifuged at 6000 rpm for 10 min, and the non-aqueous and aqueous phases were separated. The cells were recovered using a Pyrex crucible n˚3 and were washed with water. The resting cells were dried under vacuum for 24 h. These cells were extracted with a lab-scale supercritical fluid extractor (Speed SFE-Applied separations). The extraction temperature, pressure, CO_2 outflow rate, and residence time were set at 40°C, 35 MPa, 4 L•min^{-1}, and 45 min, respectively. The remaining fatty matter recovered from the supercritical CO_2 extraction of the biocatalyst was joined to the non-aqueous phase previously obtained. The resulting non-aqueous viscous liquid (113.58 g, 93 % yield) was titrated by duplicate to determine the degree of hydrolysis [35] of the fatty matter. (95% of hydrolysis degree). The fatty matter was crystallized with methanol 1/6 (w/v) at -20˚C for 24 h. The mother liquor was concentrated yielding

81.84 g of a high unsaturated fatty acid mixture. Composition (GC-FID [36]): oleic acid (55.14%), linoleic acid (30.17%), stearic acid (7.57%), palmitic acid (6.80%).

4.3.8. Preparation of DHSA from non-edible animal fat

A volume of 7 mL (61.74 mmol) of a 30% H_2O_2 solution (at 4 °C) was added to a 50-mL Falcon vial containing 10 g (41.02 mmol of double bonds) of the highly unsaturated fatty acid mixture and 1 g of immobilized CAL-B. The epoxidated fatty acids were separated from the immobilized CAL-B extracting twice with 25 mL of *t*-BuOH. This organic solution was placed in a 150 mL reaction vial containing 50 mL of distilled water. The vial was stirred magnetically in an oil bath at 130˚C for 12 h. Subsequently, the vial was brought to room temperature and the content was placed in a funnel. The aqueous phase was discarded and the organic phase was concentrated under vacuum: The final residue was dissolved in hot ethyl acetate in a solute/solvent ratio 1/1 (w/v). The organic mixture was dried over Na_2SO_4 and DHSA crystals recovered after crystallization at 4˚C for 24 h by filtration using a Pyrex crucible n˚3. The solid was washed three times with cold ethyl acetate and recrystallized in ethyl acetate at 4˚C in a solute/solvent ratio 1/5 (w/v) yielding 3.13 g of DHSA (51% yield). The reaction was repeated until get enough starting material for further enzymatic esterification reactions. The final white powder (m.p. 93.8˚C) [37] was analyzed by ^{1}H NMR.

4.3.9. Bio-catalytic preparation of octyl DHSE- Reuse study

A volume of 1 mL of octanol (6.32 mmol) was added to a 15-mL falcon tube containing 1 g (3.16 mmol) of DHSA prepared as described in subsection 4.2.8, 100 mg of biocatalyst and 10 mL of α-limonene in each tube. The falcon

tubes were fixed horizontally in a Labnet 211DS orbital oven and then shaken at 220 rpm at 40˚C during 24 h. Then, the falcon was centrifuged at 6000 rpm during 1 min, and the organic layer was separated from the biocatalyst. The organic layer was added to another 15-mL falcon and incubated on the orbital oven at 40˚C during 5 min (220 rpm) with 3 mL of a saturated solution of $NaHCO_3$. The falcon was centrifuged at 6000 rpm during 1 min and α-limonene was recovered. The ester crystals appeared when α-limonene was maintained at 4˚C during 24 h. The crystals were recovered passing them through a Pyrex crucible n˚3 and washed three times with cold α-limonene. The falcon tube containing the biocatalyst was used to repeat the reaction for the reuse study. The final white powder was analyzed by ^{1}H NMR:

Octyl DHSE: ^{1}H RMN (400 MHz, $CDCl_3$) δ ppm: 0.88 (t, J=6.9 Hz, C**H$_3$**), 1.19-1.55 (m, C**H$_2$**), 1.63 (m, β**CH$_2$**), 1.83-1.93 (s, **H**O-), 2.29 (t, J=7.4 Hz, αC**H$_2$**), 3.40 (m, **H**COH), 4.05 (t, J= 6.7 Hz, C**H$_2$**-O).

4.3.10. Bio-catalytic preparation of DHSEs: Esters from methanol to 1-tetradecanol (procedure A). Esters of 1-hexadecanol and 1-octadecanol (procedure B).

A given amount of alcohol (**Table 4.1**) was added to a 15-mL (A) or 50-mL (B) Falcon vial containing 1 g (3.16 mmol) of DHSA, prepared previously as described in subsection 4.2.8, 100 mg of immobilized CAL-B, and 10 mL (A) or 20 mL (B) of α-limonene. The vials were fixed horizontally in a Labnet 211DS orbital oven and shaken at 220 rpm at 40°C for 24 h. Subsequently, 5 mL of methanol (B) and 3 mL of a saturated solution of $NaHCO_3$ (A and B) were added to each vial, and the content was stirred at 200 rpm at 40°C for 5 min (A) or 2 min (B). The vials were centrifuged at 6000 rpm for 1 min and the organic layer was recovered. The solutions were crystallized at various

temperatures depending on the ester prepared (**Table 4.1**). Note that 1-octanyl to 1-octadecanyl esters easily crystallized when the α-limonene solutions were at room temperature. The crystals of each ester were recovered on a Pyrex crucible n°3 and washed three times with cold α-limonene. **Table 4.1** shows the yields and melting points (measured by DSC). The DHSEs were analyzed by NMR spectroscopy (see **Annex I**):

Methyl DHSE: ^{1}H RMN (400 MHz, $CDCl_3$) δ ppm: 0.89 (t, J=6.9 Hz, C**H$_3$**), 1.21-1.55 (m, C**H$_2$**), 1.63 (m, β**CH$_2$**), 2.10-2.27 (s, **H**O-), 2.31 (t, J=7.5 Hz, αC**H$_2$**), 3.40 (m, **H**COH), 3.67 (s, C**H$_3$**-O). ^{13}C RMN (400 MHz, $CDCl_3$) δ ppm: 14.09 (CH_2**C**H_3), 22.66 (**C**H_2CH_3), 24.88 (**C**H_2), 25.56, 25.67 (**C**H_2CH_2CHOH), 28.93-29.79 (**C**H_2), 31.87 (CH_3CH_2**C**H_2), 33.57, 33.63 (**C**H_2CHOH), 34.06 (α**C**H_2), 51.46 (COO**C**H_3), 74.45, 74.51 (**C**HOH), 174.34 (**C**$OOCH_3$).

Ethyl DHSE: ^{1}H RMN (400 MHz, $CDCl_3$) δ ppm: 0.86 (t, J=6.8 Hz, C**H$_3$**), 1.17-1.52 (m, C**H$_2$**), 1.60 (m, β**CH$_2$**), 2.27 (t, J=7.5 Hz, αC**H$_2$**), 3.38 (m, **H**COH), 4.11 (q, J= 7.1 Hz, C**H$_2$**-O). ^{13}C RMN (400 MHz, $CDCl_3$) δ ppm: 14.12, 14.27 (**C**H_3), 22.68 (CH_3**C**H_2), 24.93 (**C**H_2), 25.59, 25.70 (**C**H_2CH_2CHOH), 28.95-29.82 (**C**H_2), 31.89 (CH_3CH_2**C**H_2), 33.59, 33.65 (**C**H_2CHOH), 34.37 (α**C**H_2), 60.22 (COO**C**H_2CH_3), 74.48, 74.54 (**C**HOH), 173.96 (**C**$OOCH_2$).

Propyl DHSE: ^{1}H RMN (400 MHz, $CDCl_3$) δ ppm: 0.87 (t, J=6.8 Hz, C**H$_3$**), 0.93 (t, J=7.4 Hz, C**H$_3$**), 1.18-1.52 (m, C**H$_2$**), 1.62 (m, β**CH$_2$**), 2.10-2.24 (s, **H**O-), 2.28 (t, J=7.5 Hz, αC**H$_2$**), 3.38 (m, **H**COH), 4.01 (t, J= 6.7 Hz, C**H$_2$**-O). ^{13}C RMN (400 MHz, $CDCl_3$) δ ppm: 10.43 (O-CH_2CH_2**C**H_3), 14.13 (CH_2**C**H_3), 22.03 (CH_3**C**H_2CH_2O), 22.69 (**C**H_2CH_3), 24.98 (**C**H_2), 25.60, 25.71 (**C**H_2CH_2CHOH), 28.92-29.87 (**C**H_2), 31.90 (CH_3CH_2**C**H_2), 33.60, 33.66 (**C**H_2CHOH), 34.37 (α**C**H_2), 65.89 (COO**C**H_2CH_2), 74.49, 74.54 (**C**HOH), 174.05 (**C**$OOCH_2$).

Butyl DHSE: ^{1}H RMN (400 MHz, $CDCl_3$) δ ppm: 0.87 (t, J=6.8 Hz, C**H$_3$**), 0.92 (t, J=7.4 Hz, C**H$_3$**), 1.19-1.55 (m, C**H$_2$**), 1.60 (m, β**CH$_2$**), 2.07-2.24 (s, **H**O-), 2.28 (t, J=7.5 Hz, αC**H$_2$**), 3.38 (m, **H**COH), 4.05 (t, J= 6.7 Hz, C**H$_2$**-O). ^{13}C RMN (400 MHz, $CDCl_3$) δ ppm: 13.72, 14.11 (**C**H_3), 19.16, 22.72 (CH_3**C**H_2), 24.96 (**C**H_2), 25.59, 25.69 (**C**H_2CH_2CHOH), 28.80-29.96 (**C**H_2), 30.71 ($COOCH_2$**C**H_2), 31.88 (CH_3CH_2**C**H_2), 33.59, 33.65 (**C**H_2CHOH), 34.37 (α**C**H_2), 64.15 (COO**C**H_2CH_2), 74.48, 74.53 (**C**HOH), 174.03 (**C**$OOCH_2$).

Pentyl DHSE: ^{1}H RMN (400 MHz, $CDCl_3$) δ ppm: 0.84-0.93 (m, C**H$_3$**), 1.20-1.52 (m, C**H$_2$**), 1.61 (m, β**CH$_2$**), 2.07-2.20 (s, **H**O-), 2.28 (t, J=7.5 Hz, αC**H$_2$**), 3.38 (m, **H**COH), 4.05 (t, J= 6.8 Hz, C**H$_2$**-O). ^{13}C RMN (400 MHz, $CDCl_3$) δ ppm: 13.98, 14.12 (**C**H_3), 22.33, 22.68 (CH_3**C**H_2), 24.96 (**C**H_2), 25.59, 25.69 (**C**H_2CH_2CHOH), 28.10-29.85 (**C**H_2), 31.89 (CH_3CH_2**C**H_2), 33.60, 33.65 (**C**H_2CHOH), 34.37 (α**C**H_2), 64.44 (COO**C**H_2CH_2), 74.48, 74.53 (**C**HOH), 174.03 (**C**$OOCH_2$).

Hexyl DHSE: ^{1}H RMN (400 MHz, $CDCl_3$) δ ppm: 0.84-0.91 (m, C**H$_3$**), 1.20-1.52 (m, C**H$_2$**), 1.60 (m, β**CH$_2$**), 2.12-2.22 (s, **H**O-), 2.28 (t, J=7.5 Hz, αC**H$_2$**), 3.38 (m, **H**COH), 4.04 (t, J= 6.8 Hz, C**H$_2$**-O). ^{13}C RMN (400 MHz, $CDCl_3$) δ ppm: 14.01, 14.12 (**C**H_3), 22.56, 22.69 (CH_3**C**H_2), 24.97-29.81 (**C**H_2), 31.45, 31.89 (CH_3CH_2**C**H_2), 33.60, 33.66 (**C**H_2CHOH), 34.38 (α**C**H_2), 64.46 (COO**C**H_2CH_2), 74.48, 74.54 (**C**HOH), 174.03 (**C**$OOCH_2$).

Octyl DHSE: ^{1}H RMN (400 MHz, $CDCl_3$) δ ppm: 0.87 (t, J=6.7 Hz, C**H$_3$**), 1.18-1.52 (m, C**H$_2$**), 1.60 (m, β**CH$_2$**), 2.03-2.20 (s, **H**O-), 2.28 (t, J=7.5 Hz, αC**H$_2$**), 3.39 (m, **H**COH), 4.04 (t, J= 6.7 Hz, C**H$_2$**-O). ^{13}C RMN (400 MHz, $CDCl_3$) δ ppm: 14.10, 14.12 (**C**H_3), 22.65, 22.68 (CH_3**C**H_2), 24.96 (**C**H_2), 25.59, 25.69 (**C**H_2CH_2CHOH), 25.95-29.80 (**C**H_2), 31.79, 31.89 (CH_3CH_2**C**H_2), 33.59, 33.65 (**C**H_2CHOH), 34.38 (α**C**H_2), 64.46 (COO**C**H_2CH_2), 74.48, 74.53 (**C**HOH), 174.02 (**C**$OOCH_2$).

Decyl DHSE: ^{1}H RMN (400 MHz, $CDCl_3$) δ ppm: 0.87 (t, J=6.7 Hz, C**H$_3$**), 1.18-1.52 (m, C**H$_2$**), 1.59 (m, β**CH$_2$**), 2.06-2.16 (s, **H**O-), 2.28 (t, J=7.5 Hz, αC**H$_2$**), 3.38 (m, **H**COH), 4.04 (t, J= 6.7 Hz, C**H$_2$**-O). ^{13}C RMN (400 MHz, $CDCl_3$) δ ppm: 14.10 (**C**H_3), 22.67 (CH_3**C**H_2), 24.95 (**C**H_2), 25.57, 25.67 (**C**H_2CH_2CHOH), 25.93-29.79 (**C**H_2), 31.88, 31.92 (CH_3CH_2**C**H_2), 33.58, 33.64 (**C**H_2CHOH), 34.36 (α**C**H_2), 64.45 (COO**C**H_2CH_2), 74.46, 74.52 (**C**HOH), 174.00 (**C**$OOCH_2$).

Dodecyl DHSE: ^{1}H RMN (400 MHz, $CDCl_3$) δ ppm: 0.87 (t, J=6.8 Hz, C**H$_3$**), 1.18-1.52 (m, C**H$_2$**), 1.61 (m, β**CH$_2$**), 2.04-2.20 (s, **H**O-), 2.28 (t, J=7.5 Hz, αC**H$_2$**), 3.38 (m, **H**COH), 4.04 (t, J= 6.7 Hz, C**H$_2$**-O). ^{13}C RMN (400 MHz, $CDCl_3$) δ ppm: 14.11 (**C**H_3), 22.68 (CH_3**C**H_2), 24.95-29.80 (**C**H_2), 31.88, 31.92 (CH_3CH_2**C**H_2), 33.59, 33.65 (**C**H_2CHOH), 34.37 (α**C**H_2), 64.46 (COO**C**H_2CH_2), 74.47, 74.52 (**C**HOH), 174.02 (**C**$OOCH_2$).

Tetradecyl DHSE: ^{1}H RMN (400 MHz, $CDCl_3$) δ ppm: 0.87 (t, J=6.9 Hz, C**H$_3$**), 1.20-1.52 (m, C**H$_2$**), 1.61 (m, β**CH$_2$**), 1.87-1.97 (s, **H**O-), 2.28 (t, J=7.5 Hz, αC**H$_2$**), 3.37 (m, **H**COH), 4.05 (t, J= 6.8 Hz, C**H$_2$**-O). ^{13}C RMN (400 MHz, $CDCl_3$) δ ppm: 14.11 (**C**H_3), 22.68 (CH_3**C**H_2), 24.95-29.80 (**C**H_2), 31.88, 31.92 (CH_3CH_2**C**H_2), 33.59, 33.65 (**C**H_2CHOH), 34.36 (α**C**H_2), 64.46 (COO**C**H_2CH_2), 74.48, 74.54 (**C**HOH), 174.00 (**C**$OOCH_2$).

Hexadecyl DHSE: ^{1}H RMN (400 MHz, $CDCl_3$) δ ppm: 0.87 (t, J=6.8 Hz, C**H$_3$**), 1.18-1.52 (m, C**H$_2$**), 1.61 (m, β**CH$_2$**), 1.87-1.95 (s, **H**O-), 2.28 (t, J=7.5 Hz, αC**H$_2$**), 3.39 (m, **H**COH), 4.05 (t, J= 6.8 Hz, C**H$_2$**-O). ^{13}C RMN (400 MHz, $CDCl_3$) δ ppm: 14.12 (**C**H_3), 22.69 (CH_3**C**H_2), 24.96-29.80 (**C**H_2), 31.88, 31.92 (CH_3CH_2**C**H_2), 33.59, 33.65 (**C**H_2CHOH), 34.37 (α**C**H_2), 64.46 (COO**C**H_2CH_2), 74.49, 74.54 (**C**HOH), 174.01 (**C**$OOCH_2$).

Octadecyl DHSE: ^{1}H RMN (400 MHz, $CDCl_3$) δ ppm: 0.87 (t, J=6.9 Hz, C**H$_3$**), 1.18-1.52 (m, C**H$_2$**), 1.60 (m, β**CH$_2$**), 1.98-2.06 (s, **H**O-), 2.28 (t, J=7.5 Hz, αC**H$_2$**), 3.39 (m, **H**COH), 4.05 (t, J= 6.8 Hz, C**H$_2$**-O). ^{13}C RMN (400 MHz, $CDCl_3$) δ ppm:

14.12 (**C**H_3), 22.69 (CH_3**C**H_2), 24.96 (**C**H_2), 25.58, 25.68 (**C**H_2CH_2CHOH), 25.95-29.81 (**C**H_2), 31.88, 31.92 (CH_3CH_2**C**H_2), 33.59, 33.65 (**C**H_2CHOH), 34.37 (α**C**H_2), 64.46 (COO**C**H_2CH_2), 74.48, 74.54 (**C**HOH), 174.00 (**C**$OOCH_2$).

4.4. Results and Discussions

4.4.1. Chemo-enzymatic epoxidation of commercial oleic acid

The chemo-enzymatic epoxidation of oleic acid was first described in 1995 by Warwel et al. [38]. As depicted in **Chapter I** (see **Figure 1.14**), the peroxyoleic acid produced via lipase-catalytic peroxidation of oleic acid with hydrogen peroxide is the reagent that oxidizes the double bond of the alkyl chain to form the corresponding epoxide [38-40]. The chemo-enzymatic epoxidations were performed in Falcon vials as previously described for the bio-catalytic hydrolysis of non-edible animal fat in **Chapter II** [35]. The use of such vials facilitates the separation of product and biocatalyst by centrifugation at the end of the reaction.

Warwel et al. [38] reported the self-epoxidation of oleic acid in toluene catalyzed by immobilized CAL-B when a given amount of 60% hydrogen peroxide was added every 15 min. This stepwise addition appeared to be required to prevent enzyme inactivation by 60% hydrogen peroxide during the long reaction periods (10-66 h) described in their procedure. Orellana-Coca et al. [40] presumably supposed this issue in their solvent-free chemo-enzymatic reaction by adding 30% hydrogen peroxide in aliquots every 15 min during the first 4 h. Nevertheless, here we show that 30% hydrogen peroxide can be added to the reaction mixture at 4°C and in one step, thereby simplifying the procedure. The reaction was completed in 150 min.

The organic layer was recovered, and the biocatalyst was extracted for later reuse using supercritical CO_2. A similar approach has been reported in a fat biocatalytic hydrolysis (see **Chapter II**) [35]. This process allows recovery of the remaining product from the biocatalyst. The combination of the non-aqueous layer and the extracted product achieves the actual yield. In addition, this extraction methodology permits the reuse of the biocatalyst. **Figure 4.2** shows the yields of the epoxidation procedure in five consecutive reaction cycles. Epoxide purity was determined by ^{1}H NMR [17], comparing the integration value of the signal at 2.34 ppm corresponding to αC**H**$_2$ and the signal at 2.90 ppm corresponding to the **H**COC**H** protons of the epoxide group. The enzyme catalyzed the full conversion of the oleic acid during the first (R0) and second (R1) cycles. Nevertheless, the yield decreased dramatically from the third cycle (R2) onwards. Warwel et al. [38] reused the immobilized CAL-B in the presence of toluene fifteen times. However, that epoxidation was performed with an excess of oleic acid, and the yield was referred to the hydrogen peroxide added. Orellana-Coca et al. [40] described good results for the reutilization of CAL-B to epoxidize methyl oleate in a solvent-free medium during six cycles, considering the methyl oleate conversion in the first five cycles (above 85%) and a dramatic decrease to 20% in the sixth cycle. However, although the authors described the chemo-enzymatic epoxidation of oleic acid, they reported only the recycling capacity of the biocatalyst to epoxidize methyl oleate.

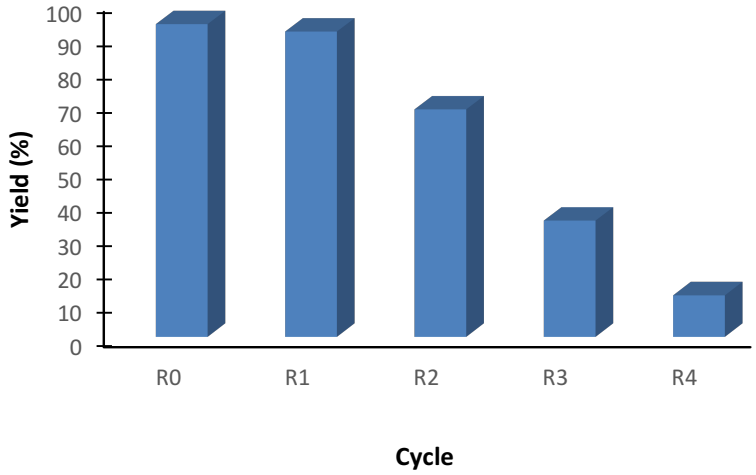

Figure 4.2. Epoxidation yields of commercial oleic acid. The epoxidation was performed at 55˚C for 150 min in a solvent-free medium using immobilized CAL-B as biocatalyst. Data corresponds to 5 experiments using supercritical CO_2 for the biocatalyst extraction after each cycle. (4.2.4. Chemo-enzymatic epoxidation of commercial oleic acid – Reuse study).

To complete the chemo-enzymatic epoxidation study, the immobilized CAL-B was extracted with common solvents and α-limonene, instead of using supercritical CO_2. Subsequently, the reaction was repeated with the washed bio-catalyst. Indeed, an aliquot from the epoxide of the second cycle reaction (R1) was analyzed by ^{1}H NMR. As all the biocatalyst of that second cycle reaction was not extracted, the total mass of product was not known. Thus, the results are shown in terms of oleic acid conversion rather than epoxide yield. In this regard, the integration value of the signal at 5.10 ppm corresponding to the two remaining **H**C=C**H** protons of the alkene group was compared with the value of the two **H**C=C**H** protons of a commercial oleic

acid ^{1}H NMR sample. **Figure 4.3** shows oleic acid conversion on the first reuse (R1) of immobilized CAL-B. The extraction of immobilized CAL-B with non-polar solvents such as α-limonene or hexane resulted in higher activity than that extracted with acetone, ethyl acetate, or *t*-BuOH. The oleic acid conversion of α-limonene (98%) and hexane (95%) sets gave promising results. Nevertheless, according to (IMI)-CHEM21, hexane is classified as hazardous and the substitution of this kind of solvent is a priority [41].

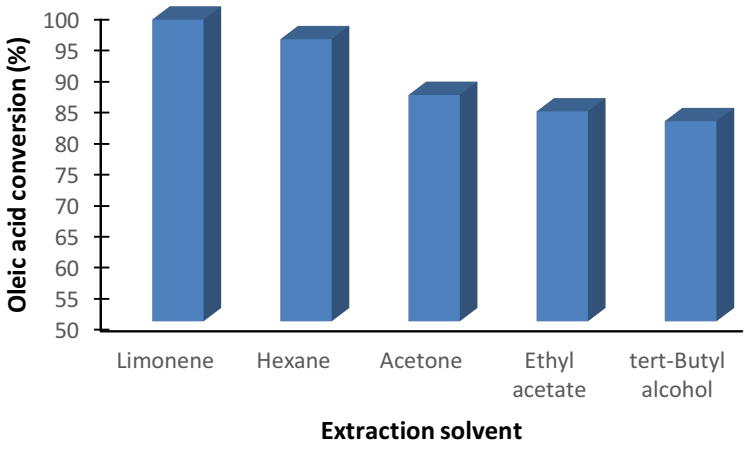

Figure 4.3. Oleic acid conversion on the first reuse (R1) of immobilized CAL-B on the epoxidation of commercial (90%) oleic acid at 55˚ C for 150 min reaction in a solvent-free medium. (4.2.5. Chemo-enzymatic epoxidation of commercial oleic acid – remaining activity of the enzyme).

4.4.2. Preparation of DHSA from oleic acid

Lab-scale preparation of DHSA from oleic acid is usually afforded by few common procedures. In 1959, Swern et al. [23] described the synthesis of

DHSA from commercial oleic acid. A high amount of hazardous formic acid and hydrogen peroxide were mixed with oleic acid to produce a highly exothermic reaction. Once the formic acid had been removed by distillation, sodium hydroxide was added to hydrolyze the ester group. Finally, hydrochloric acid was added to obtain the free fatty acids. The method described by Herrmann et al. [42] in 1991 using the expensive catalyst methyltrioxorhenium for olefin oxidations has also been adapted to the synthesis of DHSA from oleic acid [19]. In this synthesis, considerable amounts of anhydrous $MgSO_4$ are used and the excess of hydrogen peroxide is decomposed by adding Na_2SO_3. In addition, the mixture is crystallized in hexane, and column chromatography is used to achieve the desired product. Greener approaches for the preparation of DHSA using enzymes to hydrolyze *cis*-9,10-epoxystearic acid have been studied since 1967 [43]. Soluble *Pseudomona* bacterial enzyme [43, 44], mammalian epoxide hydrolases [45], and soybean epoxide hydrolases [46] have been used to tackle the enzymatic hydrolysis of *cis*-9, 10-epoxystearic acid to DHSA, affording distinct results. Whereas the bacterial enzyme mediated the hydrolysis of half of the racemic epoxy acid to optically pure (+)-DHSA, mammalian and soybean epoxide hydrolases completely hydrolyzed the racemic epoxide to DHSA. Although these epoxide hydrolases could offer an interesting approach for the preparation of green DHSA, these studies were focused on enzyme behavior and the final stereochemistry of the product rather than on the preparation of DHSA at gram scale.

During our attempts to develop a straightforward and green approach to synthesize DHSA, the processes devoted to epoxide hydrolysis with hot water [47] and epoxide-opening cascades in water [48] acquired importance. Wang et al. [47] described the hydrolysis of epoxides as styrene oxide in

water only and in water:organic solvent (1:1) mixtures, the former giving the highest yield (98%). In the case of the DHSA synthesis, in the present work a co-solvent was mandatory in order to keep the mixture solubilized, thereby preventing the formation of estolides between the epoxide group and the carboxylic acid.

The epoxide present in the various solvents used in the evaluation of immobilized CAL-B activity was tested in the first screening (results not shown). These solutions with *c.a.* 10% (w/w) of epoxide were placed in reaction vials and the same amount of water as organic solvent was added. The vials were magnetically stirred at 130°C (to keep the water boiling) for 16 h, and subsequently an aliquot was collected and concentrated under N_2. ^{1}H NMR revealed that the epoxide group (2.90 ppm, m, **H**COC**H**) was still present in the α-limonene and hexane tests while it was not observed in the tests that used acetone, ethyl acetate and *t*-BuOH. In addition, estolides appeared to be considerable in α-limonene, hexane and ethyl acetate, as determined by the presence of two signals at 3.58 ppm and 4.83 ppm, which can be assigned to **H**-COH (hydrogen bonded to a secondary alcohol) and $R_1COOC\mathbf{H}R_2$ (hydrogen bonded to a secondary alcoxyester), respectively [17]. With respect to acetone and *t*-BuOH, the former presented a partial conversion of the diol moiety into an acetal (3.55 ppm, m, **H**COCO**H**) [49] whereas the latter presented the best selectivity towards diol moiety formation (3.40 ppm, m, **H**-COH).

In order to achieve a straightforward process to produce DHSA, we expected an optimal amount of *t*-BuOH to allow epoxide hydrolysis and also crystallization of the diol once the reaction had finished. In addition, although *t*-BuOH is not a suitable crystallization solvent due to its high melting point (~25 °C), the azeotropic mixture with water lowers the melting point, thereby

allowing crystallizations in the fridge (4°C). It must be remarked that complete epoxide hydrolysis using an open reactor equipped with a reflux condenser required at least 48 h (results not shown), while 12 h were sufficient to open the epoxide using pressurized reaction vials at 130°C. By combining chemo-enzymatic epoxidation, hydrolysis with hot water, and crystallization on the same reaction solvent, we achieved a DHSA yield of 55%. Indeed, this process allows a greener and easier preparation of DHSA from oleic acid at lab scale compared to common syntheses using formic acid [23] or methyltrioxorhenium as catalysts [18].

4.4.3. Preparation of DHSA from non-edible animal fat

Triacylglycerides were hydrolyzed using water and *R. oryzae* cells, and saturated acids were recovered by crystallization. The evaporation of the mother liquor yielded a highly unsaturated fatty acid mixture. This mixture was epoxidized, maintaining the double bonds: hydrogen peroxide (1:1.5) ratio used in the oleic acid epoxidation. The crude epoxide yielded crude DHSA using the hot water-*t*-BuOH approach. However, poor yields (~25%) were achieved by direct crystallization of DHSA in *t*-BuOH, probably due to the low percentage of oleic acid in the starting unsaturated mixture (55.14%). *t*-BuOH was evaporated and the organic residue was recrystallized from ethyl acetate to increase the DHSA yield (51%). This final DHSA had the same ^{1}H NMR and melting point as that prepared from commercial oleic acid. Hence, the DHSA prepared from non-edible animal fat was used as the starting material for the synthesis of DHSEs.

4.4.4. Synthesis of DHSEs from DHSA using a biocatalyst and the corresponding alcohol

Given our interest in preparing green bio-based DHSEs and testing their thermal properties, a lipase-catalyzed esterification was required. Manufacturers commonly mix fatty acids or hydroxy fatty acids with alcohols at high temperature in the presence of chemical catalysts, a process that leads to undesired side reactions. In contrast, lipase-catalyzed reactions take place under mild conditions, thereby preventing the degradation of the starting materials and thus reducing side reactions [33, 50]. Lokotsch et al. [50] described a solvent-free esterification of DHSA and transesterification of methyl DHSE with 1-decanol using a 3:1 alcohol excess and immobilized *R. miehei* lipase as catalyst in a fixed-bed reactor. Furthermore, crystallization with hexane or CH_3OH/H_2O was used on the purification step of the various compounds synthesized. Unfortunately, 1-dodecanol, 1-tetradecanol, 1-hexadecanol and 1-octadecanol are solid at room temperature. Consequently, the esterification of DHSA with these alcohols under mild conditions is not feasible in a solvent-free system. The preparation of DHSEs in solution using a biocatalyst has been achieved by means of immobilized *R. miehei* lipase [33, 34, 50, 51], immobilized *T. lanuginosus* lipase [51], and immobilized CAL-B lipase [33]. Awang et al. [33] studied the esterification of DHSA with 1-octanol in various solvents, including hexane and acetone catalyzed by immobilized *R.miehei* lipase and immobilized CAL-B lipase. They reported lower activity of lipase in polar solvents compared with non-polar ones. They also prepared and purified by column chromatography DHSEs of 1-decanol, 1-dodecanol, 1-tetradecanol, 1-hexadecanol and 1-octadecanol catalyzed by immobilized *R. miehei* in hexane.

The present method combines the approach proposed by Awang et al. [33] to prepare DHSEs of distinct alcohol lengths, with the crystallization method described by Lokotsch et al. [50]. The proposed method substitutes the hexane by α-limonene. Certainly, α-limonene provides a green alternative to petroleum-based hexane [52]. Moreover, the immobilized CAL-B extracted with α-limonene on the epoxidation of oleic acid retained high activity **(Figure 4.3)**.

Given that the bio-catalytic esterification of DHSA with 1-octanol in hexane has been widely studied [33, 34, 51], this chapter studies this reaction using α-limonene as solvent. Upon completion of the reaction, the mixture was washed with a saturated solution of $NaHCO_3$ to isolate the remaining free acid, and the final product was recovered by crystallization. **Figure 4.4** shows the yields achieved in five consecutive cycles of esterification of DHSA with 1-octanol catalyzed by immobilized CAL-B or *R. oryzae* resting cells using the same amount of biocatalyst. The use of resting cells to prepare DHSEs and the determination of final yields in the reuse study are a novelty. The yield achieved for the synthesis of octyl DHSE by the two biocatalysts was maintained at around 60% during the first four cycles and decreased to 50% on the fifth. *R. oryzae* resting cells achieved slightly lower yields in most of the cycles. However, the catalytic performance of the two biocatalysts was similar. Indeed, 0.1 g of immobilized CAL-B or *R. oryzae* cells yielded 4.75 g and 4.56 g of pure octyl DHSE, respectively.

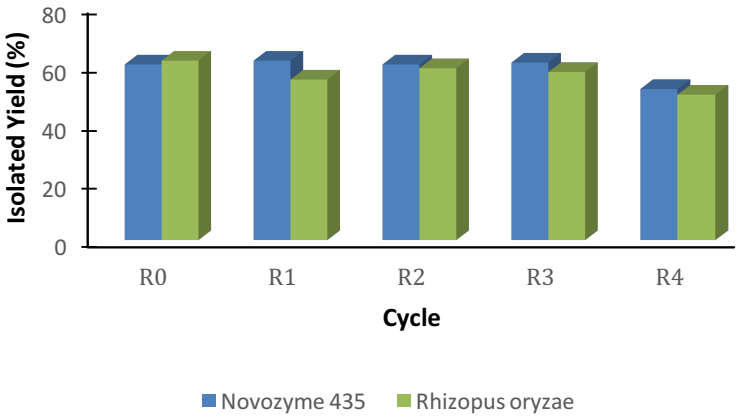

Figure 4.4. Isolated yield on the esterification of 1-octanol with DHSA catalyzed by immobilized CAL-B or *R. oryzae* resting cells at 40˚ C for 24 h in α-limonene. Data corresponds to 5 experiment cycles using the same recovered biocatalyst. (4.3.9. Bio-catalytic preparation of octyl DHSE-Reuse study).

Finally, immobilized CAL-B was used as a biocatalyst to prepare various DHSEs. An alcohol excess ranging 5:1 to 1.1:1 was studied (results not shown). **Table 4.1** shows the best alcohol:DHSA ratios for the preparation of each ester. The crystallization temperatures and the yields achieved are also shown. To the best of our knowledge, although solvents such as α-limonene have been used in lipase esterifications with fatty acids [53, 54], this is the first study to report the preparation of DHSEs using α-limonene as solvent. Awang et al. [33] purified several DHSEs by column chromatography; however, the isolated yield of such esters was not provided. In the present study, the use of α-limonene and a suitable crystallization temperature allowed the recovery of the esters without solvent evaporation. In addition,

most of the yields achieved were higher than those reported by Swern et al. [37] using naphthalene-α-sulfonic acid as catalyst. The melting points shown in **Table 4.1** (determined by DSC) are similar to those described by Swern et al. [37].

4.4.5. Thermal properties and cycling reliability of the DHSEs from non-edible animal fat

In **Chapters II** and **III**, animal fat was hydrolyzed and crystallized to prepare eutectic mixtures of palmitic and stearic acids [4, 35]. With a melting point around 55°C, these mixtures can be used to improve the efficiency of domestic hot water (DHW) tanks [55, 56] and air conditioning condensation heat recovery systems [7]. Otherwise, each DHSE presents a distinct melting temperature, thereby increasing the potential applications of PCMs derived from animal fat waste. **Table 4.1** shows the thermal properties of the twelve DHSEs prepared. The melting temperatures of these esters ranged from 52.45 to 76.88°C and the solidification temperatures from 40.04 to 70.82°C. These phase-change temperatures meet the requirements of the following: domestic hot water tanks [55, 56], air conditioning condensation heat recovery systems [7], and low temperature industrial waste heat (IWH) recovery in industries such as those devoted to food and beverage, textile, paper, and non-metallic mineral processes, among others [57]. However, sub-cooling ranging from 17.15 to 7.20°C was observed in the DSC analysis. This effect may be related to the DSC analysis method and sample mass [58]. Nevertheless, the diol moiety of these DHSEs could be responsible of such sub-cooling since the DSC analysis of some polyols, such as erythritol [59] and galactitol [60], also revealed this effect. DSC curves of the bio-based mixtures

prepared from non-edible fats showed a sharp endothermic peak during melting and a sharp exothermic peak during solidification, thereby indicating that only one substance was obtained at the end of the synthetic process. The non-cycled melting latent heats of the esters prepared ranged from 136.83 to 234.22 $kJ \bullet kg^{-1}$ and latent heat of solidification from 122.68 to 229.71 $kJ \bullet kg^{-1}$. These DHSEs showed some similarities when compared to analogous stearates studied for PCM purposes. As an example, odd carbon-numbered alcohol esters such as methyl and propyl stearates presented higher latent heats than even carbon-numbered esters such as ethyl and butyl stearates [28, 61]. However, the melting temperatures of these four alcolxyl stearates were around 30°C lower than their DHSE counterparts. Indeed, to prepare stearates as PCMs with melting temperatures of around 60°C, high-chain esters such as octadecyl stearate (59.22°C) are required [29]. Some of these DHSEs showed interesting enthalpy values, an example being paraffin, which has a latent heat of solidification in the range of 180 to 230 $kJ \bullet kg^{-1}$ [9]. On the other hand, some of the described commercial fatty acid bio-based PCMs [11, 12, 14] from feedstocks and the bio-based eutectic mixture from non-edible animal fat prepared in **Chapter III** [4] presented latent heat of solidification from 149.2 [11, 12, 14] to around 180 $kJ \bullet kg^{-1}$ [4]. As the DHSEs prepared from non-edible animal fat presented promising latent heat, the thermal cycling reliability of the products with higher enthalpies (above 200 $kJ \bullet kg^{-1}$) were studied. Thermal cycling tests are essential to ensure the applicability of a PCM since its working principle relies on repeated melting and freezing cycles. The purpose of such tests is to ensure that the thermo-physical properties of a PCM remain constant after cycling or do not show a variation of more than ± 20% compared to their initial value [62].

The variation of solidification and melting enthalpies after 100 thermal cycles ranged from a gain of 0.99% to a loss of 2.94% (see **Table 4.2**). Losses below 20% after thermal cycling indicate that the material shows good thermal cycling stability [63]. Moreover, of all the materials tested, octyl DHSE showed the highest latent heat after 100 heating/cooling cycles: 230.05 $kJ \bullet kg^{-1}$ (fusion enthalpy), 228.69 $kJ \bullet kg^{-1}$ (solidification enthalpy). In addition, only the phase-change solidification temperature of hexyl DHSE presented outstanding changes (13.34%). Given these findings, thermal cycling stability tests were taken one step further, and 1000 thermal cycles were performed following the same methodology.

The results from the 1000 thermal cycles (**Table 4.2**) reveal that solidification and melting enthalpies varied from a gain of 5.36% to a loss of 11.78%. On the one hand, dodecyl DHSE showed the most significant reduction in thermal performance with an 11.78% loss of melting enthalpy. On the other hand, octyl DHSE again showed the highest melting and solidification enthalpies after 1000 heating/cooling cycles (223 and 218 $kJ \bullet kg^{-1}$, respectively). Of the distinct esters prepared, hexyl DHSE presented the best thermal cycling stability since melting and solidification enthalpies did not decreases more than 4% after thermal cycling stability tests.

Table 4.1. Synthetic specifications and thermal properties of the DHSEs prepared from non-edible animal fat (see **Annex III**).

Material	Synthetic			Thermal			
	Isolated Yield (%)	Reaction molar ratio alcohol: DHSA	Crystallization temperature (°C)	$H_{melting}$ (kJ•kg^{-1})	$H_{solidification}$ (kJ•kg^{-1})	$T_{melting}$ (°C)	$T_{solidification}$ (°C)
Methyl DHSE	72	3:1	-20	181.40 ± 0.08	156.26± 0.83	69.31± 0.00	53.86± 0.37
Ethyl DHSE	75	3:1	-20	142.29 ± 1.65	140.70± 0.01	57.06± 0.01	47.50± 0.09
Propyl DHSE	74	3:1	-20	148.82 ± 2.52	138.03± 1.71	58.75± 0.01	43.25± 0.42
Butyl DHSE	60	5:1	-20	136.83 ± 1.88	122.68± 2.62	52.45± 0.01	40.04± 0.00
Pentyl DHSE	77	3:1	-20	155.54 ± 1.90	145.01± 2.04	55.34± 0.14	42.51± 0.63
Hexyl DHSE	69	2:1	-20	213.30 ± 0.30	201.91± 0.54	63.93± 0.05	48.37± 0.23
Octyl DHSE	60	2:1	-20	234.22 ± 3.47	229.71± 3.13	72.65± 0.04	64.57± 0.15
Decyl DHSE	70	2:1	-20	216.62 ± 0.55	203.31± 2.15	72.27± 0.01	55.12± 0.28
Dodecyl DHSE	79	2:1	-20	215.41 ± 2.87	200.31± 2.80	70.70± 0.02	55.63± 0.98
Tetradecyl DHSE	90	2:1	4	191.74 ± 1.26	147.27± 0.91	71.12± 0.01	60.60± 0.01
Hexadecyl DHSE	90	2:1	4	178.77 ± 2.75	175.45± 5.99	71.61± 0.01	64.41± 0.23
Octadecyl DHSE	58	1.1:1	25	160.83 ± 11.29	168.50± 6.43	76.88± 0.06	70.82± 0.08

Table 4.2. Thermal cycling stability results of DHSEs with high thermal storage capacity (see **Annex III**).

Material	Reliability	$H_{melting}$ ($kJ \bullet kg^{-1}$)	$H_{solidification}$ ($kJ \bullet kg^{-1}$)	$T_{melting}$ (°C)	$T_{solidification}$ (°C)
Hexyl DHSE	Cycled 100	213.55±6.25	200.46±4.38	63.99±0.03	41.92±0.08
	Property loss (%)	-0.12	0.72	-0.10	13.34
	Cycled 1000	212.84±0.78	194.33±5.13	64.03±0.04	40.98±1.22
	Property loss (%)	0.21	3.75	-0.16	15.28
Octyl DHSE	Cycled 100	230.05±0.06	228.69±1.04	72.78±0.04	64.65±0.02
	Property loss (%)	1.78	0.44	-0.18	-0.12
	Cycled 1000	221.61±4.59	217.82±12.60	72.55±0.23	60.45±4.14
	Property loss (%)	5.38	5.17	0.14	6.37
Decyl DHSE	Cycled 100	218.78±2.55	209.22±2.41	72.52±0.02	57.07±0.08
	Property loss (%)	-0.99	-2.90	-0.35	-3.54
	Cycled 1000	217.52±6.06	214.22±1.00	72.33±0.01	58.25±2.68
	Property loss (%)	-0.41	-5.36	-0.09	-5.67
Dodecyl DHSE	Cycled 100	209.26±2.35	200.87±2.81	70.74±0.06	55.52±0.23
	Property loss (%)	2.86	-0.28	-0.06	0.21
	Cycled 1000	190.03±3.25	194.74±4.04	70.06±0.16	56.34±0.21
	Property loss (%)	11.78	2.78	0.90	-1.27

From the phase-change temperature point of view, none of the materials tested experienced a temperature change of more than 16%. Nevertheless, the results suggest that thermal cycling increases the sub-cooling effect in several materials. For example, the solidification temperature of hexyl DHSE and octyl DHSE decreased from 48 to 40°C and from 65 to 60°C, respectively. The principal drawback of these materials as PCMs is their sub-cooling, which was increased in some cases by thermal cycling, at least at lab scale. However, some PCMs showed no sub-cooling or less sub-cooling when tested at higher scales, such as hundreds of kilograms, amounts closer to real applications [64].

On the basis of the experimentally obtained thermal properties and thermal cycling tests results, we conclude that the esters prepared from non-edible animal fat in a green and bio-catalytic process can be considered potential PCM candidates. Thus, the preparation of DHSEs improved the thermal stability of DHSA and expanded the application scope. Besides, the diol moiety could easily be modified to groups such as ketals [49] or acetals [21, 49], which allows the substantial decrease of the melting points. Demonstration of the satisfactory thermal properties of these compounds would boost the scope of fatty acid bio-based PCMs.

4.5. Conclusions

Non-edible animal fat waste was transformed successfully into DHSEs that showed good thermal properties as PCMs. These DHSEs were prepared by sustainable reactions such as hot water hydrolysis and bio-catalytic reactions. Biocatalyst reusability was also studied in terms of productivity, whereby immobilized CAL-B successfully afforded the chemo-enzymatic epoxidation and the enzymatic esterification during various cycles. In

addition, *R. ozyzae* resting cells showed a similar performance in the esterification process. α-Limonene showed a high capacity to preserve bio-catalyst activity and also as a solvent to crystalize the DHSEs. The preparation and thermal analysis of these esters is a step forward. On the one hand, we applied green approaches and used non-edible animal fat. On the other hand, regarding thermal energy storage applications, the PCMs developed extend the applications of these esters (bio-PCM) thanks to the high enthalpies achieved (up to 234 $kJ \bullet kg^{-1}$), attractive range of operation (52.45 to 76.88°C) and also good thermal stability after 1000 cycles.

4.6. References

[1] Bongaarts J. Human population growth and the demographic transition. Philos Trans R Soc B, Biol Sci 2009;364:2985–90.

[2] Irshad A, Sureshkumar S, Shalima Shukoor A, Sutha, M. Slaughter house by-product utilization for sustainable meat industry- a review. IJDR 2015,06:4725-34.

[3] Öner C, Altun Ş. Biodiesel production from inedible animal tallow and an experimental investigation of its use as alternative fuel in a direct injection diesel engine. Appl Energy 2009;86:2114–20.

[4] Gallart-Sirvent P, Martín M, Villorbina G, Balcells M, Solé A, Barrenche C, Cabeza L.F, Canela-Garayoa R. Fatty acids and derivatives from non-edible animal fat as phase change materials. RSC Adv 2017; 7: 24133-9.

[5] Yuan Y, Zhang N, Tao W, Cao X, He Y. Fatty acids as phase change materials: A review. Renew Sustain Energy Rev 2014;29:482–98.

[6] Zalba B, Marín JM, Cabeza LF, Mehling H. Review on thermal energy storage with phase change: materials, heat transfer analysis and applications. Appl Therm Eng 2003,23:251-83.

[7] Zhang N, Yuan Y, Du Y, Cao X, Yuan Y. Preparation and properties of palmitic-stearic acid eutectic mixture/expanded graphite composite as phase change material for energy storage. Energy 2014;78:950–6.

[8] Farid MM, Khudhair AM, Razack SAK, Al-Hallaj S. A review on phase change energy storage: Materials and applications. Energy Convers Manag 2004;45:1597–615.

[9] Hu W, Yu X. Thermal and mechanical properties of bio-based PCMs encapsulated with nanofibrous structure. Renew Energy 2014;62:454–8.

[10] Hu W, Yu X. Encapsulation of bio-based PCM with coaxial electrospun ultrafine fibers. RSC Adv 2012;2:5580–4.

[11] Yu S, Jeong SG, Chung O, Kim S. Bio-based PCM/carbon nanomaterials composites with enhanced thermal conductivity. Sol Energy Mater Sol Cells 2014;120:549–54.

[12] Jeong SG, Chung O, Yu S, Kim S, Kim S. Improvement of the thermal properties of bio-based PCM using exfoliated graphite nanoplatelets. Sol Energy Mater Sol Cells 2013;117:87–92.

[13] Kosny J, Kossecka E, Brzezinski A, Tleoubaev A, Yarbrough D. Dynamic thermal performance analysis of fiber insulations containing bio-based phase change materials (PCMs). Energy Build 2012;52:122–31.

[14] Jeong SG, Lee JH, Seo J, Kim S. Thermal performance evaluation of bio-based shape stabilized PCM with boron nitride for energy saving. Int J Heat Mass Transf 2014;71:245–50.

[15] Atabani AE, Silitonga AS, Ong HC, Mahlia TMI, Masjuki HH, Badruddin IA. Non-edible vegetable oils: A critical evaluation of oil extraction, fatty acid compositions, biodiesel production, characteristics, engine performance and emissions production. Renew Sustain Energy Rev 2013;18:211–45.

[16] Li A, Li K. Pressure-sensitive adhesives based on epoxidized soybean oil and dicarboxylic acids. ACS Sustain Chem Eng 2014;2:2090–6.

[17] Wu Y, Li A, Li K. Pressure sensitive adhesives based on oleic acid. J Am Oil Chem Soc 2015;92:111–20.

[18] Meier M a R, Metzger JO, Schubert US. Plant oil renewable resources as green alternatives in polymer science. Chem Soc Rev 2007;36:1788–802.

[19] Kulik A, Martin A, Pohl M-M, Fischer C, Köckritz A. Insights into gold-catalyzed synthesis of azelaic acid. Green Chem 2014;16:1799-1806.

[20] Kulik A, Janz A, Pohl MM, Martin A, Köckritz A. Gold-catalyzed synthesis of dicarboxylic and monocarboxylic acids. Eur J Lipid Sci Technol 2012;114:1327–32.

[21] Filley J. New lubricants from vegetable oil: Cyclic acetals of methyl 9, 10-dihydroxystearate. Bioresour Technol 2005;96:551–5.

[22] Koay GFL, Chuah T, Zainal-abidin S, Ahmad S, Choong TSY. Development , characterization and commercial application of palm based dihydroxystearic acid and its derivatives : an overview. J Oleo Sci 2011;265:237–65.

[23] Swern, D, Scanlan JT, Dickel GB. 9, 10-Dihydroxystearic Acid. Org Synth 1959;39:15.

[24] Palm oil-based hydroxy fatty acids. EP., EP001588999A2, 2005.

[25] Gaveau DL, Wich S, Epting J, Juhn D, Kanninen M, Leader-Williams N. The future of forests and orangutans (Pongo abelii) in Sumatra: predicting impacts of oil palm plantations, road construction, and mechanisms for reducing carbon emissions from deforestation. Environ Res Lett 2009;4:19.

[26] Fitzherbert EB, Struebig MJ, Morel A, Danielsen F, Brühl CA, Donald PF, et al. How will oil palm expansion affect biodiversity? Trends Ecol Evol 2008;23:538–45.

[27] Koh LP, Wilcove DS. Is oil palm agriculture really destroying tropical biodiversity? Conserv Lett 2008;1:60–4.

[28] Suppes GJ, Goff MJ, Lopes S. Latent heat characteristics of fatty acid derivatives pursuant phase change material applications. Chem Eng Sci 2003;58:1751–63.

[29] Alper Aydn A. High-chain fatty acid esters of 1-octadecanol as novel organic phase change materials and mathematical correlations for estimating the thermal properties of higher fatty acid esters homologous series. Sol Energy Mater Sol Cells 2013;113:44–51.

[30] Alper Aydın A, Aydın A. High-chain fatty acid esters of 1-hexadecanol for low temperature thermal energy storage with phase change materials. Sol Energy Mater Sol Cells 2012;96:93–100.

[31] Alper Aydn A, Okutan H. High-chain fatty acid esters of myristyl alcohol with odd carbon number: Novel organic phase change materials for thermal energy storage - 2. Sol Energy Mater Sol Cells 2011;95:2417–23.

[32] Alper Aydn A, Okutan H. High-chain fatty acid esters of myristyl alcohol with odd carbon number: Novel organic phase change materials for thermal energy storage - 2. Sol Energy Mater Sol Cells 2011;95:2417–23.

[33] Awang R, Basri M, Ahmad S, Salleh AB. Enzymatic esterification of dihydroxystearic acid. J Am Oil Chem Soc 2000;77:609–12.

[34] Awang R, Basri M, Ahmad S, Salleh AB. Lipase catalyzed esterification of palm based 9, 10-dihydroxystearic acid and 1-octanol in hexane – a kinetic study. Biotechnol Lett 2004;26:11–4.

[35] Gallart-Sirvent P, Yara E, Villorbina G, Balcells M, Sala N, Canela-Garayoa R. Recycling Rhizopus oryzae resting cells as biocatalyst to prepare near eutectic palmitic-stearic acid mixtures from non-edible fat. J Mol Catal B Enzym 2016;134:172–7.

[36] Eras J, Montañes F, Ferran J, Canela R. Chlorotrimethylsilane as a reagent for gas chromatographic analysis of fats and oils. J Chromatogr A 2001;918:227–32.

[37] Swern D, Jordan EF. Aliphatic Esters of the 9, 10-Dihydroxystearic acids. J Am Chem Soc 1945;67:902–3.

[38] Warwel S, Rüsch gen. Klaas M. Chemo-enzymatic epoxidation of unsaturated carboxylic acids. J Mol Catal B Enzym 1995;1:29–35.

[39] Törnvall U, Orellana-Coca C, Hatti-Kaul R, Adlercreutz D. Stability of immobilized Candida antarctica lipase B during chemo-enzymatic epoxidation of fatty acids. Enzyme Microb Technol 2007;40:447–51.

[40] Orellana-Coca C, Törnvall U, Adlercreutz D, Mattiasson B, Hatti-Kaul R. Chemo-enzymatic epoxidation of oleic acid and methyl oleate in solvent-free medium. Biocatal Biotransformation 2005;23:431–7.

[41] Prat D, Wells A, Hayler J, Sneddon H, McElroy CR, Abou-Shehada S. CHEM21 selection guide of classical- and less classical-solvents. Green Chem 2016;18:288–96.

[42] Herrmann WA, Fischer RW, Marz DW. Methyltrioxorhenium als katalysator fur die olefin-oxidation. Angew Chem 1991;33:1706-09.

[43] Niehaus WG, Schroepfer GJ. Enzymic stereospecificity in the hydration of epoxy fatty acids. Stereospecific incorporation of the oxygen of water. J Am Chem Soc 1967; 89: 4227-8.

[44] Niehaus WG, Kisic A, Torkelson A, Bednarczyk DJ, Schroepfer GJ. Stereospecific hydration of cis- and trans- 9,10-epoxyoctadecanoic acids. J Biol Chem 1970; 245:3802-09.

[45] Watabe T, Akamatsu K. Stereoselective hydrolysis of acyclic olefin oxides to glycols by hepatic microsomal epoxide hydrolase. BBA 1972;279:297-305.

[46] Blee E, Schuber F. Occurrence of fatty acid epoxide hydrolases in soybean (Glycine max). Purification and characterization of the soluble form. Biochem J 1992;282:711–4.

[47] Wang Z, Cui YT, Xu ZB, Qu J. Hot water-promoted ring-opening of epoxides and aziridines by water and other nucleopliles. J Org Chem 2008;73:2270–4.

[48] Morten CJ, Byers JA, Van Dyke AR, Vilotijevic I, Jamison TF. The development of endo-selective epoxide-opening cascades in water. Chem Soc Rev 2009;38:3175–92.

[49] Godard A, Thiebaud-Roux S, De Caro P, Vedrenne E, Mouloungui Z. New one-pot syntheses of ketals and acetals from oleic acid. Ind Crops Prod 2014;52:111–7.

[50] Lokotsch W, Lang S, Mbius D, Wagner F. Biocatalytical synthesis and monolayer studies of multiple hydroxylated wax esters 1996;73:1459–64.

[51] Awang R, Basri M, Ahmad S, Salleh A. Thermomyces lanuginosus lipase-catalyzed esterification of 9, 10-dihydroxystearic acid and monohydric alcohol. J Oleo Sci 2005;54:305–9.

[52] Yara-Varón E, Selka A, Fabiano-Tixier AS, Balcells M, Canela-Garayoa R, Bily A. Solvent from forestry biomass. Pinane a stable terpene derived from pine tree byproducts to substitute n-hexane for the extraction of bioactive compounds. Green Chem 2016;18:6596–608.

[53] Paggiola G, Hunt AJ, McElroy CR, Sherwood J, Clark JH. Biocatalysis in bio-derived solvents: an improved approach for medium optimisation. Green Chem 2014;16:2107–10.

[54] Lanctôt AG, Attard TM, Sherwood J, McElroy CR, Hunt AJ. Synthesis of cholesterol-reducing sterol esters by enzymatic catalysis in bio-based solvents or solvent-free. RSC Adv 2016;6:48753–6.

[55] Cabeza LF, Castell A, Barreneche C, De Gracia A, Fernández AI. Materials used as PCM in thermal energy storage in buildings: A review. Renew Sustain Energy Rev 2011;15:1675–95.

[56] Kousksou T, Bruel P, Cherreau G, Leoussoff V, El Rhafiki T. PCM storage for solar DHW: From an unfulfilled promise to a real benefit. Sol Energy 2011;85:2033–40.

[57] Brückner S, Liu S, Miró L, Radspieler M, Cabeza LF, Lävemann E. Industrial waste heat recovery technologies: An economic analysis of heat transformation technologies. Appl Energy 2015;151:157–67.

[58] Günther E, Hiebler S, Mehling H, Redlich R. Enthalpy of phase change materials as a function of temperature: Required accuracy and suitable measurement methods. Int J Thermophys 2009; 30: 1257–69.

[59] Sari A, Eroglu R, Biçer A, Karaipekli A. Synthesis and thermal energy storage properties of erythritol tetrastearate and erythritol tetrapalmitate. Chem Eng Technol 2011;34:87–92.

[60] Sari A, Biçer A, Lafçi Ö, Ceylan M. Galactitol hexa stearate and galactitol hexa palmitate as novel solid-liquid phase change materials for thermal energy storage. Sol Energy 2011;85:2061–71.

[61] Feldman D, Banu D, Hawes D. Low chain esters of stearic acid as phase change materials for thermal energy storage in buildings. Sol Energy Mater Sol Cells 1995;36:311–22.

[62] Solé A, Neumann H, Niedermaier S, Cabeza LF, Palomo E. Thermal stability test of sugar alcohols as phase change materials for medium temperature energy storage application. Energy Procedia 2014;48:436–9.

[63] Solé A, Neumann H, Niedermaier S, Cabeza LF, Palomo E. Thermal stability test of sugar alcohols as phase change materials for medium temperature energy storage application. Energy Procedia 2014; 48: 436–9.

[64] Gil A, Barreneche C, Moreno P, Solé C, Inés Fernández A, Cabeza LF. Thermal behaviour of d-mannitol when used as PCM: Comparison of results obtained by DSC and in a thermal energy storage unit at pilot plant scale. Appl. Energy 2013; 111: 1107–13.

Chapter V

Preparation of pressure-sensitive adhesives from tung oil via Diels-Alder reaction

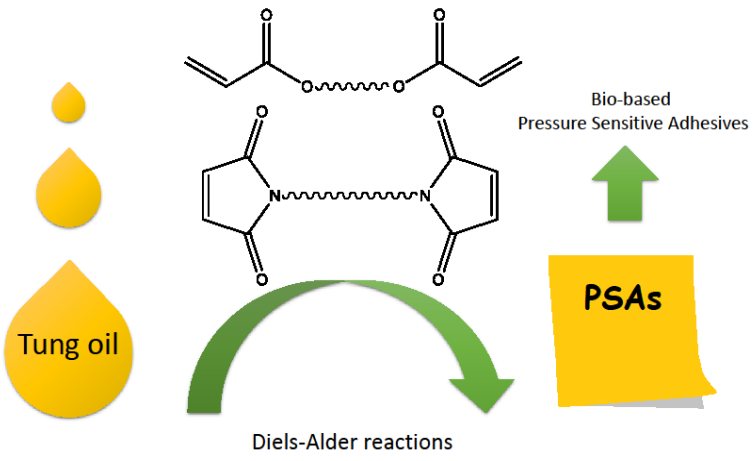

Part of the results described in this chapter were realized in the Oregon State University under the supervision of professors Kaichang Li and Anlong Li.

Part of the results contained in this chapter has been submitted to: International Journal of Adhesives.

5.1. Abstract

In this study, tung oil was polymerized with a dimaleimide (4,4'-methylene-bis(*N*-phenylmaleimide) (MPMI) and two diacrylates (poly(propylene glycol) diacrylate (PPGDA) and bisphenol A glycerolate diacrylate (BPAGDA) *via* Diels-Alder reaction (DA reaction) to prepare pressure-sensitive adhesives (PSAs). On the one hand, the polymer of tung oil and MPMI was readily prepared however it was too rigid to serve as a PSA. On the other hand, the polymerization of tung oil with PPGDA or BPAGDA resulted in PSAs with peel strengths ranging from 0.1 to 0.2 N•cm^{-1} and loop tacks ranging from 0.4 to 0.5 N. Nevertheless, tung oil reacted readily with acrylic acid to form adducts (TOAA) with lower content of conjugated diene groups than those of tung oil. The use of TOAAs instead of tung oil to polymerize PPGDA failed to increase the peel strength of the resulting PSAs. However, polymerizations of TOAAs with BPAGDA resulted in PSAs with much higher peel strengths and much higher loop tacks than the polymerization of tung oil with BPAGDA. In addition, the introduction of small amount of MPMI in the polymerization of TOAA and PPGDA significantly shortened the curing time.

Keywords: Pressure-sensitive adhesive, peel, tung oil, Diels-Alder reaction, non-edible vegetable oil.

Abbreviations of this chapter: BPAGDA, bisphenol A glycerolate diacrylate; CDG, conjugate diene group; DA reaction, Diels-Alder reaction; DG, dienophile group; ESO, epoxidized soy bean oil; MPMI, 4,4'-methylene-bis(N-phenylmaleimide); PET, polyethylene terephthalate; PPGDA, poly(propylene glycol) diacrylate; PSA, pressure-sensitive adhesive; TOAA, an adduct from the reaction of tung oil and acrylic acid.

5.2. Introduction

Pressure-sensitive adhesives (PSA) are a category of adhesives that are tacky, can quickly bond with adherents when a light pressure is applied, and can be removed from the adherents due to their sufficient cohesion strength [1]. PSAs are widely used in industry and everyday life in forms of PSA tapes, labels and protective films, *etc*. At present, commercial PSAs are mainly based on petrochemical-derived polymers such as acrylate-based copolymers, styrene-based block copolymers, ethylene-vinyl acetate copolymers, polyisobutylenes, and polyurethanes [2–4]. Nevertheless, these PSAs are not based on renewable materials and thus not sustainable.

The use of renewable natural materials to replace petrochemicals can slow down the depletion of petroleum and promote more sustainable industries. As PSAs are consuming a large amount of petrochemicals every year; the development of PSAs from renewable materials appears to be inherent. Recently, the development of PSAs from renewable plant oils acquired great importance [2–7]. Indeed, it has been demonstrated that PSAs could be developed from polymerizations of epoxidized soybean oil (ESO) with carboxylic acids [2], polymerization of ESO with phosphoric acid [6], polymerization of epoxidized oleic acid [4, 5], polymerization of a mixture of epoxidized fatty acids that is prepared directly from ESO [7], and polymerization of acrylated epoxidized methyl oleate [3]. These new PSAs are mainly based on soybean oil that is an edible plant oil. Edible plant oils are mainly used as food [8], therefore, it is better desirable to use non-edible plant oils as an alternative for the preparation of the PSAs.

In that regard, tung oil is a non-edible plant oil containing about 80% of α-eleostearic acid and a small amount of β-eleostearic acid [9]. As

highlighted, both α-eleostearic acid and β-eleostearic acid contain a conjugated diene group that can readily undergo Diels-Alder (DA) reaction with dienophiles such as maleic anhydride, maleimides and acrylates [10-12]. Indeed, the DA reaction was recently used to develop PSAs from tung oil [13]. Tung oil was functionalized with maleic anhydride (MA) to prepare an adduct and then, was further polymerized with diols such as poly (propylene glycol) for the PSAs [13].

In this study, a new approach has been developed for the preparation of PSAs through the direct DA polymerization of tung oil or acrylic acid-modified tung oil with chemicals containing two dienophile groups. The resulting polymers were evaluated for their PSA properties such as peel strength, loop tack, shear adhesion and aging resistance. The effects of the molecular structures and usages of the monomers on the PSA properties of the final polymers were discussed.

5.3. Experimental section

5.3.1. Materials

Tung oil, bisphenol A glycerolate diacrylate (BPAGDA), poly(propylene glycol) diacrylate (PPGDA) with a number-averaged molecular weight of 800, and acrylic acid (purity, 99%) were purchased from Sigma-Aldrich Corp. (St. Louis, MO). 4,4'-Methylene-bis(N-phenylmaleimide) (MPMI) (purity, 95%) was purchased from Alfa Aesar (Ward Hill, MA). All reagents were used as received. Poly (ethylene terephthalate) (PET) film (thickness, ~50 μm) was obtained from Henkel Corp. (Rochy Hill, CT) and used as a backing material for the PSAs obtained in this study.

5.3.2. Analyses

^{1}H NMR spectra were recorded with a MERCURY plus NMR Spectrometer Systems VARIAN Imant AS operating at 400 MHz. FT-IR spectra were recorded with a Thermo Nicolet Nexus 470 FT-IR spectrometer (Thermo Nicolet Corp., Madison, WI) coupled with a Smart Golden Gate diamond ATR accessory in a scanning range of 650-4000 cm^{-1} for 32 scans at a spectral resolution of 2•cm^{-1}.

5.3.3. Syntheses

5.3.3.1. Polymerization of tung oil and MPMI

Tung oil (3.93 g, 11.8 mmol of conjugated diene groups (CDG)) and MPMI (2.22 g, 11.8 mmol of dienophile groups (DG)) were placed in a round-bottom flask equipped with a silicone oil bath and a magnetic stirrer. The resulting mixture was stirred at 200 rpm and bubbled with nitrogen gas for 5 min at room temperature. The reaction mixture was stirred at 105˚C for 25 min when the mixture became an orange gel. The gel was further heated at 140˚C for 35 min to give a tough appeared as a solid.

5.3.3.2. Preparation of PSAs from tung oil and PPGDA

Tung oil (3.50 g, 10.3 mmol of CDG) and PPGDA (4.13 g, 10.3 mmol of DG) were placed in a round-bottom flask equipped with a silicone oil bath and a magnetic stirrer. The resulting mixture was stirred at 200 rpm and bubbled with nitrogen gas for 5 min at room temperature. The reaction mixture was stirred at 160˚C for 8 h to give a clear, light brown–yellow and viscous polymer. The polymer while still hot and spreadable was then coated onto a sheet of PET film at a coating thickness of about 3.5 mg/cm^{2} with a HLCL-

1000 hot-melt coater (ChemInstruments, Inc., Fairfield, OH). The polymer on the PET film was further cured in an air-circulating oven at 150˚C until FT-IR spectra of the coating showed that the characteristic conjugated diene peak of tung oil at 990 cm^{-1} disappeared, which took about 3 h. The polymer/PET film laminate (designated as a PSA tape) was taken out of the oven, and measured for its PSA properties.

5.3.3.3. Preparation of PSAs from tung oil and BPAGDA

Tung oil (4.00 g, 11.8 mmol of CDG) and BPAGDA (2.86 g, 11.8 mmol of DG) were placed in a round-bottom flask equipped with a silicone oil bath and a magnetic stirrer. The resulting mixture was stirred at 200 rpm and bubbled with nitrogen gas for 5 min at room temperature. The reaction mixture was stirred at 160˚C for 1 h to give a clear, light brown–yellow and viscous polymer. The polymer was then coated on a sheet of PET film and cured with the same procedures as described in the section 5.3.3.2. After a curing time of 3 h, the polymer/PET film laminate was measured for its PSA properties.

5.3.3.4. Preparation of the tung oil-acrylic acid adducts (TOAA)

A typical procedure for the preparation of TOAA was described as follows. Tung oil (40.00 g, 0.118 mol of CDG) and acrylic acid (3.40 g, 0.0472 mol of DG) were placed in a round-bottom flask equipped with a silicone oil bath and a magnetic stirrer. The resulting mixture was stirred at 200 rpm and bubbled with nitrogen gas for 5 min at room temperature. The reaction mixture was stirred at 160˚C for 6 h to give clear, light yellow and viscous oil. This TOAA was prepared with 0.4 molar ratio of the DG of acrylic acid to the CDGs of tung oil (DG/CDG), and was thus designated as TOAA0.4 in this

paper. Likewise, another TOAA was prepared with a DG/CDG molar ratio of 0.3, and was designated as TOAA0.3.

5.3.3.5. Preparation of PSAs from TOAA0.4 and BPAGDA

A typical procedure using TOAA0.4 as a modified tung oil for the preparation of a PSA was described as follows. TOAA0.4 (5.10 g, 8.32 mmol of CDG) and BPAGDA (2.02 g, 8.32 mmol of DG) were placed in a round-bottom flask equipped with a silicone oil bath and a magnetic stirrer. The resulting mixture was bubbled with nitrogen gas for 5 min and stirred at 200 rpm at room temperature. The reaction mixture was stirred at 160˚C for 2.5 h to give a clear, light brown–yellow and viscous polymer. The polymer was then coated on a sheet of PET film and cured with the same procedures as described in section 5.3.3.2. After a curing time of 2 h, the polymer/PET film laminate was measured for its PSA properties.

5.3.3.6. Preparation of PSAs from TOAAs and PPGDA

A typical procedure using TOAA0.4 as a modified tung oil for the preparation of a PSA was described as follows. TOAA0.4 (4.34 g, 7.08 mmol of CDG) and PPGDA (2.83 g, 7.08 mmol of DG) were placed in a round-bottom flask equipped with a silicone oil bath and a magnetic stirrer. The resulting mixture was stirred at 200 rpm and bubbled with nitrogen gas for 5 min at room temperature. The reaction mixture was stirred at 160˚C for 4 h to give a clear, light brown–yellow and viscous polymer. The polymer was then coated on a sheet of PET film and cured with the same procedures as described in the section 5.3.3.2. After a curing time of 1.5 h, the polymer/PET film laminate was measured for its PSA properties.

5.3.3.7. Preparation of PSAs from TOAA0.4, PPGDA and MPMI

TOAA0.4 (4.14 g, 6.55 mmol of CDG) and PPGDA (1.75 g, 4.36 mmol of DG) were placed in a round-bottom flask equipped with a silicone oil bath and a magnetic stirrer. The resulting mixture was stirred at 200 rpm and bubbled with nitrogen gas for 5 min at room temperature. The reaction mixture was stirred at 160˚C for 8 h. To this reaction mixture, a solution of MPMI (0.41 g, 2.18 mmol of DG) in acetone (3 mL) was added. The resulting mixture was then stirred for 20 min at room temperature to give a clear, light orange and viscous solution. The solution was coated onto a sheet of PET film with a coater. The coating on the PET film was placed in a fume hood for about 20 min, allowing complete evaporation of acetone. The coating on the PET film was then placed in an air-circulating oven maintained at 150˚C for curing. After a curing time of 0.5 h, the polymer/PET film laminate was measured for its PSA properties.

5.3.4. Measurements of the properties of the PSAs and the aging test

The measurements of peel strength, shear adhesion and loop tack, and the aging test at 60˚C for the PSA tapes were performed in accordance with the conditions and methods described in the previous studies [2, 4, 5, 7, 13]. More specifically, measurement of the peel strength was carried out on a stainless steel panel in accordance with Test Method F of ASTM D3330/D3330M-04 (Standard Test Method for Peel Adhesion of Pressure-Sensitive Tape). Three strips with a size of 25 mm by 150 mm were cut from each of the PSA tapes as prepared in previous sections. One end of the PSA strip was applied onto the panel and then pressed with a roller with a weight of 2040 g twice in the lengthwise direction. The test panel was then fixed at

the bottom grip of a tensile tester. The free end of the PSA strip was fold back and attached to the upper grip that was connected to the load cell of the tester. The PSA strip was then peeled upwards at about 180˚ angle at a speed of 5 mm•s^{-1}; the force required to peel off the strip from the test panel was recorded as peel strength. Three specimen strips were tested for each PSA tape sample and the averaged value in N•cm^{-1} was reported as the peel strength.

The loop tack of the PSA tapes was measured on a stainless steel panel (Type 302) in accordance with Test Method A of ASTM D6195-03 (Standard Test Methods for Loop Tack). Three strips with a size of 25 mm by 150 mm were cut from each of the PSA tapes as prepared in previous sections. A loop with the PSA facing outwards was prepared from each PSA strip. The loop was brought into contact with the test panel with a contact area of 25 by 25 mm without an external pressure applied. The loop was then immediately pulled away from the test panel at a speed of 5 mm•s^{-1}; the maximum force required to remove the PSA loop from the test panel was recorded as the loop tack.

The shear adhesion was measured on a stainless steel panel (Type 302) in accordance with ASTM D3654/D3654M-06 (Standard Test Methods for Shear Adhesion of Pressure-Sensitive Tapes). PSA strips with a size of 25 mm by 120 mm were cut from each of the PSA tapes as prepared in previous sections. Each PSA strip was applied onto the test panel with a contact area of 24 by 24 mm, the PSA strip was then pressed with a roller with a weight of 2040 g twice in lengthwise direction. The test panel with the applied PSA strip was then fixed on a stand at a tilt angle of 2° relative to the vertical direction. After 20 min, the free end of the PSA strip was attached to a mass of 1000 g. The time to failure, i.e., the time between the attachment of the

mass and complete separation of the PSA strip from the test panel, was used as an indication of shear adhesion.

The test on the aging resistance for the PSAs was performed in accordance with the following procedure. Briefly, PSA tapes as prepared in previous sections were placed in an Isotemp 625D incubator (Thermo Fisher Scientific Inc., Waltham, MA) maintained at 60°C. After one week, the PSA tape was taken out of the incubator and conditioned at 23 ± 1°C and 40 ± 5 % relative humidity for about one day. PSA strips were then cut from the aged sample tapes and measured for their peel strength, shear adhesion and loop tack in accordance with the methods described previously.

5.3.5. Statistical analysis

The data of the peel strength, loop tack and shear adhesion were statistically analyzed with a two-sample t-test using Microsoft Excel (version 2010, Microsoft Corp., Redmond, WA). All comparisons were based on a 95% confidence interval.

5.4. Results and Discussion

5.4.1. Polymerization of tung oil with MPMI, PPGDA or BPAGDA, and preparation of PSAs from these polymers

From the two fatty acids presenting conjugated groups in tung oil, α-eleostearic acid has two C=C bonds in *trans* configuration (C11 and C13, **Figure 5.1**) and one C=C bond in *cis* configuration (C9, **Figure 5.1**), and β-eleostearic acid has all three C=C bonds in *trans* configuration (**Figure 5.1**). In terms of reactivity, it has been demonstrated that the *trans*–*trans* conjugated C=C bonds in tung oil can readily undergo Diels-Alder (DA)

reaction with dienophiles such as maleic anhydride, maleimides and acrylates [10–12]. Each fatty chain of α-eleostearic acid or β-eleostearic acid accounts for one CDG since each chain can only react with one DG (i.e., one C=C bond) *via* the DA reaction. Thus, tung oil should be able to function as a monomer to polymerize with a chemical containing two DGs *via* the DA reaction because each triglyceride molecule of tung oil contains at least two CDGs.

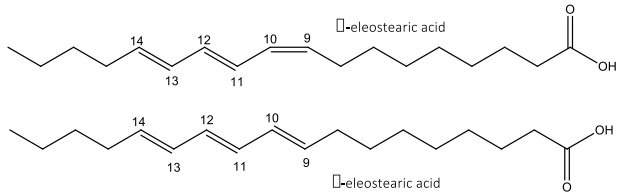

Figure 5.1. Chemical structures of α-eleostearic acid and α-eleostearic acid.

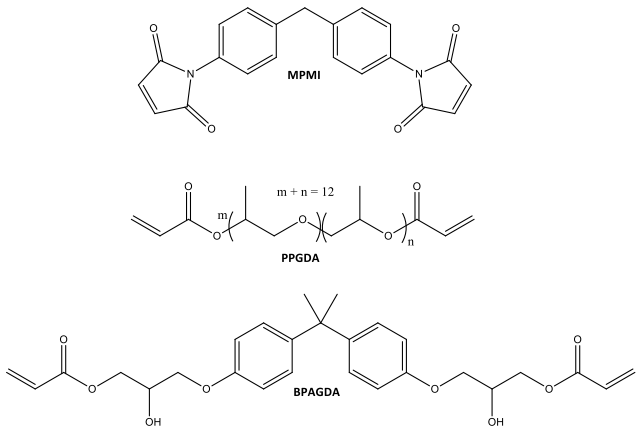

Figure 5.2. Chemical structures of the monomers used to polymerize tung oil or TOAA via the DA reaction.

Chemicals containing two DGs used in this study are shown in **Figure 5.2**. Polymers were prepared from reactions of tung oil with each chemical shown

in **Figure 5.2**, and were evaluated if they have desirable PSA properties. The first polymer was made from the reaction of tung oil with MPMI at the 1:1 molar ratio of the CDGs of tung oil to the DGs of the dimaleimide in the absence of any catalysts. The reaction proceeded readily at 105 °C, resulting in a semi-solid gel in 25 min. The gel was characterized with FT-IR. The FT-IR spectrum showed that the peak of the CDGs of tung oil at 990 cm^{-1} and the peak of the DGs of MPMI at 825 cm^{-1} were still obviously observed (**Figure 5.3**, bottom), which indicated that the CDGs and the DGs were not fully reacted. Further heating at a higher temperature of 140 °C for an additional 35 min resulted in a tough solid. FT-IR spectrum of the solid showed that the peaks of the CDGs and DGs almost disappeared (**Figure 5.3**, top), which indicated that most of the CDGs had reacted with the DGs *via* the DA reaction. The resulting (tung oil)-MPMI polymer was neither soft nor tacky, which indicated that it was too rigid to serve as a PSA.

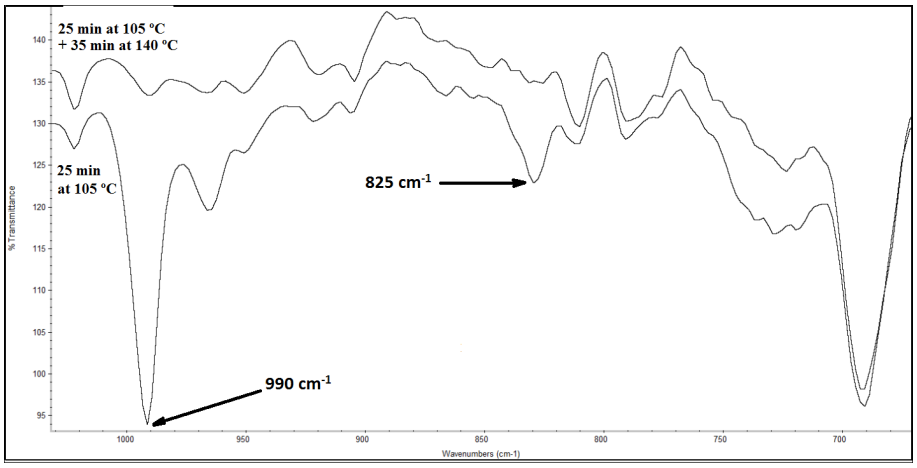

Figure 5.3. FT-IR spectra of the reaction mixture of tung oil and MPMI that was heated at 105˚C for 25 min (bottom) and further heated at 140˚C for another 35 min (top), respectively.

The second polymer, also a gel, was made from the reaction of tung oil with PPGDA. The reaction had to be conducted at a higher reaction temperature of 160 °C than that (105 °C) used in the (tung oil)-MPMI reaction, and a longer reaction time of 8.5 h than that (about 0.5 h) for the latter, which is consistent with the fact that the DGs of MPMI are more reactive to CDGs than the acrylic DGs of PPGDA. The resulting polymer was tacky, which was a good sign that it might be used as a PSA. For further evaluation of its PSA properties, the polymer was coated on a backing material of PET film for forming a PSA tape. The peel strength and loop tack of the resulting tape are shown as the entry 1 in **Table 5.1** and are in the low end of all commercial PSA-based tapes and labels. Therefore, the resulting PSA might be used for applications such as post-it® notes or protective films that only require low strength. After aging at 60 °C for one week, the peel strength and loop tack of the tape did not significantly change as compared with those before aging (entry 1, **Table 5.1**), which indicated that the resulting PSA was fairly aging resistant. For typical petrochemical-based PSAs, one week of aging at 60 °C is equivalent to 9 months of natural aging, i.e., storage at room temperature [13]. If this is applicable to the PSA from tung oil and PPGDA, it is stable for at least 9 months under natural conditions. The PSA tape from the polymer of tung oil and BPAGDA also had a low peel strength and a low loop tack (entry 2, **Table 5.1**). However, the PSA tape lost its tackiness after its aging at 60 °C for one week, which indicated that the PSA was not aging resistant.

Table 5.1. PSA properties of the polymers prepared from tung oil or TOAA with PPGDA or BPAGDA.

Entries	tung oil or TOAA	Other monomers	Peel strength ($N \bullet cm^{-1}$)	Loop tack (N)	Shear adhesion (h)	Peel strength after aging ($N \bullet cm^{-1}$)	Loop tack after aging (N)
1	tung oil	PPGDA	0.1	0.4	nm*	0.1	0.3
2	tung oil	BPAGDA	0.2	0.5	nm	0	0
3	TOAA0.3	BPAGDA	0.9	3.9	nm	nm	nm
4	TOAA0.4	BPAGDA	1.1	5.1	At least 168	0.9	4.2
5	TOAA0.4	PPGDA	0.1	0.6	At least 168	nm	nm
6	TOAA0.4	PPGDA+MPMI	0.1	1.4	At least 168	0.1	1.3

* nm stands for “not measured”.

Tung oil has an average of about 2.6 CDGs per triglyceride molecule [13] and is viewed as a multifunctional monomer, whereas PPGDA and BPAGDA have two DGs and are difunctional monomers. The disappearance of the characteristic peak of CDGs in the FT-IR spectra of the (tung oil)-PPGDA and (tung oil)-BPAGDA polymers confirmed that the polymerizations were through the DA reaction. According to a theory developed by Flory and Stockmayer [14], step-growth polymerization of a multifunctional monomer with a difunctional monomer would result in a gel that contained crosslinked polymer networks. The conversion of the CDGs or DGs at the gel point (“the gel-point conversion”, p_c) can be calculated from the Equation (1) derived by Flory and Stockmayer [14].

$$pc = 1/[r(f_{CDG} -1)(f_{DG} -1)]^{1/2} \qquad \textit{Equation (1)}$$

Wherein, r is the initial CDG/DG molar ratio, f_{CDG} is the number of CDGs per molecule of tung oil, f_{DG} is the number of DGs per molecule of a diacrylate.

For the polymerization of tung oil and a diacrylate with the CDG/DG molar ratio of 1, i.e., r =1, and given that f_{CDG} = 2.6 and f_{DG} = 2 for tung oil and the diacrylate, respectively, *pc* was 0.79 from the Equation (1). This implied that crosslinked polymer networks started to form and the reaction mixture became a gel when the conversion of the CDGs or DGs reached 79%. For a step-growth polymerization, the degree of polymerization (*Xn*) and hence the number-averaged molecular weight are related to the conversion (*p*) of CDGs or DGs in accordance with Carothers' equation, Equation (2) [14].

$$Xn = 1/(1-p) \qquad \textit{Equation (2)}$$

At the gel-point conversion of 79%, the X_n was 4.8 from Equation (2). This implied that the reaction resulted in mostly oligomers at the gel point. Once a gel was formed, the mobility of the oligomers and unreacted monomers was greatly reduced. When the gel was further cured with heat, the remaining high amount of CDGs and DGs would react locally. It is reasonably assumed that the local reactions between CDGs and DGs would result in polymers with high crosslinking density, but low average molecular weights between crosslinks (M_c). Such polymers were expected to have low strength, which is consistent with the low peel strength of the PSAs from the polymerization of tung oil with PPGDA or BPAGDA (**Table 5.1**). BPAGDA in the PSA polymer chains has rigid phenylene moieties that can stack together through π-electron interactions, commonly known as π-electron stacking [2], thus resulting in physical crosslinks among the polymer chains. In addition, BPAGDA has a high amount of hydroxyl groups (−OH) that can form hydrogen bonds, i.e., crosslinks among the polymer chains. The aging process appeared to facilitate the π-electron stacking and the hydrogen bond formation, thus

turning a tacky material into non-tacky one, which explains the poor aging resistance of the PSA from tung oil and BPAGDA.

5.4.2. Preparation of PSAs from polymerization of TOAA with PPGDA or BPAGDA

For having desirable PSA properties, PSA polymers must have sufficiently long polymer chains, and the polymer chains also have to be slightly crosslinked so that they are strong enough to stay together, i.e., do not leave any residues when the PSA tape is peeled off an adherent. However, the crosslinking density has to be sufficiently low so that the polymer networks are still soft and flexible enough to readily deform under light pressure for wetting an adherent, thus resulting in high tack and high peel strength. Therefore, our attention was diverted to increasing the molecular weight and decreasing the crosslinking density of the polymers to see if the tack and peel strength could be improved.

Under otherwise the same conditions, i.e., r =1 and f_{DG} = 2, the Equation (1) could be simplified as Equation (3).

$$p_c = 1/[(f_{CDG}-1)]^{1/2} \qquad \textit{Equation (3)}$$

Per the Equation (3), decreasing f_{CDG} would increase the gel-point conversion, p_c. According to the Equation (2), a higher conversion of the functional groups would result in a higher X_n and hence a higher molecular weight of the resulting polymers, which would theoretically increase the adhesive strength of the polymers. In addition, when a higher conversion of functional groups was achieved before a polymerization mixture became a gel, there would be a smaller amount of functional groups left to form new crosslinks;

accordingly, the final polymers would have a lower crosslinking density and a higher M_c.

For the reduction of CDGs of tung oil, a small amount of acrylic acid was used as a dienophile for the modification of tung oil. The modification also introduced carboxylic acid groups (-COOH) onto the modified tung oil and eventual PSA polymers. The -COOH groups on the PSA polymers could improve wetting of the PSAs on adherents and improve the bond strength of the PSAs to the adherents through formation of hydrogen bonds and/or other non-covalent interactions [2, 4, 5, 13].

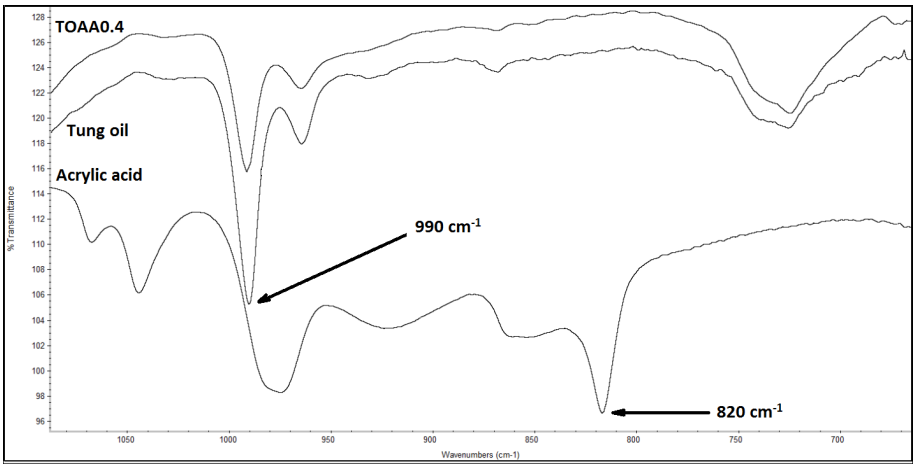

Figure 5.4: FT-IR spectra of TOAA0.4 (top), tung oil (middle) and acrylic acid (bottom).

Acrylic acid-modified tung oil, TOAA0.4, was prepared by reacting a mixture of tung oil and acrylic acid at the 0.4 molar ratio of the DG of acrylic acid to the CDGs of tung oil (DG/CDG). The reaction proceeded readily at 160 °C and was monitored with FT-IR (**Figure 5.4**). It was found that the peak corresponding to the DG of acrylic acid at 820 cm^{-1} completely disappeared in 6 h, and the intensity of the peak at 990 cm^{-1} corresponding to CDGs of

tung oil gradually decreased and remained constant after 6 h. The ^{1}H NMR spectrum of the reaction product also showed new peaks at 3.0-3.6 ppm that were corresponding to the proton on carbon n° 54 in the newly formed cyclohexene rings (**Figure 5.5**). Likewise, TOAA0.3 was readily prepared at a DG/CDG of 0.3, which had a higher f_{CDG} than TOAA0.4 because a smaller amount of acrylic acid was used for the consumption of the CDGs of tung oil in its preparation.

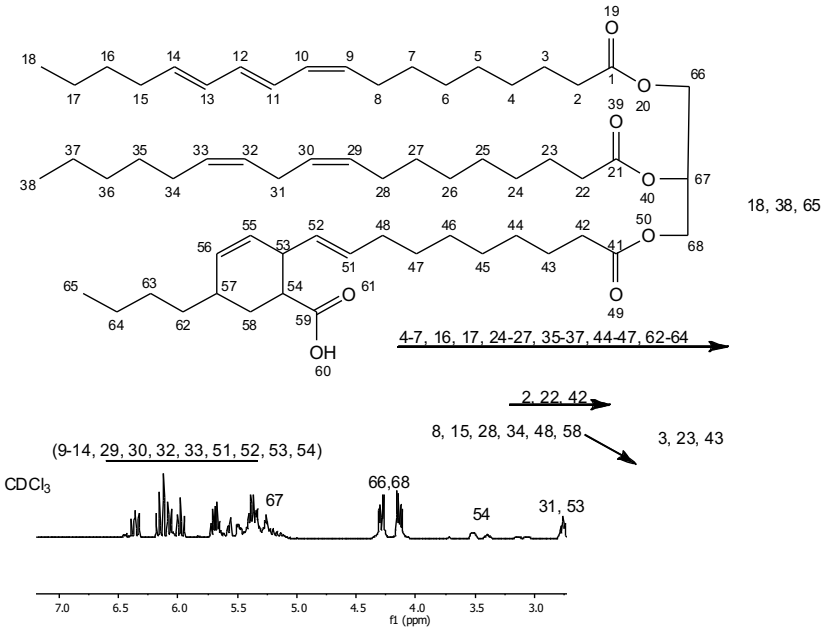

Figure 5.5. ^{1}H NMR spectra of the TOAA0.4 obtained from the reaction of tung oil and acrylic acid, and a representative chemical structure of TOAA0.4.

The PSA from BPAGDA and TOAA0.3 (entry 3, **Table 5.1**) had a higher peel strength and a higher loop tack than that from BPAGDA and unmodified tung oil (entry 2, **Table 5.1**). The replacement of TOAA0.3 with TOAA0.4 increased the peel strength and the loop tack of the resulting PSAs (entry 4, **Table 5.1**).

As discussed previously, a high CDG content may decrease the molecular weight and increase the crosslinking density of the resulting polymers, thus lowering the peel strength and loop tack. That TOAA0.4 had a lower CDG content than TOAA0.3 may account for the increase in the peel strength and the loop tack when TOAA0.3 was replaced by TOAA0.4. The optimum CDG content of TOAA warranted further investigation. The PSA from BPAGDA and TOAA0.4 had a good shear adhesion of more than 168 h (the true shear adhesion of the PSA was unknown because the shear test was terminated at 168 h that was a typical value for commercially available PSAs [15]). After aging at 60 °C for one week, the peel strength and loop tack of the PSA did not change significantly (entry 4, **Table 5.1**), which indicated that the PSA was aging resistant.

From previous discussion, the combination of the low molecular weight and the increased crosslinking density during the aging was believed to be responsible for the poor aging resistance of the PSA from tung oil and BPAGDA. The CDG content of TOAA0.4 was substantially lower than that of tung oil; TOAA0.4-BPAGDA polymers are thus supposed to have a higher molecular weight than (tung oil)-BPAGDA polymers, which implied that chains of TOAA0.4-BPAGDA polymers were less mobile than those of (tung oil)-BPAGDA polymers for π-electron stacking and hydrogen bond formation during the aging. The BPAGDA content (28.4 wt%) of TOAA0.4-BPAGDA polymers was much lower than that (41.7%) of (tung oil-BPAGDA) polymers, which implied that TOAA0.4-BPAGDA polymers had much lower contents of phenylene and –OH groups than (tung oil-BPAGDA) polymers for the formation of new crosslinks during the aging. The combination of the lower mobility of the polymer chains and the lower chances of forming new

crosslinks accounted for the better aging resistance of the TOAA0.4-BPAGDA polymer than the (tung oil)-BPAGDA polymer (entry 2, **Table 5.1**).

The PSA from TOAA0.4 and PPGDA had a lower peel strength than that from TOAA0.4 and BPAGDA (**Table 5.1**). Unlike BPAGDA, PPGDA did not have phenylene and hydroxyl groups for the formation of crosslinks. The insufficient crosslinking density of the PSA from TOAA0.4 and PPGDA is speculated to be responsible for the low peel strength of the PSA. The PSA from TOAA0.4 and PPGDA was supposed to have a higher molecular weight than that from tung oil and PPGDA because of the reduced f_{CDG} of TOAA0.4, thus increasing the peel strength. However the reduced f_{CDG} would reduce the amount of CDGs and DGs available for the curing reactions, thus reducing the crosslinking density and the peel strength. These two opposite effects may account for the results that the PSA from TOAA0.4 and PPGDA had the peel strength and tack similar to that from tung oil and PPGDA.

As discussed previously, phenylene groups that were incorporated into polymers might stack together through π-electron interactions and thus resulted in physical crosslinks among the polymer chains. MPMI contains two phenylene groups per molecule. It was hoping that addition of a small amount of MPMI in the pre-polymers of TOAA0.4 and PPGDA during the curing might increase the crosslinking density and thus increase the peel strength and tack of the polymer. PPGDA was first polymerized with TOAA0.4 with the molar ratio of the CDGs of TOAA0.4 to the DGs of PPGDA being slightly greater than one. After all the DGs of PPGDA were consumed, polymers containing a small amount of unreacted CDGs were obtained. MPMI was then added to the reaction mixture for curing the polymers. The addition of MPMI did not increase the peel strength of the resulting PSA as expected (entry 6, **Table 5.1**). It appears that the

incorporated MPMI chains were not able to stack together for forming extra crosslinks. However, the addition of MPMI significantly increased the loop tack and shortened the curing time from 1.5 h to 0.5 h, which is consistent with the fact that the DGs of MPMI are more reactive to CDGs than the acrylic DGs of PPGDA. The exact reasons for the increased loop tack are not well understood.

The PSAs obtained in this study had peel strengths ranging from 0.1 to 1.1 $N \bullet cm^{-1}$ that falls in the required range of peel strength for some commercial PSA products such as Post-it® notes [16], ultra-removable protective films [17] and some technical film labels [18]. In addition to tung oil, other components for the new PSAs could be fully or partially prepared from renewable materials. For example, acrylic acid can be prepared from renewable lactic acid [19]. PPGDA and BPAGDA can be partially based on renewable glycerol. And maleic anhydride that is used for preparation of MPMI can also be prepared from renewable materials [20].

5.5. Conclusions

The polymerization of tung oil and MPMI proceeded fast and efficiently *via* the DA reaction between the CDGs of tung oil and the DGs of MPMI; but the resulting polymer was too rigid to serve as a PSA. The polymerization of tung oil with PPGDA or BPAGDA required a higher reaction temperature and a longer reaction time than that for the polymerization of tung oil with MPMI. The PSAs from tung oil and PPGDA or BPAGDA had peel strengths ranging from 0.1 to 0.2 $N \bullet cm^{-1}$ and loop tacks ranging from 0.4 to 0.5 N. Tung oil could readily react with acrylic acid to give TOAAs that had lower contents of CDGs than tung oil. The use of TOAAs instead of tung oil to polymerize

PPGDA failed to result in PSAs with increased peel strength. However, the PSAs from the polymerization of BPAGDA with TOAAs had higher peel strengths and higher loop tack than those from the polymerization with unmodified tung oil. The addition of a small amount of MPMI to the pre-polymers of TOAA0.4 and PPGDA during the curing process did not increase the peel strength, but significantly increase the loop tack, and significantly shortened the curing time. In addition, most tung oil-based PSAs obtained in this study had a superior shear adhesion of up to 168 h and a good aging resistance.

5.6. References

[1] Benedek I, Feldstein MM. Handbook of pressure-sensitive adhesives and products: Fundamentals of pressure sensitivity. vol. 1. Boca Raton, FL: Taylor & Francis Group; 2009.

[2] Li A, Li K. Pressure-sensitive adhesives based on epoxidized soybean oil and dicarboxylic acids. ACS Sustain Chem Eng 2014;2:2090–6.

[3] Maassen W, Meier MAR, Willenbacher N. Unique adhesive properties of pressure sensitive adhesives from plant oils. Int J Adhes Adhes 2016;64:65–71.

[4] Wu Y, Li A, Li K. Pressure sensitive adhesives based on oleic acid. J Am Oil Chem Soc 2015;92:111–20.

[5] Wu Y, Li A, Li K. Development and evaluation of pressure sensitive adhesives from a fatty ester. J Appl Polym Sci 2014;131:1–8.

[6] Ahn BK, Kraft S, Wang D, X Susan Sun. Thermally stable, transparent, pressure-sensitive adhesives from epoxidized and dihydroxil soybean oil. Biomacromolecules 2011;12:1839–43.

[7] Li A, Li K. Pressure-sensitive adhesives based on soybean fatty acids. RSC Adv 2014;4:21521–30.

[8] Atabani AE, Silitonga AS, Ong HC, Mahlia TMI, Masjuki HH, Badruddin IA. Non-edible vegetable oils: A critical evaluation of oil extraction, fatty acid compositions, biodiesel production, characteristics, engine performance and emissions production. Renew Sustain Energy Rev 2013;18:211–45.

[9] Bickford WG, Hoffmann JS, Heinzelman DC, Fore SP. Kinetics of Diels-Alder reactions of eleostearic acids with maleic anhydride and substituted maleic anhydrides J Org Chem 1957;22:1080–3.

[10] Trumbo DL, Mote BE. Synthesis of tung oil – diacrylate copolymers via the Diels- Alder reaction and properties of films from the copolymers. J Appl Polym Sci 2001;80:2369–75.

[11] Huang K, Zhang P, Zhang J, Li S, Li M, Xia J, et al. Preparation of biobased epoxies using tung oil fatty acid-derived C21 diacid and C22 triacid and study of epoxy properties. Green Chem 2013;15:2466–75.

[12] Huang K, Liu Z, Zhang J, Li S, Li M, Xia J. Epoxy monomers derived from tung oil fatty acids and its regulable thermosets cured in two synergistic ways. Biomacromolecules 2014;15:837–43.

[13] Li A, Li K. Pressure-sensitive adhesives based on tung oil. RSC Adv 2015;5:85264–71.

[14] Chanda M. Introduction to polymer science and chemistry: A problem-solving approach. 2nd ed. Boca Raton, FL: CRC Press Taylor & Francis Group; 2013.

[15] Ozturk GI, Pasquale AJ, Long TE. Melt Synthesis and characterization of aliphatic low-Tg polyesters as pressure sensitive adhesives. J Adhes 2010;86:395–408.

[16] Bunker SP, Wool RP. Synthesis and characterization of monomers and polymers for adhesives from methyl oleate. J Polym Sci Part A Polym Chem 2002;40:451–8.

[17] Pressure-sensitive adhesive sheet for surface protection, US Pat., 8962136B2, 2015.

[18] Ichemco general catalog PDF, http://ichemco.it/eng/Ichemco_catalog.pdf ; 2017 [accessed 01.29.2017].

[19] Zhang J, Zhao Y, Pan M, Feng X, Ji W, Au C-T. Efficient acrylic acid production through bio lactic acid dehydration over NaY zeolite modified by alkali phosphates. ACS Catal 2011; 1; 32-41.

[20] Lan J, Chen Z, Lin J, Yin G. Catalytic aerobic oxidation of renewable furfural to maleic anhydride and furanone derivatives with their mechanistic studies. Green Chem 2014, 16, 4351-8.

GENERAL DISCUSSION

From **Chapter II** to **IV** non-edible animal fat has been demonstrated as a source to prepare PCMs by distinct approaches. Besides, the preparation of these PCMs was performed according to sustainability and following as much as possible the Green Chemistry principles. Indeed, in **Chapter II** animal fat was hydrolyzed by using resting cells of *R.oryzae* achieving the higher yields in hydrolysis of animal fats by resting cells. The hydrolysis splits glycerol and fatty acids, which can be afterwards divided into saturated and unsaturated fatty acids.

Commonly, fatty acids and derivatives evaluated as PCMs come from hydrogenations of unsaturated sources. Nevertheless, in **Chapter III** we demonstrated that the hydrolysis and crystallization of animal fat allowed the preparation of a eutectic mixture of PA-SA showing good properties and good reliability as PCMs during 1000 cycles. To demonstrate that hydrogenation reduces the applications of triacylglycerols, the unsaturated fatty acids were converted to DHSA. The hydroxyl moieties of DHSA increase the melting point of the fatty acid when compared to its saturated counterparts such as stearic acid. Indeed, DHSA was postulated as an interesting fatty acid to test its properties as PCMs since every distinct phase-change temperature can undergo new applications. However, the chemical and thermal stability was committed presumably to the formation of estolides while the alternative to prepare and test some DHSA salts became in products with poor thermal interest. Moreover, no polymorphism was observed in all the fatty acids and derivatives tested by DSC. However, the. DSC response of calcium DHSA salt (**Figure A3-27**) shows an unexpected behavior and it cannot be concluded whether it is due to polymorphism or to a mixture of two substances.

As esters of fatty acids haven shown good properties as PCMs, we realized that the preparation of DHSEs could match the problems presented by DHSA and also achieve distinct phase-change temperatures by preparing several esters. Additionally, in **Chapter VI**, to prepare DHSA and DHSEs we sought to apply the Green Chemical principles by employing biocatalysis and using the less amount of reactants. Indeed, solvents such as *t*-BuOH or α-limonene were used to perform both reaction and crystallization to prepare pure compounds. In that way, esterification of DHSA with alcohols from methanol to 1-octadecanol lead to twelve DHSEs and four of them presented enthalpies beyond 200 $kJ \bullet kg^{-1}$. According to the DSC results, no polymorphism was observed in these PCM. The thermal reliability of these four esters during 100 and 1000 cycles was also promising. Indeed, the use of biocatalysts and Green Chemistry to prepare PCM materials was a novelty.

Thus, along **Chapters II**, **III** and **IV** we demonstrated that the hydrolysis and crystallization of animal fat allows the preparation of distinct compounds. The hydrogenation of unsaturated sources is not mandatory to prepare fatty acids for PCM purposes since PA-SA eutectic mixtures can be prepared from animal fat hydrolyzed by chemical as well as enzymatic approaches. Additionally, the preservation of the unsaturated fatty acids allows the preparation of DHSA by chemical and enzymatic approaches. Moreover, DHSEs have showed new applications by presenting good properties as PCMs.

The preparation of PSAs from a non-edible source such as tung oil is now possible by direct polymerization. Indeed, direct polymerization allows the preparation of non-generating wastes polymers. **Chapter V** shown that the use of two diacrylates such as PPGDA and BAPGDA to polymerize tung oil resulted in PSAs with low peel strength. Nevertheless, the preparation of a TOAA adduct and posterior polymerization with BAPGDA and PPGDA increased the peel strength and loop tack of the polymers prepared with BAPGDA while resulted unsuccessful in PPGDA. In order to improve the PSA properties of the polymer with TOAA and PPGDA we added MPMI. However, this addition just only improved the curing time.

GENERAL CONCLUSIONS

We have demonstrated the possibility to use non-edible fats and vegetable oil to prepare products with commercial interest by using suitable approaches. Regarding to the proposed objectives and considering the results achieved, the following conclusions have been established:

1. The hydrolysis of non-edible animal fat with biocatalysts was successful. Whereas immobilized CAL-B partially hydrolyzed non-edible animal fat, *R.oryzae* resting cells hydrolyzed animal fat with excellent yields. Indeed, the degree of hydrolysis was the highest among the values reported using resting cells.
2. The extraction of resting cells extracted with supercritical CO_2 allowed the reusing of the biocatalyst with better hydrolysis degrees than the extracted with common solvents.
3. The separation of hydrolyzed non-edible animal fat in saturated and unsaturated fatty acids was possible using solvents such as ethyl acetate, acetone, ethanol, hexane and methanol. Besides, the uncorrected melting points as well as composition of the mixture of saturated fatty acids were similar to those reported as PA-SA eutectic mixtures for PCM purposes.
4. The evaluation of the thermal properties of these PA-SA eutectic mixtures prepared from non-edible animal fat revealed good latent heats and good thermal reliability.
5. The preparation of pure DHSA from the unsaturated fatty acids using chemical approaches was successful. Nevertheless, the thermal evaluation of DHSA and some of their salts revealed poor properties as PCMs. The acid and diol moieties presumably reacted by themselves leading to estolides when DHSA is heated.

6. The preparation of DHSEs via green and bio-catalytic approaches from non-edible animal fat was possible by using biocatalysts, hydrogen peroxide, hot water and α-limonene.
7. Supercritical CO_2 and α-limonene were used to reuse the biocatalyst on the chemo-enzymatic epoxidation and the enzymatic esterification, respectively. Besides, those solvents allowed the biocatalysts to retain higher activity than the common solvents studied.
8. The thermal stability of DHSA was improved by preparing DHSEs. Indeed, the thermal reliability of four of these esters was evaluated during 100 and 1000 cycles without outstanding changes in the enthalpy. However, the hysteresis of two of them increased once cycled.
9. The polymerization of tung oil with PPGDA or BPAGDA resulted in PSAs with low peel strength and loop tack.
10. The preparation of polymers of PPGDA and BPAGDA with TOAAs partial adducts presented distinct behavior. While the peel strength and loop tack was not improved on the polymer prepared with PPGDA and TOAA. Polymerizations of TOAA with BPAGDA resulted in PSAs with much higher peel strengths and loop tacks.
11. The addition of MPMI to the polymerization of TOAA and PPGDA did not improve the PSA properties. Nevertheless, it shortened the curing time.

ANNEXES

Annexes contents

Annex I. NMR spectra

^{1}H spectra of the Chapter III

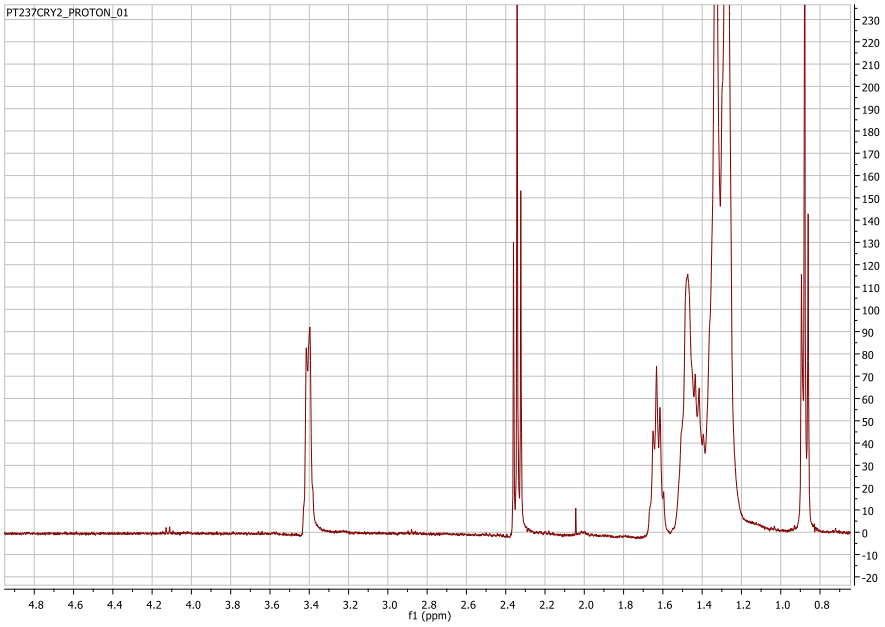

Figure A1-1. ^{1}H NMR Spectra of the DHSA before the DSC analysis.

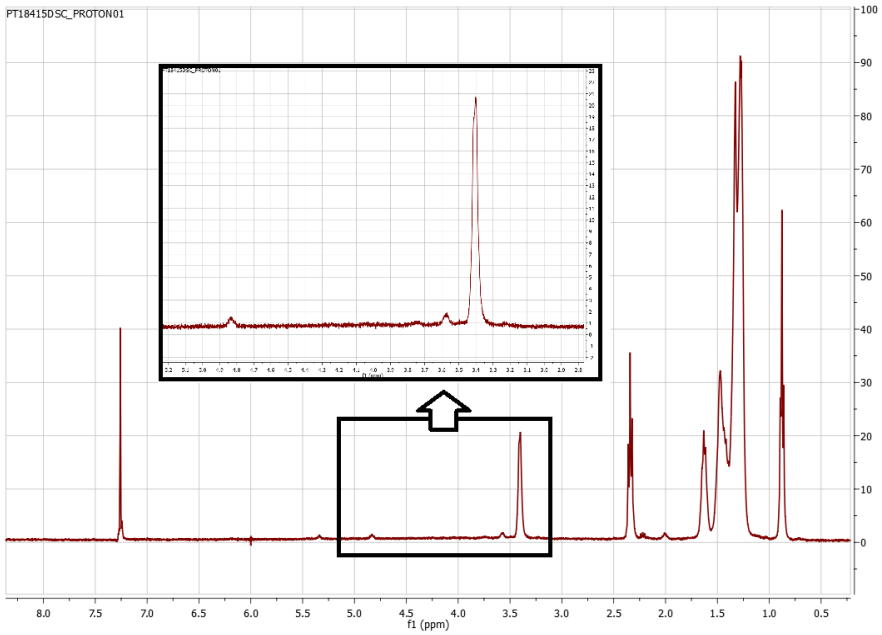

Figure A1-2. ^{1}H NMR Spectra of the DHSA after the DSC analysis. Contains the detailed part from 5.2 to 2.8 ppm.

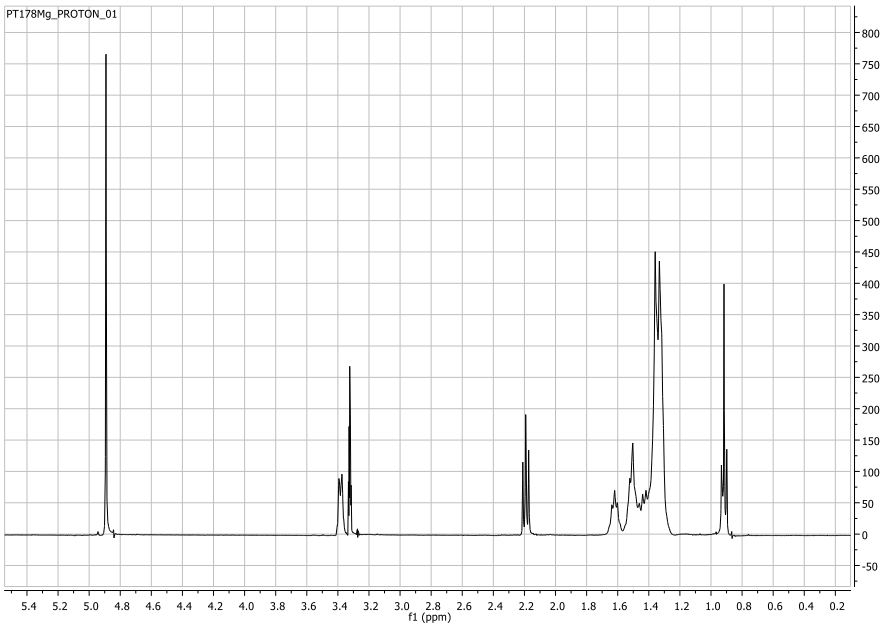

Figure A1-3. ^{1}H NMR Spectra of the magnesium DHSA.

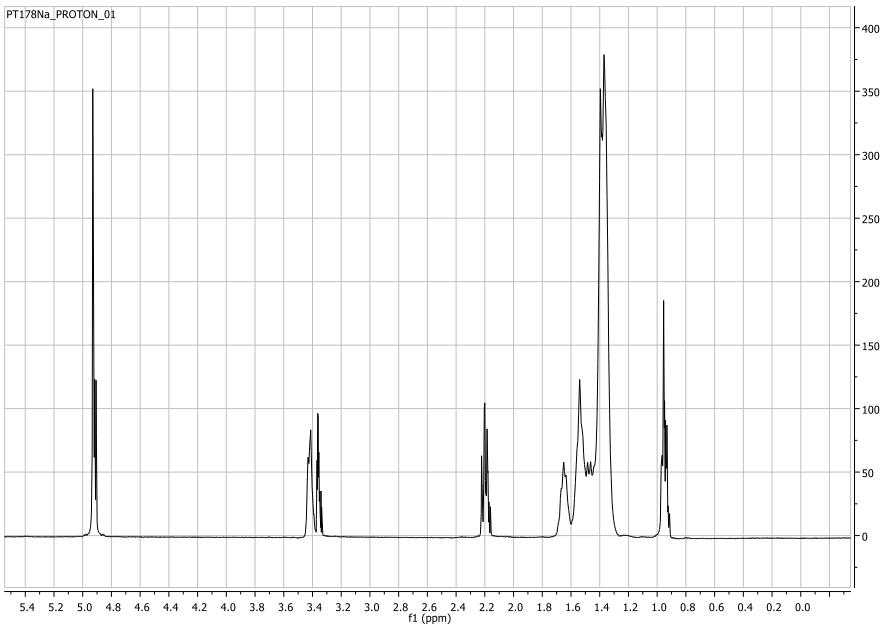

Figure A1-4. ^{1}H NMR Spectra of the sodium DHSA.

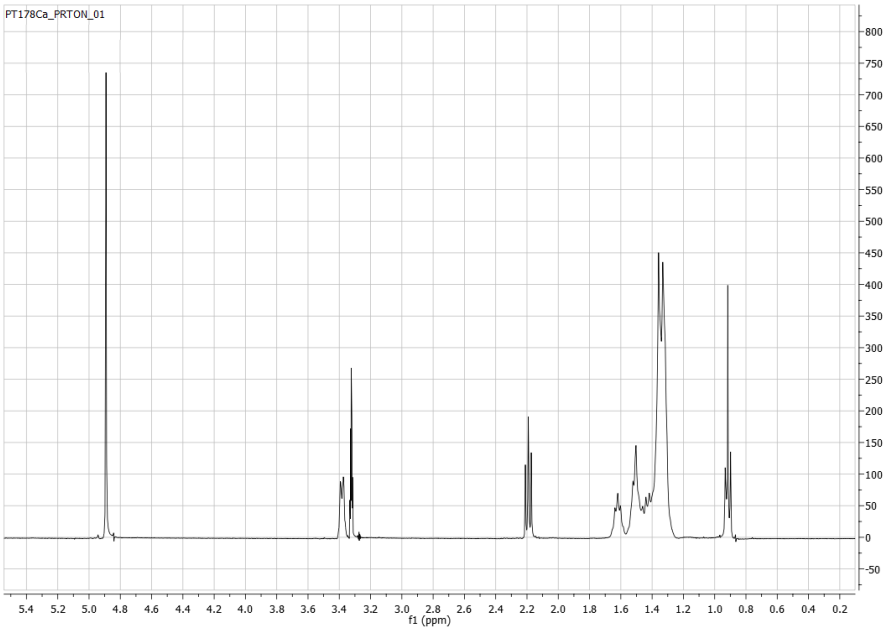

Figure A1-5. ^{1}H NMR Spectra of the calcium DHSA.

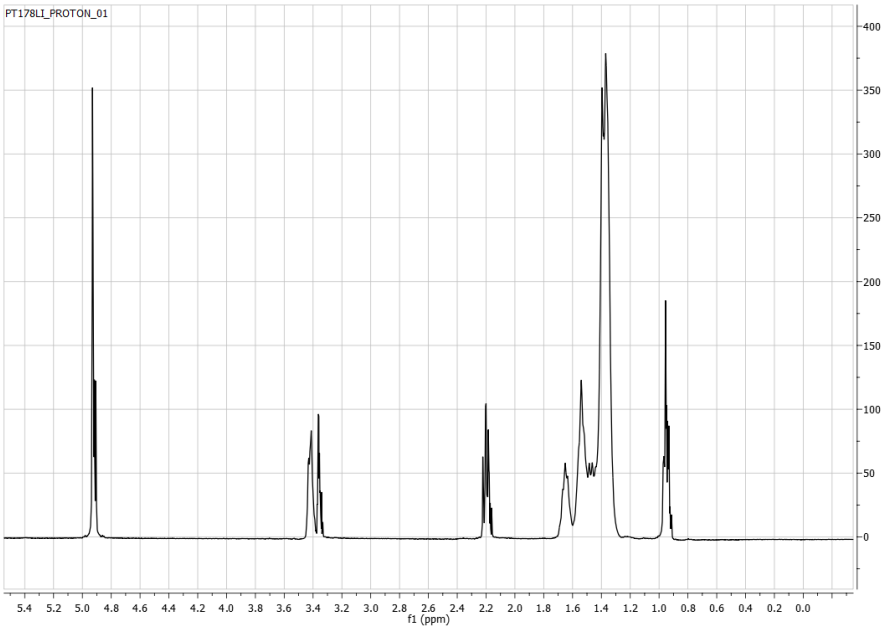

Figure A1-6. ^{1}H NMR Spectra of the litium DHSA.

^{1}H spectra of the Chapter IV

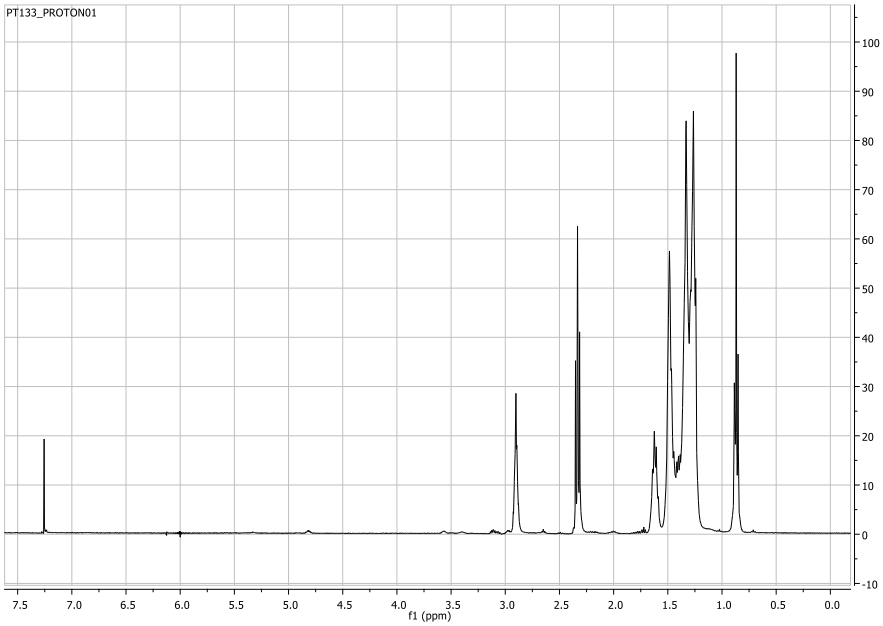

Figure A1-7. ^{1}H NMR Spectra of the *cis*-9, 10-epoxyestearic acid.

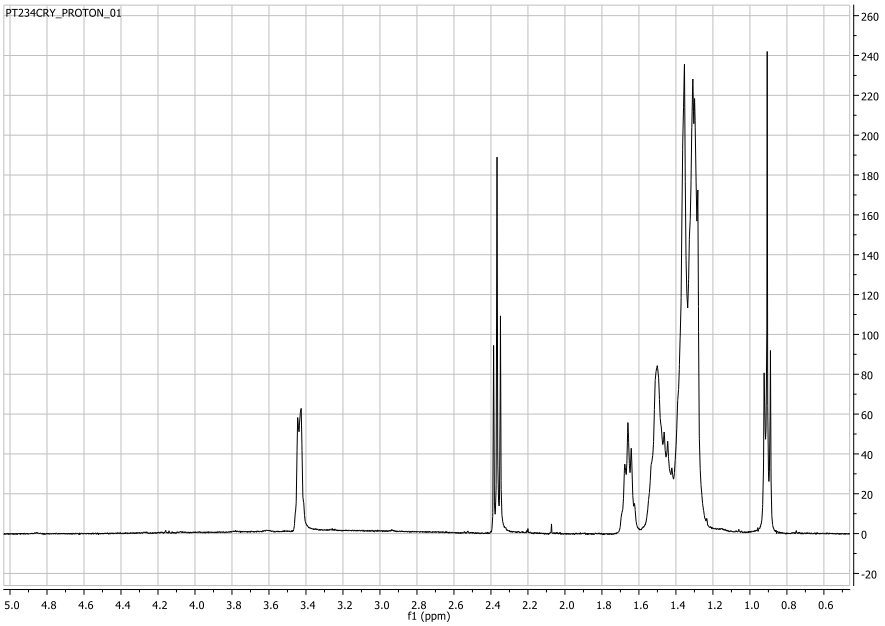

Figure A1-8. ^{1}H NMR Spectra of the DHSA.

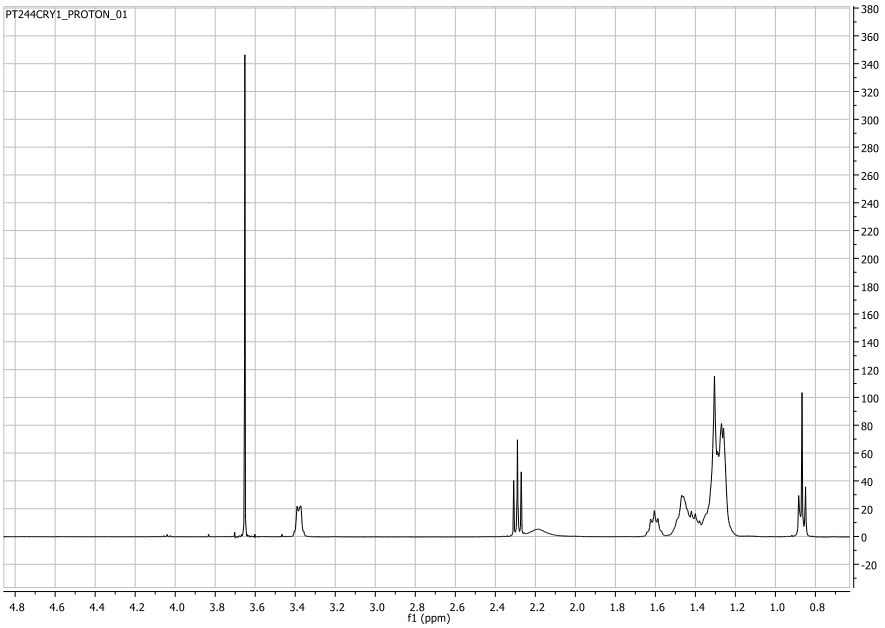

Figure A1-9. ^{1}H NMR Spectra of the methyl DHSE.

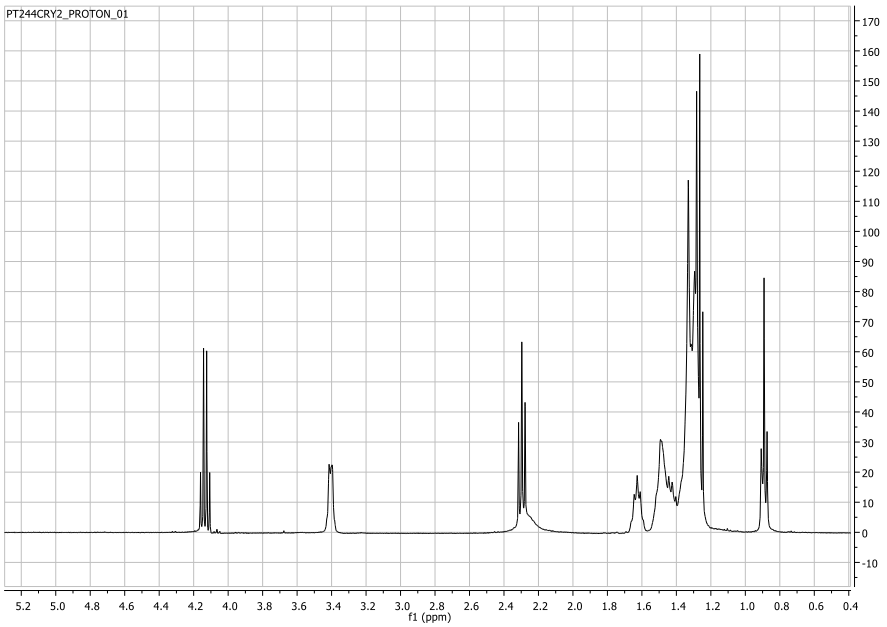

Figure A1-10. ^{1}H NMR Spectra of the ethyl DHSE.

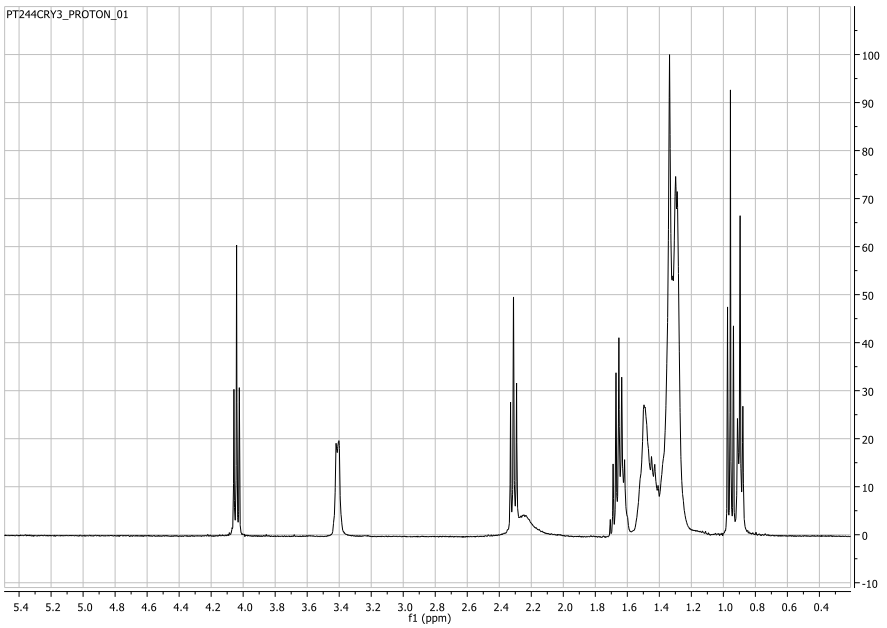

Figure A1-11. ^{1}H NMR Spectra of the propyl DHSE.

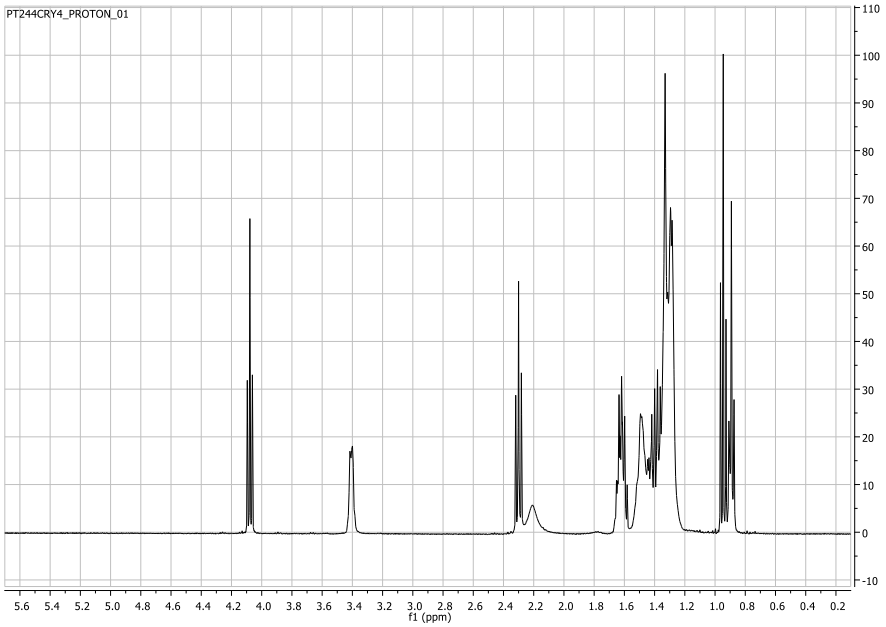

Figure A1-12. ^{1}H NMR Spectra of the butyl DHSE.

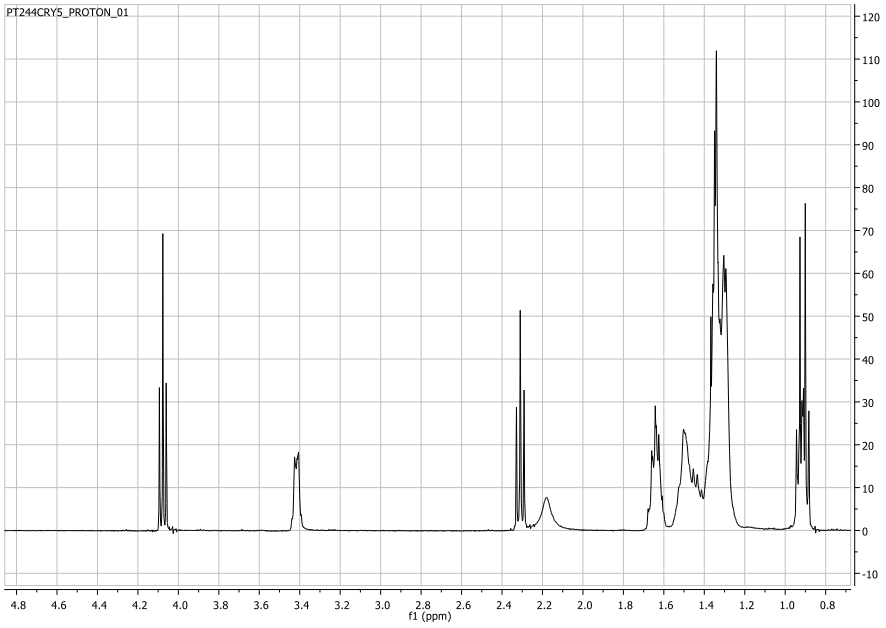

Figure A1-13. ^{1}H NMR Spectra of the penthyl DHSE.

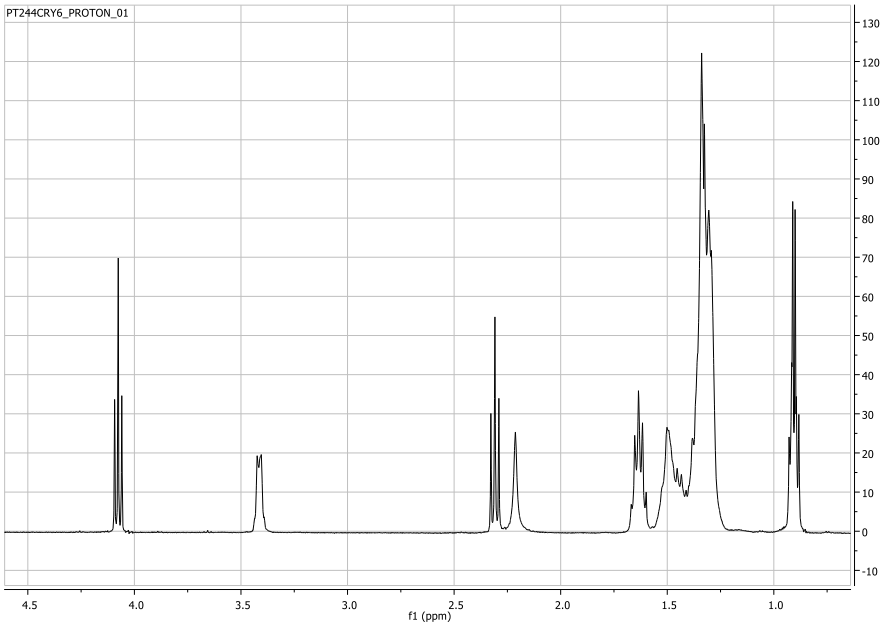

Figure A1-14. ^{1}H NMR Spectra of the hexyl DHSE.

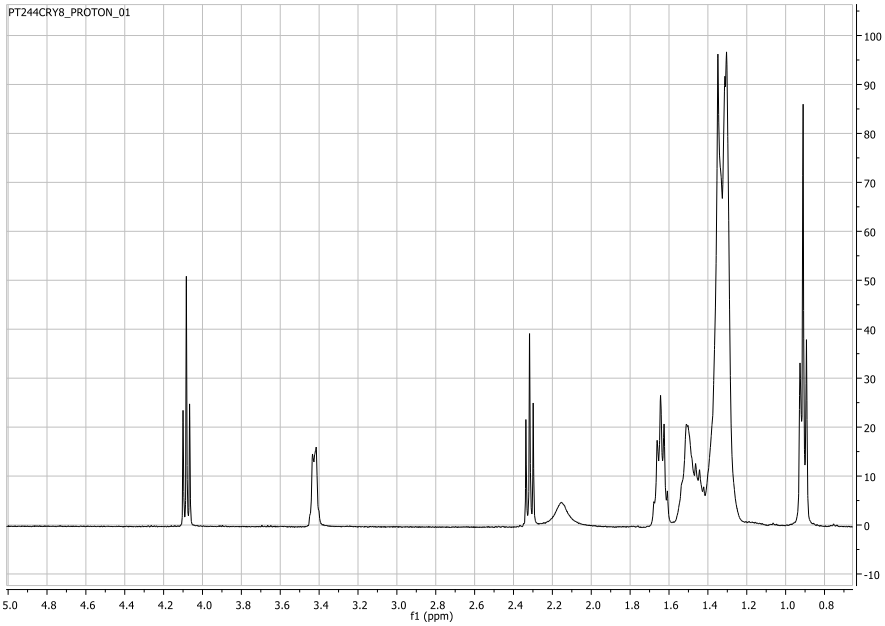

Figure A1-15. ^{1}H NMR Spectra of the octyl DHSE.

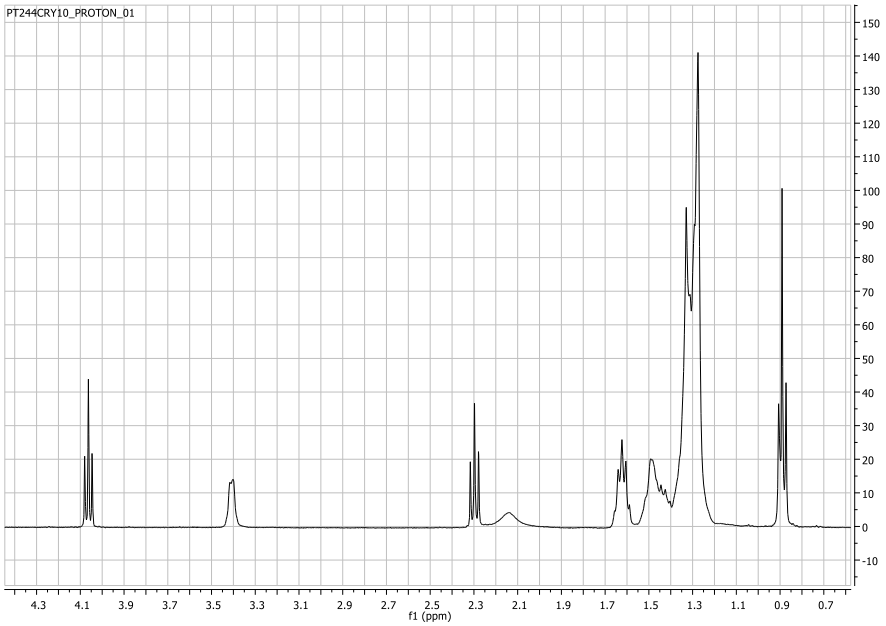

Figure A1-16. ^{1}H NMR Spectra of the decyl DHSE.

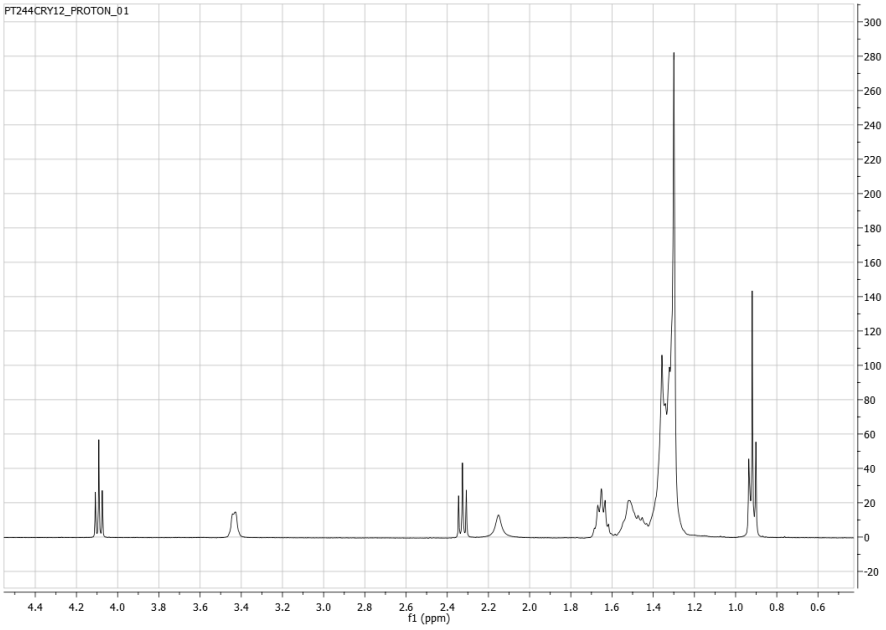

Figure A1-17. ^{1}H NMR Spectra of the dodecyl DHSE.

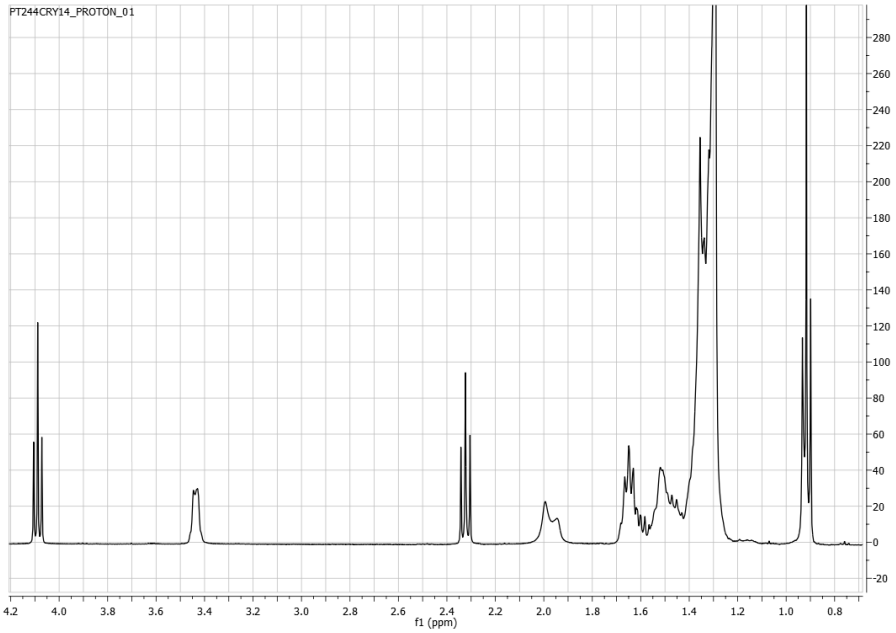

Figure A1-18. ^{1}H NMR Spectra of the tetradecyl DHSE.

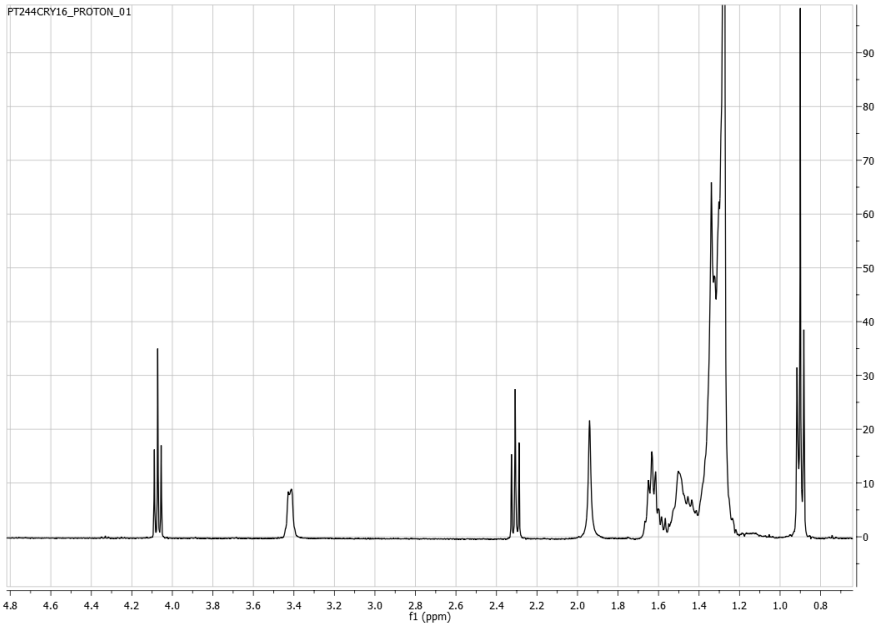

Figure A1-19. ^{1}H NMR Spectra of the hexadecyl-DHSE.

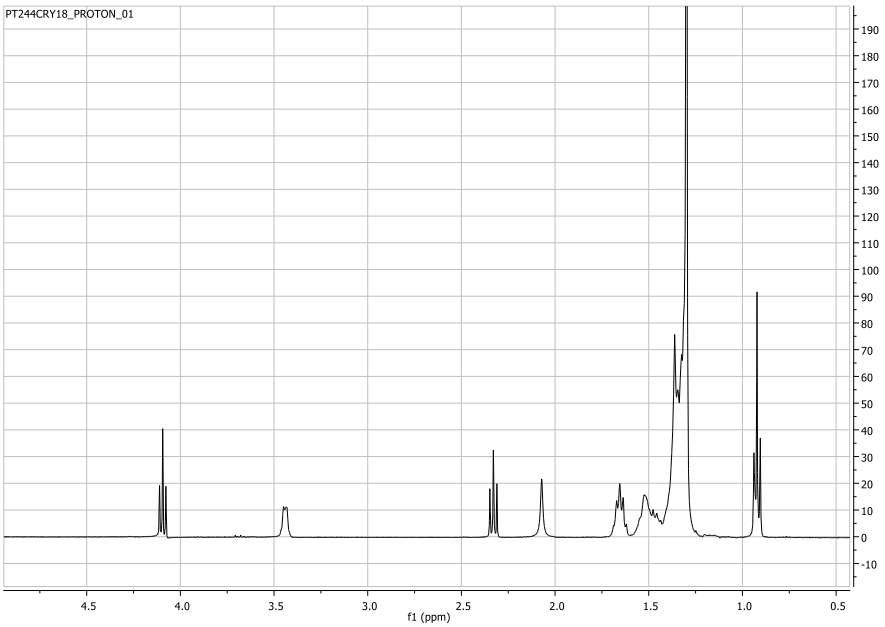

Figure A1-20. ^{1}H NMR Spectra of the octadecyl DHSE.

^{13}C spectra of the Chapter III

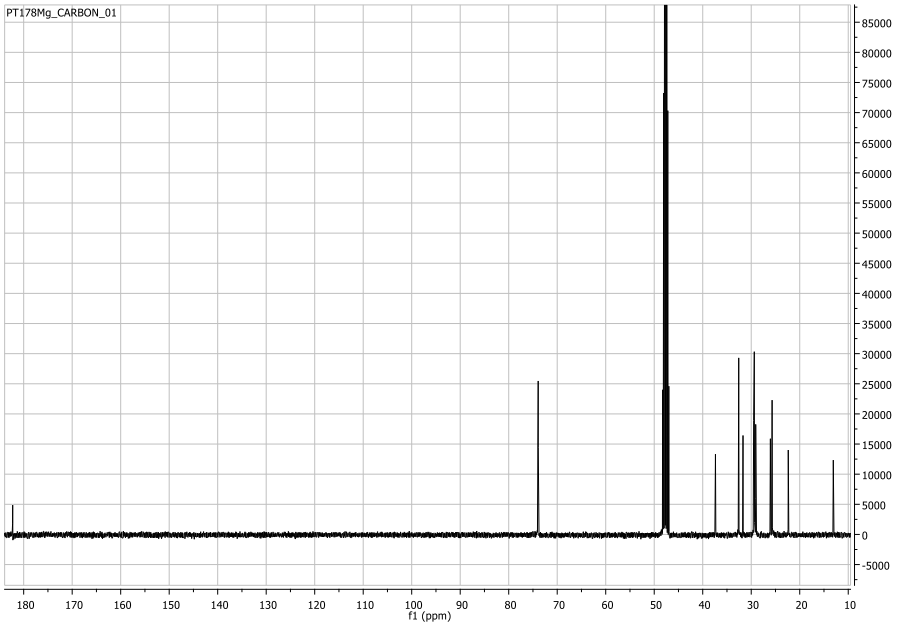

Figure A1-21. ^{13}C NMR Spectra of the magnesium DHSA.

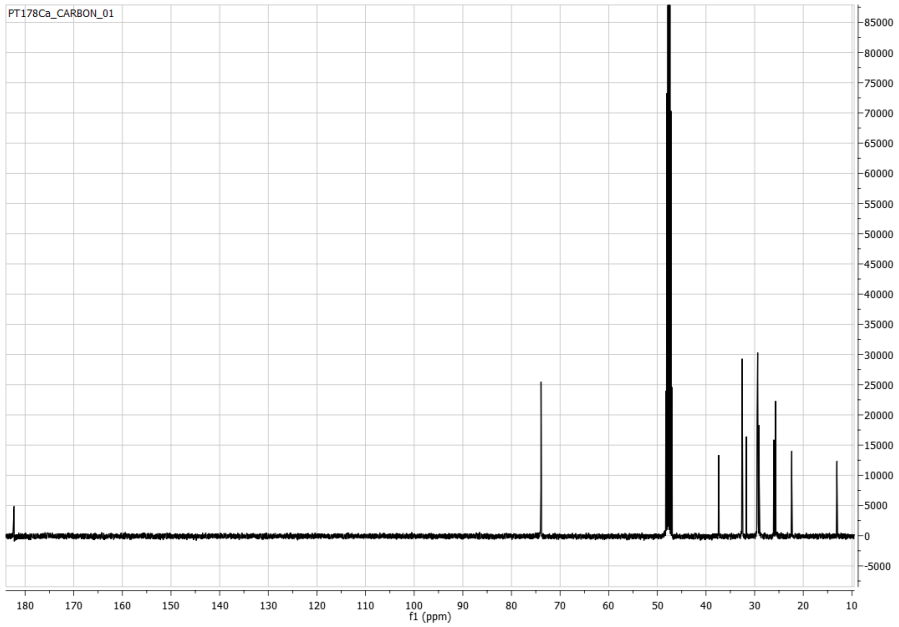

Figure A1-22. ^{13}C NMR Spectra of the calcium DHSA.

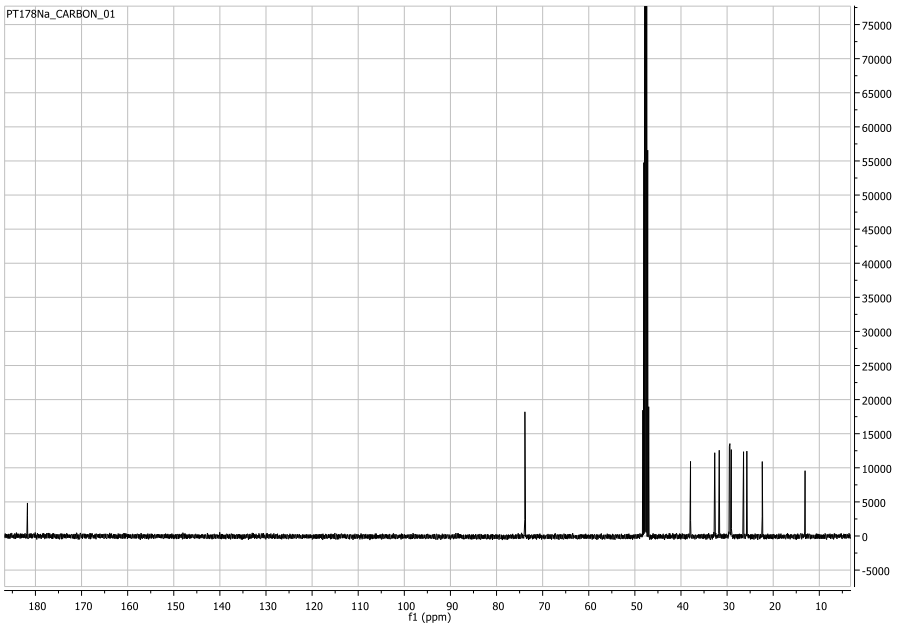

Figure A1-23. ^{13}C NMR Spectra of the sodium DHSA.

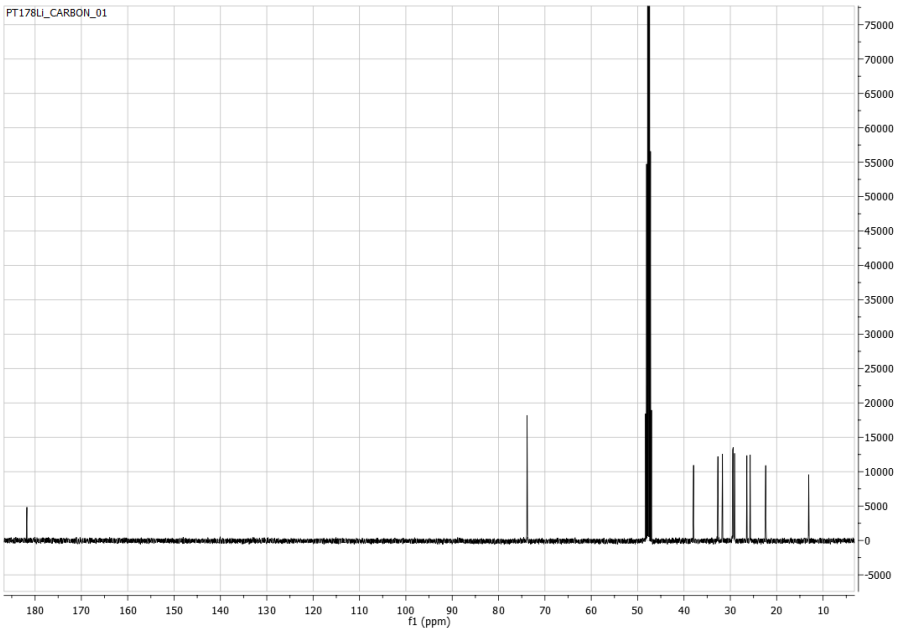

Figure A1-24. ^{13}C NMR Spectra of the litium DHSA.

^{13}C spectra of the Chapter IV

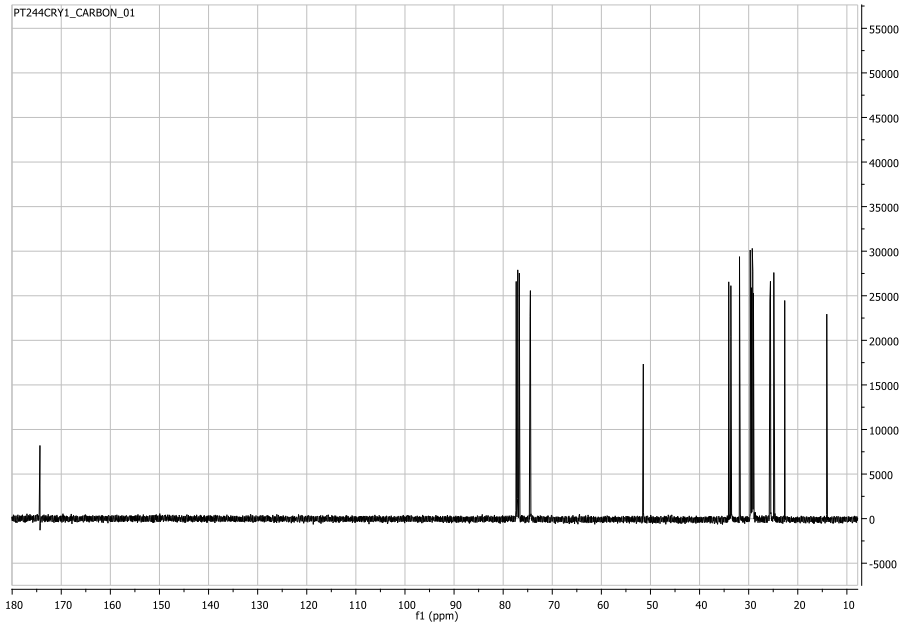

Figure A1-25. ^{13}C NMR Spectra of the methyl DHSE.

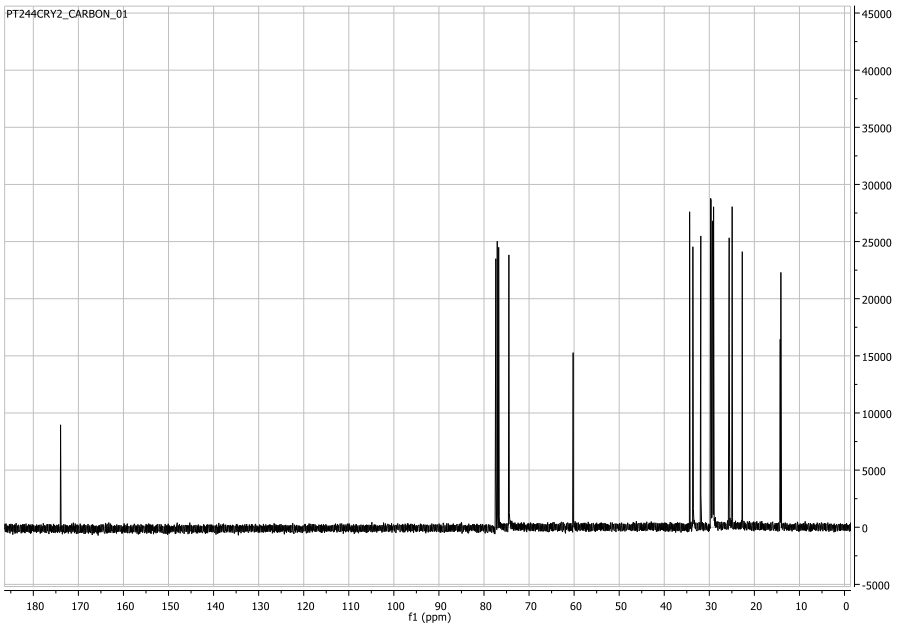

Figure A1-26. ^{13}C NMR Spectra of the ethyl DHSE.

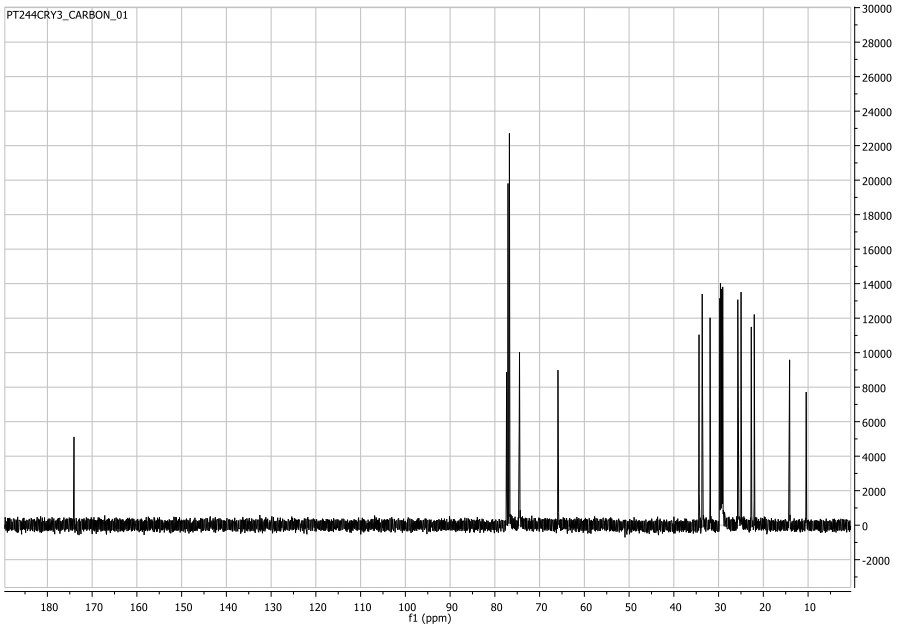

Figure A1-27. ^{13}C NMR Spectra of the propyl DHSE.

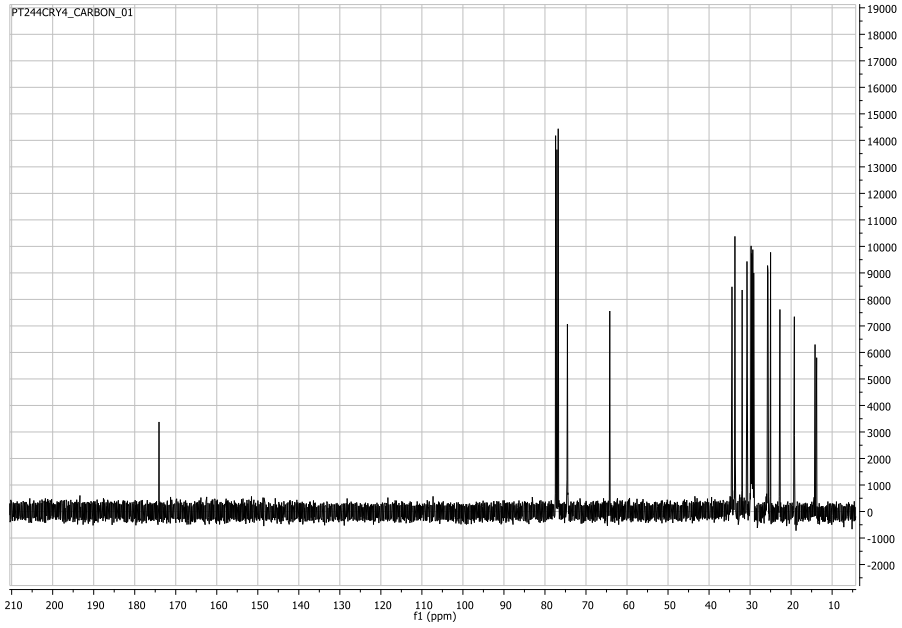

Figure A1-28. ^{13}C NMR Spectra of the butyl DHSE.

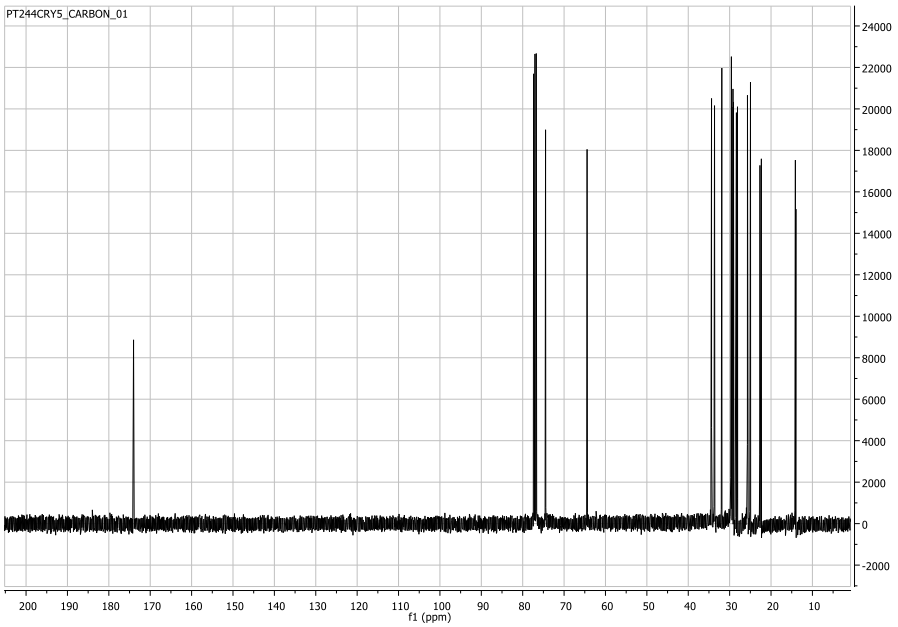

Figure A1-29. ^{13}C NMR Spectra of the penthyl DHSE.

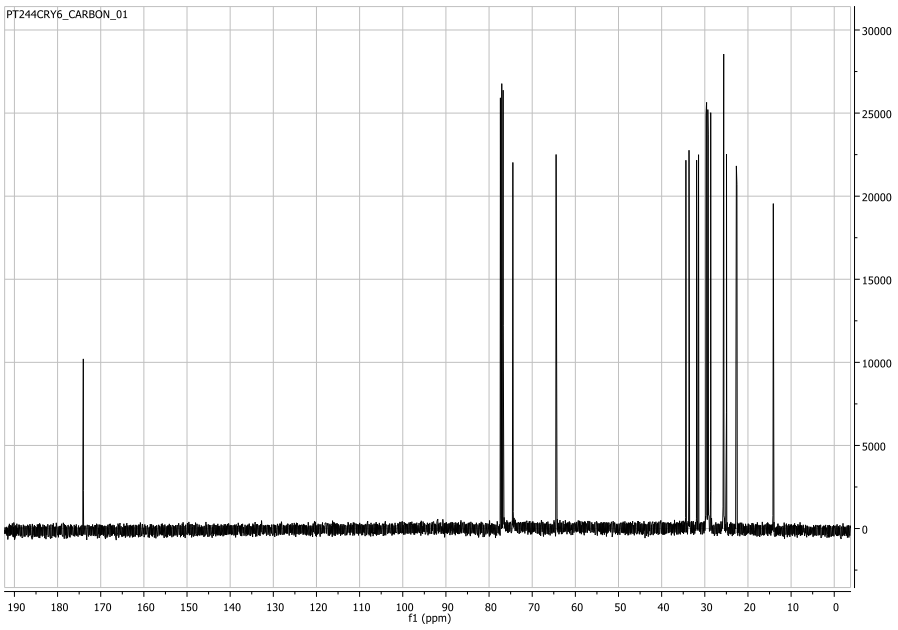

Figure A1-30. ^{13}C NMR Spectra of the hexyl DHSE.

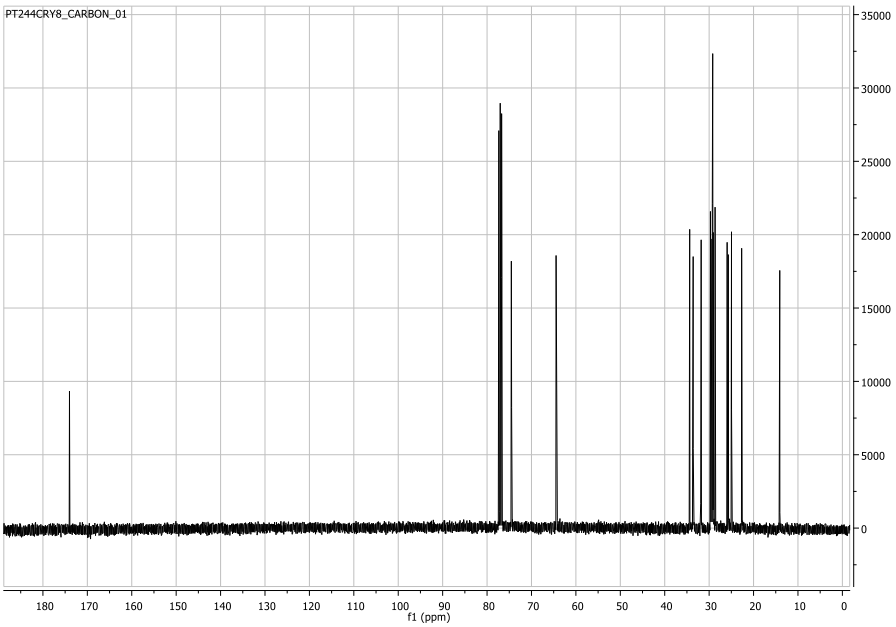

Figure A1-31. ^{13}C NMR Spectra of the octyl DHSE.

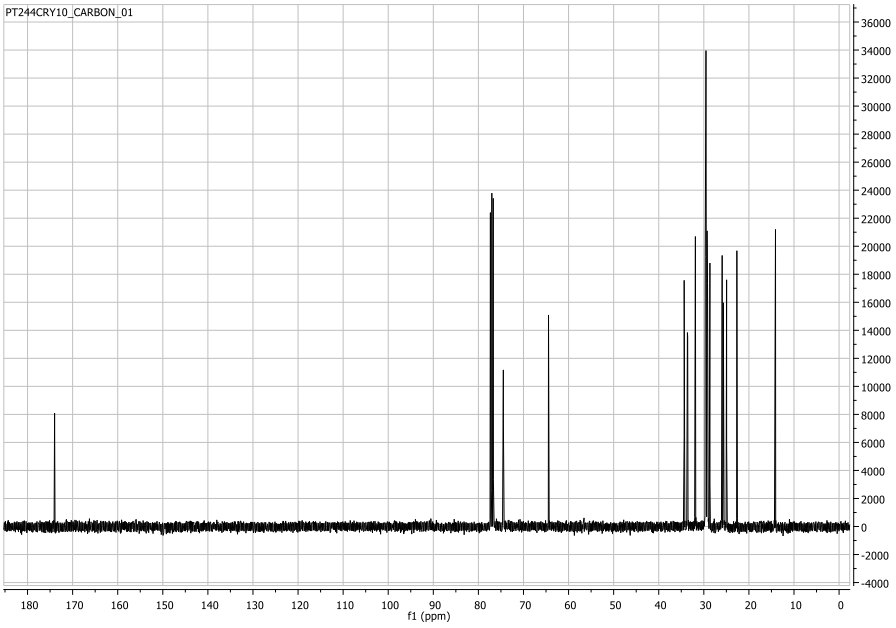

Figure A1-32. ^{13}C NMR Spectra of the decyl DHSE.

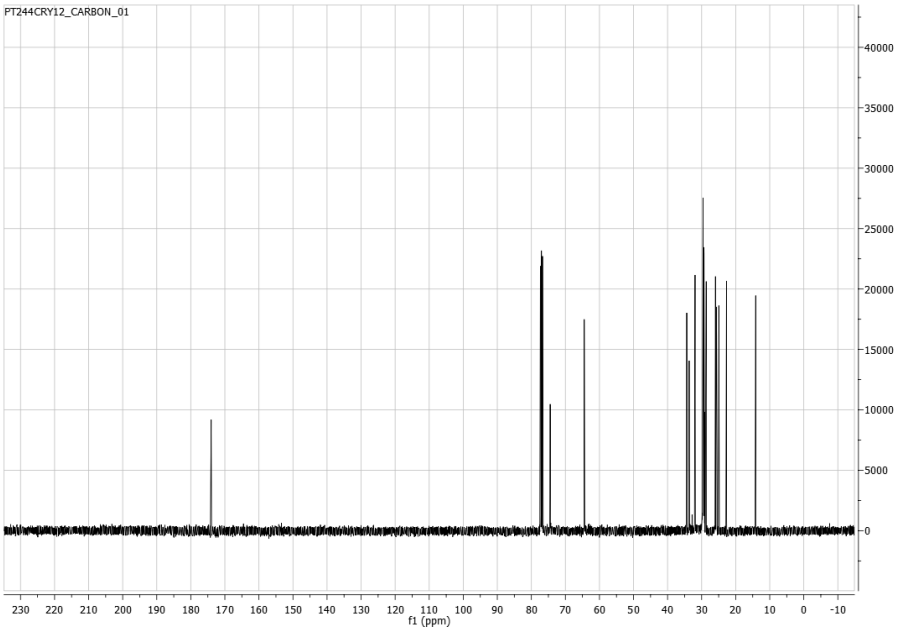

Figure A1-33. ^{13}C NMR Spectra of the dodecyl DHSE.

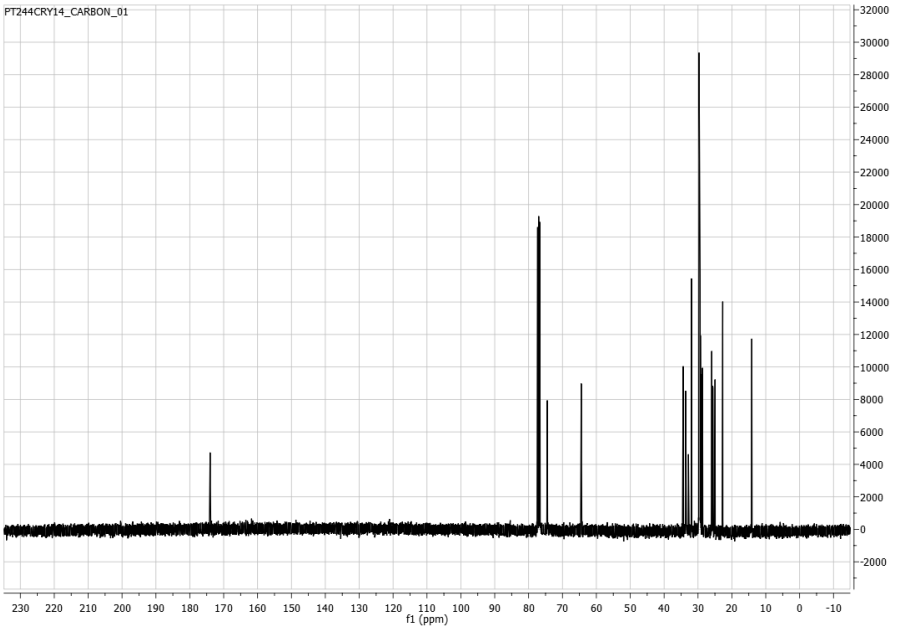

Figure A1-34. ^{13}C NMR Spectra of the tetradecyl DHSE.

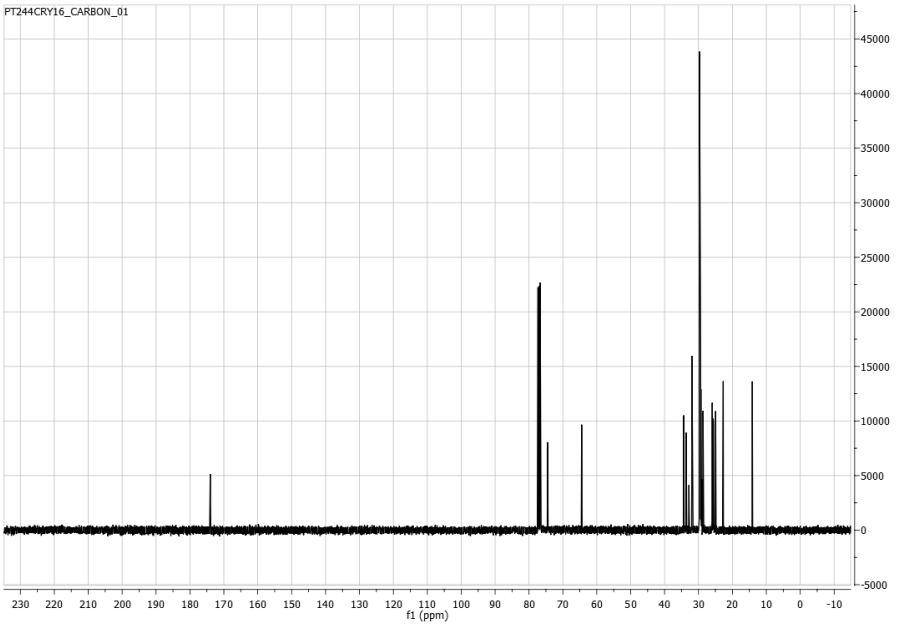

Figure A1-35. ^{13}C NMR Spectra of the hexadecyl-DHSE.

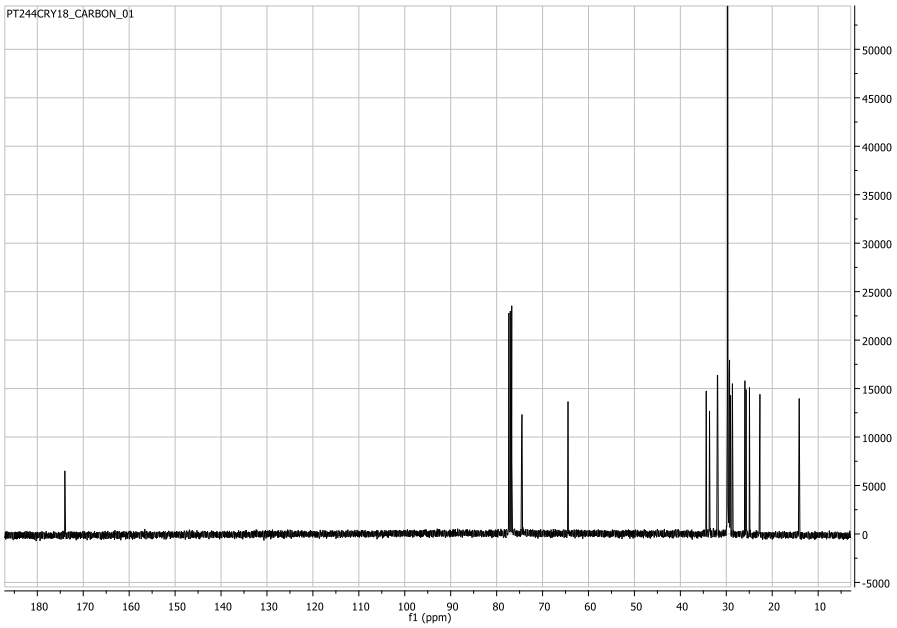

Figure A1-36. ^{13}C NMR Spectra of the octadecyl DHSE.

Annex II. FT-IR spectra

FT-IR spectra of the Chapter III

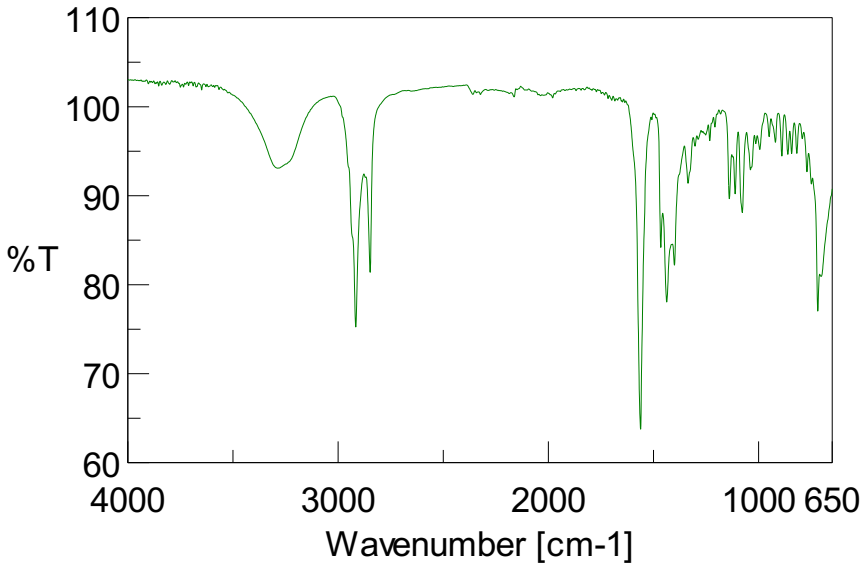

Figure A2-1. Litium salt of DHSA.

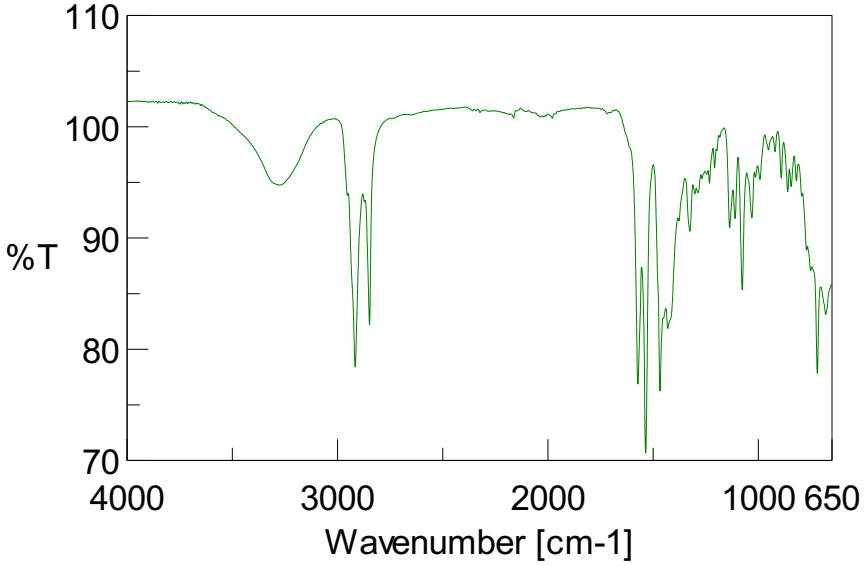

Figure A2-2. Calcium salt of DHSA.

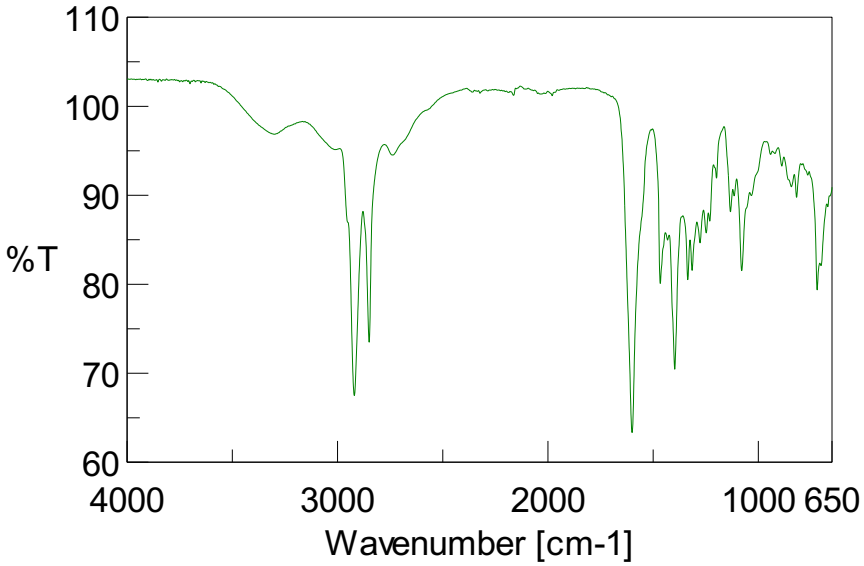

Figure A2-3. Magnesium salt of DHSA.

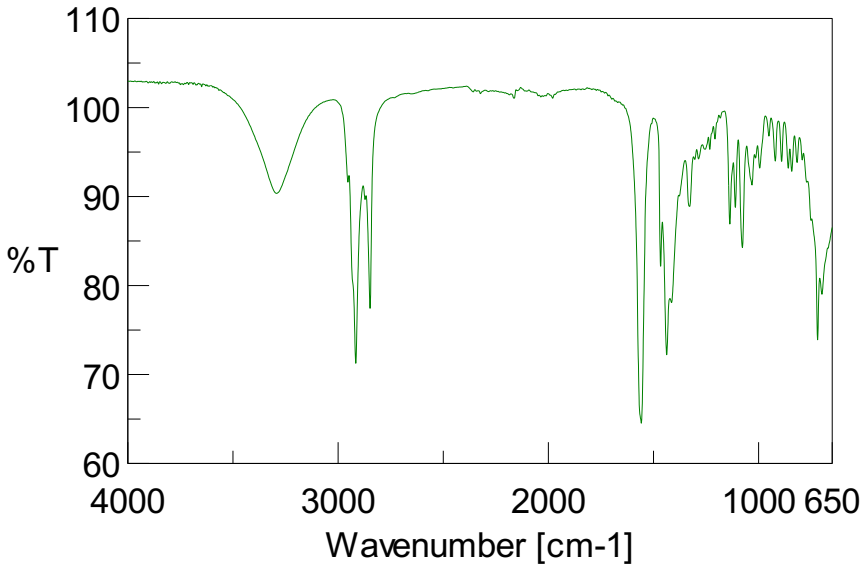

Figure A2-4. Sodium salt of DHSA.

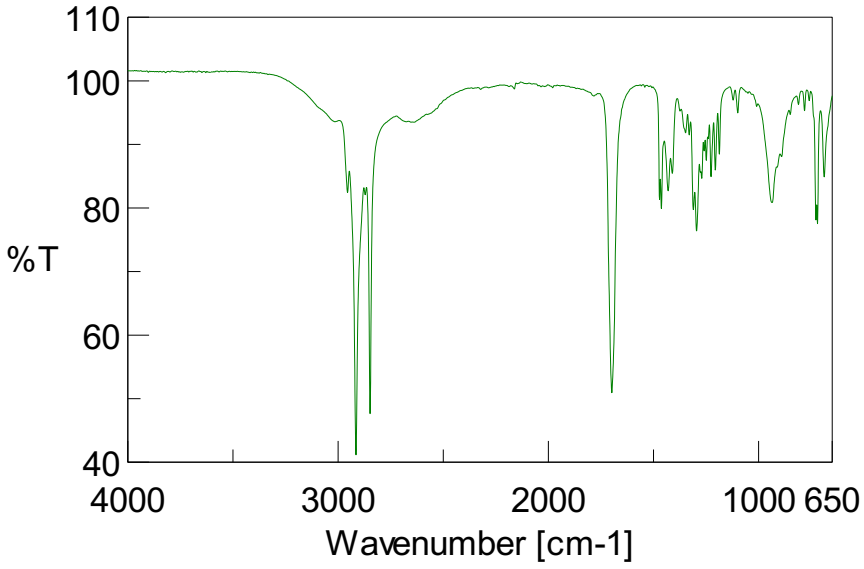

Figure A2-5. PA-SA mixture.

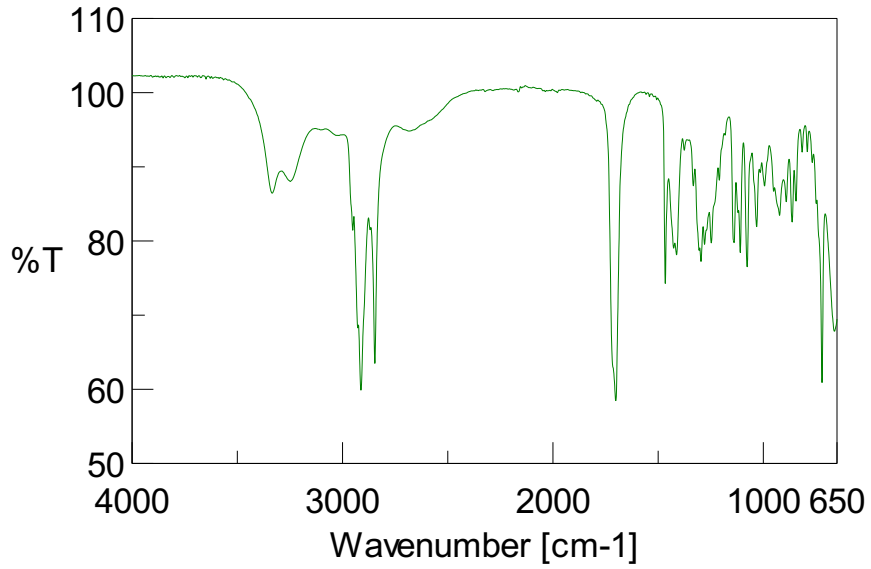

Figure A2-6. DHSA.

Annex III. DCS analysis data

DSC analysis of the Chapter III

DSC analysis of the PA-SA mixtures:

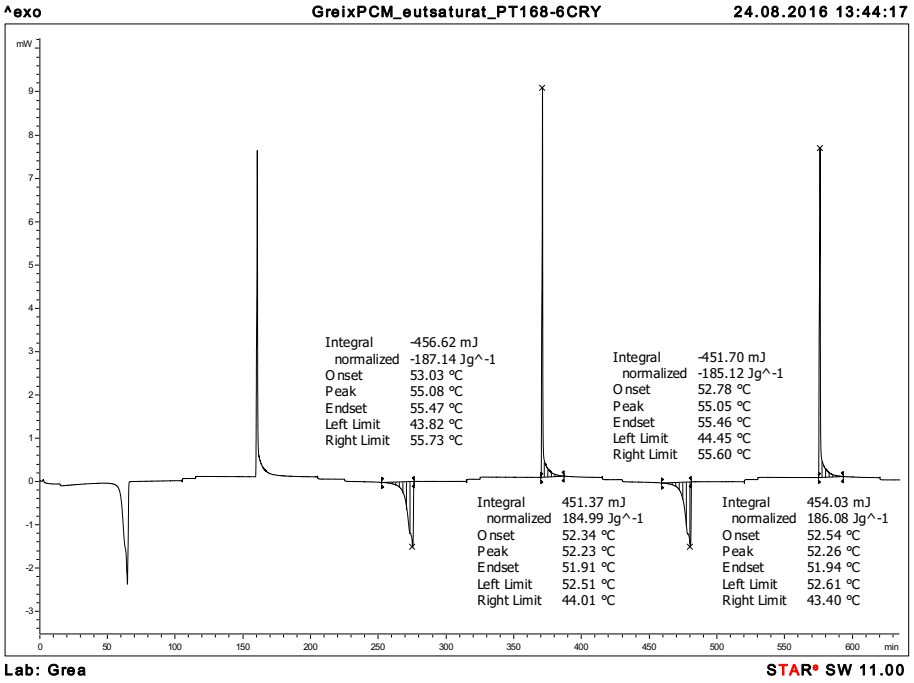

Figure A3-1. DSC response and evaluation of the material crystallized from acetone. Not-cycled sample 1, three cycles.

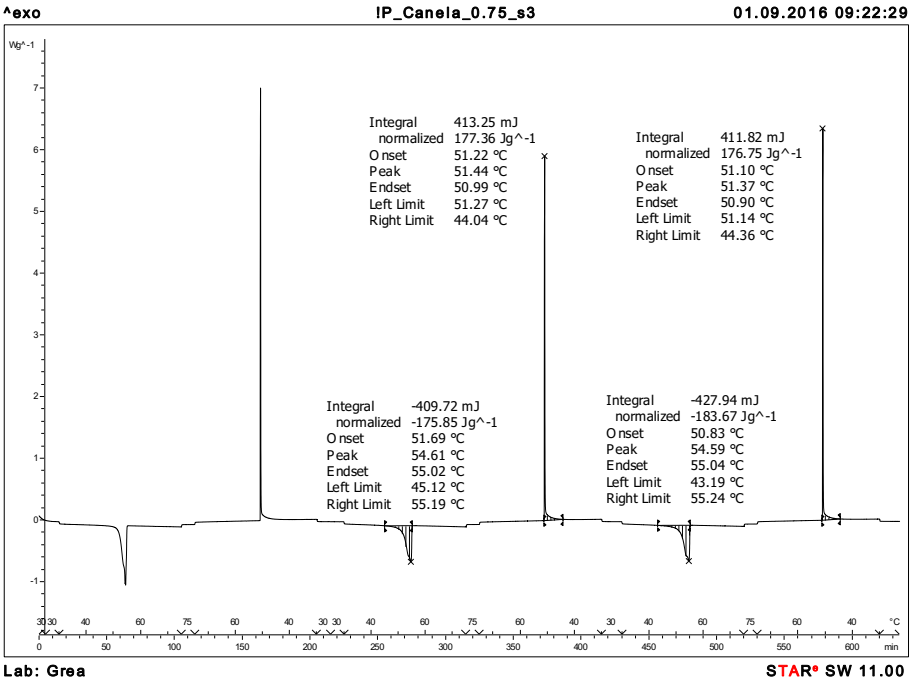

Figure A3-2. DSC response and evaluation of the material crystallized from acetone. Not-cycled sample 2, three cycles.

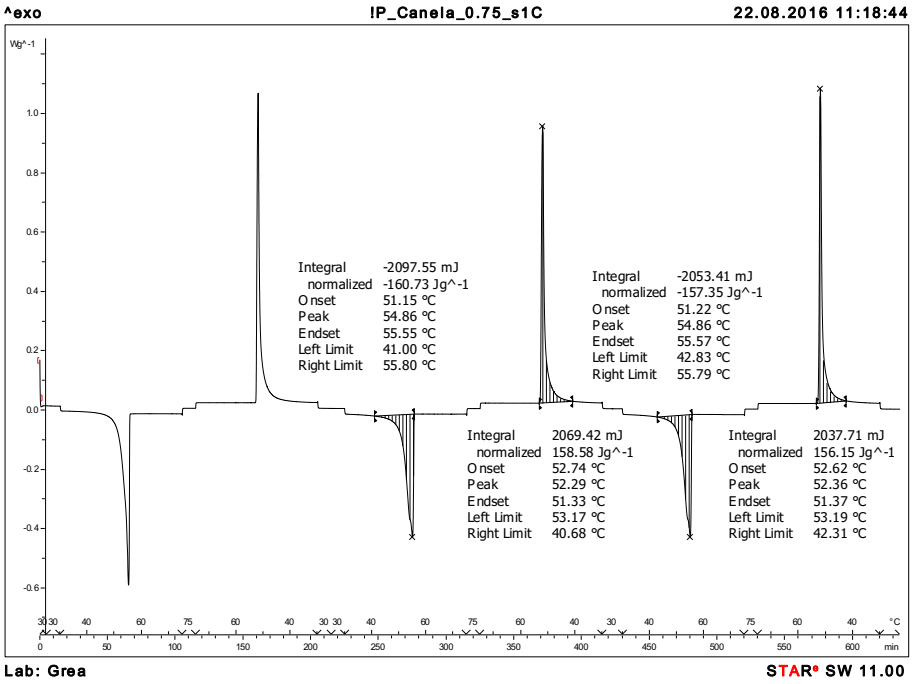

Figure A3-3. DSC response and evaluation of the material crystallized from acetone. Cycled sample 1, three cycles.

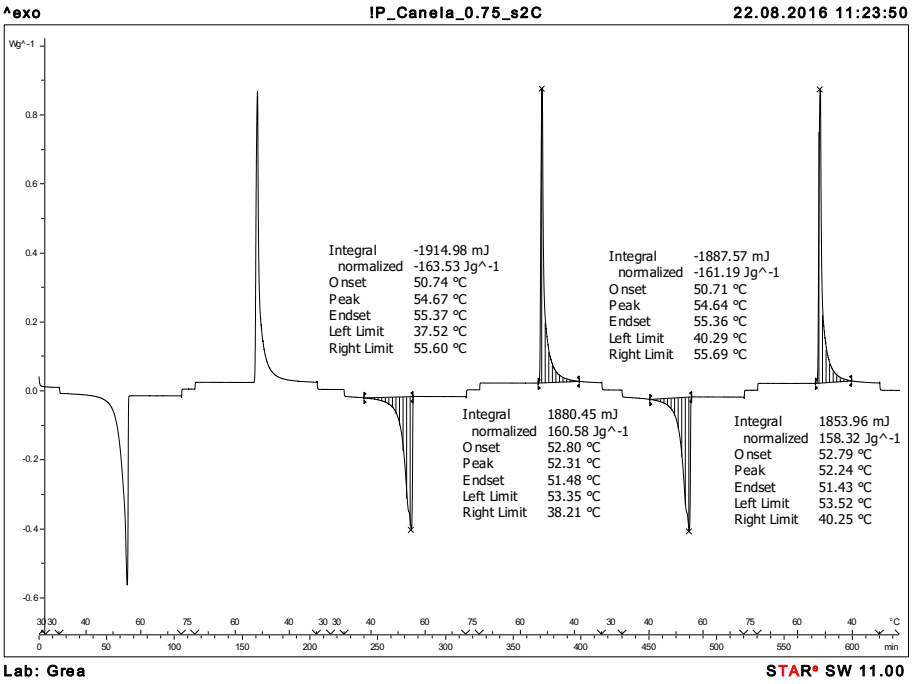

Figure A3-4. DSC response and evaluation of the material crystallized from acetone. Cycled sample 2, three cycles.

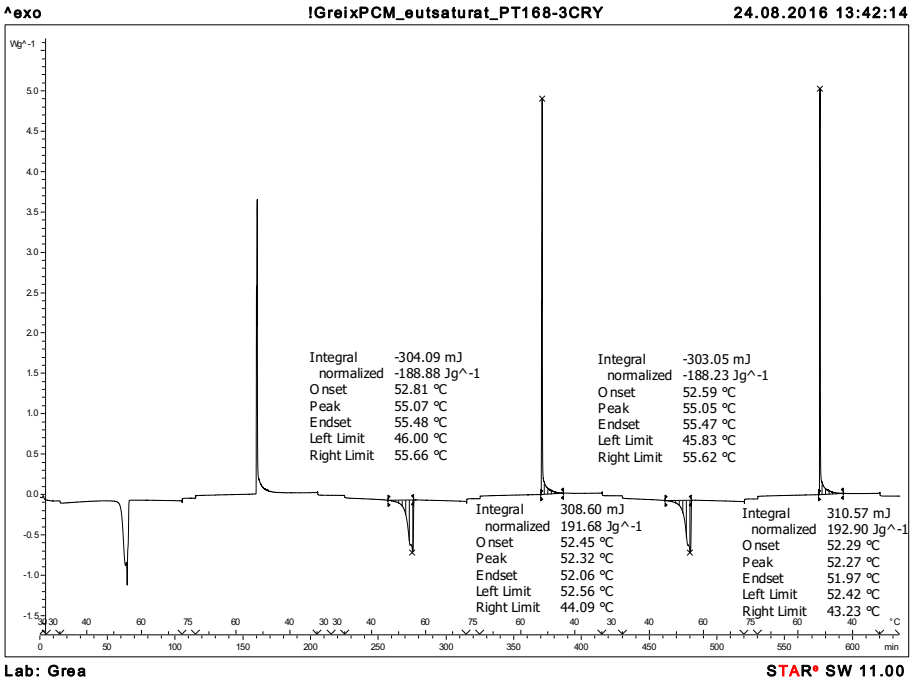

Figure A3-5. DSC response and evaluation of the material crystallized from ethyl acetate. Not-cycled sample 1, three cycles.

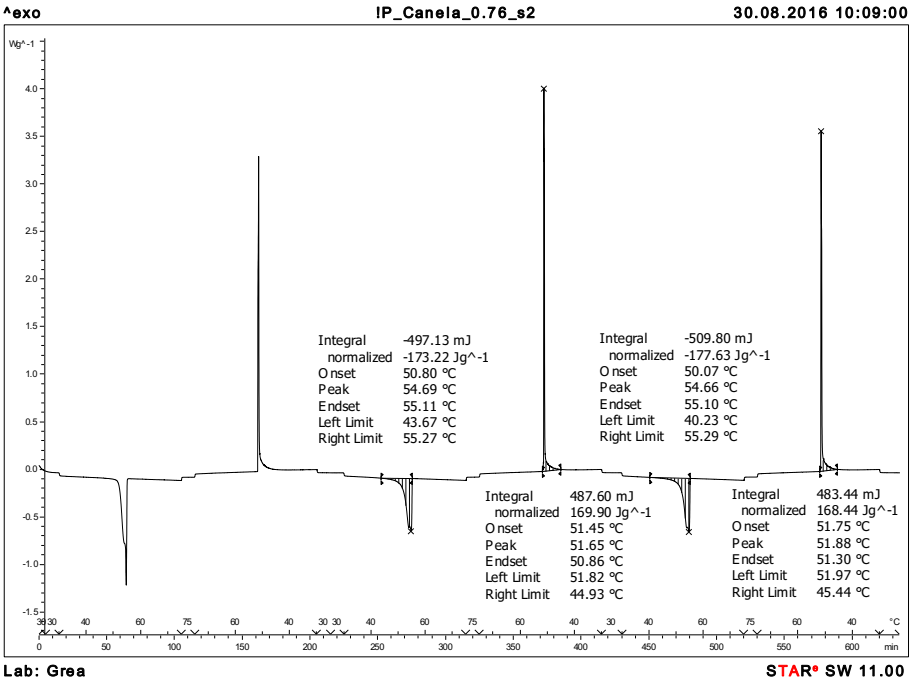

Figure A3-6. DSC response and evaluation of the material crystallized from ethyl acetate. Not-cycled sample 2, three cycles.

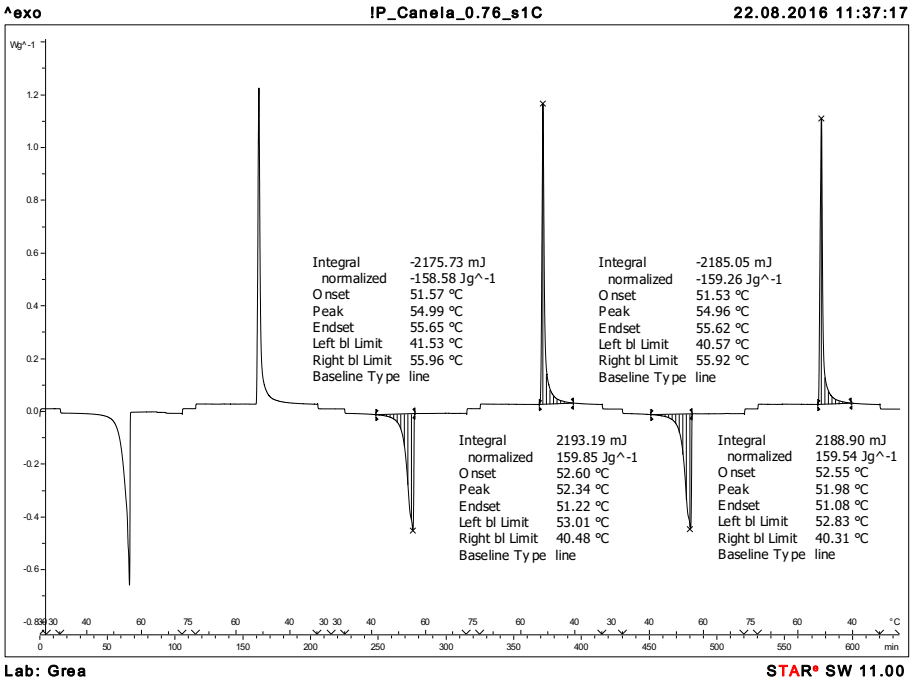

Figure A3-7. DSC response and evaluation of the material crystallized from ethyl acetate. Cycled sample 1, three cycles.

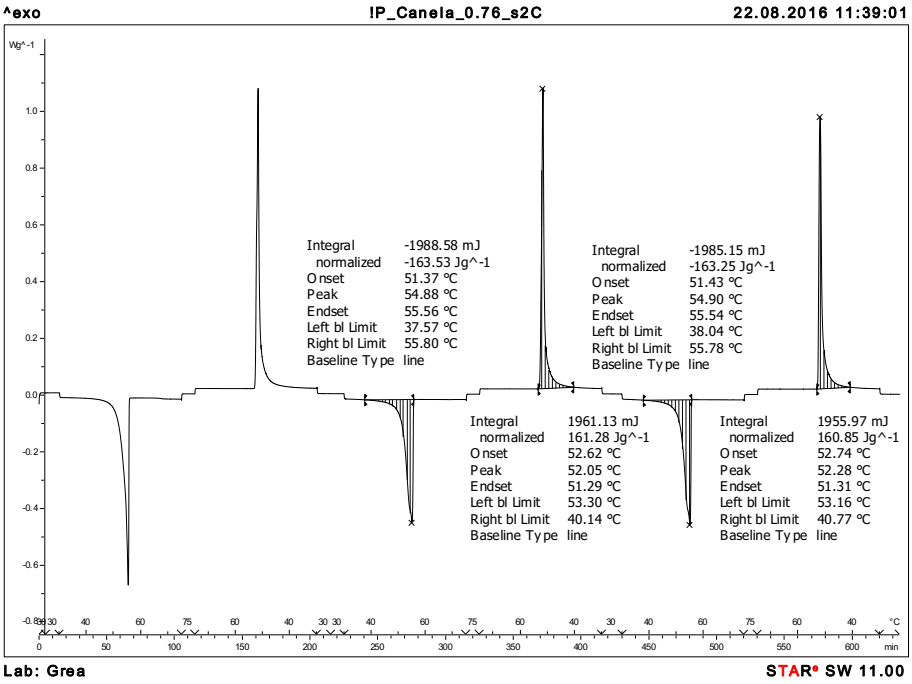

Figure A3-8. DSC response and evaluation of the material crystallized from ethyl acetate. Cycled sample 2, three cycles.

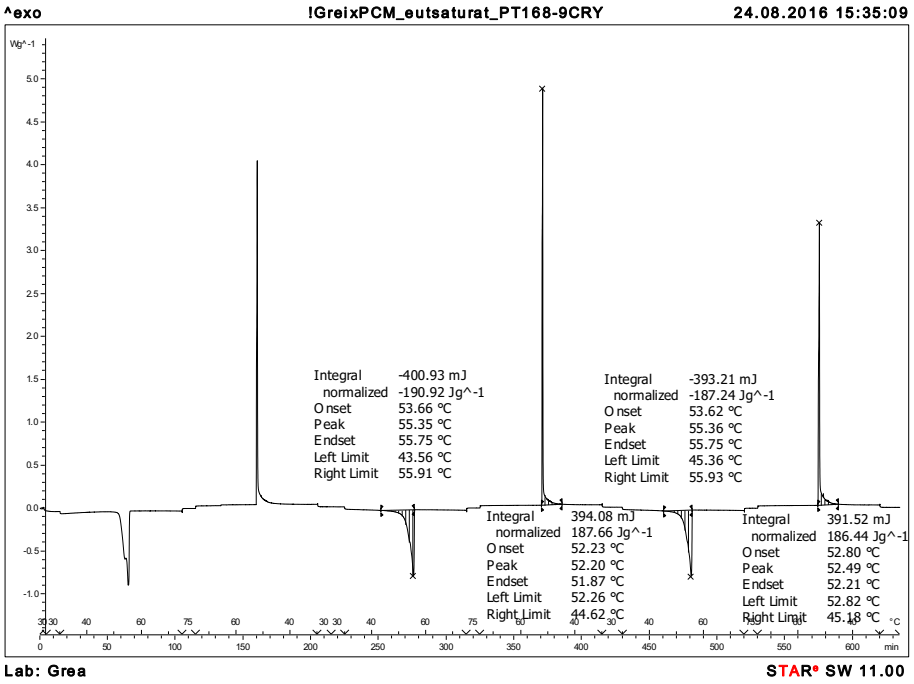

Figure A3-9. DSC response and evaluation of the material crystallized from ethanol. Not-cycled sample 1, three cycles.

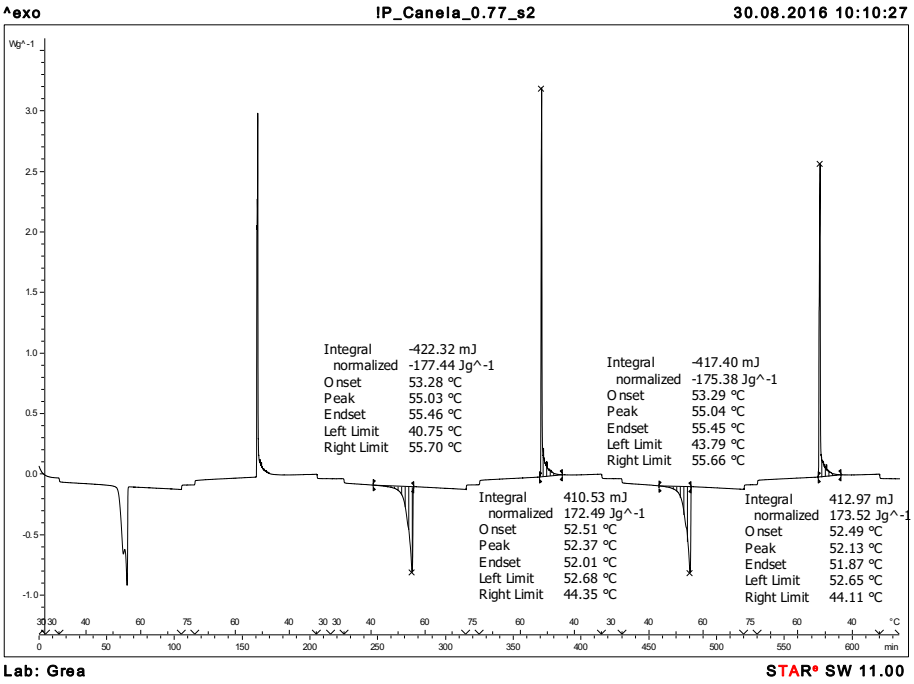

Figure A3-10. DSC response and evaluation of the material crystallized from ethanol. Not-cycled sample 2, three cycles.

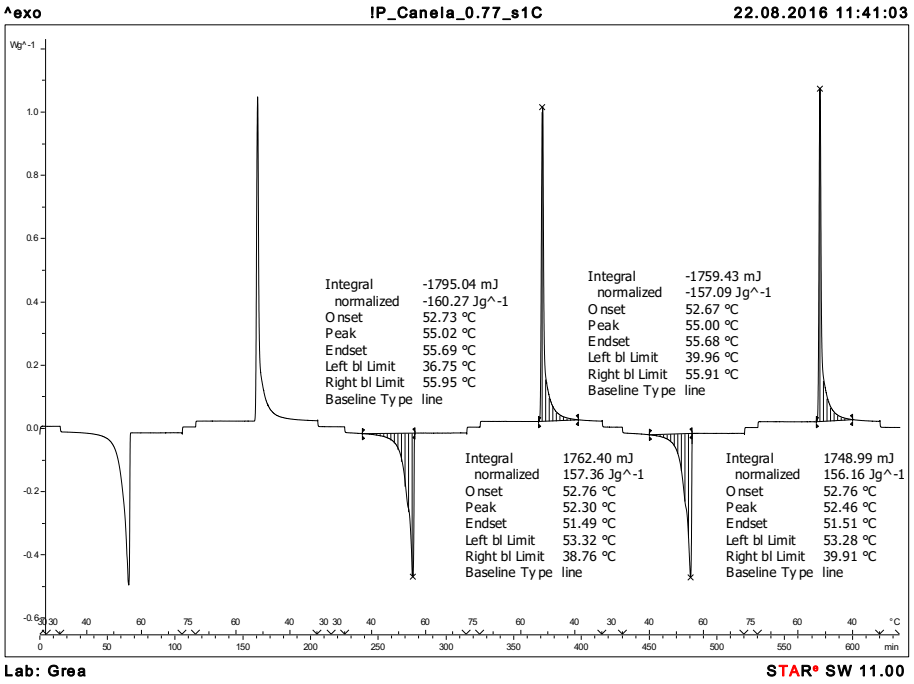

Figure A3-11. DSC response and evaluation of the material crystallized from ethanol. Cycled sample 1, three cycles.

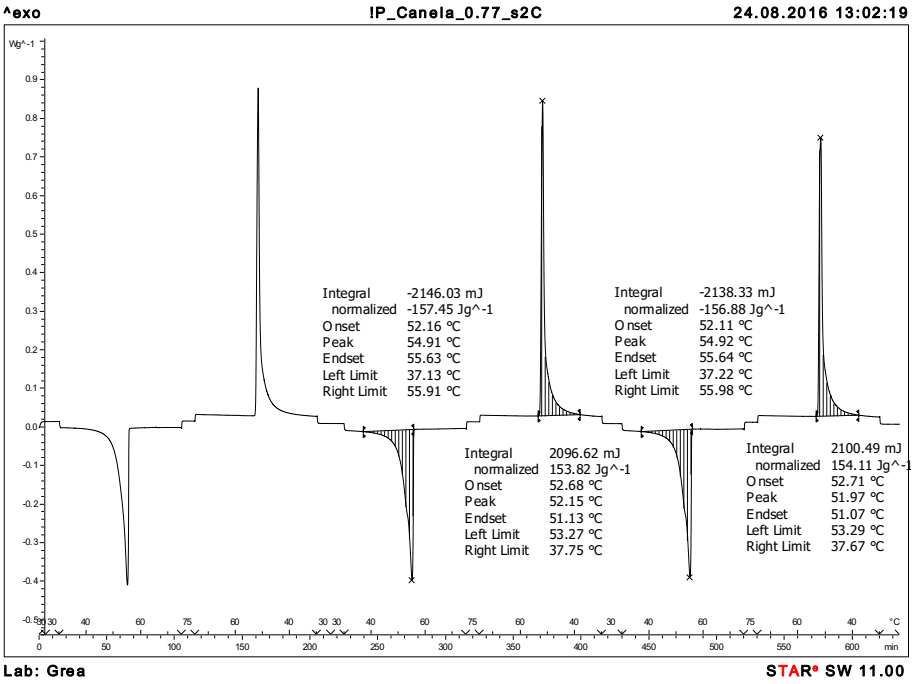

Figure A3-12. DSC response and evaluation of the material crystallized from ethanol. Cycled sample 2, three cycles.

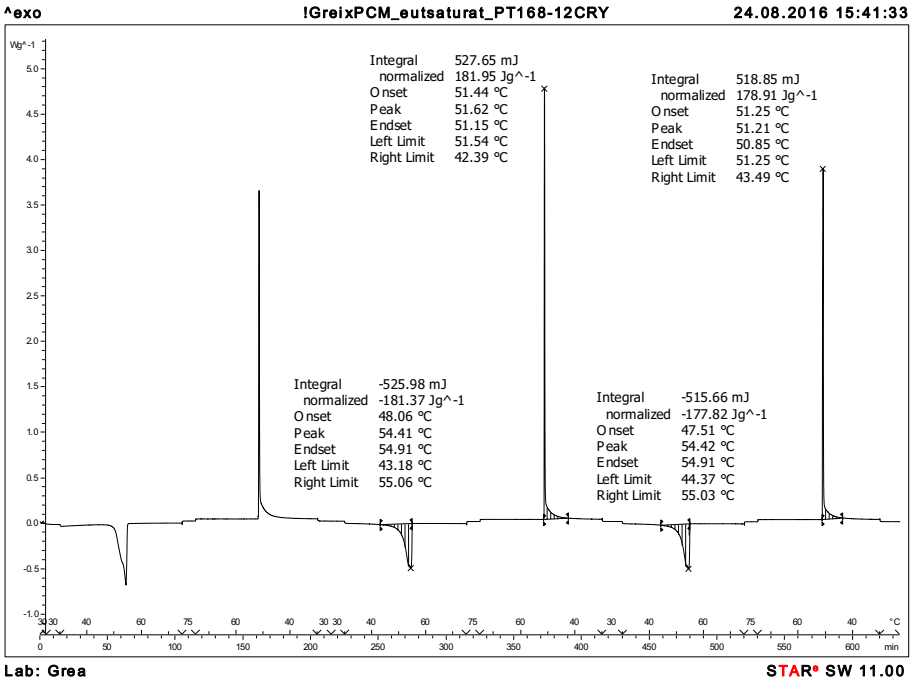

Figure A3-13. DSC response and evaluation of the material crystallized from hexane. Not-cycled sample 1, three cycles.

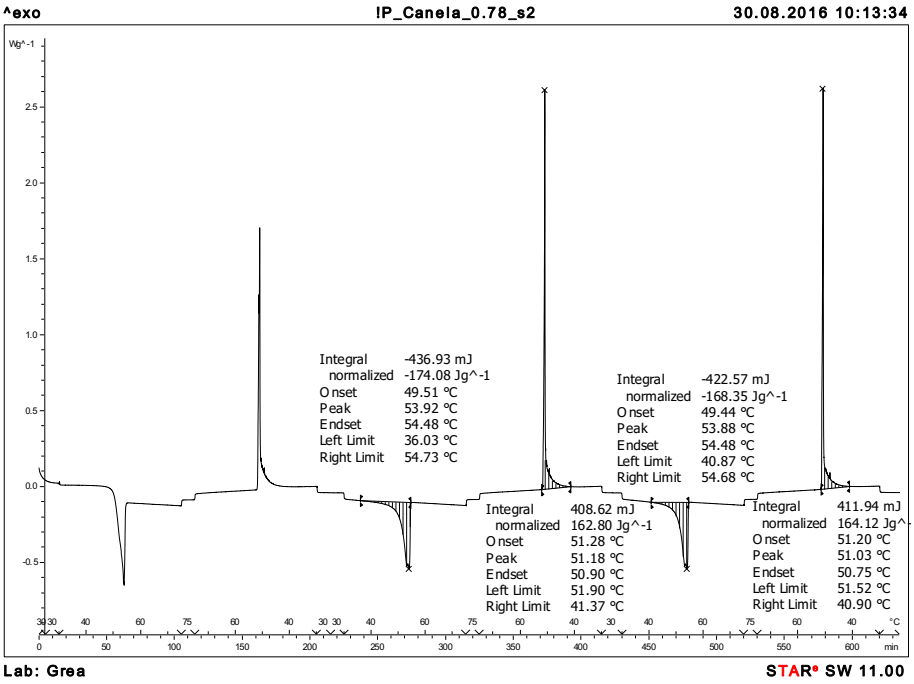

Figure A3-14. DSC response and evaluation of the material crystallized from hexane. Not-cycled sample 2, three cycles.

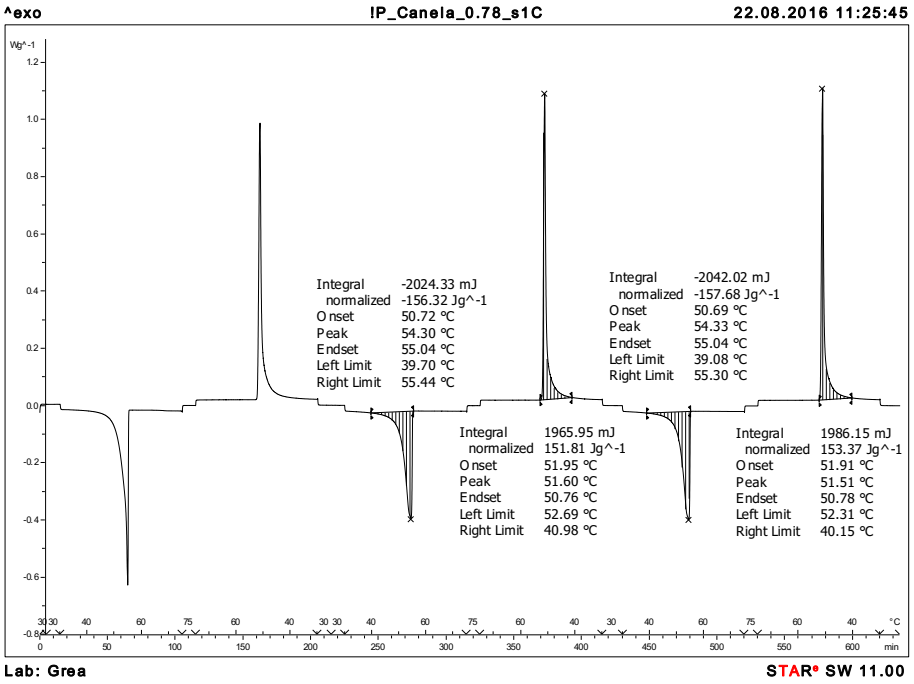

Figure A3-15. DSC response and evaluation of the material crystallized from hexane. Cycled sample 1, three cycles.

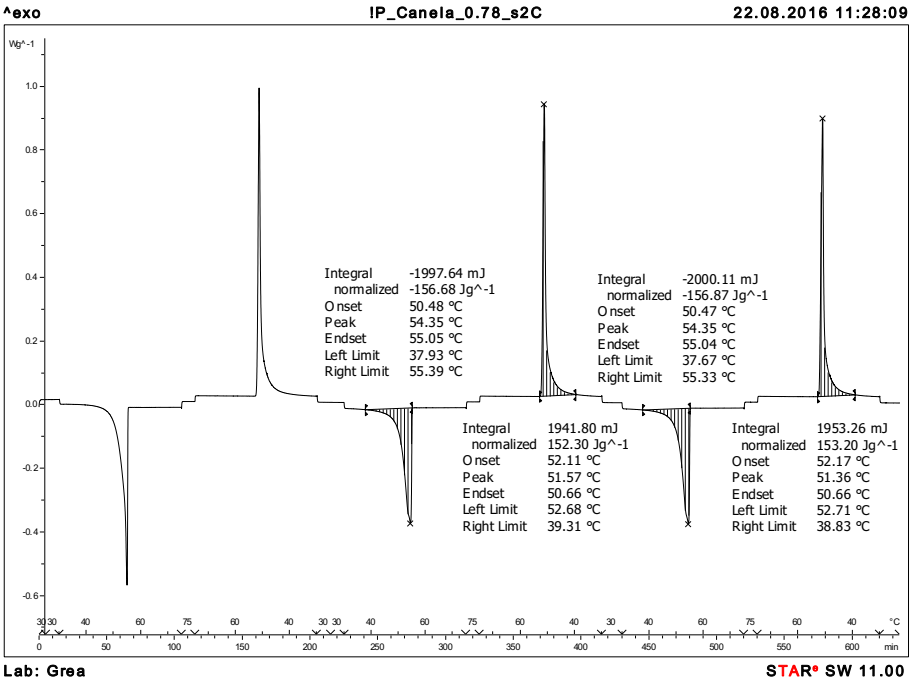

Figure A3-16. DSC response and evaluation of the material crystallized from hexane. Cycled sample 2, three cycles.

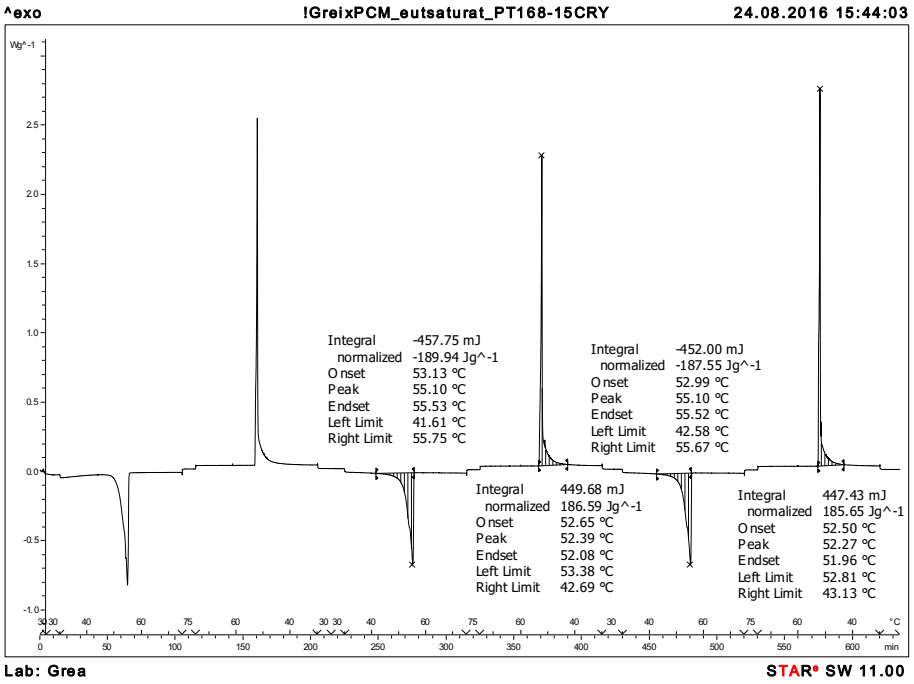

Figure A3-17. DSC response and evaluation of the material crystallized from methanol. Not-cycled sample 1, three cycles.

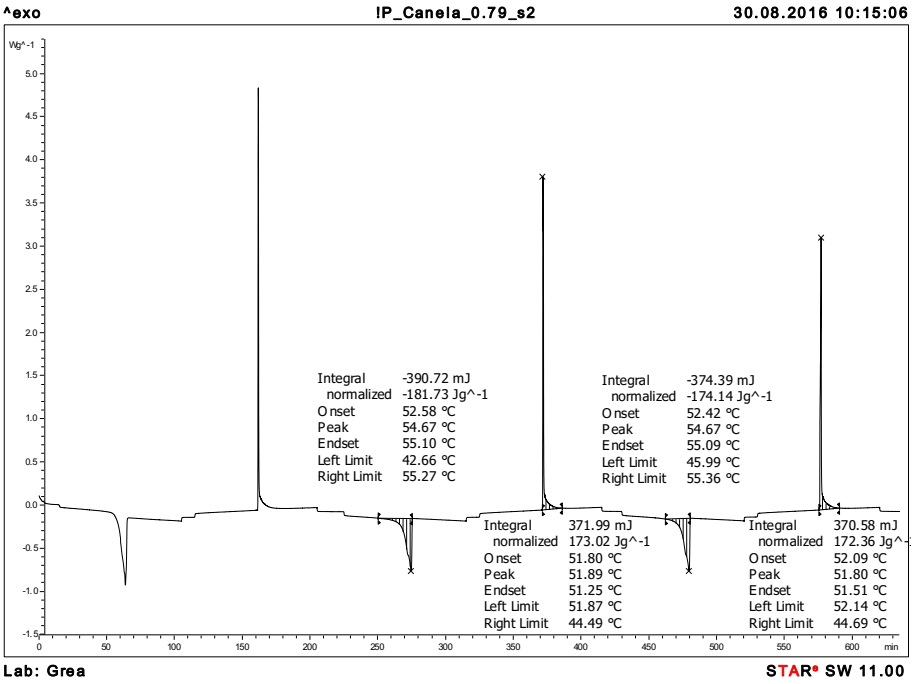

Figure A3-18. DSC response and evaluation of the material crystallized from methanol. Not-cycled sample 2, three cycles.

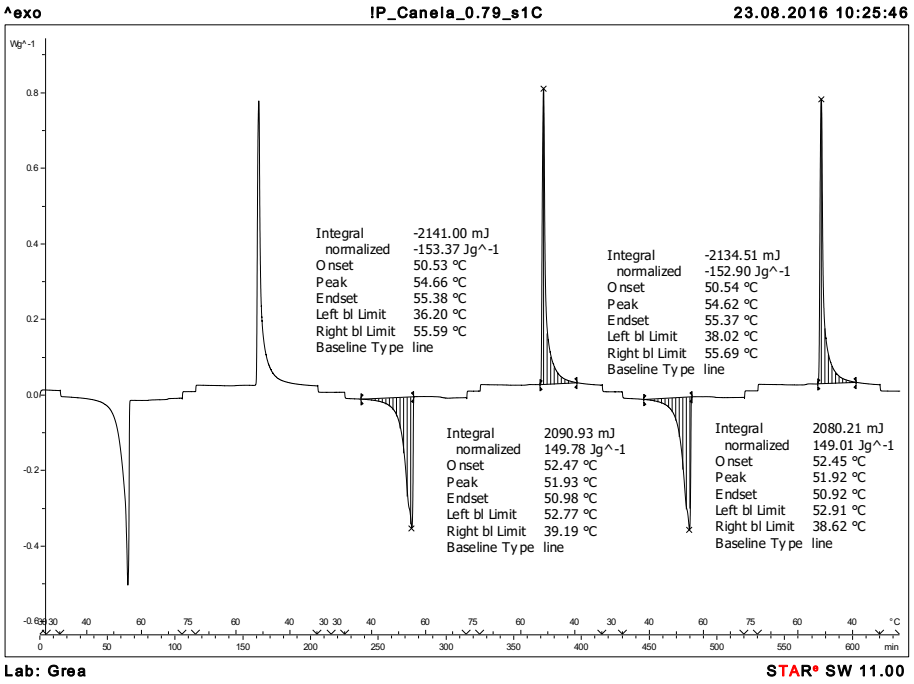

Figure A3-19. DSC response and evaluation of the material crystallized from methanol. Cycled sample 1, three cycles.

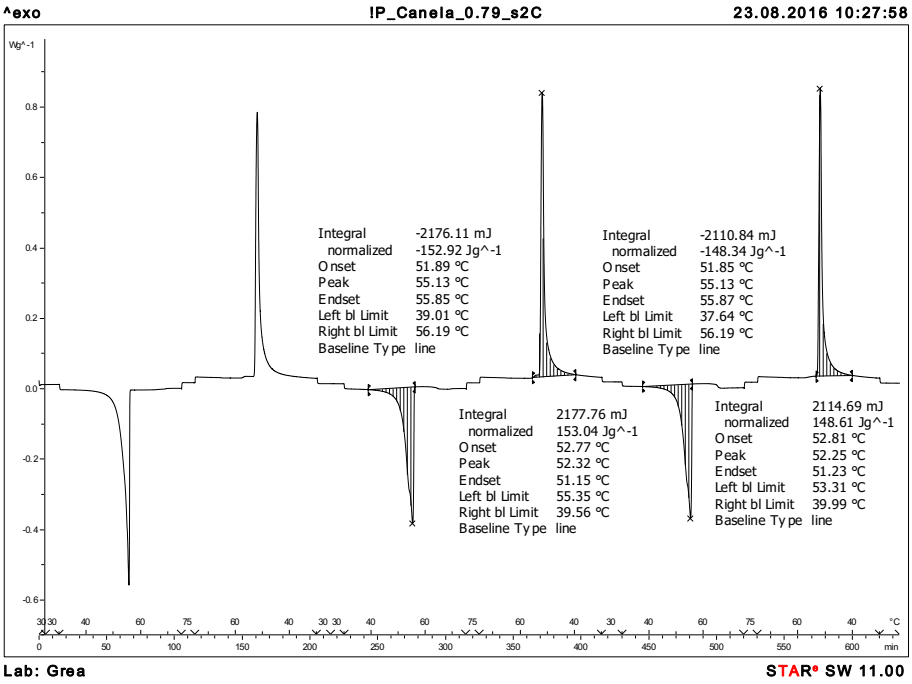

Figure A3-20. DSC response and evaluation of the material crystallized from methanol. Cycled sample 2, three cycles.

DSC analysis of DHSA and their salts:

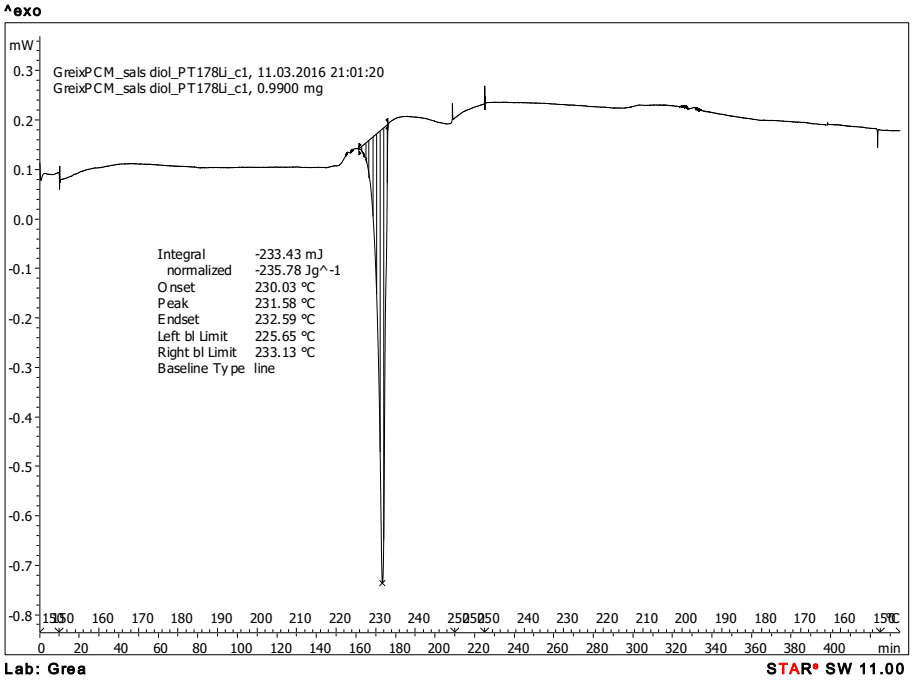

Figure A3-21. DSC response of lithium DHSA salt, 1st cycle.

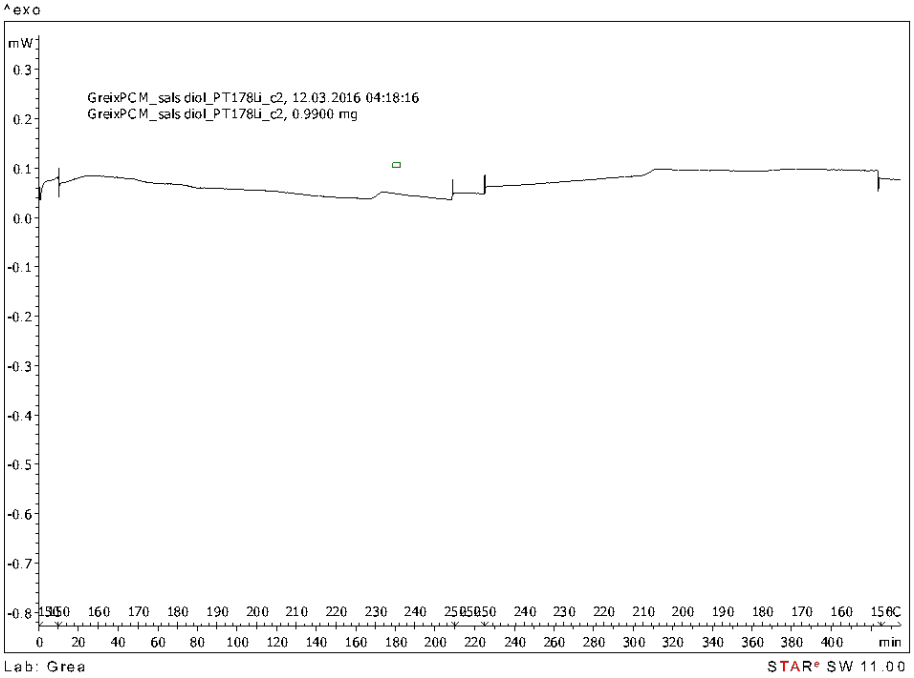

Figure A3-22. DSC response of lithium DHSA salt, 2nd cycle.

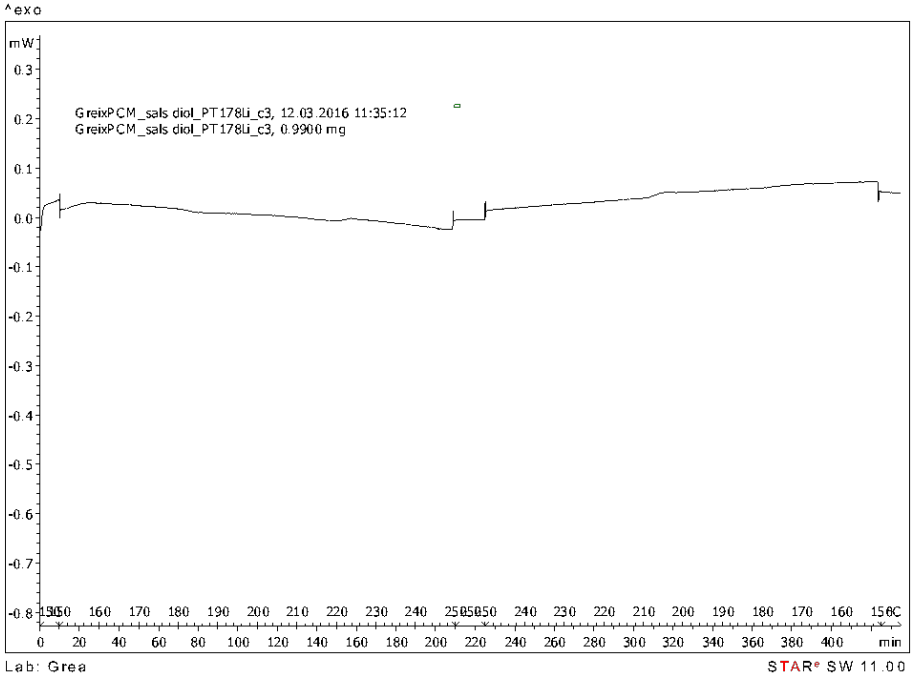

Figure A3-23. DSC response of lithium DHSA salt, 3rd cycle.

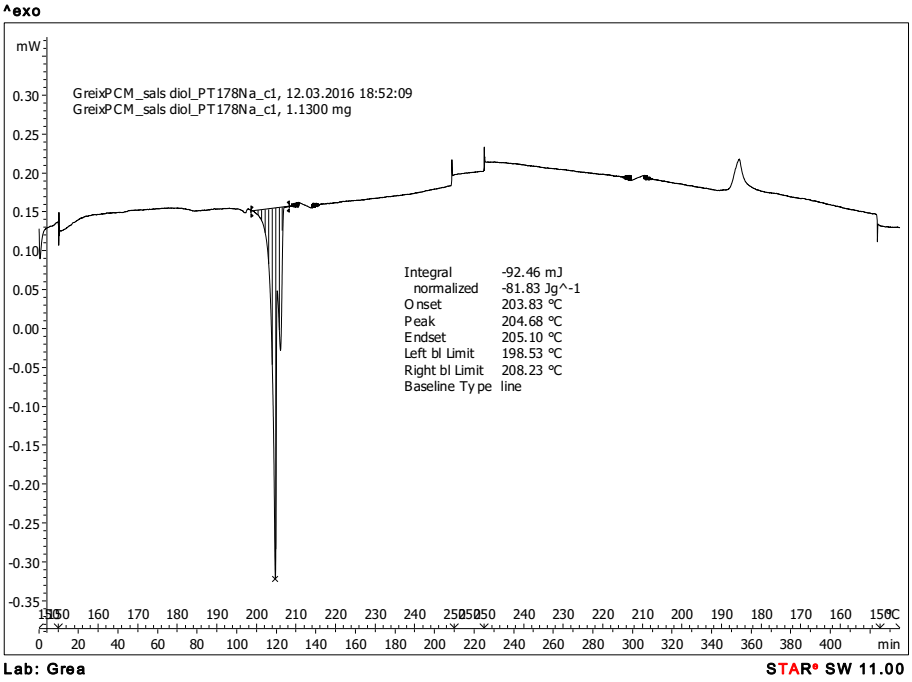

Figure A3-24. DSC response of sodium DHSA salt, 1st cycle.

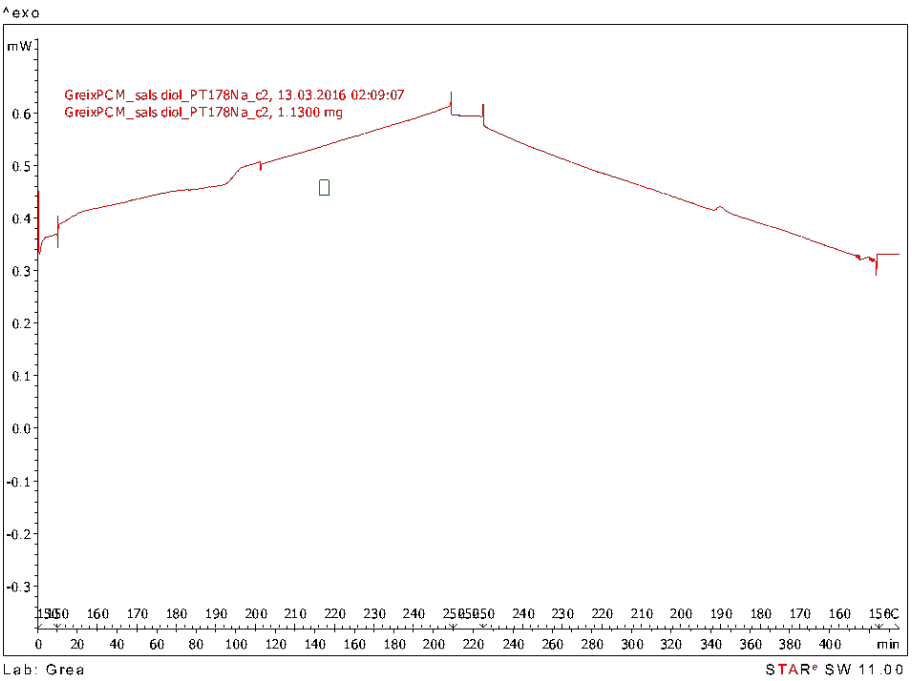

Figure A3-25. DSC response of sodium DHSA salt, 2nd cycle.

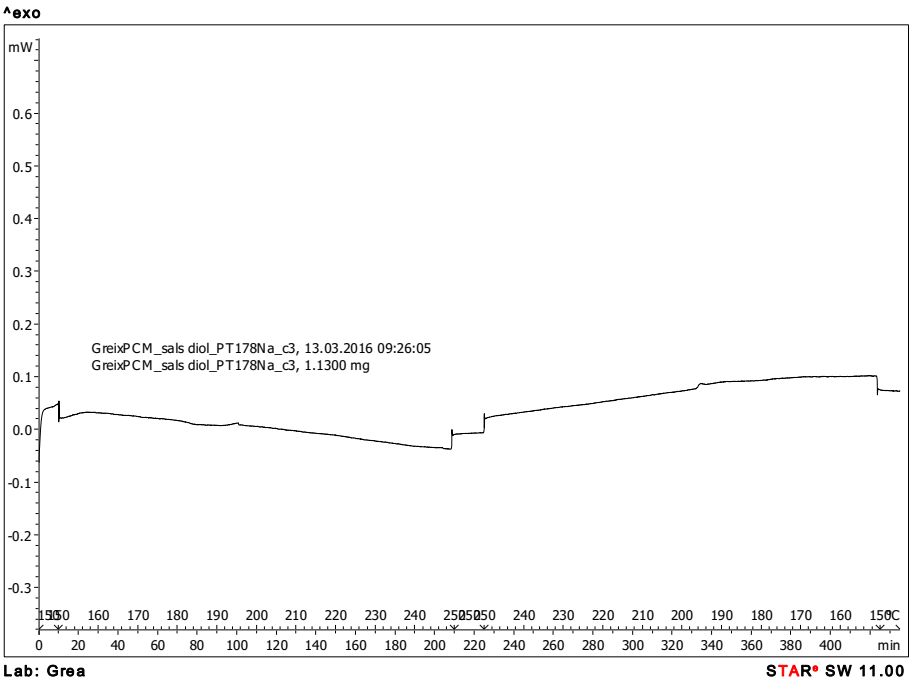

Figure A3-26. DSC response of sodium DHSA salt, 3rd cycle.

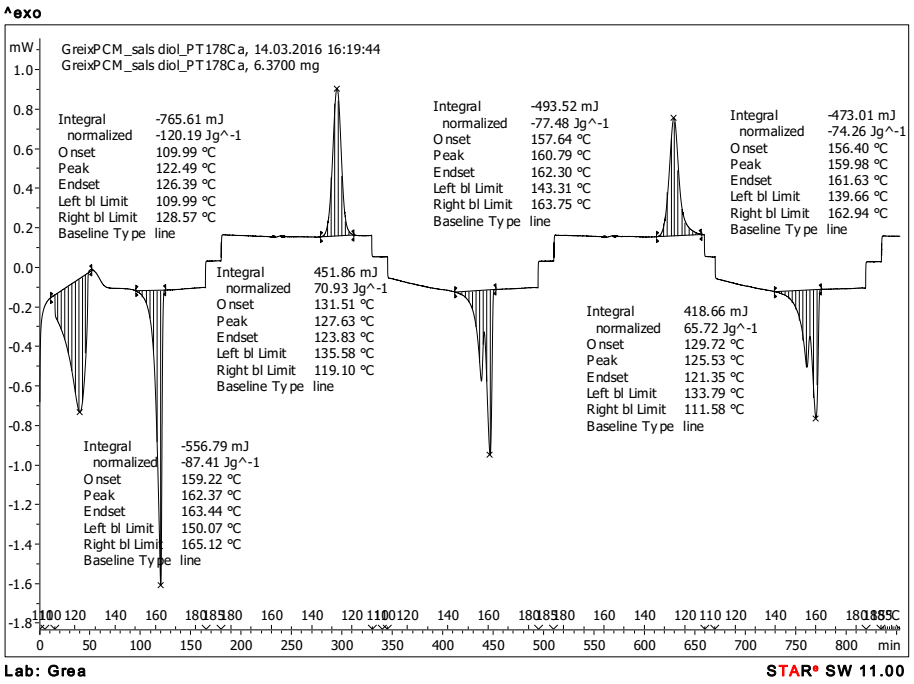

Figure A3-27. DSC response of calcium DHSA salt, three cycles.

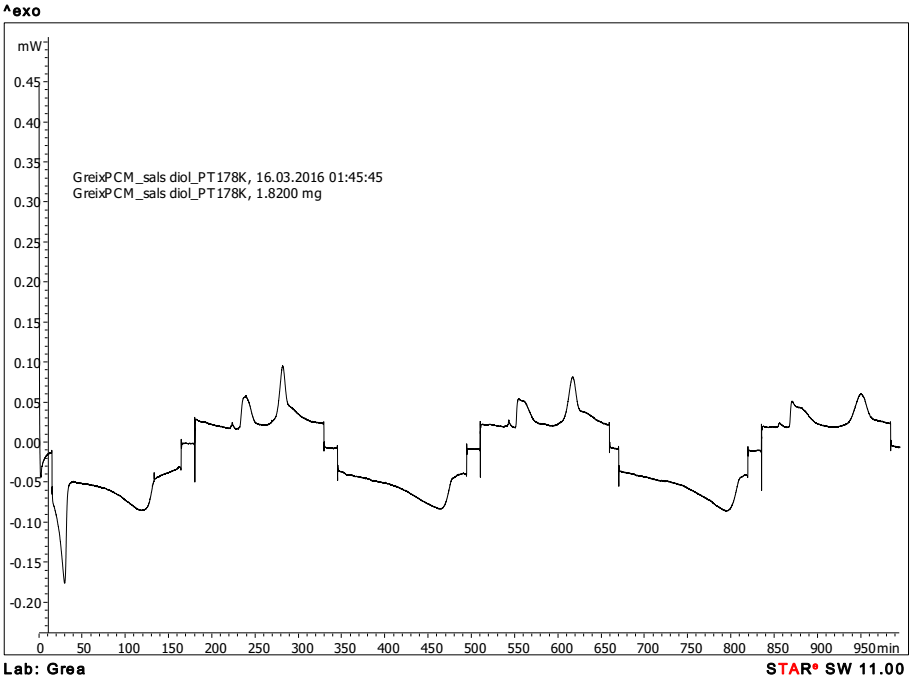

Figure A3-28. DSC response of magnesium DHSA salt, three cycles.

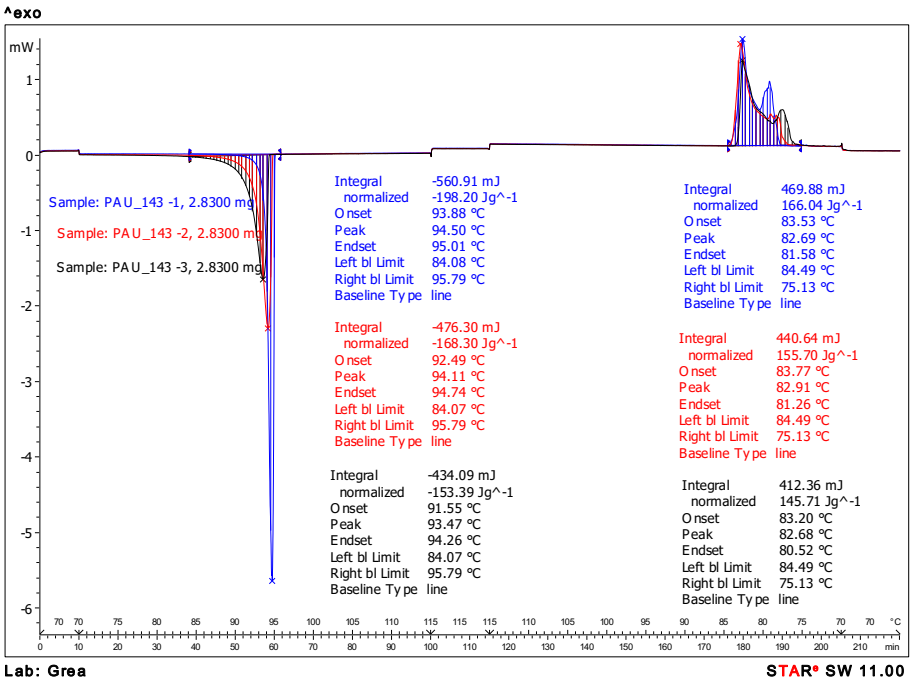

Figure A3-29. DSC response of DHSA, three cycles.

DSC analysis of the Chapter IV

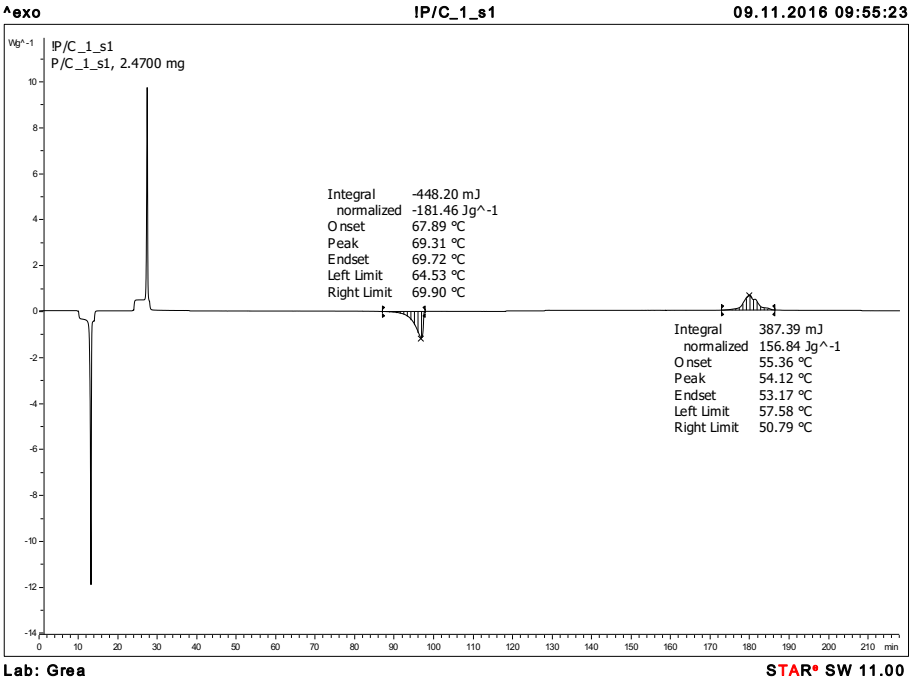

Figure A3-30. DSC response and evaluation of the material crystallized from methyl DHSE. Not cycled sample 1.

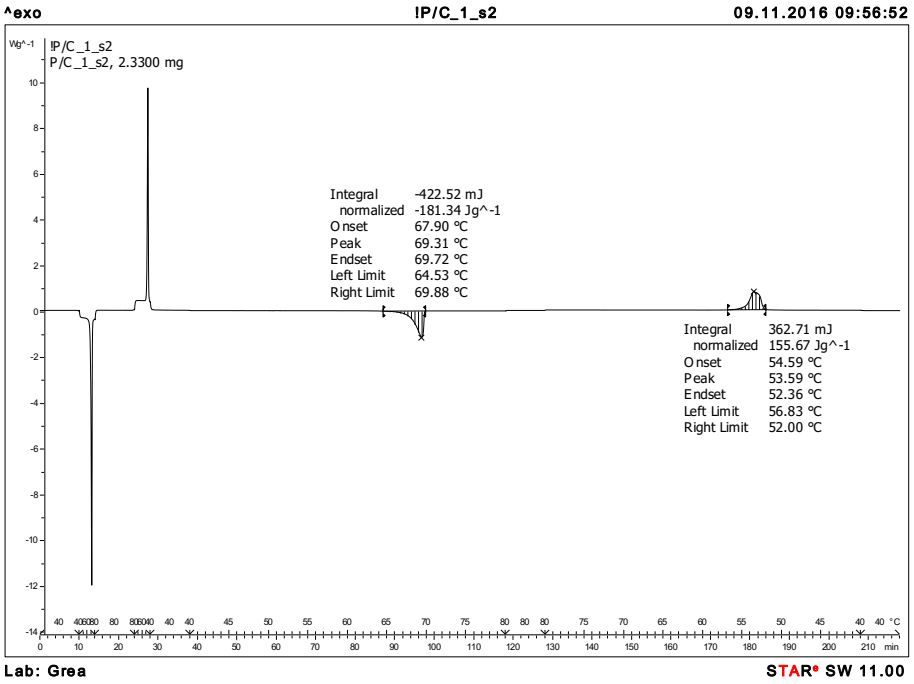

Figure A3-31. DSC response and evaluation of the material crystallized from methyl DHSE. Not cycled sample 2.

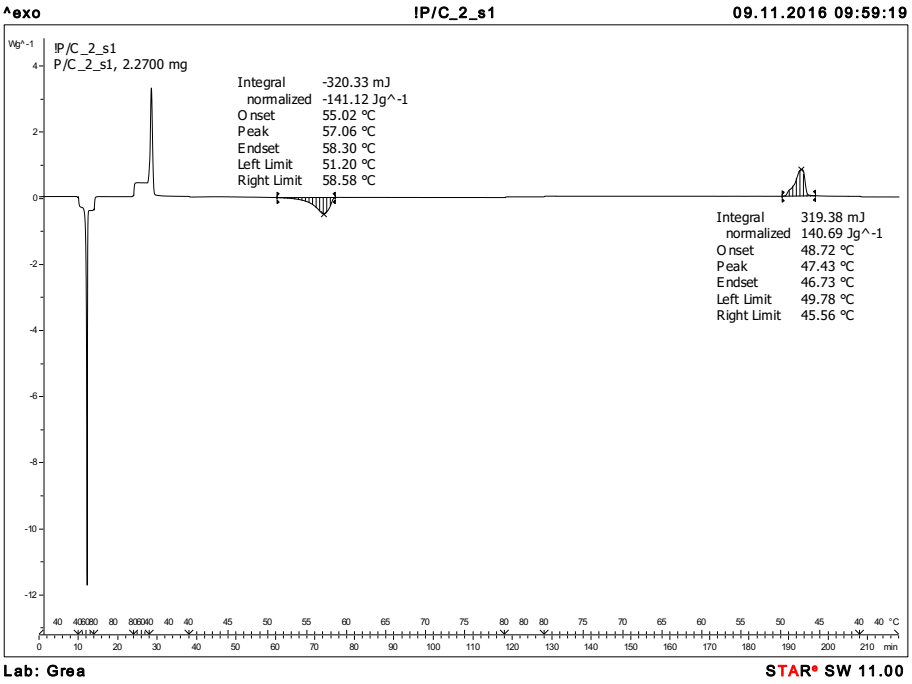

Figure A3-32. DSC response and evaluation of the material crystallized from ethyl DHSE. Not cycled sample 1.

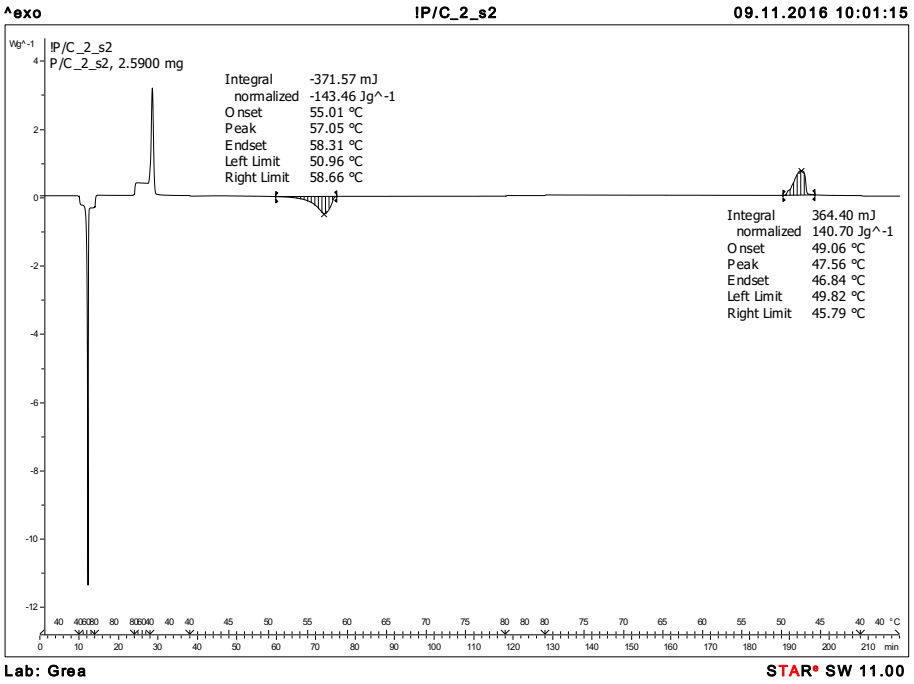

Figure A3-33. DSC response and evaluation of the material crystallized from ethyl DHSE. Not cycled sample 2.

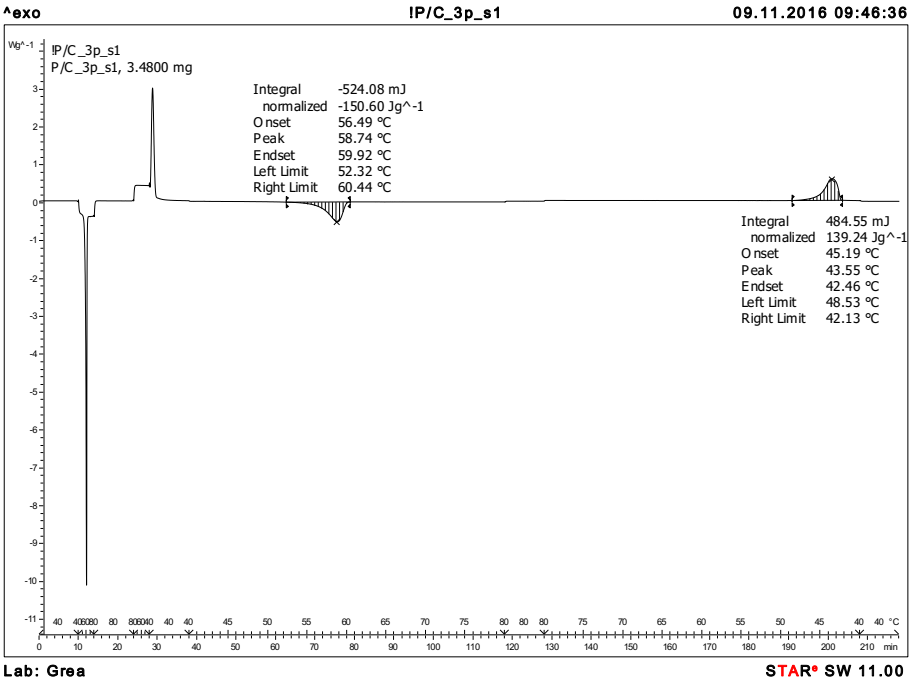

Figure A3-34. DSC response and evaluation of the material crystallized from propyl DHSE. Not cycled sample 1.

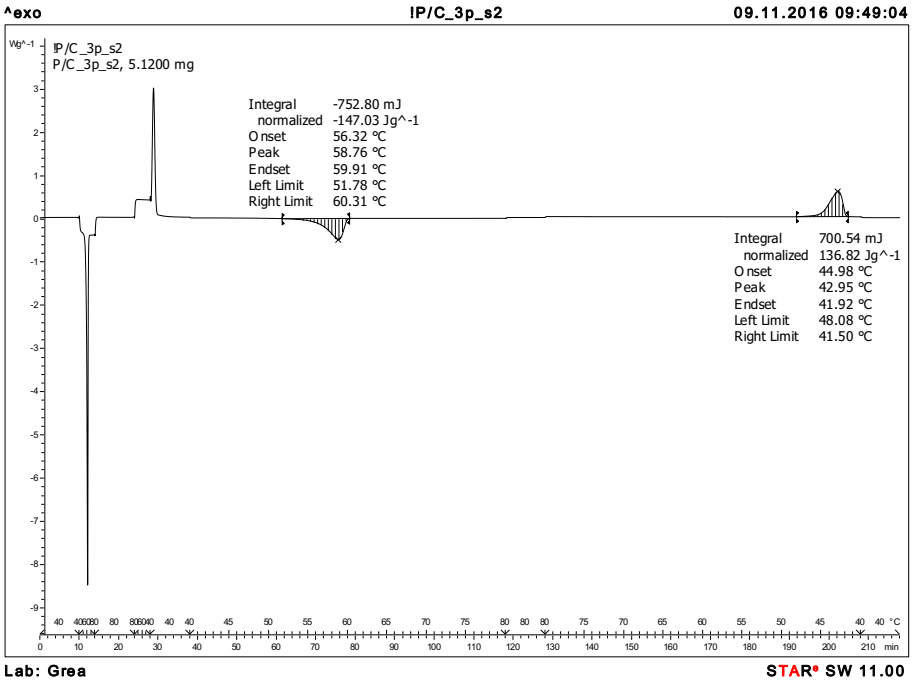

Figure A3-35. DSC response and evaluation of the material crystallized from propyl DHSE. Not cycled sample 2.

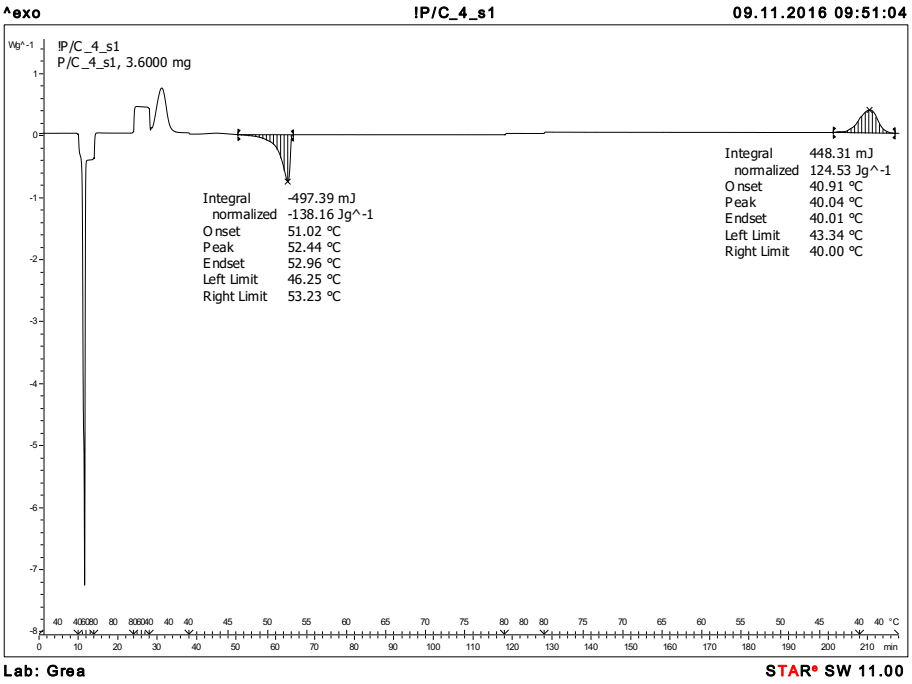

Figure A3-36. DSC response and evaluation of the material crystallized from butyl DHSE. Not cycled sample 1.

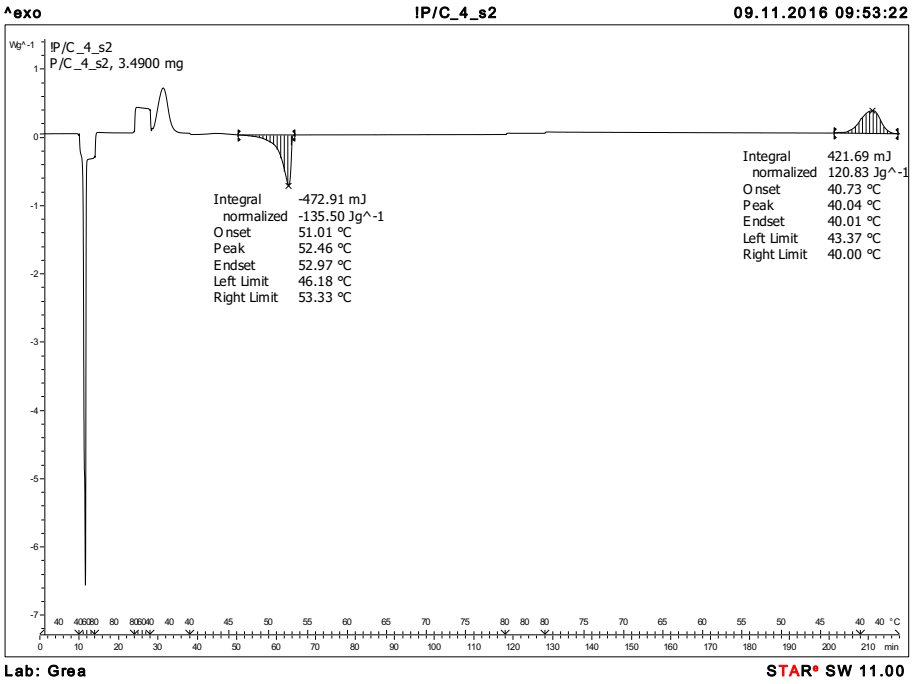

Figure A3-37. DSC response and evaluation of the material crystallized from butyl DHSE. Not cycled sample 2.

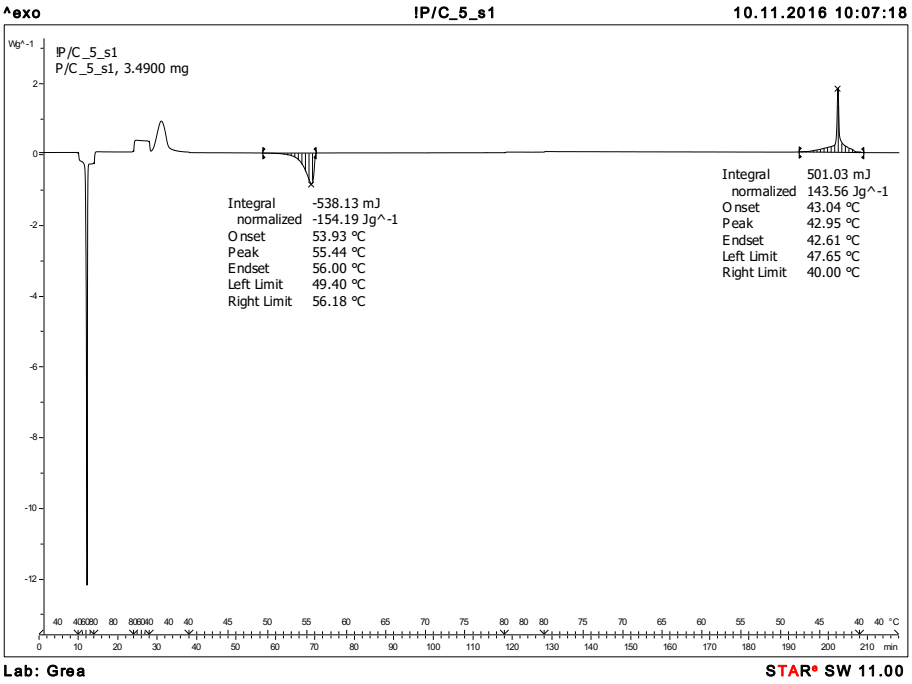

Figure A3-38. DSC response and evaluation of the material crystallized from pentyl DHSE. Not cycled sample 1.

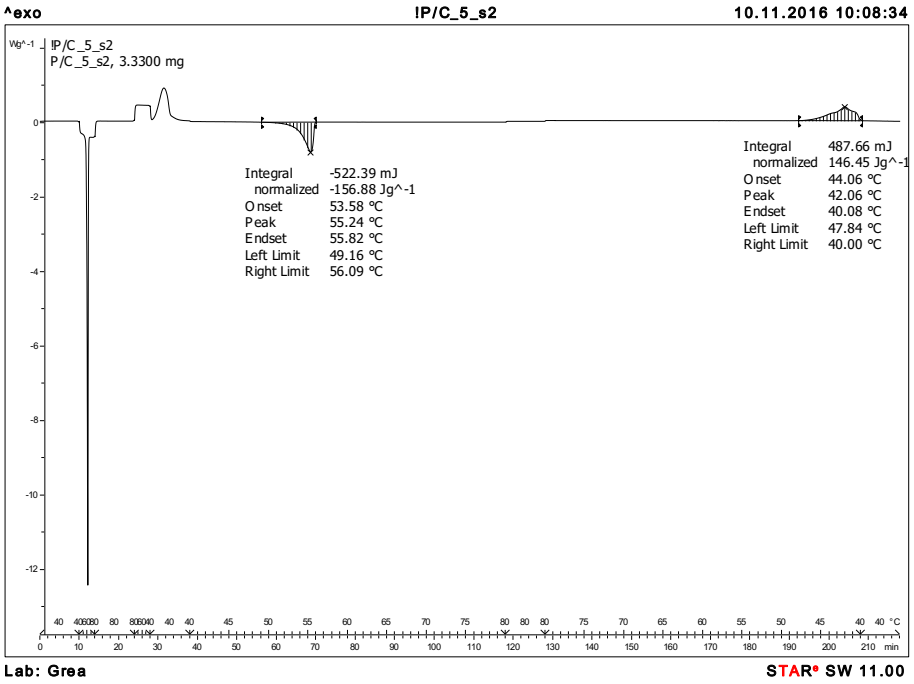

Figure A3-39. DSC response and evaluation of the material crystallized from pentyl DHSE. Not cycled sample 2.

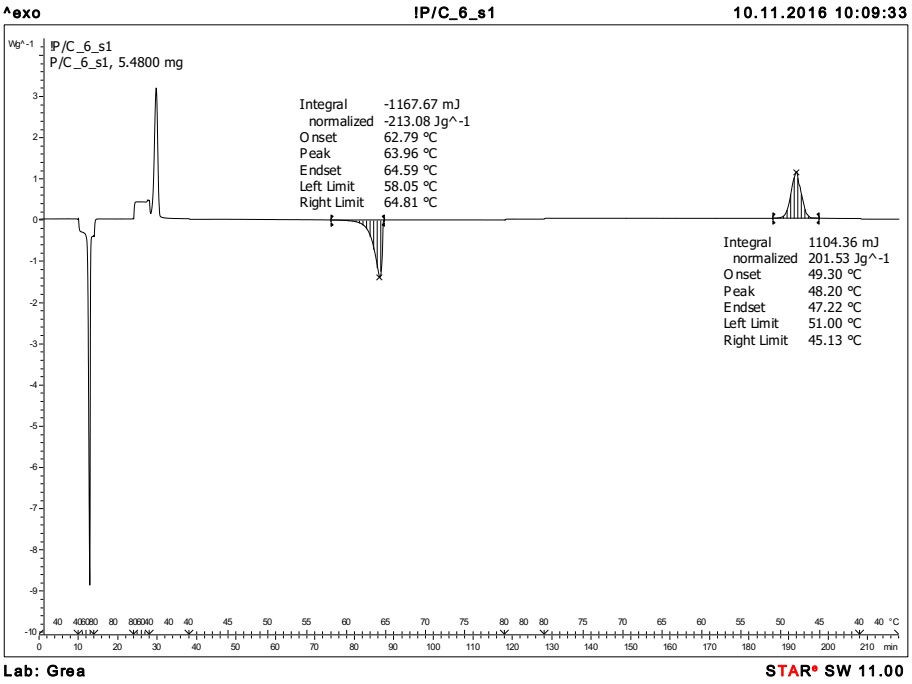

Figure A3-40. DSC response and evaluation of the material crystallized from hexyl DHSE. Not cycled sample 1.

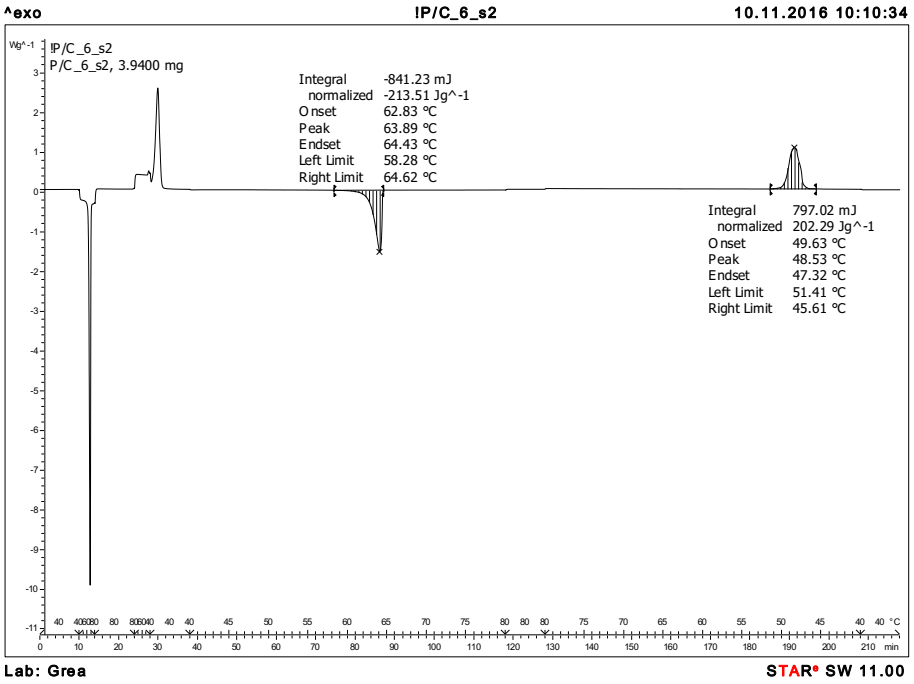

Figure A3-41. DSC response and evaluation of the material crystallized from hexyl DHSE. Not cycled sample 2.

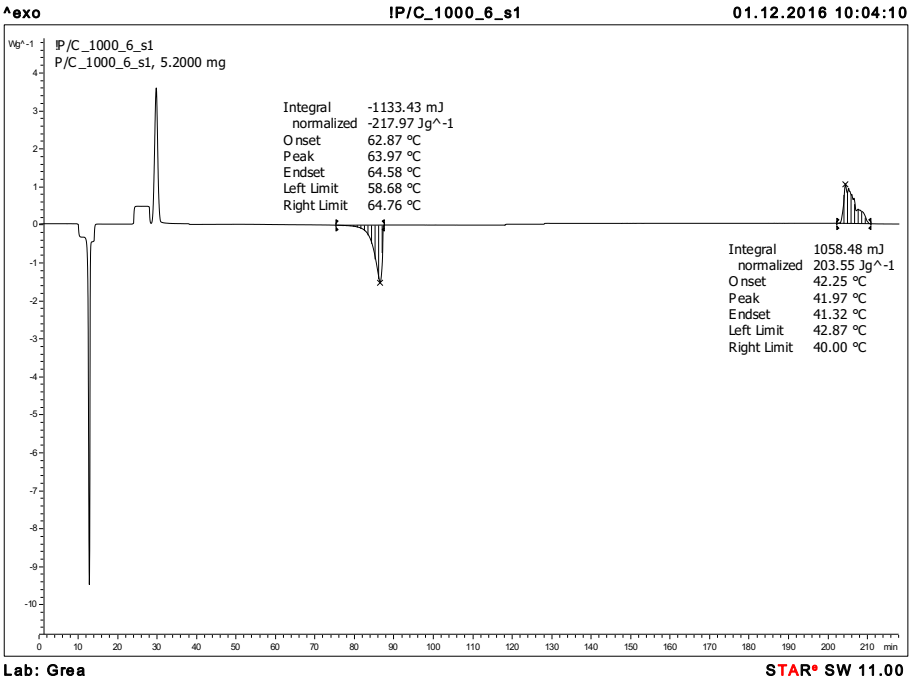

Figure A3-42. DSC response and evaluation of the material crystallized from hexyl DHSE. Cycled sample 1. 100 cycles.

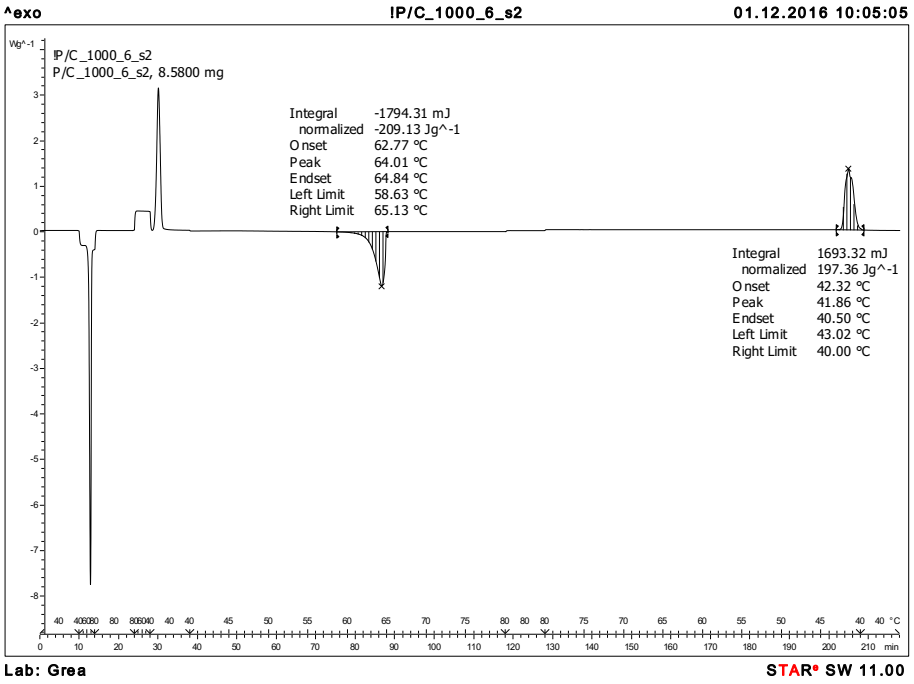

Figure A3-43. DSC response and evaluation of the material crystallized from hexyl DHSE. Cycled sample 2. 100 cycles.

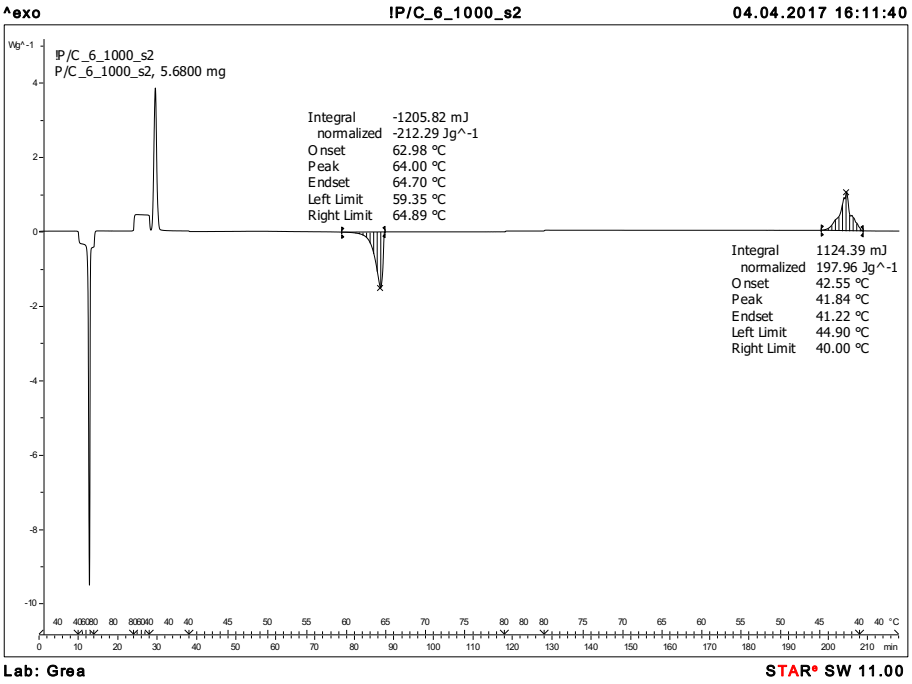

Figure A3-44. DSC response and evaluation of the material crystallized from hexyl DHSE. Cycled sample 1. 1000 cycles.

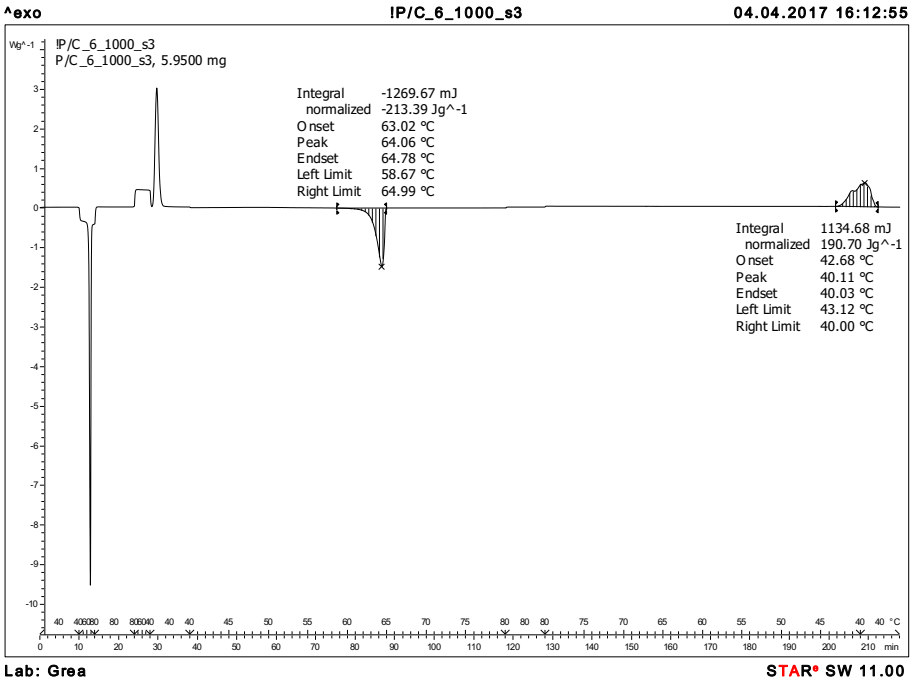

Figure A3-45. DSC response and evaluation of the material crystallized from hexyl DHSE. Cycled sample 2. 1000 cycles.

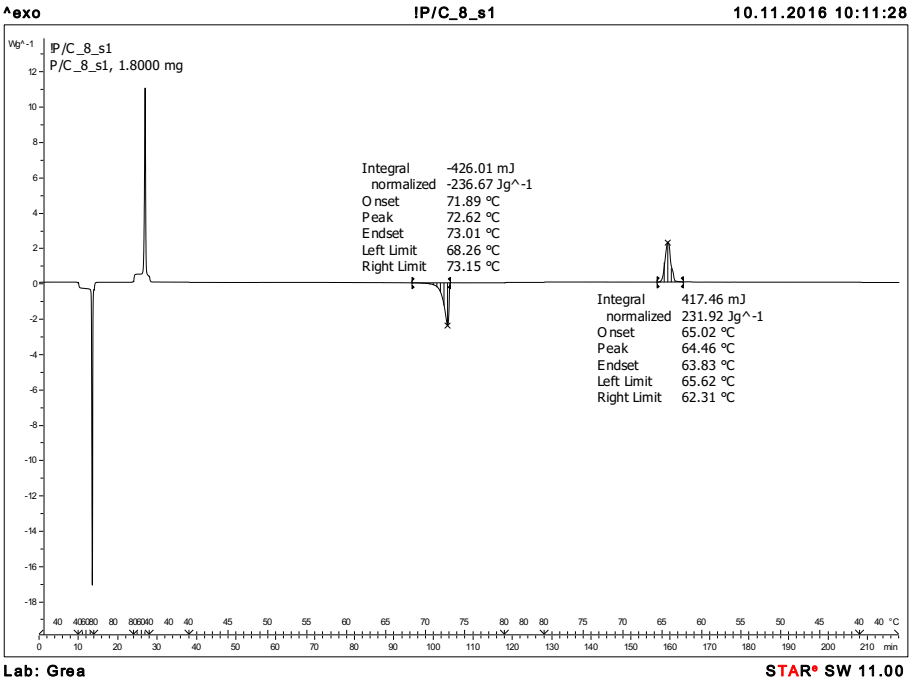

Figure A3-46. DSC response and evaluation of the material crystallized from octyl DHSE. Not cycled sample 1.

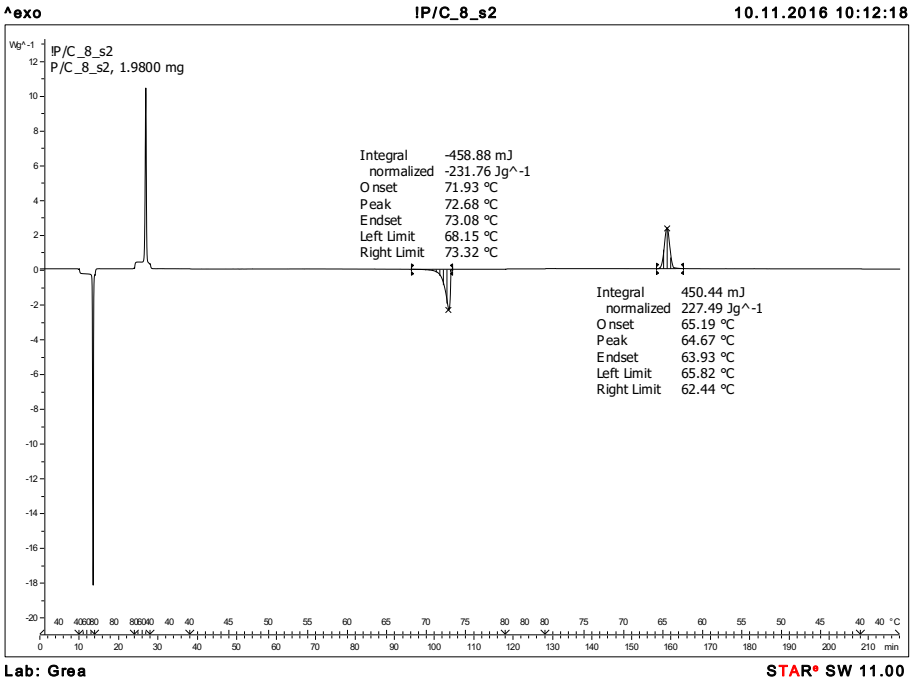

Figure A3-47. DSC response and evaluation of the material crystallized from octyl DHSE. Not cycled sample 2.

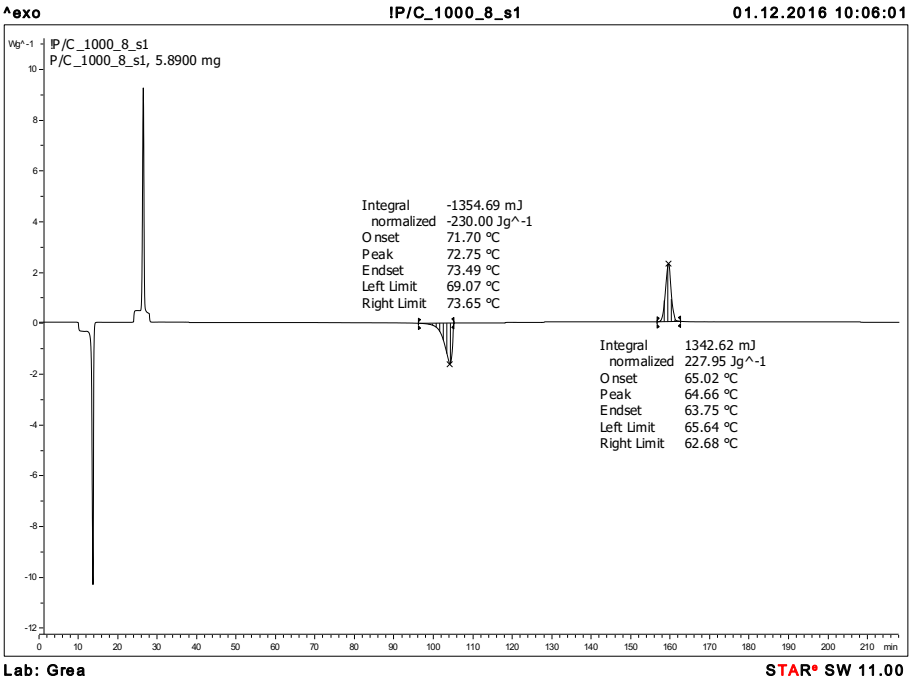

Figure A3-48. DSC response and evaluation of the material crystallized from octyl DHSE. Cycled sample 1. 100 cycles.

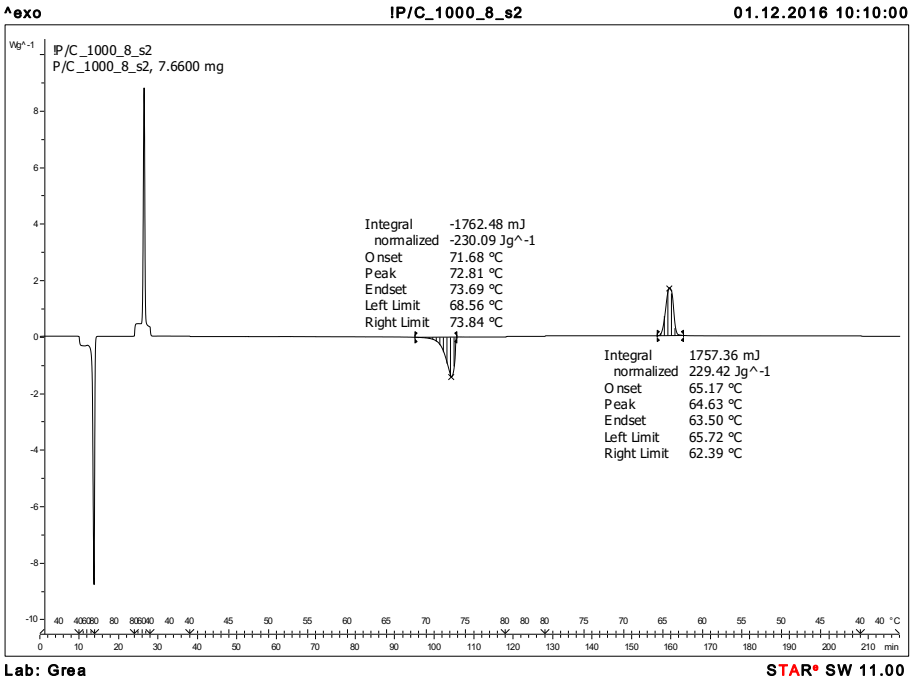

Figure A3-49. DSC response and evaluation of the material crystallized from octyl DHSE. Cycled sample 2. 100 cycles.

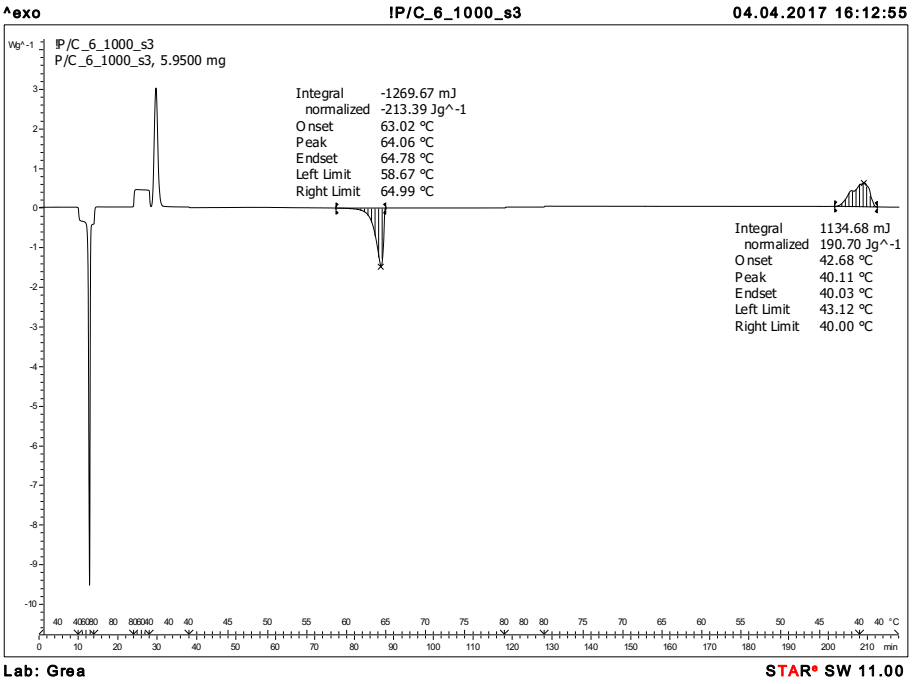

Figure A3-50. DSC response and evaluation of the material crystallized from octyl DHSE. Cycled sample 1. 1000 cycles.

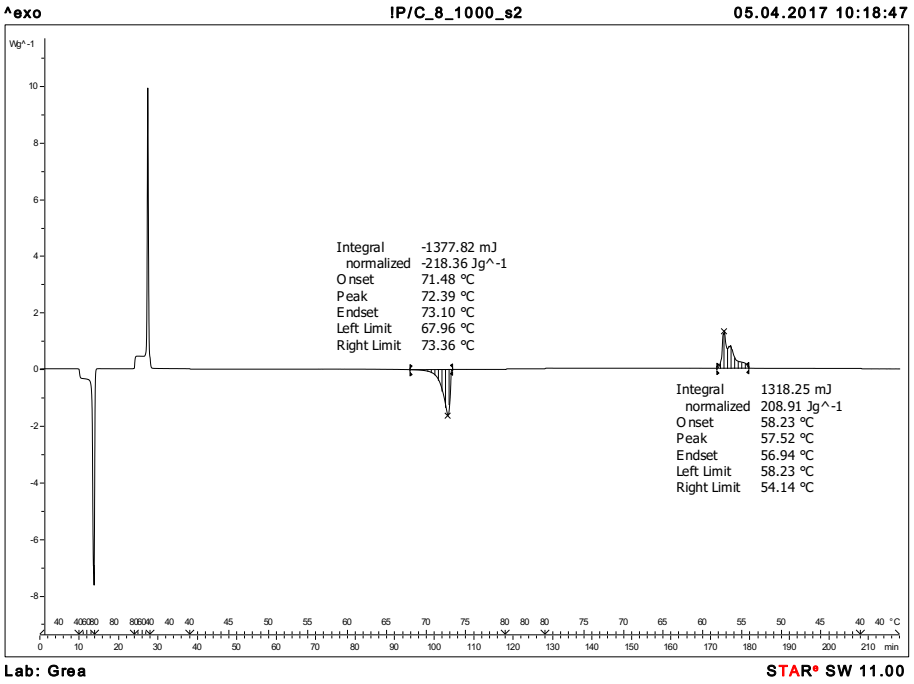

Figure A3-51. DSC response and evaluation of the material crystallized from octyl DHSE. Cycled sample 2. 1000 cycles.

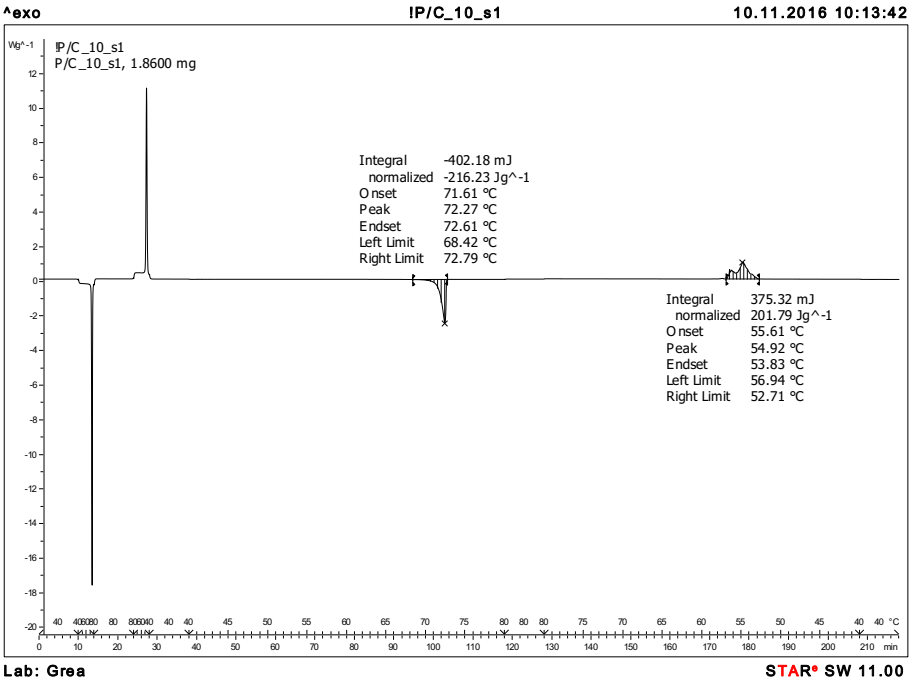

Figure A3-52. DSC response and evaluation of the material crystallized from decyl DHSE. Not cycled sample 1.

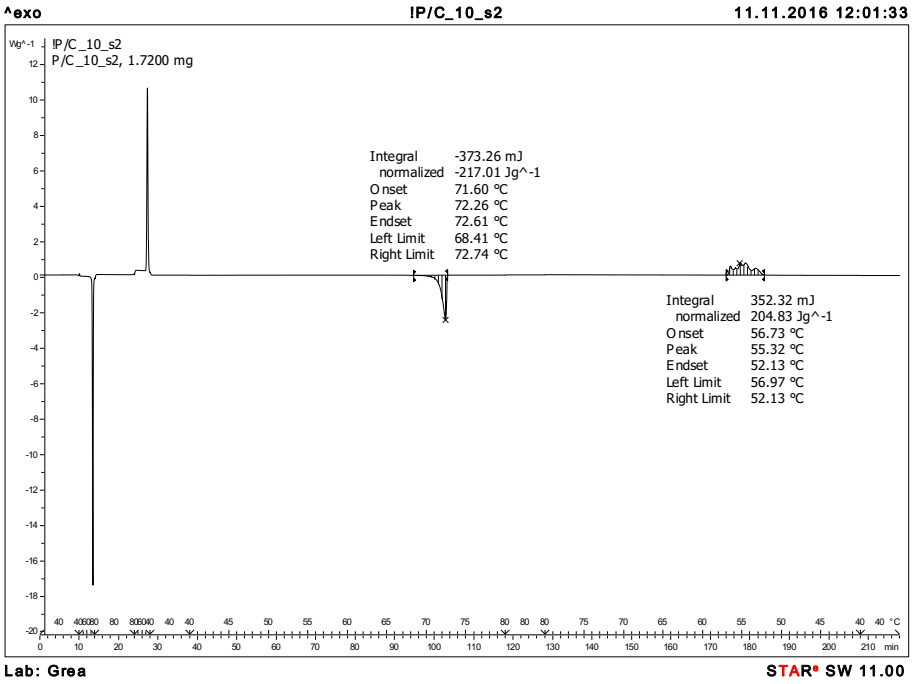

Figure A3-53. DSC response and evaluation of the material crystallized from decyl DHSE. Not cycled sample 2.

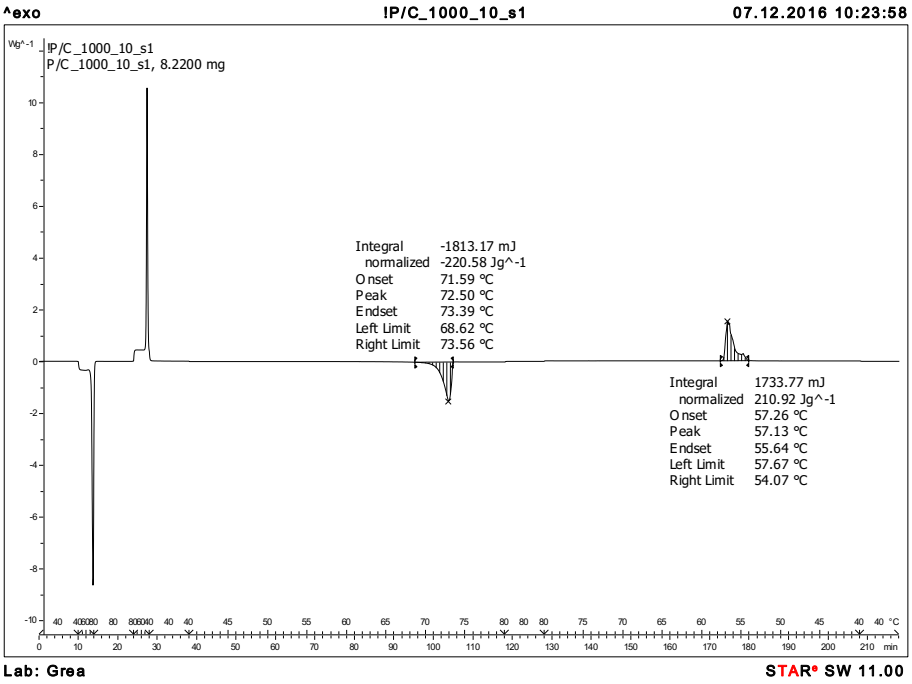

Figure A3-54. DSC response and evaluation of the material crystallized from decyl DHSE. Cycled sample 1. 100 cycles.

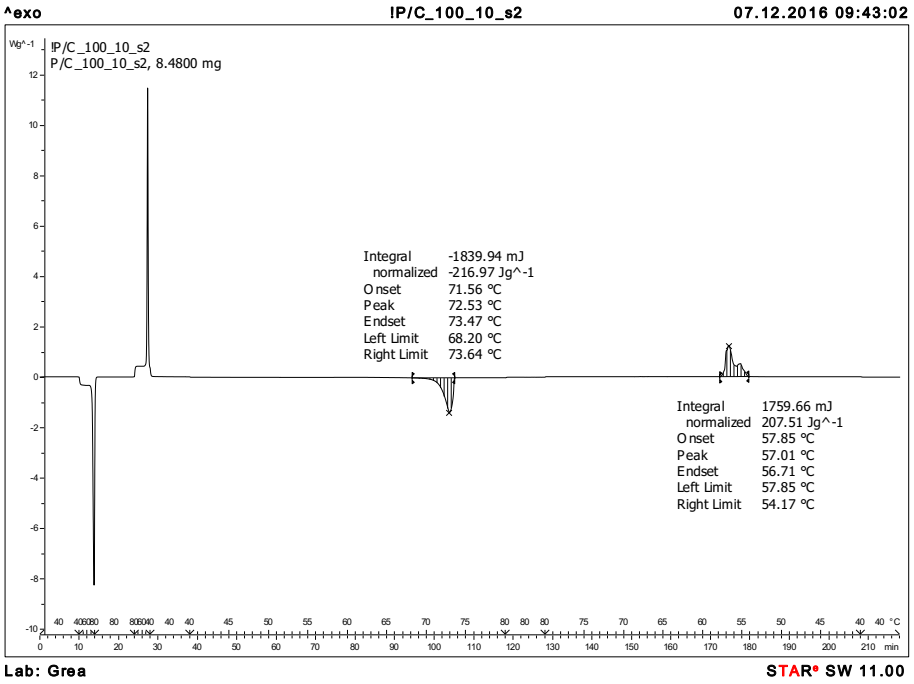

Figure A3-55. DSC response and evaluation of the material crystallized from decyl DHSE. Cycled sample 2. 100 cycles.

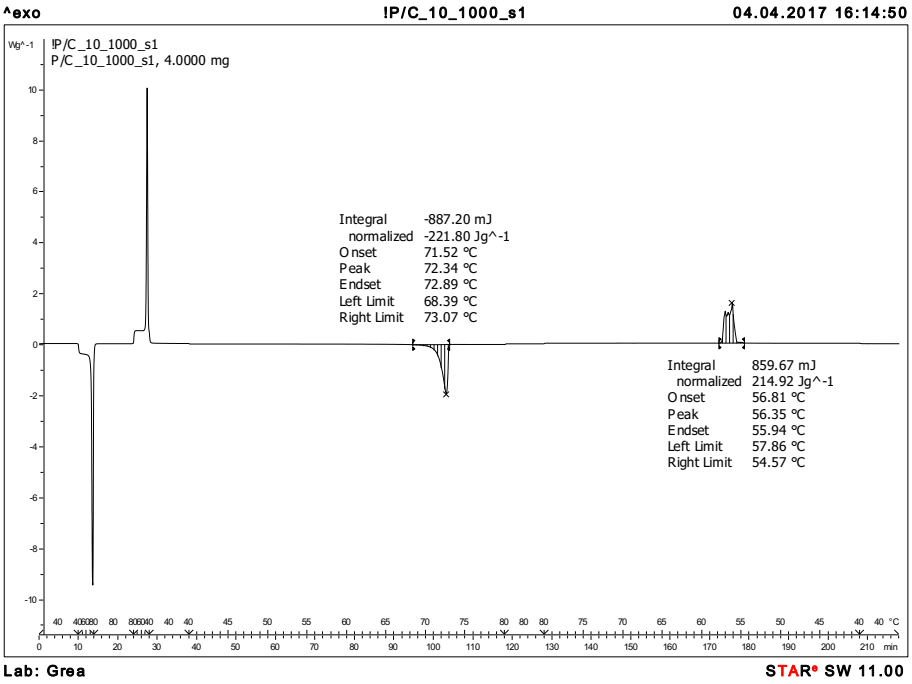

Figure A3-56. DSC response and evaluation of the material crystallized from decyl DHSE. Cycled sample 1. 1000 cycles.

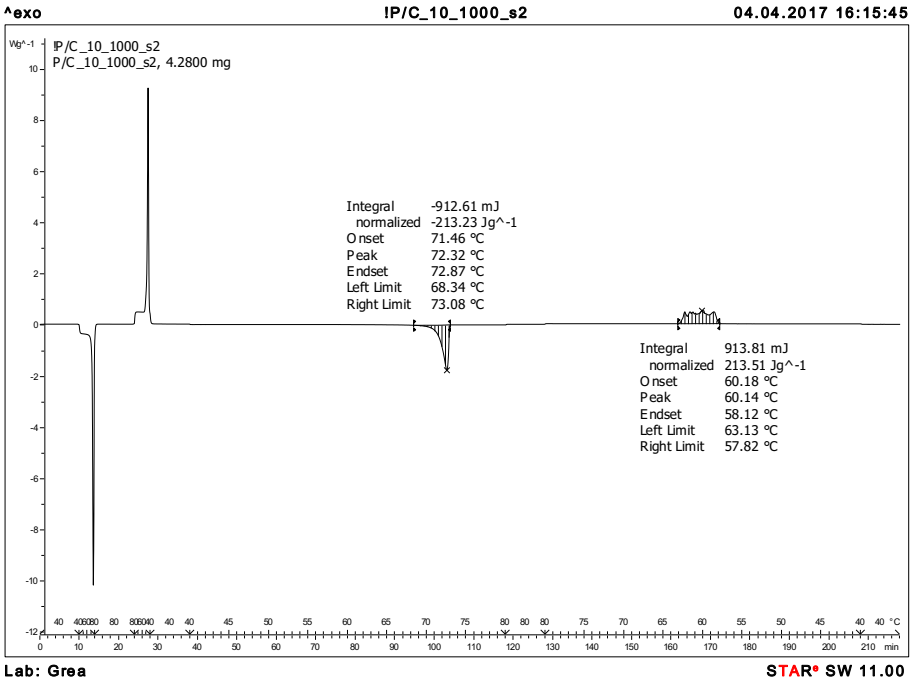

Figure A3-57. DSC response and evaluation of the material crystallized from decyl DHSE. Cycled sample 2. 1000 cycles.

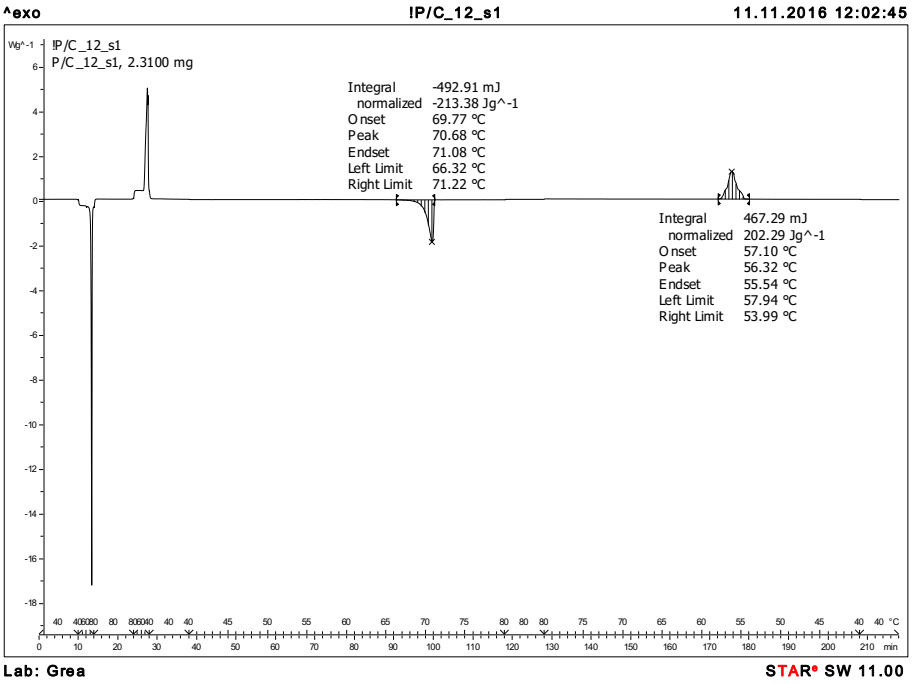

Figure A3-58. DSC response and evaluation of the material crystallized from dodecyl DHSE. Not cycled sample 1.

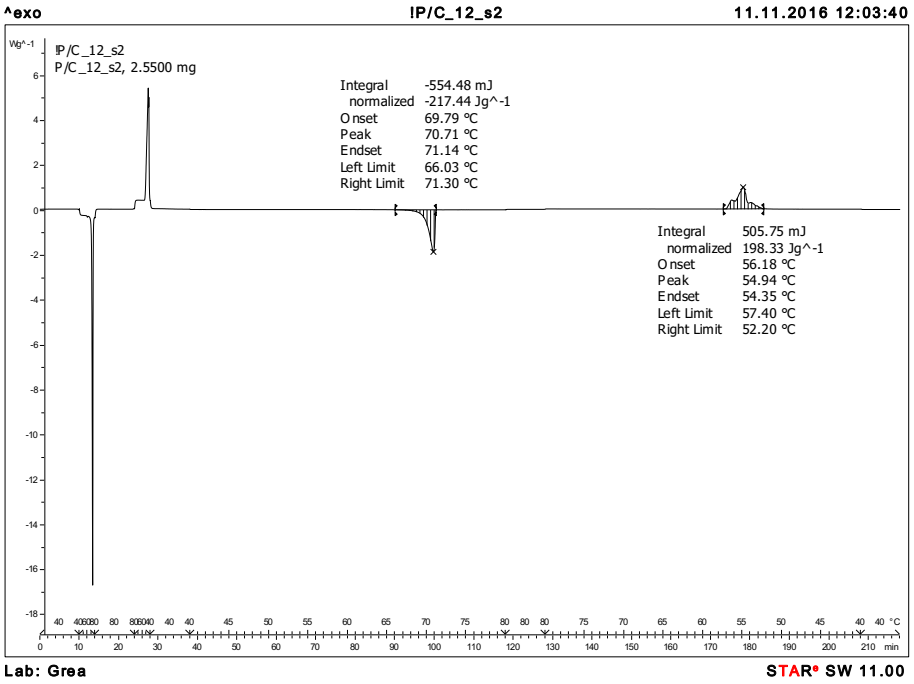

Figure A3-59. DSC response and evaluation of the material crystallized from dodecyl DHSE. Not cycled sample 2.

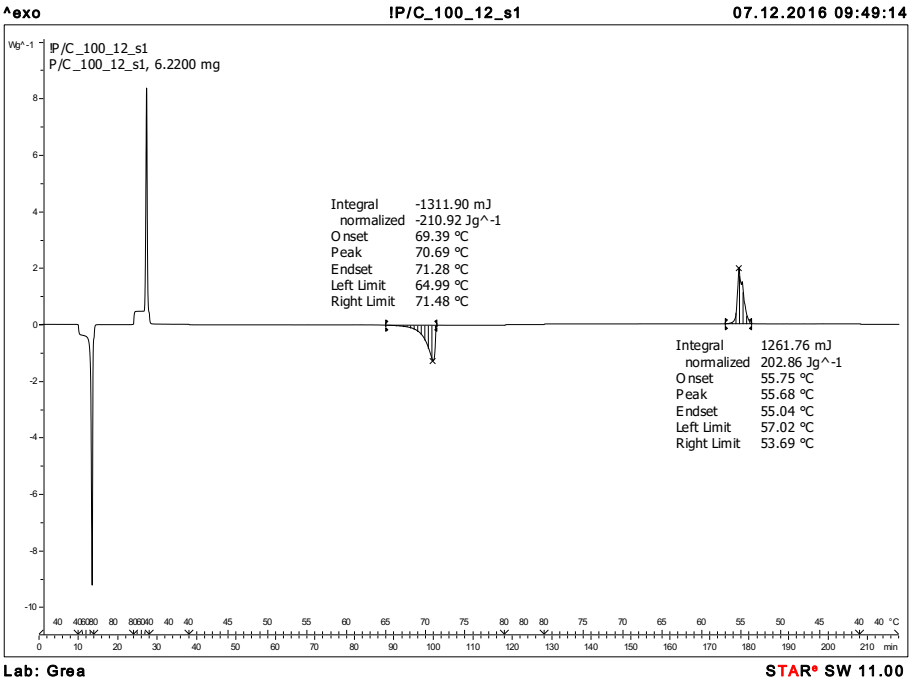

Figure A3-60. DSC response and evaluation of the material crystallized from dodecyl DHSE. Cycled sample 1. 100 cycles.

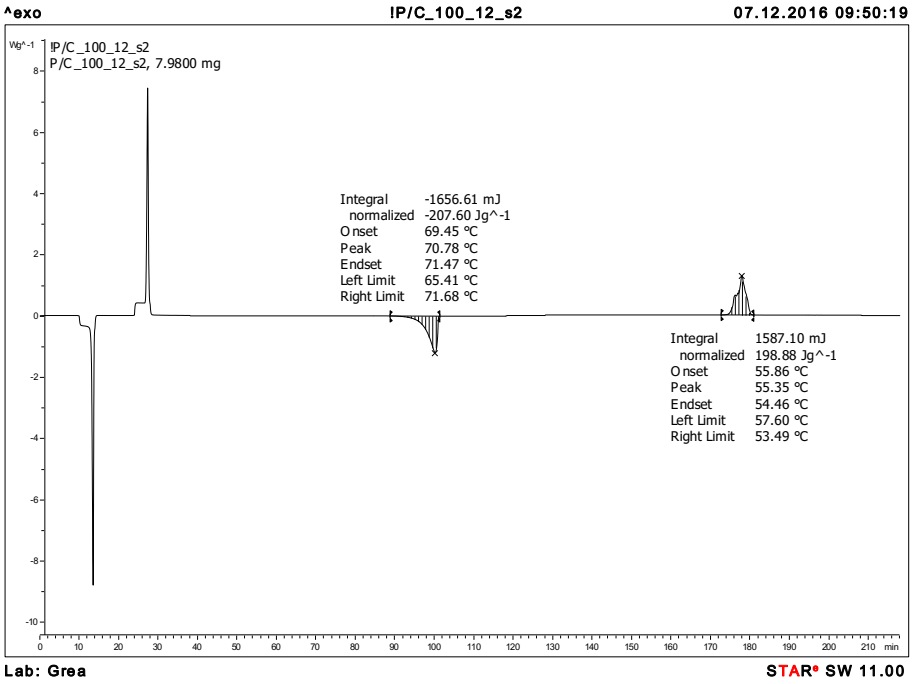

Figure A3-61. DSC response and evaluation of the material crystallized from dodecyl DHSE. Cycled sample 2. 100 cycles.

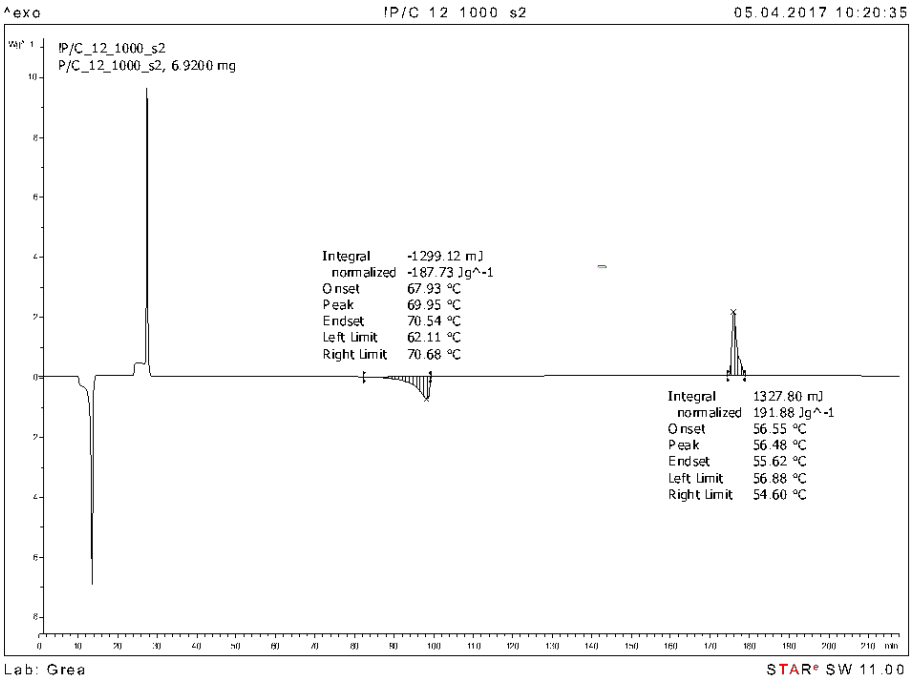

Figure A3-62. DSC response and evaluation of the material crystallized from dodecyl DHSE. Cycled sample 1. 1000 cycles.

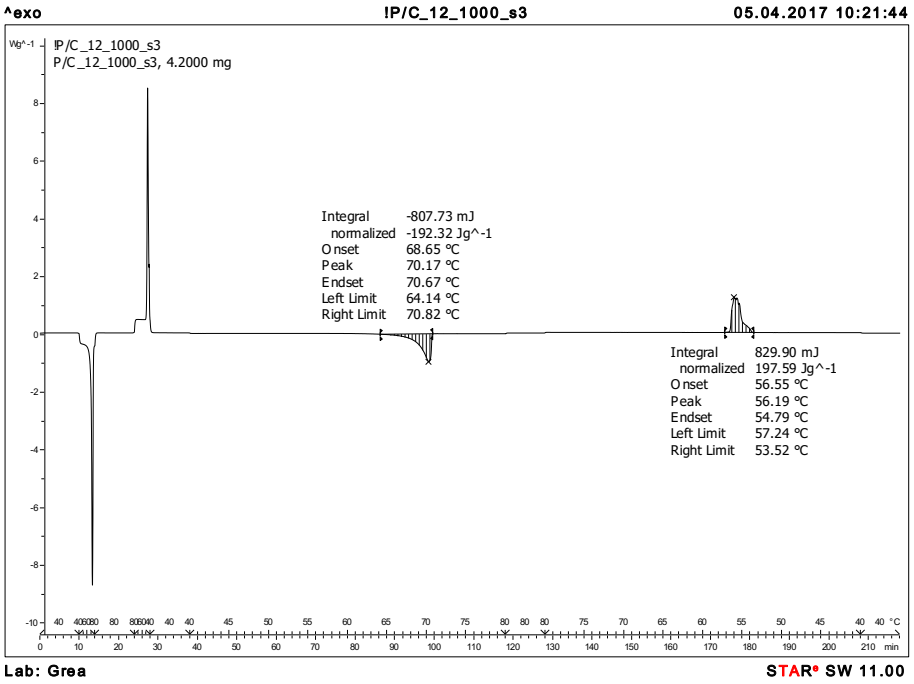

Figure A3-63. DSC response and evaluation of the material crystallized from dodecyl DHSE. Cycled sample 2. 1000 cycles.

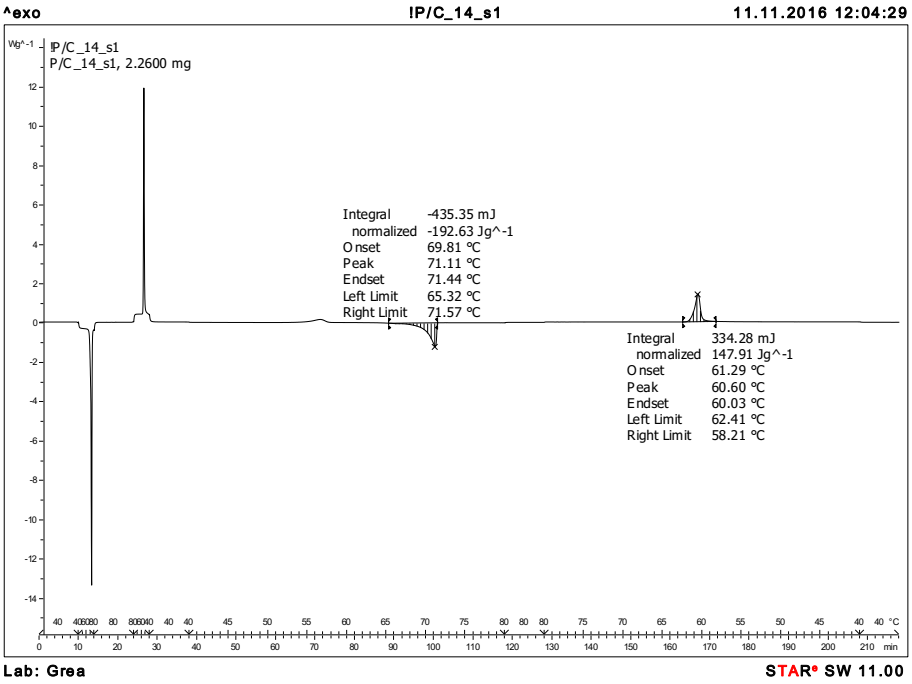

Figure A3-64. DSC response and evaluation of the material crystallized from tetradecyl DHSE. Not cycled sample 1.

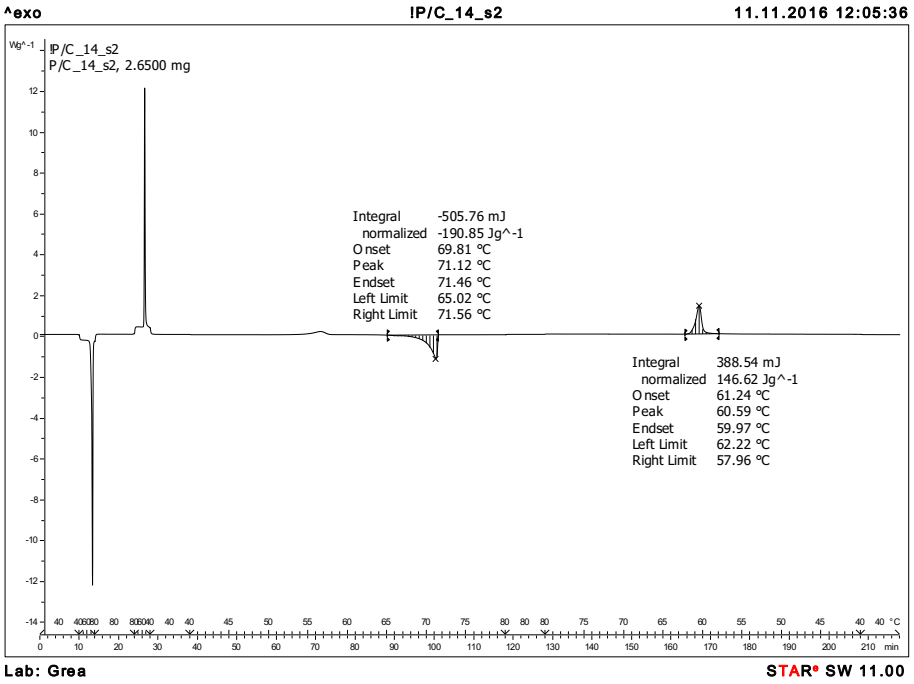

Figure A3-65. DSC response and evaluation of the material crystallized from tetradecyl DHSE. Not cycled sample 2.

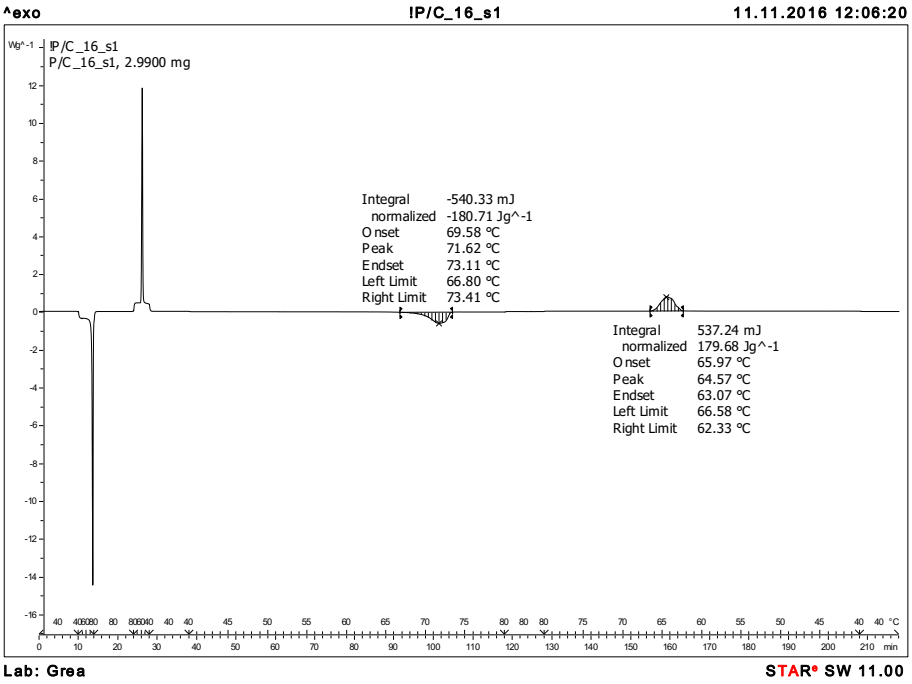

Figure A3-66. DSC response and evaluation of the material crystallized from hexadecyl DHSE. Not cycled sample 1.

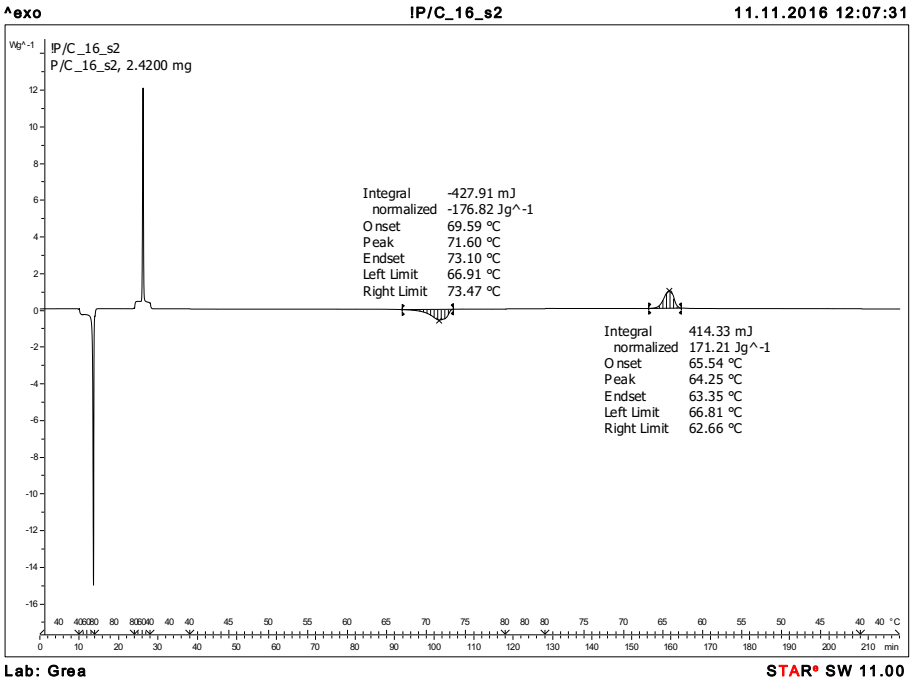

Figure A3-67. DSC response and evaluation of the material crystallized from hexadecyl DHSE. Not cycled sample 2.

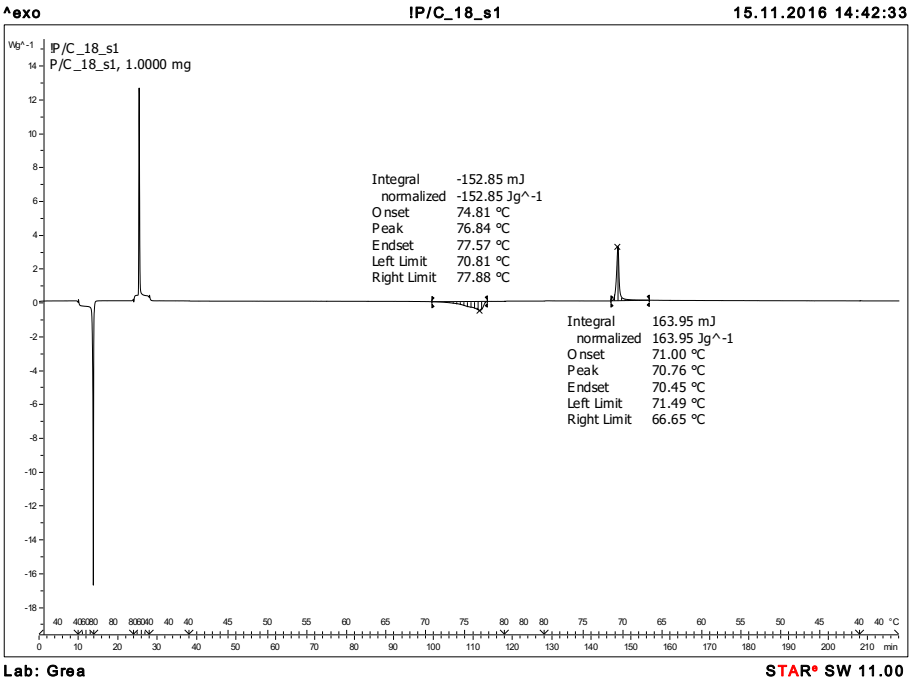

Figure A3-68. DSC response and evaluation of the material crystallized from octadecyl DHSE. Not cycled sample 1.

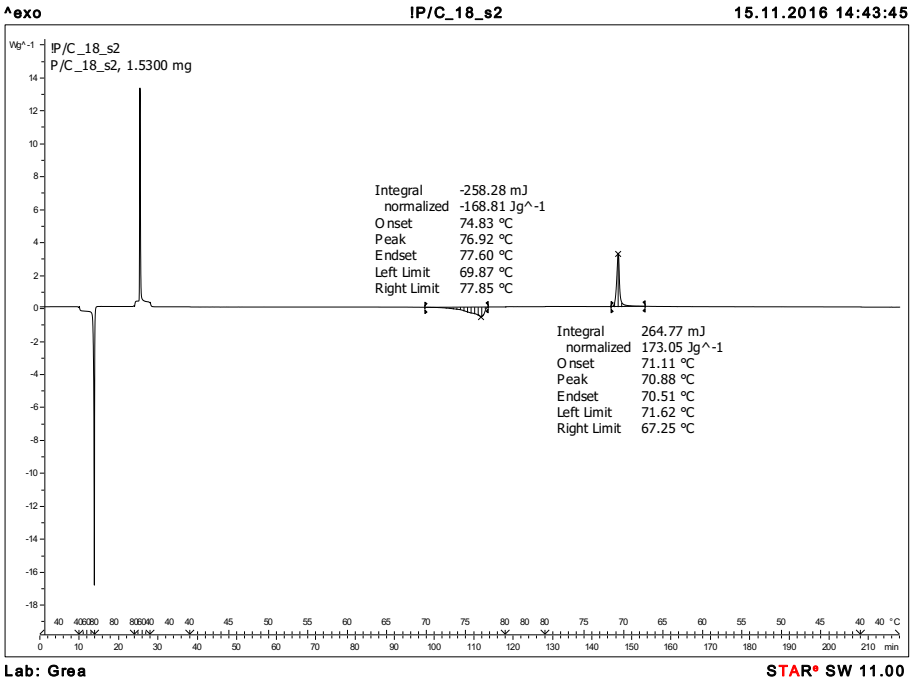

Figure A3-69. DSC response and evaluation of the material crystallized from octadecyl DHSE. Not cycled sample 2.